Using cell type specific transcriptomics to understand how *Arabidopsis* roots respond to *Sinorhizobium meliloti*

By
Jo Hulsmans

Thesis
Submitted to the University of Warwick
For the degree of

Doctor of Philosophy

Department of systems biology
September 2014

Table of Contents

Acknowledgments

At the start of this project, a PhD was described to me as a marathon, rather than a sprint, and these two pages feel far too short to acknowledge everyone who has helped me reach the end.

First and foremost, Miriam Gifford, my promotor, for her insights and her patience, for her perpetually positive attitude even when things appeared bleakest, for encouraging me to participate and present in science congresses in the UK and abroad, and for teaching me to write and analyze critically and scientifically.

I also want to thank Nigel Burroughs, my co-promotor, for the monthly meetings with discussions on gene clusters and inference networks. My advisory committee, Jim Beynon, Andrew Mead and Sascha Ott for always giving me constructive advice and being as helpful as possible.

I also want to thank everyone from our group for their insights, support and for all the good times we had in the lab. Roxana Bonyadi and Antony Carter were excellent friends during the work hours, Sanjeev, Yin, Jesper and Dhaval helped me a lot with their advice and support, especially when I needed some sleep in between FACS sessions.

The systems biology DTC gave me the opportunity to attain my MSc and helped me secure funding for my PhD, for which all the people involved deserve my gratitude, with special thanks to Hugo Vandenbergh, and his many emails prior to my enrolment.

Of course there is a life beyond academia as well and I want to thank all the wonderful people I lived with during my 4 years in England: Ali, Phil,

Dennis, Sang and Andrew, thank you for the great times. And especially Sharon, my wonderful girlfriend, whom I met halfway through, thank you for being so patient with me and for making me a happier man.

Finally, it is fitting in the acknowledgement for a thesis in life sciences to end by thanking those with whom I have the closest genetic links. My parents Marc and Conny, and my dear brother Jeroen. Your patience, support and understanding throughout all my life can never be repaid, and will never be forgotten.

Declarations

This thesis is presented in accordance with the regulations for the degree of Doctor of Philosophy. It has been composed by myself and has not been submitted in any previous application for any degree. The work in this thesis has been undertaken by myself unless otherwise stated.

Abstract

Roots are key organs for the uptake of nutrients in plants. Leguminous plants form nodules, providing a niche for symbiotic nitrogen-fixing bacteria, enabling plants to colonize nitrogen depleted soils. Lateral root formation shares genetic regulation, as well as developmental features, with nodulation. This led us to investigate whether shared genetic control can be revealed in lateral root development responses of *Arabidopsis thaliana* to rhizobia.

The phenotypic response of *Arabidopsis* to *Sinorhizobium meliloti* was analyzed. *Arabidopsis* lateral root length was found to be shorter, indicating a potential link between bacterial perception and lateral root development, even in a non symbiotic host plant. To gain more insight, a transcriptome time series was carried out. The response of *Arabidopsis* to *Sinorhizobium* inoculation compared to the response of nitrogen treatment were analyzed. In order to identify highly localized, yet important minimal regulatory cues and maximize the spatial specificity of the data, this analysis was carried out in isolated cortical and pericycle cells. Combined, in response to the two treatments approximately a 20% of the *Arabidopsis* genome is differentially expressed during the first 48 hours. Bioinformatic tools (clustering and network inference) were used to obtain a chronology of different responses, highlighting which metabolic processes change over time and identify potential gene regulatory mechanisms. The data and approach presented here present a unique analysis of the response to *Sinorhizobium* and nitrogen treatment and open the way to further tissue specific analysis of transcriptional regulation in plants.

The similarities and differences between the response to *Sinorhizobium* (a potentially neutral bacteria) and *Ralstonia* (a pathogen of *Arabidopsis* roots) were evaluated using an analysis of gene expression at two early time points after inoculation. There was significant overlap in transcriptional response to both treatments, as well as striking differences: we find pathogen defense genes in the response to *Sinorhizobium,* rather than *Ralstonia*. We also find a core of 11 auxin responsive genes that have similar differential expression between treatments.

Our results show that *Rhizobium* has a distinct transcriptional and phenotypic effect on *Arabidopsis* roots that is distinct from a pathogenic interaction. Several network hub genes are proposed as potential targets for further studying this effect.

Supplemental materials

S1: BATS DE genes for all time series

S2: GP2S analysis of time series data

S3: Gene ontology enrichment analysis for CN

S4: Gene ontology enrichment analysis for CR

S5: Gene ontology enrichment analysis for PN

S6: Gene ontology enrichment analysis for PR

S7: Gene regulatory inference network data

S8: *Ralstonia solanacearum* treated plants DE data

Supplemental materials can be found on the following link: https://www.dropbox.com/sh/mxs1hg4wgq0747v/AAD0aRX8h3kugwEXJ_eNlXm6a?dl=0

Abbreviations

ABA	Abscisic acid
AM	Arbuscular mycorhizae
BF	Bayesian factor
CN	Cortex nitrogen treatment
CR	Cortex *Sinorhizobium* treatment
CS	Cortex standard treatment
DE	Differential expression/differentially expressed
ETI	Effector triggered immunity
GO	Gene ontology
HR	Hypersensitivity response
JA	Jasmonic acid
PAMP	Pathogen associated molecular pattern
N	Nitrogen
PN	Pericycle nitrogen treatment
PR	Pericycle *Sinorhizobium* treatment
PS	Pericycle standard treatment
PTI	Plant triggered immunity
SA	Salicylic acid
TF	Transcription factor

Chapter 1

Literature review and thesis aims

Plants are essential for human life. Through direct consumption as food crops, indirect consumption as fodder, through their conversion of atmospheric CO_2 to O_2, as well as newer applications such as biofuel production, modern human society is completely dependent on plants for survival. With the human population projected to reach 9-11 billion by 2050 (Bongaarts, 2009) from 7 billion currently, the pressure on available land will increase steadily. This is compounded by global climate change and thus the ecological constraints in which we perform agriculture will be tightened through increasing population and ecological pressure.

Nitrogen (N) availability is one of the major limiting factors to plant and crop growth (Oldroyd and Downie, 2008). In the developed world, farmers use large, unsustainable amounts of inorganic fertilizers as N supplementation in crop production (Tilman et al., 2011). In undeveloped countries, farmers are usually unable to afford these fertilizers and suffer poor crop yields as a result (Tilman et al., 2011).

N is very abundant on earth, mostly as N_2, making up roughly 80% of the atmosphere. However, N_2 is unavailable to eukaryotes, because of the chemical stability of the triple bond between the N atoms. Only bacteria and archaea have evolved the ability to convert N_2 into ammonia through the nitrogenase enzyme (Downie, 2014). Some plants, more specifically the legume family as well as the non-legume *Parasponia,* have evolved the ability to

associate with N-fixing bacteria, known as rhizobia. This activity is in most species localized to nodules, specialized organs that provide a suitable environment for N_2 fixation (Oldroyd et al., 2011). In nodule development rhizobia-derived signal molecules (Nod factors) are sensed in root epidermal cells. Concomitantly with bacterial entry, cortical cell division is induced, enabling formation of a niche to host the bacteria. Inside a functional nodule, rhizobia fix atmospheric N into a form useable by the plant. In exchange the plant supplies the bacteria with a mixture of carbon compounds and amino acids (Lodwig and Poole, 2003; Oldroyd et al., 2011; Oldroyd, 2013).

Enabling associations of all non-legumes with rhizobia could provide an enormous advantage, reducing the need for inorganic N supplementation through fertilizers. This would address a financial as well as an ecological burden for agricultural systems worldwide. To even begin to be able to do this, a much deeper understanding of the interactions of rhizobia and plants is needed and some outstanding questions need to be resolved, including: why is it that the symbiotic interaction is almost exclusively limited to a single plant family? Is there any type of interaction between other plants and rhizobia?

Within the context of this thesis, responses of the non-legume *Arabidopsis thaliana* to *Sinorhizobium meliloti* are analyzed in parallel and compared to other environmental factors that plants respond to that might be related: N treatment and pathogen invasion. It is these three processes (nodulation and interaction with rhizobia, N deficiency and pathogen invasion) and their connections that will be explored in this review of literature.

1.1 Nitrogen and the N cycle

Nitrogen is an essential macronutrient for plants and a core component of artificial fertilizers. Most non-legume plants require N at a ratio of 20-50 g of N for 1 kg of dry biomass (Xu et al., 2012). Nitrate fertilizer production accounts for 1% of world energy use and the production of N fertilizer accounts for 50% of agricultural greenhouse gas emissions. Reducing agricultural reliance on inorganic fertilizers is a major challenge for the agricultural industry going forward and relies on a better understanding of N uptake and signaling in root systems.

In ecosystems, N is found in several forms: N_2, NH_4^+, NO_2^- and NO_3^- and organically bound N. It is most abundant as triple bonded N_2 in the atmosphere. This bond must be broken before N can become available to plants. Conversion of N_2 into NH_4^+ is carried out by N fixing organisms such as *Rhizobium* bacteria and Cyanobacteria (Galloway, 1998). In addition to biological N fixation there is N fixation as a result of lightning, although the amount of N fixed through lightning is roughly 2 orders of magnitude lower than in biological N fixation (Galloway, 1998). In the 20^{th} century, humans have added a third source of N into the ecosystem through industrial N fixation in the Haber-Bosch cycle for the production of fertilizers (reviewed by Erisman et al., 2008).

Nitrogen fixed through N fixing bacteria is quickly taken up into soil organisms (typically the bacteria itself or a host plant) and incorporated into organic N compounds (Pidwirny, 2006). After the death of an organism, the N stored in tissues and cells is reconverted into NH_4^+ in a process called

mineralization (Pidwirny, 2006). A portion of the released NH_4^+ is converted into NO_2^- by *Nitrosomonas* bacteria, which can in turn be converted into NO_3^- by *Nitrobacter* bacteria (Painter, 1970). In the soil, NH_4^+ is typically absorbed onto negatively charged clay particles and therefore immobile (Pidwirny, 2006). Nitrates however, are negatively charged, which prohibits them from absorbing onto clay particles and thus renders nitrates very mobile and easily leached out of the soil into the oceans (Pidwirny, 2006).

Plants can take up both ammonium and nitrates from the environment. Typically plants adapted to anaerobic conditions and low pH tend to assimilate NH_4^+, whereas plants adapted to aerobic conditions and higher pH assimilate NO_3^- (Maathuis, 2009)

1.1.1 Nitrate uptake from the soil

Nitrate is present in the soil but the concentration is highly heterogeneous (Cain et al., 1999). Furthermore, nitrate is easily dissolved in water due to its polar nature, making it very mobile. Thus, plants have to employ a variety of strategies to maximize nitrate assimilation from the soil (Miller et al., 2007). Physiological studies have shown that plants have evolved three nitrate transport systems, specialized to take up nitrate when it is at low concentrations in the soil (Crawford and Glass, 1998). Two of these are high affinity transport systems, specialized to take up low concentrations of nitrate (1 μM to 1 mM). One of these systems is constitutive, active even in the complete absence of nitrates, whereas the other is inducible, requiring the presence of nitrate for the transporter genes to be expressed. At nitrate concentrations above 1mM, low affinity systems become the dominant source of nitrate influx, as the high affinity

systems are downregulated and/or saturated (Miller et al., 2007; Krapp et al., 2014).

Four major gene families have been identified as potential candidates for encoding nitrate transporters: The nitrate transporter 1 family (NRT1), the nitrate transporter 2 family (NRT2), the chloride channel family (CLC), and slow anion channel associated homologues (SLAC), with respectively 53, 7, 7 and 5 members in *Arabidopsis* (Krapp et al., 2014). Only the first two are involved in N influx in the roots. The latter two predominantly play a role in nitrate transport into vacuoles and redistribution of nitrate across the plant.

1.1.2 The NRT1 family

Proteins from the NRT1 family are not limited to transporting nitrate, they have recently been found to transport multiple compounds such as amino acids, peptides and hormones such as auxin and ABA (Léran et al., 2014). For example, NRT1.1 has been found to transport auxin (Krouk et al., 2009) and function as a sensor for nitrate (Gojon et al., 2011). Nitrate transporters in this family are typically low affinity, being functional when nitrate is abundant. The one exception is the well characterized NRT1.1, since it is able to function as both a low and high affinity transporter (Liu et al., 1999). The switch from low to high affinity transport function for NRT1.1 occurs through phosphorylation of a threonine residue on the protein. When the external nitrate concentration rises, the phospho- group is removed (Liu and Tsay, 2003), switching the protein to low affinity-mode, lowering the rate of nitrate assimilation.

NRT family genes do not only function as nitrate influx importers, for example, NAXT is located in cortical root cells and has been shown to be a

nitrate exporter, activated when nitrate concentrations in cell plasma reach a threshold concentration (Segonzac et al., 2007).

1.1.3 The NRT2 family

All identified *Arabidopsis NRT2* family members are high-affinity transporters and appear to specifically transport nitrate only (Krapp et al., 2014). In most higher plants the nitrate transport function depends on the presence of a separate protein, NRT3 (Orsel et al., 2006). In *Arabidopsis*, two *NRT3* genes have been identified, but only one of them (*NRT3.1*) appears to be essential for the uptake of nitrates (Orsel et al., 2006; Li et al., 2007). Experiments with yeast two-hybrid systems show that virtually all *Arabidopsis* NRT2-family proteins interact with NRT3.1 (Kotur et al., 2012).

Several NRT2 proteins have been confirmed to have nitrate transport activity (Remans et al., 2006; Kiba et al., 2012). NRT2.1 is the main component of high affinity transport in most nitrate concentration ranges (Li et al., 2007). *NRT2.4* expression is increased during long-term N starvation and is predominantly expressed in the root epidermis, in a location enabling nitrate uptake when soil concentrations are lowest (Kiba et al., 2012).

NRT2.1 and all proteins of the NRT2 family require interaction with another protein, NRT3.1 (Orssel et al., 2006). Mutations in *NRT3.1* cause similar phenotypes to mutations in *NRT2.1* (Orsel et al., 2006) and lack correct localization of NRT2.1 to the plasma membrane (Wirth et al., 2007). The NRT2.1 - NRT3.1 protein complex is thought to exist of 2 subunits each of NRT2.1 and NRT3.1 (Yong et al., 2010).

1.1.4 Transport of nitrate through the plant

Nitrate transport throughout the plant is predominantly controlled by other *NRT1* family genes. *NRT1.5* is predominantly expressed in pericycle cells and is involved in loading nitrate into the xylem (Lin et al., 2008), while *NRT1.8* is expressed mainly in xylem parenchyma cells and functions to export nitrate from the xylem (Li et al., 2010). NRT1.9 also acts in a location-specific pattern to specifically transport nitrate out of the phloem (Wang and Tsay, 2011). Together, these studies show how long distance transport of nitrates throughout the plant is highly co-ordinated and cell type specific.

Plants are not limited to external sources of N. Plants can remobilize N from mature to younger leaves, aided by NRT1.7 (Fan et al., 2009), giving plants rapid access to N, when external N sources are depleted. Similarly, NRT1.11 and NRT1.12, which are mainly expressed in fully grown leaves, have been shown to function as redistributors of N from source to sink organs. This redistribution is critical for optimal plant growth (Hsu and Tsay, 2013). Finally, *NRT1.6*, which is expressed in *Arabidopsis* reproductive organs, the funiculus and the silique, has been shown to function to channel available nitrate into seeds. *Nrt1.6* mutant plants exhibit a phenotype with strongly reduced N content in the seeds and an increased seed abortion rate as a result (Almagro et al., 2008).

1.1.5 Nitrogen availability signaling

As well as being an essential structural and metabolic element, nitrate also has a role as a signaling molecule. In the context of this thesis, the focus will mostly be on how this signal regulates root development and the expression of nitrate-related genes, also known as the primary N response.

Plants have the ability to adjust nitrate assimilation based on availability in the environment. Regulation of gene expression in response to changing N availability can be very rapid. During the first 20 minutes after the addition of nitrate to N starved *Arabidopsis* seedlings there is a steady increase in expression levels of a limited set of genes, related to ribosome and hormone biosynthesis, transcription and RNA processing, nucleic acid biosynthesis and N assimilation (Wang et al., 2004; Castaings et al., 2011). However, many of these genes are downregulated soon after and thus can be missed in experiments that analyze responses at 1 hour and later (Castaings et al., 2011).

1.1.5.1 NRT1.1 has a dual role as a nitrate transceptor

Nitrate sensing, as well as nitrate transport, have been described in NRT1.1 as two independent functions. The first evidence for this was the description of a mutation in the *NRT1.1* gene, which had lost transport functionality, but retained N sensing ability (Ho et al., 2008). As discussed earlier, phosphorylation of NRT1.1 is important for the functional switch between high and low affinity transport modes, and it appears that phosphorylation also plays a role in nitrate sensing. CIPK23, a nitrate-inducible kinase, which has also been shown to be involved in potassium starvation responses (Li et al., 2006), is able to phosphorylate NRT1.1 in response to low nitrate concentrations. This results in a reduced primary transcriptional response to nitrate as well as switching the overall nitrate transport mode to high affinity (Ho et al., 2008).

Additional insights to the role of NRT1.1 were gained when it was shown that NRT1.1 enables basipetal auxin transport under low nitrate conditions, inhibiting the accumulation of auxin in lateral root initiation sites.

When expressed at high concentrations, NRT1.1 dependent transport of auxin is inhibited, auxin can accumulate in lateral root initiation sites and lateral root growth is promoted (Krouk et al., 2010). Thus *Arabidopsis* has a mechanism that directly combines nutrient sensing with hormone directed organ development.

1.1.5.2 NRT2.1 and NRT1.1 are potentially able to direct root growth to N-rich patches of soil

Root systems demonstrate a strong local response to nitrate availability, directing lateral root growth into regions of soil where nitrate concentrations are higher (Zhang and Forde, 1998). Being able to adapt root growth specifically to nitrate-rich patches in the soil confers a huge evolutionary advantage to an otherwise sessile plant. In *Arabidopsis,* the nitrate-responsive ANR1 is a known promoter of local lateral root growth in response to patches with elevated concentrations of nitrate (Zhang et al., 1998).

Two nitrate transporter genes are known to play a critical role in directing root growth to nitrate-rich patches of soil. *Arabidopsis* seedlings defective in *NRT1.1* have a similar phenotype to seedlings defective in *ANR1,* suggesting that NRT1.1 is an upstream regulator of *ANR1* (Remans et al., 2006). NRT2.1 is thought to be involved in sensing nitrate-rich patches in the soil and directing root growth. *NRT2.1* encodes a major component of the high affinity transport system for nitrate in the root (Cerezo et al., 2001; Li et al., 2007). It is induced by low concentrations of nitrate while being repressed by constitutive high concentrations of nitrate (Lejay et al., 1999; Zhuo et al., 1999; Girin et al., 2007). *Nrt2.1* mutants show a reduced repression of lateral root primordia when grown on low nitrate media. Little et al. (2005), suggested that NRT2.1 acts as a nitrate responsive repressor of lateral root initiation. As described for NRT1.1,

this sensing role has been found to be fully independent from its function as a nitrate transporter (Little et al., 2005; Remans et al., 2006a).

1.1.5.3 Transcriptional activation of the primary nitrate response through NLP7

In recent years, additional transcription factors (TF) controlling nitrate signaling have been identified. Members of the NIN-like protein family (*NLP*) have a major role in plant responses to changing nitrate concentrations (Konishi and Yanagisawa, 2013; Marchive et al., 2013). These TFs are homologous to the NIN (NODULE INCEPTION) protein. NIN was originally identified in *Lotus japonicus* with a role in regulating formation of infection threads in the initiation of nodulation (Stougaard et al., 1999). In *Arabidopsis*, NLP7 has been shown to bind to the promotors of 851 genes in response to an increase in nitrate concentration (Marchive et al., 2013). NLP7 is found in the nucleus of cells playing a role in N transport (root hairs, emerging lateral roots (LR) and stem vascular tissues), and N starvation causes NLP7 delocalization to the cytosol. Thus, through some as yet unknown mechanism, it appears that nitrate inhibits the export of NLP7 from the nucleus, and that nuclear accumulation of NLP7 in the nucleus leads to transcriptional activation of many nitrate assimilation and signaling genes (Marchive et al., 2013).

Transcriptional activation in the response to an increase in nitrate concentration is not restricted to *NLP* family genes. Three members of the *LOB (*Lateral organ boundaries) *domain* gene family (LBD37, LBD38 and LBD39) have been shown to act as negative regulators of N-responsive genes (these include, among others, *NRT1.1, NRT2.1* and *NRT2.4*) (Rubin et al., 2009). Another TF linked to nitrate signaling is ANR1, a MADS-box TF (Zhang and

Forde, 1998), with *anr1* mutant plants showing reduced lateral root proliferation in nitrate-rich zones (Zhang and Forde, 1998). For an overview of nitrate signaling in roots, see Figure 1.1.

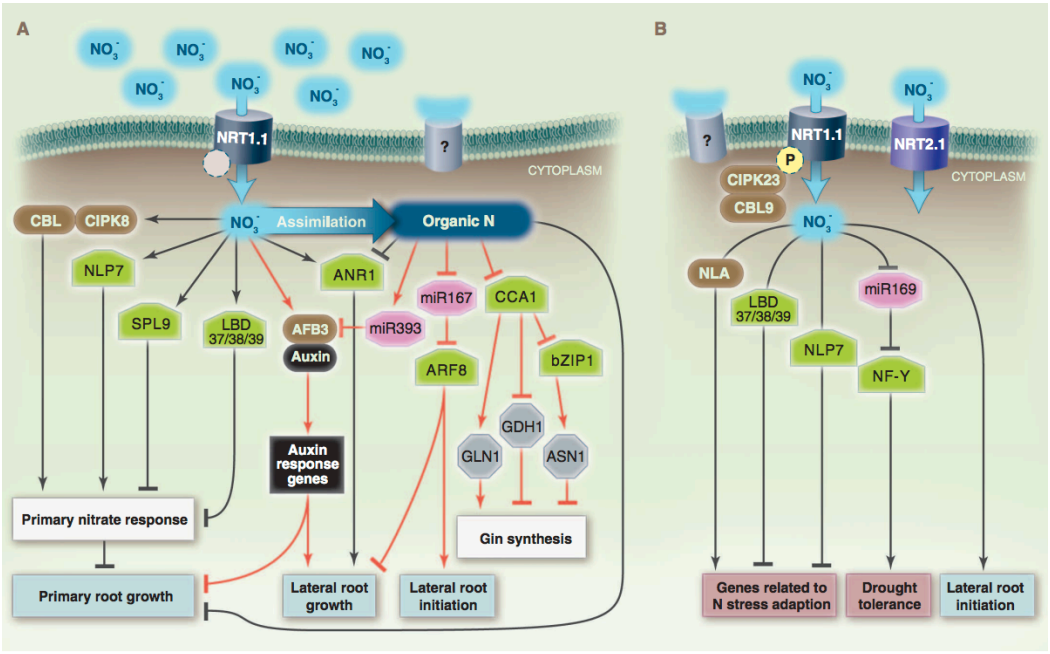

Figure 1.1 Simplified summary of known regulatory components controlling *Arabidopsis* responses to nitrate at the cell-soil interface. (A) Under high nitrate conditions (>1mM), NRT1.1 functions as a low affinity nitrate transporter. Nitrate activates several TFs (NLP7, SPL9, ANR1). NLP7 as well as CBL-CIPK8 coordinate transcription of regulatory genes in response to high concentrations of nitrates (Castaings et al., 2009; Hu et al., 2009). Members of the Lateral Organ Boundary Domain (LBD37/38/39) repress known N responsive genes (Rubin et al., 2009). CCA1 co-ordinates the organic N response by binding to bZIP1 TFs (which in turn regulates ASN1), Glutamate dehydrogenase (GDH) and Glutamine synthethase (GLN1) (Gutiérrez et al., 2008; McClung et al., 2010). Another target of organic N inhibition is miRNA167, which in turn inhibits ARF8, an activator of LR initiation and an inhibitor of LR growth. Thus nitrate treatment represses miRNA167, which increases concentrations of ARF8, leading to an increase in the ratio between initiating and emerging roots (Gifford et al., 2008). Induction of AFB3 gene expression by nitrate leads to auxin responses in primary and lateral roots. Under sufficient N nutrition, miR393 is induced, repressing AFB3 expression and auxin sensitivity. This allows the plant to control root architecture in response to N signals from inside and outside the root (Vidal et al., 2010). (B) Under low nitrate conditions (<1mM), NRT1.1 is phosphorylated and functions as a high affinity nitrate transporter, while NRT2.1 may play an additional role as signaler. Repression of miRNA169 by N limitation may lead to drought tolerance by NF-Y, a crucial TF for drought tolerance genes (Pant et al., 2009). Green shapes represent TFs, grey octagons represent enzymes, pink octagons represent miRNAs, and brown shapes represent other regulatory molecules. Black lines represent relationships obtained by molecular genetic approaches, red lines represent relationships discovered by systems biology approaches. Figure from (Gutiérrez, 2012).

1.2 Symbiotic interactions in plant roots

Many plants develop symbiotic interactions with micro-organisms in their immediate environment and we know that the rhizosphere is a complex mixture of physical, microbial and chemical properties (McCully, 1999; Yodler, 1999). The rhizosphere has gained increased interest in recent years due to the availability of new visualization techniques. Transparent soil in combination with confocal microscopy allows for quantitative imaging of in-situ root-microbe dynamics or high throughput screening of root phenotypes (Downie et al., 2012). Automatized root tomography methods allow for analysis of root phenotypes in different soil types (Mairhofer et al., 2012). These new techniques can be combined with recent whole microbial community sequencing methods (Bulgarelli et al., 2013; Schlaeppi et al., 2014).

Plant root interactions with mutualistic arbuscular mycorrhiza (AM) and ectomycorrhiza are particularly prevalent (in 70%-90% of land plants) (Parniske, 2008). In this interaction, plants provide the fungi with carbon, while the association with the fungus enhances the supply of water, N, phosphate as well as other nutrients to the host plant (Parniske, 2008). Uniquely among the different families of plants, legumes (as well as the non-legume genus exception *Parasponia* (Akkermans et al., 1978)) have evolved the ability to interact with N-fixing soil bacteria, referred to as rhizobia, within specialized root nodule structures similar to lateral roots (Desbrosses and Stougaard, 2011). In this mutualistic interaction, the bacteria express nitrogenase, which catalyzes the conversion of N_2 into NH_3. The ammonium is exported and assimilated into the plant, which in turn supplies the bacteria with access to carbon sources (Figure 1.2).

Bacterial endosymbiosis is also found outside the legume family. *Frankia,* an actinomycete, forms actinorhizal root nodules on a wide range of host plants. All plants that possess the ability to form an endosymbiotic relationship with *Frankia* are part of the Eurosid 1 clade (Soltis et al., 1995), which also contains legume species. It appears that the ability to nodulate developed several times independently in the evolution of this clade (Doyle, 2011), indicating that there could be some preexisting genetic mechanism to enable nodulation that is common to all members of the Eurosid 1 clade (Markmann and Parniske, 2009).

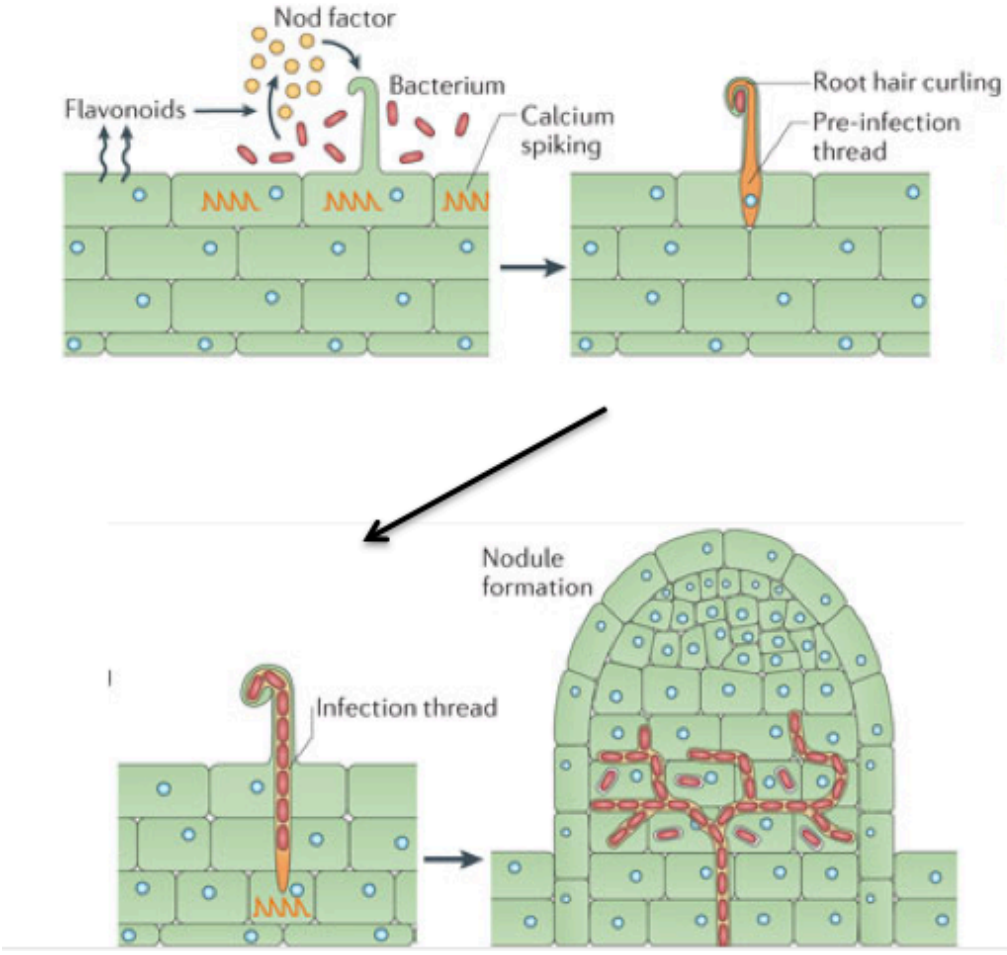

Figure 1.2 Rhizobial and mycorrhizal colonization of plant roots. Flavonoids released by the plant root signal rhizobia in the soil, inducing the production of Nod factors that are recognized by the plant, activating the symbiosis signaling pathway, leading to calcium oscillations and further signaling. Rhizobia enter the plant through root hair cells growing around the bacteria, trapping the bacteria inside the root hair curl. Infection threads form and nodules initiate below the site of bacterial infection. Image from Oldroyd (2013).

Nodulation is part of a complex endosymbiotic interaction, which probably evolved through co-option of one or more signaling and developmental pathways. Candidates for these pathways are lateral root development, and AM symbiosis, which is itself possibly related to bacterial defense (Markmann and Parniske, 2009; Liang et al., 2014).

1.2.1 Signal transduction through root cell layers during nodulation response in legumes

The nodulation response in legumes starts when legumes recognize NOD factors from *Rhizobia* bacteria in their immediate environment (Oldroyd et al., 2013). This NOD factor recognition will ultimately lead to nodulation of cells in the inner cortex and pericycle. It is thus clear that the nodulation signal has to successfully traverse several layers of different cell types before successful nodulation can occur (Figure 1.3).

Recognition of NOD factors by the NOD factor receptors leads to a signal cascade involving several transducing proteins, including SYMRK (Stracke et al., 2002), NUP85 (Saito et al., 2007), Castor and Pollux (Charpentier et al., 2008), which eventually causes Ca^{2+}-oscillations in the epidermis (Erhardt et al., 1996). These Ca^{2+}-oscillations are perceived by CcaMK (Lévy et al., 2004) which activates several TF downstream (NIN1, ERN1) (Marsh et al., 2007; Andrianka et al., 2007). This signal cascade serves a dual role: initiation of bacterial infection at the epidermis and the promotion of cell division in the cortex via an unknown diffusible signal (Oldroyd et al., 2013).

In cortex cells, nuclear factor induced cytokinin signaling is recognized by the cytokinin receptor LHK1/CRE1 (Plet et al., 2011), resulting in further

downstream signaling through the TFs NSP1, NSP2 and NIN (Heckman et al., 2006; Smit et al., 2005) and the suppression of polar auxin transport (Plet et al., 2011), which results in the promotion of nodule organogenesis in cortical and pericycle cells, rather than lateral root formation.

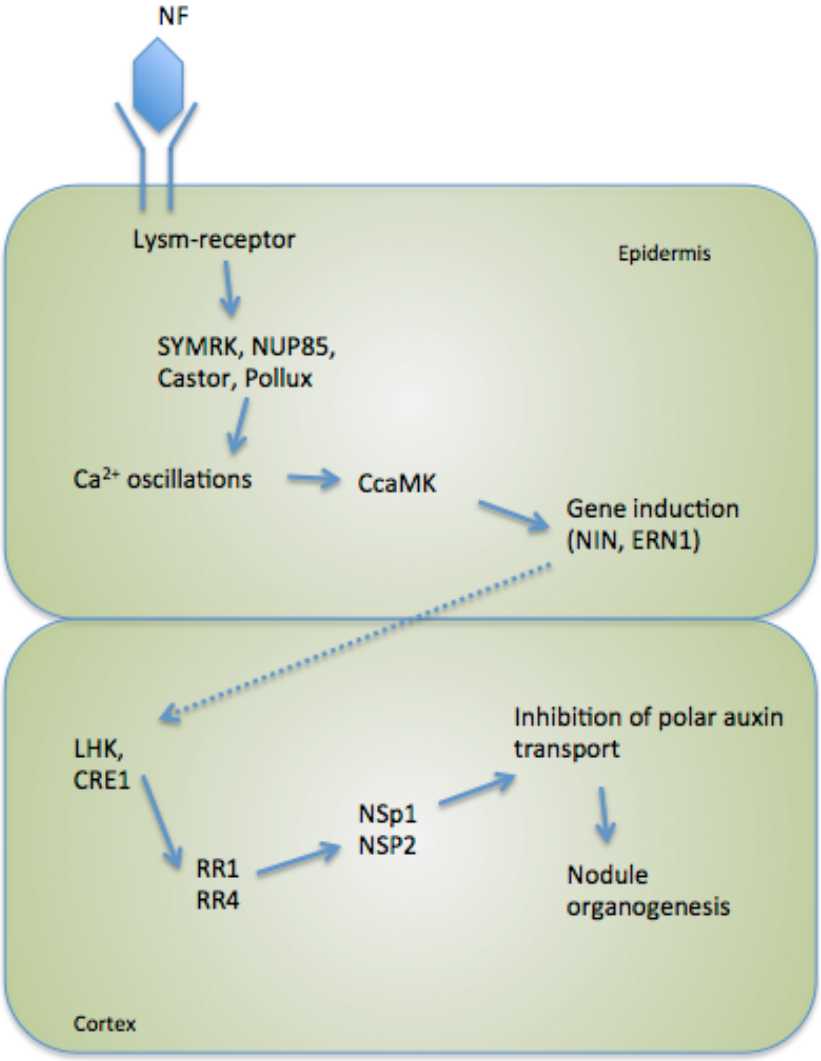

Figure 1.3 A schematic representation of genetic pathways involved in the activation of the establishment of symbiosis in the legume-rhizobia interaction. Epidermal cells are capable of perceiving Nod factor through lysM-receptor kinases (Madsen et al., 2003) that activate Ca^{2+}-oscillations through several signaling proteins, including symbiosis receptor like kinases (SYMRK) (Stracke et al., 2002), components of the nuclear pore (NUP85) (Saito et al., 2007) and Castor and pollux, two cation channels located on the nuclear envelope (Charpentier et al., 2008). The Ca^{2+}-oscillations are perceived through the calcium and calmodulin dependent kinase (CcaMK) (Lévy et al., 2004) which activates gene expression through TFs such as Nodule inception (NIN) (Marsh et al., 2007) and ERF required for nodulation (ERN1) (Andriankaja et al., 2007). An unknown signal (dotted line) transduces the signal into the cortex where polar auxin transport will be repressed through another signaling pathway, starting with cytokinin receptors Lotus histidine kinase (LHK) (Tirichine et al., 2007) and cytokinin response 1 (CRE1) (Murray et al., 2007; Plet et alk., 2011), through response regulators (RR1, RR4) (Plet et al., 2011; Gonzalez et al., 2006) and nodulation signalling pathway proteins (NSP1, NSP2) (Heckman et al., 2006), ultimately leading to the inhibition of polar auxin transport and the promotion of nodule growth. Reproduced from Oldroyd et al. (2011).

1.2.2 LysM receptor kinases link different biological interactions at the cell wall

Plants are exposed to a wide range of micro-organisms in soils. Successful elicitation of a response requires a first establishment of communication between the plant and the micro-organism that will to interact with it, whether this interaction is beneficial (symbiosis) or not (pathogenic) (Oldroyd et al., 2013). The major messenger molecules involved in early organism crosstalk are Myc factors (in AM), Nod factors (in rhizobial symbiosis), both lipo-chitin oligosaccharides (Maillet et al., 2011; Liang et al., 2014) and pathogen associated molecular patterns (PAMPs, in pathogenic interactions) (Jones and Dangl, 2006). Nod factor, Myc factor and certain PAMPs such as chitin, carry a strong structural similarity (Liang et al., 2014) and thus their signaling receptors are thought to be closely related (Figure 1.4). For many years, leucine-rich repeat receptor proteins have been established as the major binding protein for PAMPs (Boller and Felix, 2009). More recent evidence points to another class of cell-surface receptor kinases, the LysM family, also playing a role in PAMP-recognition (Miya et al., 2007; Willmann et al., 2011; Brotman et al., 2012). These LysM-receptor kinases were also earlier identified as the proteins responsible for Nod-factor recognition in the *Rhizobium* symbiosis in legume plants *Lotus japonicus* (Madsen et al., 2003) and *Medicago truncatula* (Amor et al., 2003; Arrighi et al., 2006).

In AM symbiosis, it was long hypothesized that there would be a diffusible factor similar to the Nod factor. This hypothetical Myc factor was discovered based on the hypothesized structural similarity with Nod factors and PAMPs (Maillet et al., 2011; Gust et al., 2012). Interestingly, in *Parasponia*, the

only nonlegume with endosymbiotic interactions with rhizobia, the LysM-receptor kinase regulating *Rhizobium* interactions also regulates interactions with AM (Op den Camp et al., 2011), suggesting that LysM-receptors were recruited from the AM-symbiosis during the evolution of rhizobial symbiosis. This is consistent with the pre-existence of AM interactions before the evolution of nodulation ~60 MYA. AM interactions are thought to have evolved ~400 MYA (Redecker et al., 2000) to enable colonization of land by plants .

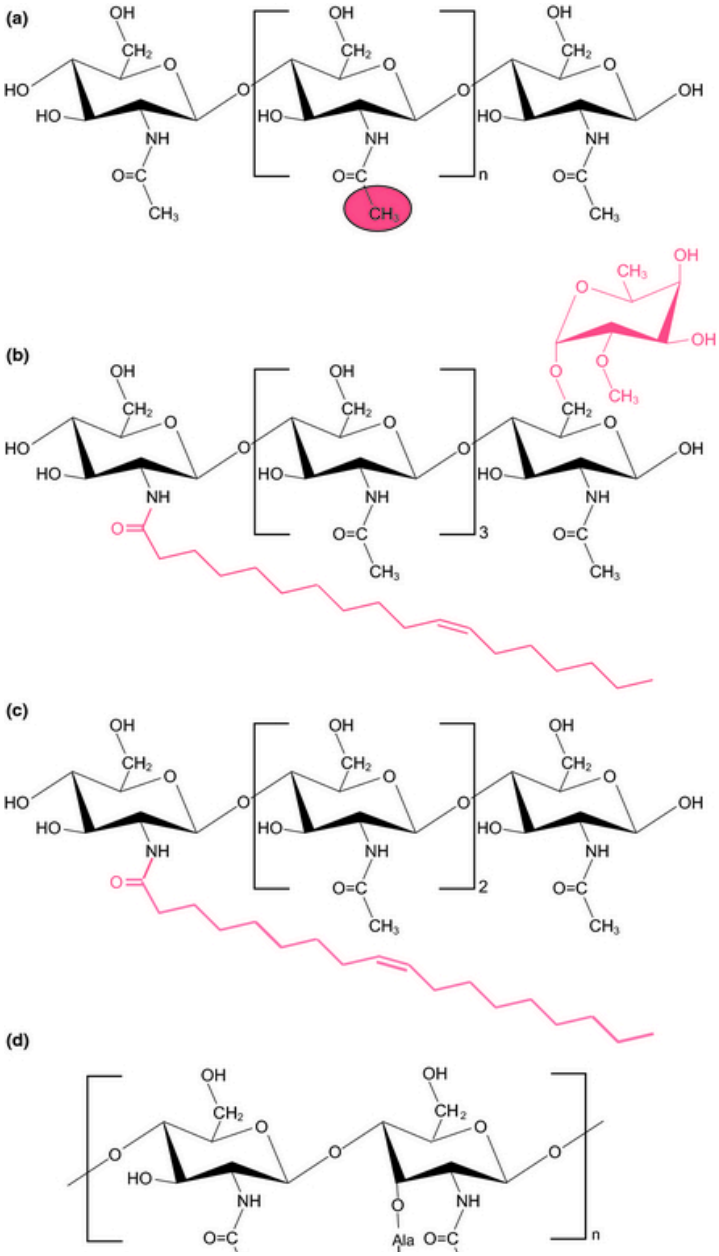

Figure 1.4 Structure of chitin, representative of Nod factor, Myc factor and peptidoglycan, highlighting their structural similarities. (a) Chitin, a polymer of N-acetylglucosamine. (b) Nod factor produced by *Bradyrhizobium japonicum*. (c) Myc factor produced by *Glomus intraradices.* (d) Monomer of peptidoglycan produced by *Escherichia coli.* Figure from Liang et al., 2014.

1.2.3 Legume plants are able to distinguish between *Sinorhizobium* and AM even though primary signal transduction is highly similar

If the primary signaling event between plants and *Rhizobium*/AM are so similar, legumes would require an additional signal to differentiate between the two. After transduction through *LysM*-receptors in epidermis cells, the symbiotic

interaction signal follows a signaling cascade, ultimately resulting in calcium spiking in the nucleus of the epidermal cells (Figure 1.3). These fluctuations in Ca^{2+}-concentrations are perceived by a calcium and calmodulin dependent protein kinase and translated through different signaling steps into gene transcription and activation of nodulation (Figure 1.4). In *Rhizobium* interactions, these spikes are highly regular (Sieberer et al., 2009), whereas in the response to AM they can be highly irregular (Chabaud et al., 2011). It is possible that differences in the calcium spiking step codes for specificity (Kosuta et al., 2008), however other studies show that calcium spikes in response to different micro-organisms are indistinguishable and should be interpreted as a reflection of the progression of the symbiotic interaction (Sieberer et al., 2012). Rather than the pattern, it is also possible that signal strength is the selecting factor in the establishment of interaction: rhizobia and fungi-associated symbioses have different binding requirements for calmodulin to bind to the calcium calmodulin dependent receptor kinase (CCaMK) (Shimoda et al., 2012), indicating a differential activation mechanism of gene transcription distinguished by differential regulation by calmodulin.

Recent work (Genre et al., 2013) indicates that short AM-associated chitin oligomers trigger calcium oscillations dependent on the symbiosis pathway but are independent of the presence of Nod factor. This suggests their role in signal specificity and suggests that the specificity for interaction with AM is signaled by a combination of Myc-factors and these short chitin oligomers.

1.2.4 Parallels between plant-pathogen and plant-mutualist interactions

In pathogen recognition in plants, the first step is recognition of PAMPs. These are recognized by plant pattern recognition receptors, leading to induction of

innate immunity, also known as PAMP-triggered immunity (PTI). To avoid this, pathogens have evolved to deliver effector proteins to the plant cells, often through specialized secretion systems. Plants in turn express resistance genes that recognize these effector proteins. This second line of defense is referred to as effector triggered immunity (ETI) (for a review, see Jones and Dangl, 2006).

As noted before, there is a strong structural similarity between Nod-factors, Myc-factors and specifically chitin PAMPs, yet at the same time they can trigger opposite (symbiosis/plant defense) responses in plants (Liang et al., 2014). For example, plants can produce chitinases that hydrolyze chitin in fungal hyphal tips (Punja and Zhang, 1993), releasing long-chain chitooligosaccharides that elicit plant innate immunity (Stacey and Shibuya, 1997; Shibuya and Minami, 2001). Certain pathogens can produce effector proteins that compete for chitin binding with the chitin receptor. These are thought to sequester the chitooligosaccharides, preventing them from triggering ETI (de Jonge et al., 2010; Mentlak et al., 2012). These chitooligosaccharides are recognized by LysM-type receptors (Shimizu et al., 2010), which have been demonstrated to be able to bind chitin. Receptors of this type have also been shown to recognize peptidoglycan, a major component of bacterial cell walls (Willmann et al., 2011; Liu et al., 2012).

Parallel to these pathogen-triggered signaling responses, Nod factors and Nod factor receptors have in the past been shown to cross talk with plant innate immune responses. In the legume *Medicago truncatula*, mutants with defective Nod factor receptors are more susceptible to fungal invasion (Ben et al., 2013), and addition of Nod factor to *Arabidopsis* triggers the production of reactive oxygen species (Wang et al., 2014), as well as suppression of innate

immune responses (Liang et al., 2013). This opens up the possibility that Nod-factor receptors were originally regulators of pathogen defense.

1.2.5 Evolution of plant-microbe interactions

The discovery of the common symbiotic pathway between AM and *Sinorhizobium* interactions indicates an evolutionary connection, and fits with AM interactions predating plant-rhizobia (Markmann and Parniske, 2009). The origins of the evolution of plant innate immunity are unclear, but LysM domains recognizing fungal elicitors are thought to be ancient and found in proteins in algal lineages that predate the emergence of higher plants (Zhang et al., 2007). Thus it can by hypothesized that the AM-interaction evolved from the plant innate immunity and was later adapted by pathogens to create molecules to suppress PTI. Myc-factor production by AM fungi could originally be an adaptation to PTI, suppressing innate immunity, with their role in the establishment of symbiosis and development a later evolved trait, a role which was later co-opted again in the rhizobia-legume symbiosis (Liang et al., 2014).

1.3 *Ralstonia solanacearum* is a broad spectrum root-invasive plant pathogen

Studying plant-microbe interactions in *Arabidopsis* has always focused on pathogenic interactions, as *Arabidopsis* forms no symbiotic interactions with either rhizobia or mycorrhizae (Vance, 2001). However, as has been discussed, there are strong indications of a common evolutionary origin of symbiotic and pathogenic interactions (Liang et al., 2014). Thus to gain a complete insight of plant responses to rhizobia it is necessary to analyze them in a comparison to

pathogenic bacteria. The pathogen *Ralstonia solanacearum* represents an ideal species to compare rhizobial responses to, since it is a pathogen of the root, with a highly cell specific infection mechanism.

Ralstonia solanacearum is a β-proteobacterium and a pathogen to over 200 species in 50 botanical families (Denny, 2006). It is found in tropical regions of all continents (Genin et al., 2012), but is known to be able to infect *Arabidopsis* (Hu et al., 2008). It can survive for years in moist soils (Álvarez et al., 2008) until it encounters a susceptible host which it invades through wounds in the root cortex and openings of lateral root primordia (Denny, 2006), after which it colonizes the xylem vessels and spreads to shoots through the vascular system. Wilting results from vascular dysfunction caused by colonization of the root system within 5 to 8 days (Genin and Denny, 2012).

Research in the relationship between *Ralstonia* and *Arabidopsis* has predominantly focused on the type 3 secretion system, which the bacteria uses to deliver effector molecules into plant cells in order to suppress the plant's immune system (Deslandes et al, 2014). Thus far, thirteen effectors with ubiquitin ligase activity have been identified in *R. solanacearum* (Remigi et al., 2011; Peeters et al., 2012), indicating the importance of subversion of the plant proteasome during infection. Targeting of the proteasome is thought to mainly have evolved as a mechanism of shutting down plant hormonal regulation of defense responses (Deslandes et al., 2014).

Several *R. solanacearum* strains carry transcription activator-like effectors, mimicking the action of TFs (Doyle et al., 2013). Binding sites and precise mechanisms of action for these remain to be identified (Deslandes and Genin, 2014). Recently it has been confirmed that they locate to the nucleus upon

injection into eukaryote cells (de Lange et al., 2013), enabling them to bind to DNA.

1.4 Cell type specific transcriptomics to profile plant-microbe interactions

In trying to understand plant-microbe interactions, profiling plant gene expression changes during microbial responses can provide insight. Gene expression is a dynamic process, highly regulated at different spatial, developmental and temporal levels. Typically genes are expressed together, in regulatory networks, in order to concertedly carry out specific functions ranging from plant defense to flower development (Less et al., 2011; De Lucas and Brady, 2013; Pajoro et al., 2014). In the past, transcriptomics studies have relied on quantifying gene expression of whole organisms or organs, and provided a wealth of information, yielding a genome-wide view of transcriptional regulation within an organism (Kreps et al., 2002; Guo et al., 2004; Buchanan-Wollaston et al., 2005; Windram et al., 2012).

Higher organisms are characterized by having a large number of different and very specialized tissues with specific genetic regulatory functions (Birnbaum et al., 2003). Quantifying gene expression to understand the regulation of developmental features may thus be very different when determined in sepals or roots. Despite this, many transcriptomics studies start by homogenizing all cell types from a whole organ of the plant, effectively destroying any spatial nuance in the data, obscuring regulatory interactions that are very cell type specific in a mix of data. With the advent of high throughput methods for selecting specific tissues from a sample such as fluorescence

activated cell sorting (FACS) and laser capture microdissection, it is now possible to perform large-scale transcriptomics studies on specific cell types or tissues (Carter et al., 2013).

In a whole genomic microarray analysis of plant roots it was shown that this method could be used to detect novel cell specific expression patterns that were masked in parallel analyses of whole root cells. This expression was highly cell type specific or showed a mixture of induction and repression patterns across cell types (Birnbaum et al., 2003; Brady et al., 2007).

The N response in *Arabidopsis* is known to be be highly cell specific for transporter genes when nitrate is not evenly distributed along the roots (Little et al., 2005; Remans et al., 2006). In a study of transcriptional responses to low nitrate concentrations in *Arabidopsis* roots, a cell specific approach has been shown to greatly increase the sensitivity of identifying nitrate-regulated genes, particularly those expressed in single cell types, or that have mixed N-induction/N-repression patterns in different cell types. It also demonstrated pericycle-localized regulation of the N-response by *miRNA167*, which would have been obscured in a traditional whole root analysis (Gifford et al., 2008).

1.5 Conclusion

Understanding the genetic basis of the response to *Rhizobia,* and being able to situate it in the context of N starvation as well as pathogenic *(Ralstonia)* responses will help in understanding whether *Arabidopsis* perceives *Rhizobia* as a pathogen, a symbiont or neither. This will provide insight into how the host range of Rhizobia bacteria can be expanded to develop nodulation outside the legume family. In this thesis, the following broad research goals are investigated:

- Gain a better understanding of the root morphological response to Rhizobial bacteria
- Understand the response to high N and *Sinorhizobium meliloti* on the level of individual cell types, and identify any commonalities or apparent differences between treatment and cell types.
- Compare the root transcriptomic response between a pathogenic and non-pathogenic bacteria.

Chapter 2

Materials and methods

2.1 Plant growth

2.1.1 Plant materials

Unless otherwise stated, all *Arabidopsis thaliana* wild type seeds are of ecotype Columbia (*Col-0*) and were obtained from the *Arabidopsis* biological research center (Nordberg lines, Lamesch et al., 2012). *Arabidopsis thaliana* GFP lines in the Col-0 background were selected to mark the pericycle (line E3754, Gifford et al., 2008) and cortex (line *pCo2::YFP*$_{H2B}$, Heidstra et al., 2004) cells in the root (Figure 2.1). Pericycle and cortical cells were chosen based on availability and existing data (Gifford et al., 2008).

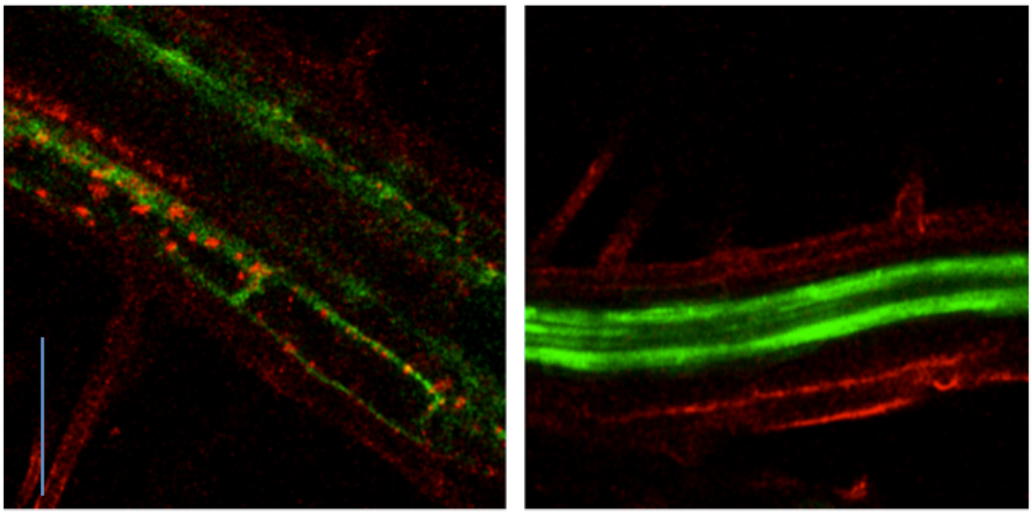

Figure 2.1 Localized GFP expression in marker lines. (a) Cortex labeled line; (b) pericycle labeled line. Images obtained using confocal microscope at 25x magnification. Cell walls stained with propidium iodide (red) to aid cellular identification. Blue line indicates 100 µM.

A set of 34 *Arabidopsis* ecotypes (Table 2.1) were obtained from ABRC (Ohio state university).

Table 2.1 Overview of Arabidopsis ecotypes used, with corresponding germplasm/stock accession number

Ecotype	Accession	Ecotype	Accession
An-1	CS22626	Knox-18	CS22567
Bil-7	CS22579	Ler-1	CS22618
Bor-1	CS22590	Lp2-2	CS22594
Bur-0	CS22656	Mr-0	CS22640
Cibc-17	CS22603	Nd-1	CS22619
Col-0	CS22625	Nfa-10	CS22599
Eden-2	CS22573	Ra-0	CS22632
Est-1	CS22629	Ren-1	CS22610
Fab-2	CS22576	Rmx-A02	CS22568
Fab-4	CS22577	RMX-A180	CS22569
Fei-0	CS22645	Se-0	CS22646
Ga-0	CS22634	Sorbo	CS22653
Got-22	CS22609	Sq-1	CS22600
Gu-0	CS22617	TSU-1	CS22641
Gy-0	CS22631	Uod-1	CS22612
Hr-10	CS22597	Uod-7	CS22613
Hr-5	CS22596	Wei-0	CS22622

2.1.2 *Arabidopsis* seed sterilization

Seeds were sterilized in either 0.5 mL or 1.5 mL tubes (Eppendorf, Hamburg, Germany), depending on the number. Seeds were first washed with 300-500 µl of 70% Ethanol in water (v/v) while being inverted regularly for 5 minutes. The Ethanol was removed and 300-500 µl of bleach (Sigma-Aldrich, New road, Dorset, SP8 4XT) in water 50% (v/v) (made in the lab) was added. After 5 minutes with regular inverting the bleach was removed and seeds were washed five times with sterile deionized water. Seeds were stored in the dark at 4°C in a 0.1% (w/v) agar solution for 2 days (stratification) prior to transfer to growth medium.

2.1.3 *Arabidopsis* growth on agar plates

After stratification, plants were transferred to 1% (w/v) agar plates containing a 1x (w/v) Murashige and Skoog (MS) basal salt micronutrient solution (1x MS salt and vitamin mix (Sigma-Aldrich M0529-1L)). This growth medium allowed for adjusting the supply of Nitrates while keeping all other nutrients at the same concentration. Medium was supplemented with sucrose (30 mM), $CaCl_2$ (1.5 mM), $MgSO_4$ (0.75 mM), KH_2PO_4 (0.625 mM) and NH_4NO_3 (concentration appropriate to the experiment). KOH was slowly added to adjust the pH to 5.7. Typically 120 µl 1 M KOH was added per 1 L of media. Media was autoclaved and when sufficiently cooled (<60°C) poured into square (12 cm x 12 cm) petri dishes, 50 mL per dish. When the experiment required rapid removal of the plants in bulk for harvesting tissue samples, a thin strip of autoclave-sterilised brown growth pouch paper (CYG™ Germination Pouch, West St. Paul, MN, United States) was placed on top of the agar 1 cm from the top of the dish.

Once the agar had solidified, seeds were transferred onto the plates using a 1000 µl aseptic pipette. For phenotypic analysis, up to 10 seeds were sown onto a plate. For bulk RNA extraction ~200 seeds were sown in a straight continuous line on the brown growth pouch paper.

The plates were sealed with microporous adhesive tape (Micropore Tape, 3M, St Paul, MN, USA). Plates were placed in opaque black polythene bags (Bagman of Cantley, Lingwood, Norfolk, UK), with only the top of the paper strip uncovered and placed vertically (seeds on top) in a temperature- and light-controlled plant incubator (MLR-351H, Sanyo, E&E Europe BV, Loughborough, UK), set to a 16 h light and 8 h darkness cycle at 22ºC, light intensity at 150 µmol m^{-2} s^{-1}.

2.2 Phenotype analysis

2.2.1 Imaging root architecture

Arabidopsis seedlings were grown on agar as section 2.1.3 and imaged to record root architecture using a flatbed scanner (HP Scanjet G2710 USB, Hewlett-Packard, Bracknell, UK) on a background of a plain black paper.

2.2.2 Image analysis of phenotypic data

ImageJ (Version 1.47, Rasband, 2013) was used to measure six key parameters of the root morphology: primary root length, average lateral root length, total lateral root length, total (primary + lateral) root length, number of lateral roots and lateral root density; the latter according to (De Smet et al., 2012) by dividing the number of lateral roots by the total root length.

2.3 Bacterial growth

2.3.1 *Ralstonia solanacearum*

Ralstonia solanacearum (GMI1000, kindly provided by Stephane Genin, INRA, Toulouse, France), was inoculated and grown on solidified bacto-agar glucose triphenyltetrazolium (BGT) media (bacto peptone (10 gL^{-1}), sucrose (5 gL^{-1}), casamino acids (1gL^{-1}), tetrazoliumchloride (0.0005% w/v) and agar (1 gL^{-1})) at 28°C for 48 h. Colonies that displayed a virulent (mucoid) phenotype were transferred to liquid BG culture media (similar to BGT media, but without agar or tetrazoliumchloride) and incubated overnight at 28°C with ~1 g shaking according to Boucher (1985). For inoculation of *Arabidopsis* plants an overnight liquid culture of *R. solanacearum* was diluted in sterile water to an OD 600 of 0.8.

2.3.2 *Sinorhizobium meliloti*

Sinorhizobium meliloti (RM1021, kindly provided by Giles Oldroyd, John Innes Centre, Norwich, UK) was inoculated and grown on solidified TY medium (bacto-tryptone (5 gL^{-1}), yeast extract (3 gL^{-1}), $CaCl_2$ (6 mM), bacto-agar (0.9 gL^{-1})) according to Journet (2006). Prior to inoculation on solid medium, bacteria were incubated for two days in liquid TY culture at 28°C with shaking at ~1 G. For inoculation of *Arabidopsis* plants an overnight liquid culture of *S. meliloti* was diluted in sterile water to an OD600 of 0.8.

2.4 Treatment of *Arabidopsis* plants

2.4.1 Inoculation of individual plants with *Sinorhizobium meliloti*

A thin layer (~400 µL) of diluted overnight culture *Sinorhizobium* solution was pipetted along the length of the roots of nine day old *Arabidopsis* GFP lines and ecotypes.

2.4.2 Time course treatments

Plants were grown for nine days on basal MS media plus 0.3 mM NH_4NO_3 (concentration chosen based on earlier work (Gifford et al., 2008)) as described earlier and subjected to various comparable treatments in section 2.1:

'Standard': The strip of plants was lifted from the agar with sterile tweezers, immersed in sterile deionized water and placed on a fresh basal MS plus 0.3 mM NH_4NO_3 plate.

'Nitrogen': The strip of plants was lifted from the agar with sterile tweezers then placed on a basal MS plus 5 mM NH_4NO_3 plate.

'*Sinorhizobium*': The strip of plants was lifted from the agar with sterile tweezers, immersed in a diluted solution of *S. meliloti* and placed on a fresh basal MS plus 0.3 mM NH_4NO_3 plate.

'*Ralstonia'*: The strip of plants was lifted from the agar with sterile tweezers, immersed in a diluted solution of *Ralstonia solanacearum* and placed on a fresh basal MS plus 0.3 mM NH_4NO_3 plate.

After treatment plants were placed back into the growth cabinet (section 2.1.3) from which they were taken. Roots were harvested at 0, 1, 2, 4, 6, 8, 10, 12, 14, 16, 20, 24, 36 and 48 hrs post treatment and either flash frozen in liquid N_2 for RNA extraction or used for FACS (section 2.5). The 0 hour time point was

sampled just prior to start of treatments, and thus represents plants that did not undergo any treatment.

2.5 Fluorescence Activated Cell Sorting (FACS) of *Arabidopsis*

FACS sorting was done with the help of Jesper Grønlund. Root samples of *Arabidopsis* lines containing cell specific GFP constructs were harvested by cutting roots of ~200 plants into a 70 μm cell strainer in a small petri dish containing protoplast-generating solution (5 ml protoplasting solution (600 mM mannitol, 2 mM MES hydrate, 10 mM KCl, 2 mM $CaCl_2$, 2 mM $MgCl_2$ and 0.1% (w/v) Bovine serum albumin, pH 5.7 with Tris HCl) with protoplast-generating enzymes, 0.015 gL^{-1} cellulase R-10 (Phytotechlab, 9245 Flint St. Overland Park, KS 66214-1739), 0.012 gL^{-1} cellulose RS (Sigma), 0.002 gL^{-1} macerozyme R-10 (Phytotechlab) and 0.0012 gL^{-1} pectinase (Phytotechlab)). (Grønlund et al., 2012). The petri dishes were placed on an orbital shaker set at ~2 G for 1 h. Cell strainers were removed and the supernatant transferred to a 50 mL tube (Falcon) and centrifuged for 5 mins at 9 G to pellet the protoplasts. The supernatant was removed and the protoplasts resuspended with a cut-tip 1000 μl pipette in 500 μl protoplast-generating solution with enzymes omitted. Finally, the suspension was filtered through a 40μm cell strainer to break up large clumps of protoplasts.

Protoplasts were sorted using a BD Influx cell sorter (BD Biosciences, Edmund Halley Road - Oxford Science Park, OX4 4DQ Oxford) fitted with a 100 μm nozzle, using FACS-Flow (BD Biosciences) as sheath fluid. Pressure was maintained at 20 psi (sheath) and 21-21.5 psi (sample), drop frequency was set to 39.5 kHZ, which yielded an event rate of <4000; these are optimal settings

on a BD influx cell sorter for the type of protoplasts described here (BD biosciences 2011). To optimise alignment of relevant lasers and detectors, Calibrite^{TM} Beads (BD Biosciences) suspended in FACS-Flow were used, and to optimise sort settings, BD^{TM} Accudrop Fluorescent Beads (BD Biosciences) suspended in FACS-Flow were used.

GFP positive protoplasts were identified using a 488 nm argon laser and plotting the output from the 580/30 bandpass filter (orange) vs. the 530/40 bandpass filter (green). GFP positive protoplasts were in the high 530/low 580 population, with non-GFP protoplasts in the low 530/low 580 population and dead/dying protoplasts and debris in the high 580 population (as Grønlund et al 2012). Sorted protoplasts were directly sorted into RNA extraction buffer (Qiagen RNA extraction kit, 27220 Turnberry Lane Suite 200. Valencia, CA 91355, USA) including β-mercaptoethanol 0.0145 molL^{-1} in tubes on dry ice, then samples stored at -80ºC. Processing of samples through cell sorting typically took between 10 and 20 minutes.

2.6 Nucleic acid techniques

RNA extraction, amplification and Microarray work were carried out by Jesper Grønlund.

2.6.1 RNA extraction and quality control

RNA was extracted using the Qiagen RNeasy mini kit (Qiagen) extraction protocol, followed by DNase treatment using the Qiagen DNase kit (Qiagen) as recommended by the manufacturer. The efficiency of DNase treatment was validated by Quantitative PCR (Power SyBR - AB bioscience) using the housekeeping gene Actin (Forward primer

TCAGATGCCCAGAAGTCTTGTTCC and Reverse primer CCGTACAGATCCTTCCTGATATCC). The quantity and quality of RNA was checked with Bioanalyzer 2100 RNA 6000 Pico Total RNA Kit (Agilent Technologies, 5301 Stevens Creek Blvd. Santa Clara, CA 95051, USA). RIN (RNA integrity number, gives an assessment of the degree of RNA degradation in the sample, with 1 being completely degraded RNA and 10 being intact RNA) threshold was set at 7.

2.6.2 RNA amplification

cDNA synthesis and amplification was performed with the Ovation® Pico WTA System (NuGEN, 9350 AC Leek, The Netherlands) according to manufacturer's guidelines but with half-reaction volumes, materials used were based on availability (depending on the quality of the cell sorting), but always within manufacturer-defined limits.

2.6.3 Microarray labeling and hybridization

Amplified cDNA was labeled using the NimbleGen (500 S Rosa Rd, Madison, WI 53719, USA) One-Color labeling kit, and hybridised using the GeneChip Hybridization kit on NimbleGen *Arabidopsis thaliana* 12 x 135k probe (3-4 probes per gene) microarrays designed for the full TAIR-10 annotation *Arabidopsis* genome (design OID 37507, see http://www.nimblegen.com/support/dna-microarray-support.html); all according to manufacturer's instructions. Hybridised arrays were incubated for 16-20 hrs (variation had no impact on signal strength) at 42°C in the NimbleGen hybridization system (NimbleGen, Roche). Post-hybridisation, microarrays were washed using the NimbleGen wash buffer kit and scanned on the MS200 Scanner (NimbleGen, Roche); all according to manufacturer's instructions.

2.7 Analysis of microarray data

Microarray data analysis was carried out by Ying Wang.

2.7.1 Quality control

Quality control of arrays was implemented by the Bioconductor package 'arrayQualityMetrics' (Kauffman et al., 2009). Outlier arrays were detected based on the between array distances (using the sum of distances as the quality metric), boxplots (using Kolmogorov-Smirnov statistic as the quality metric, Lilliefors, 1967) and MA-plots (using Hoeffding's statistic as the quality metric, Hoeffding, 1948).

2.7.2 Pre-processing

The Bioconductor 'oligo' package (version 1.32, Carvallo et al., 2010) was used to analyse the NimbleGen microarray data. The annotation package 'pd.120110.athal.mg.expr' was installed locally, which was built through pdInfoBuilder (Falcon et al., 2007) package. The RMA algorithm, which performs background subtraction, quantile normalisation and summarisation via median polish, was applied to the raw data of expression arrays to obtain the $\log_2$ normalized gene expression levels.

2.7.3 Differentially expressed genes

Differentially expressed (DE) genes within each time course were obtained using the BATS (Bayesian Analysis of Time Series, version July 2008) software (Angelini et al., 2008). BATS allows for compensating for missing data, non-uniform time intervals and a limited number of repeats. The BATS input file for each time course contained rescaled log2 gene expression values such that the vector of log2 expression values of each gene had a mean of zero and a variance

equal to 1. Genes were considered to be DE if their Bayesian Factor (BF) in the BATS output file is below a significance threshold, which was determined by the histogram of $\log_{10}$ of all Bayesian Factors and the regression plots of gene expression levels from BATS.

DE genes between treatments (standard vs high N, standard vs *Sinorhizobium*, high N vs *Sinorhizobia*) were obtained by the software GP2S (Version December 2012, Stegle et al., 2010). In the GP2S input file, the log2 expression levels of each gene for the two time courses are rescaled such that their mean is zero and their variance is one. GP2S assigned each gene a BF which equals the difference between the likelihood of the gene's expression levels in two treatments being sampled from different Gaussian processes and that from the same Gaussian process. According to the interpretation of BFs given by Jeffreys (1961) genes with BFs above five are at least substantially differentially expressed between treatments.

2.8 Clustering of differentially expressed genes

Clustering of data was carried out by Ying Wang

Hierarchical clustering of the differentially expressed genes was performed using SplineCluster (version 2/2/5, Heard et al., 2006). The mean expression level of biological replicates of a DE gene at each time point in a time course was used as input for SplineCluster. A reallocation function was implemented to reallocate outliers of each cluster into other more appropriate clusters at each agglomerative step. A prior precision value was finally determined after trying different values

and comparing their effects on clusters. Number of clusters was decided by determining the optimal number of residuals.

2.9 Gene Ontology Analysis

GOstats (version 2.34, Gentleman et al., 2005) was used to determine which GO (Gene Ontology) categories were statistically overrepresented for a group of DE genes. A hypergeometric test was implemented to identify the overrepresented GO categories for each of Biological Process, Molecular Function and Cell Component, respectively. Data was corrected for multiple comparisons using Benjamini-Hochberg correction (Benjamini and Hochberg, 1995). The whole annotated TAIR10 *Arabidopsis thaliana* genome was used as the reference set.

2.10 Gene Regulatory Network inference

Creation of the network models was carried out by Ying Wang.

The Bioconductor package GRENITS (version 1.2, Morrissey, 2013) was used for gene regulatory network inference, using a linear model with default parameters and link probability threshold above 0.4. GRENITS uses dynamic Bayesian networks and Gibbs variable selection. In the network, nodes represent genes and edges represent putative regulatory interactions between genes. The mean expression levels of biological replicates of a DE gene at each selected time point in a time course was used as input. GRENITS gives a Bayesian probability score of each link between any two genes. A link probability threshold was chosen based on the confidence required for assigning links. Then a link in the gene regulatory network exists if its posterior probability is greater than or equal to the link probability threshold. NIACS (Network interference

analysis and correction software, Version 1.0, Wang et al., 2014) was used to correct for regulator interference, which occurs when two or more regulators with similar dynamics mutually suppress both the probability of regulating a target and the associated link strength; for instance interference between two identical strong regulators reduces link probabilities by about 50%.

Chapter 3

Phenotypic response of *Arabidopsis thaliana* roots in contact with *Sinorhizobium meliloti*

3.1 Motivation

Profiling and analysing the transcriptional response to potentially symbiotic bacteria makes it possible to understand the consequential phenotypic response. The aim of this chapter is to investigate if there is a specific phenotypic response in *Arabidopsis* roots to *S. meliloti*. *Arabidopsis* root system architecture is a result of a combination of lateral root initiation, emergence, morphogenesis and growth (Malamy et al., 2005, Benfey et al., 2007). The root phenotype is essential to the way plants exploit the limited available resources in the soil (Hodge et al., 1999, Robinson et al., 1999). Most simply, phenotypes can be reduced to one-dimensional properties: root length, number of lateral roots, concentrations of metabolites in the roots. However, the field of phenotype analysis is evolving towards a more comprehensive approach, with multidimensional models (Chew et al., 2014) that are a combination of morphological and metabolic readouts associated with a combination of alleles (Gifford et al., 2013). For a more in-depth review of phenotyping in systems biology, see (Benfey and Mitchell-Olds, 2008).

3.2 The root architecture response of *Arabidopsis thaliana* to *Sinorhizobium meliloti*

The first analytical step in establishing whether *Arabidopsis* responds phenotypically to *Sinorhizobium* is to inoculate growing *Arabidopsis* roots, then assess any changes in root architecture. Of particular interest are changes in the lateral roots, as root nodules in legumes are morphologically similar to lateral root organs. In this experiment, plants were treated to determine how *Arabidopsis* responds to *S. meliloti* as well as gain an understanding of what causes the phenotype.

3.2.1 Experimental design

Arabidopsis Col-0 seedlings were planted on agar plates supplemented with MS growth medium (as methods). After six days of growth, plants were inoculated by pipetting the inoculum along the length of the root. Inoculation was performed with five treatments. Plants were treated with either i) live *S. meliloti* culture (a solution of cultured *S. meliloti* (10^{-3} OD 600, identical to that used in the transcriptomics experiments), ii) the supernatant from centrifuged *Sinorhizobium* culture (obtained by centrifuging the cells in a microcentrifuge and decanting the eluate). iii) a concentration range of Nod-factors (kindly supplied by Hugues Driguez, CERMAV-CNRS, Grenoble, France) (10^{-5}, 10^{-6}, 10^{-7} M). The concentrations were similar (10^{-6} and 10^{-7} M) or slightly higher (10^{-5} M) to what is traditionally used in literature when compatible legume plants are treated with Nod factor (Journet et al., 1994; Macchiavelli et al., 2004). Water was pipetted onto roots as a control. Seedlings were grown on agar plates (see 2.1.3) containing 5 mM KNO_3 as N-source. Measurements were taken after six

days to balance detection of significant phenotypes that are easier at later time points, with visualisation difficulties that can be caused at later time points by rhizobia colony growth.

The treatments with Nod factor are designed to give an insight to whether any observed phenotype can be directly attributable to Nod factors (that might be exuded by the *Sinorhizobium*). The supernatant treatment tests if any observed effect of the *Sinorhizobium* treatment is related to a non-Nod factor exuded secondary metabolite of *Sinorhizobium*.

For every plant, five parameters were recorded by measuring images of the roots in imageJ (Schneider et al., 2012). Primary root length, total lateral root length, average lateral root length, number of lateral roots and lateral root density (LRD) (defined as the amount of lateral roots divided by the primary root length) were recorded for $\geq$6 plants in every treatment grown on $\geq$2 separate plates. Differences between treatments were assessed by performing an unpaired t.test in R comparing each parameter and treatment to the control. Placement of agar plates in the growth cabinet was chosen to be as least influential as possible and randomized for every experiment. Each treatment was carried out on a different agar plate, with ~8 plants per plate, and two biological replicates per experiment.

3.2.2 Results - *Sinorhizobium* inoculated plants have shorter lateral roots

Significant differences were observed in plants treated with *S. meliloti* compared to the root standard, but not in the Nod factor or supernatant treatments. *S. meliloti* inoculated plants had slightly longer primary roots (6.4 cm vs 6.9 cm; $P = 0.0033$), shorter total lateral root length (10.5 cm vs 7.4 cm; $P = 0.0098$) and a lower average lateral root length (8.6 cm vs 5.4 cm, $P = 8.2 \times 10^{-6}$). Lateral root

number and lateral root density (LRD) were not significantly different in any treatment (Figure 3.1 and 3.2).

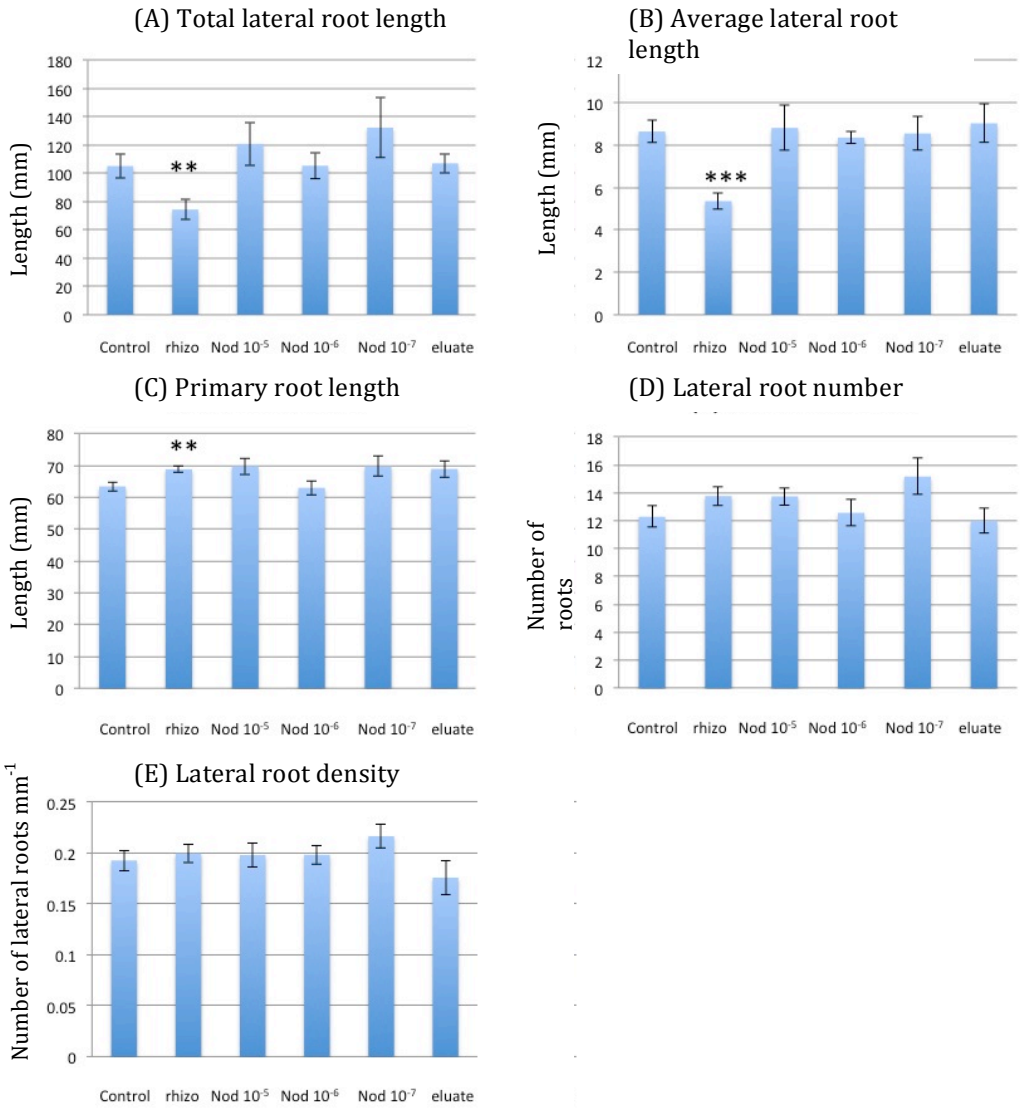

Figure 3.1 Total lateral root length (A), average lateral root length (B), primary root length (C), lateral root number (D) and lateral root density (E), for plants treated with either standard (water), *Sinorhizobium* OD 600, 10^{-5} to 10^{-7} M Nod factor, and bacterial eluate. Plants were grown for six days prior to treatment and measurements were taken 6 days post treatment. Asterisks represent significant results of t.test against the standard treatment, with p values: **=*P*<0.01, *=*P*<0.005. Error bars represent the standard error of the mean. Data was obtained from 12 plants per treatment, with 6 plants per plate.**

a

b

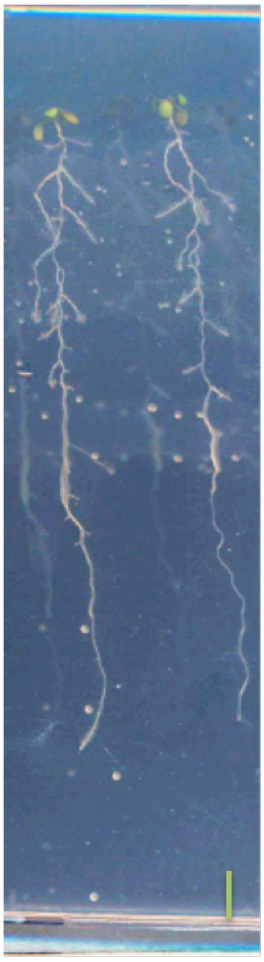

Figure 3.2 Control (standard inoculated) (a) and *Sinorhizobium* inoculated (b) *Arabidopsis* seedlings, six days post inoculation. The inoculated plants show a reduced lateral root length phenotype compared to the control. Scale bar = 1 cm.

3.3 Developmental response to *Sinorhizobium* inoculation

The observed changes in *Arabidopsis* root architecture (Figure 3.1 and 3.2) show that there is a morphological response to inoculation with a presumed incompatible bacterial symbiont (*Sinorhizobium meliloti*). However, this is one

measure of the phenotypic response. Therefore we must also consider developmental changes at the cell type level. It is necessary to test if the macroscopic change in root architecture that we observe (i.e. the change in lateral root phenotype) is reflected at the microscopic level as a qualitative or quantitative difference in the number of lateral root primordia. Four developmental stages were defined (Figure 3.3), based on work by previous groups (Malamy and Benfey, 1997, Gifford et al., 2008) and referred to as initiating, growing, emerging and fully emerged. In the previous section only fully emerged lateral roots were counted, the other stages being too small to be discerned from unaided visual inspection.

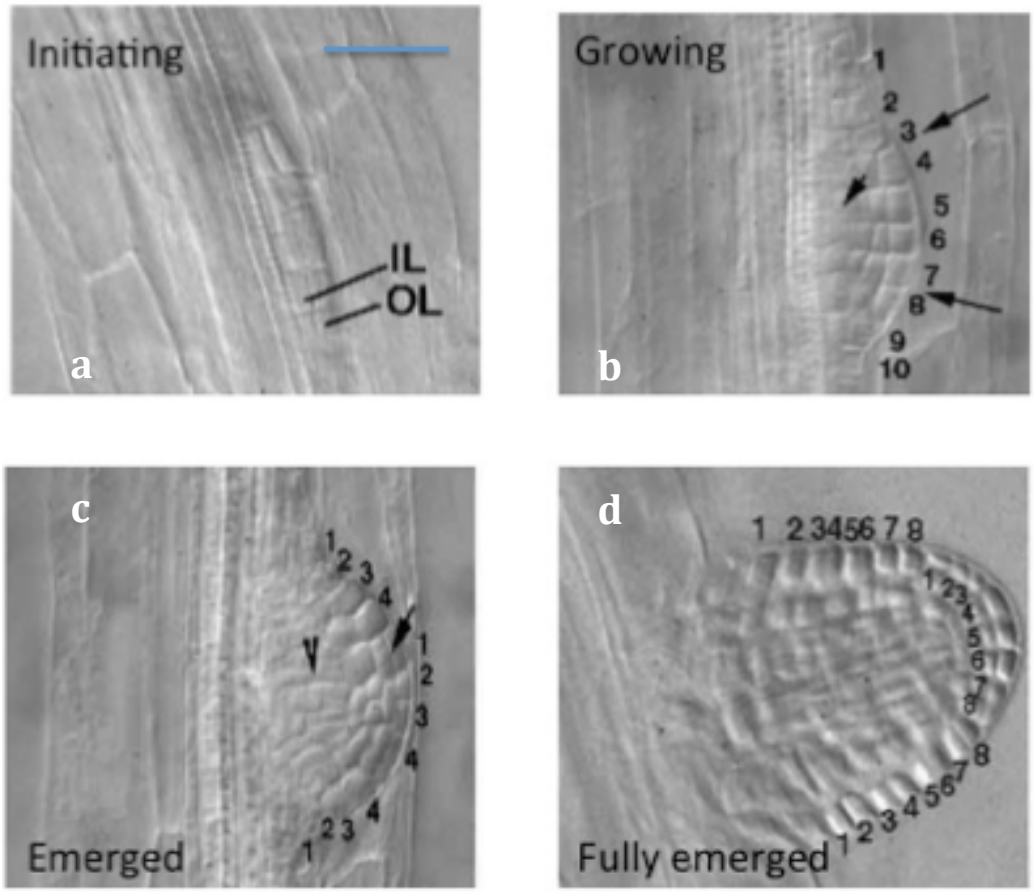

Figure 3.3 Four overall stages of lateral root development as defined after Malamy et al. (1997). (a) initiating lateral root primordium, marked by anticlinal and periclinal cell divisions. The LR primordium is divided into an inner layer (IL) and an outer layer (OL) (b) further periclinal divisions lead to initiation of a lateral root. Arrows indicate anticlinal cell divisions. The short arrow indicates the region in which cells of the IL2 undergo expansion and division, distorting the shape of IL1 and OL2. Cells in the outermost layer are numbered to indicate the constant organization at this stage. (c) A periclinal division in the OL creates a new tier of cells (arrow). Further anticlinal divisions lead to emergence of the lateral root out of the primary root. (d) Fully emerged lateral root. Cell numbering indicates that there are now more cells in the layer near the root tip, consistent with the presence of an active root apical meristem. Scale bar: 50 µm

3.3.1 Experimental design

Plants were grown as previously described on MS media for 6 days, then inoculated with *Sinorhizobium meliloti* solution or water as standard inoculation. Lateral root primordia were scored as the four stages (Figure 3.3) counted at 1, 3, 5, and 7 days after treatment. For each day/treatment combination, eight roots

coming from two plates (eight plants per plate) were scored under a light microscope. The destructive nature of the sampling did not allow for tracking a single root for multiple consecutive days, thus different roots were sampled in every experiment. Differences were assessed by performing an unpaired t-test comparing treated plants to the standard group. No significant difference in the number of emerging lateral roots at any stage of lateral root development was observed (Figure 3.4). This suggests that the previously described phenotypic change in LR length was due to effects on the LR elongation rate, rather than LR initiation.

3.3.2 Results

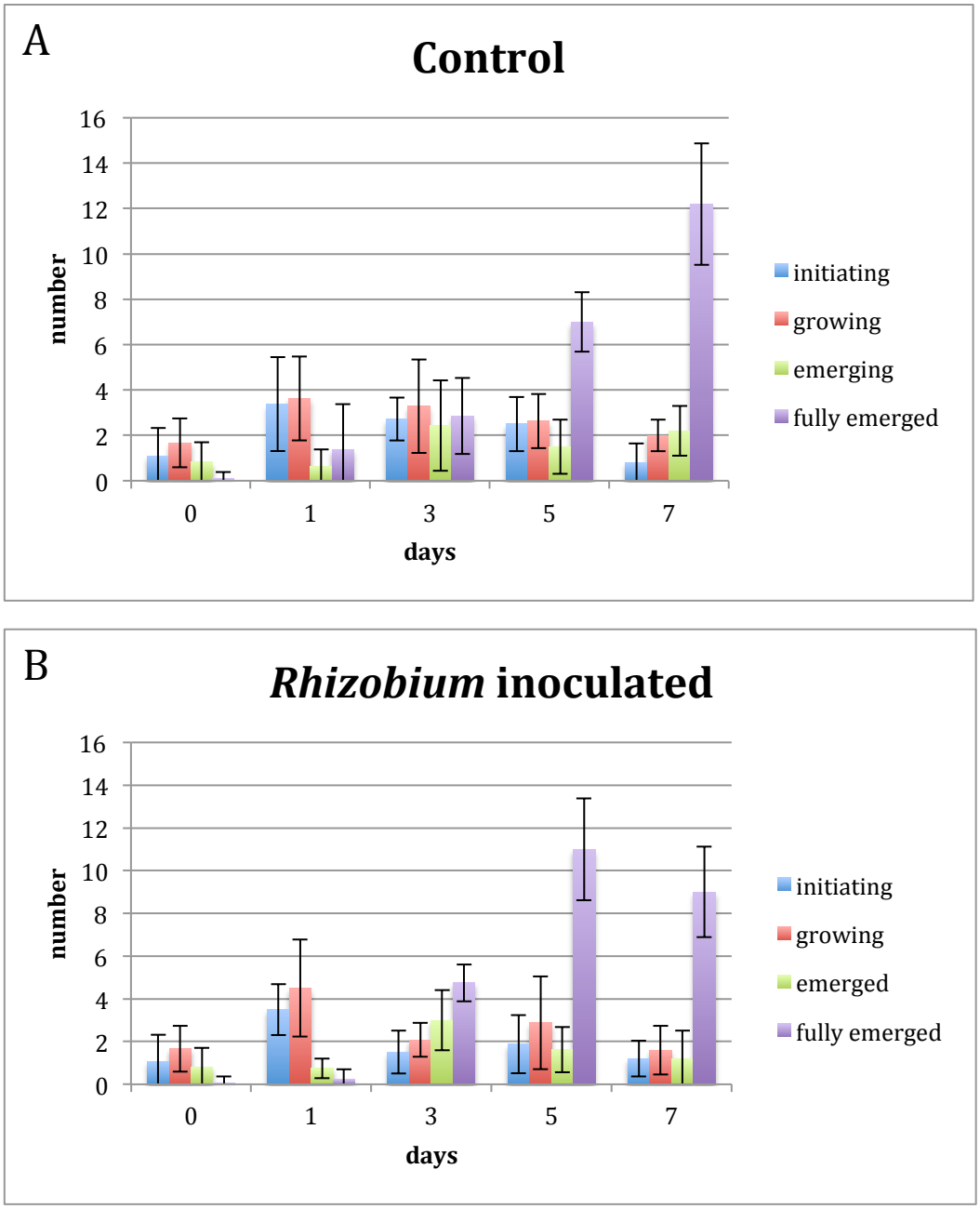

Figure 3.4 Number of lateral root primordia per day for control (A) and *Sinorhizobium* inoculated (B) plants. Error bars represent the standard error of the mean. Plants were grown for six days prior to treatment and measurements were taken up to seven days post treatment. For each day/treatment combination, eight root samples from two plates were assessed.

3.4 Natural variance in the response to *Sinorhizobium*

Probing naturally occurring genetic variation can help in elucidating the genetic nature of phenotypic responses to external stimuli (Preston et al., 2004, Gifford

et al., 2013). A set of 34 *Arabidopsis* accessions were screened for a differential response to inoculation with *S. meliloti.*

If the root response to bacteria (Figure 3.2) is correlated and under control of the same limited set of regulatory genes, natural variants should exhibit similar changes in root architecture in response to inoculation. If the response is modular, i.e. if traits are being controlled independently with respect to each other, the natural variants should fragment and exhibit a diverse range of phenotypical changes in response to treatment with *S. meliloti.* Initially the experiment was performed on 34 accessions (Table 2.1) to evaluate the potential diversity among accessions. Identifying a differential response in natural variants, opens up the possibility of further work, linking the difference in phenotype through genome wide association mapping to gene function.

3.4.1 Experimental design

A group of 34 *Arabidopsis* accessions were inoculated with either a *Sinorhizobium* culture or with water as a standard treatment as in previous experiments. For at least three seedlings in each accession the length of the primary and lateral roots and lateral root number were all measured in imageJ (Schneider et al., 2012). From this data, 6 parameters were defined: primary root length, average lateral root length, total lateral root length, total combined root length, number of lateral roots and lateral root density (defined as the amount of lateral roots per unit of primary root length). A principal components analysis and clustering of phenotype traits were carried out in Matlab (Attaway, 2013). The number of clusters was determined by calculating silhouette plots for different cluster sizes and groups were hierarchically clustered using average linkage and Euclidian distance, as described by Gifford et al. (2013).

3.4.2 Results

Accessions vary in their response to inoculation with *S. meliloti* (Figure 3.5 and 3.6). Differences in primary root length and lateral root length were assessed by an unpaired t.test and displayed on the results (Figure 3.5 and 3.6). While a reduction in lateral root length, compared to standard, as described in section 3.2 (Figure 3.2) is common, there are accessions where there is negligible difference compared to standard, such as *Gu-0* and *Wei-0* (Figure 3.6). These are accessions where the number of lateral roots was very low (1-2) in the standard treatment, potentially making it harder to observe any significant change in them. The most dramatic reduction in lateral root length was observed in *Ler-1*, which had exceptionally long lateral roots in the standard treatment, which completely disappeared when treated with *S. meliloti*. For all accessions the overall primary root response appears to either remain unchanged or significantly drop in response to *S. meliloti* treatment (see Figure 3.5 and 3.6 and Table 3.1 & 3.2).

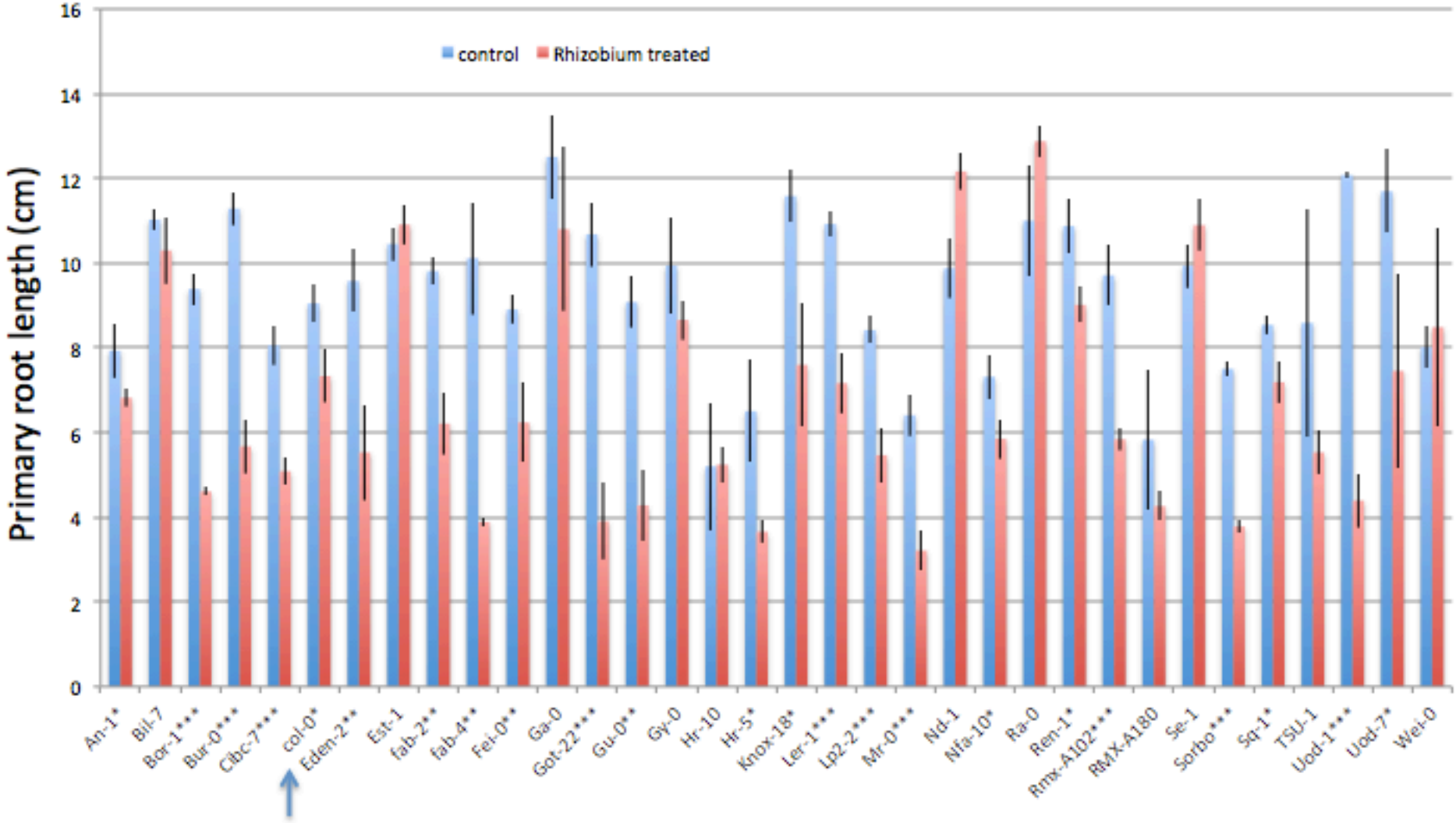
control
Rhizobium treated
Primary root length (cm)
16
14
12
10
8
6
4
2
0
An-1*
Bil-7
Bor-1***
Bur-0***
Cibc-7***
col-0*
Eden-2**
Est-1
fab-2**
fab-4**
Fei-0**
Ga-0
Got-22***
Gu-0**
Gy-0
Hr-10
Hr-5*
Knox-18*
Ler-1***
Lp2-2***
Mr-0***
Nd-1
Nfa-10*
Ra-0
Ren-1*
Rmx-A102***
RMX-A180
Se-1
Sorbo***
Sq-1*
TSU-1
Uod-1***
Uod-7*
Wei-0

Figure 3.5 (previous page) Primary root lengths of control (blue) and Sinorhizobium inoculation treatment (red) seedlings. The plot shows the overall response of a reduction in primary root length for all accessions, but illustrates the variation in the extent of the reduction. Accessions are plotted on the X-axis. Error bars represent the standard error of the mean. *Col-0* ecotype is indicated with an arrow. For each ecotype and treatment, measurements were taken from at least three viable seedlings. Stars indicate statistical significance: * *P*-value < 0.05; ** *P*-value < 0.01; * *P*-value < 0.001. Plants were grown for six days before treatment, and measurements were taken six days after treatment.**

Figure 3.6 (next page) Comparison of LR lengths between control (blue) and *Sinorhizobium* treatment (red). The plot shows the overall response of a reduction in LR length and illustrates the variation in the extent of the reduction. Accessions are plotted on the X-axis. Error bars represent the standard error of the mean. *Col-0* ecotype is indicated with an arrow. For each ecotype and treatment, measurements were taken from at least three viable seedlings. Stars indicate statistical significance: * *P*-value < 0.05; ** *P*-value < 0.01; * *P*-value < 0.001. Plants were grown for six days before treatment, and measurements were taken six days after treatment.**

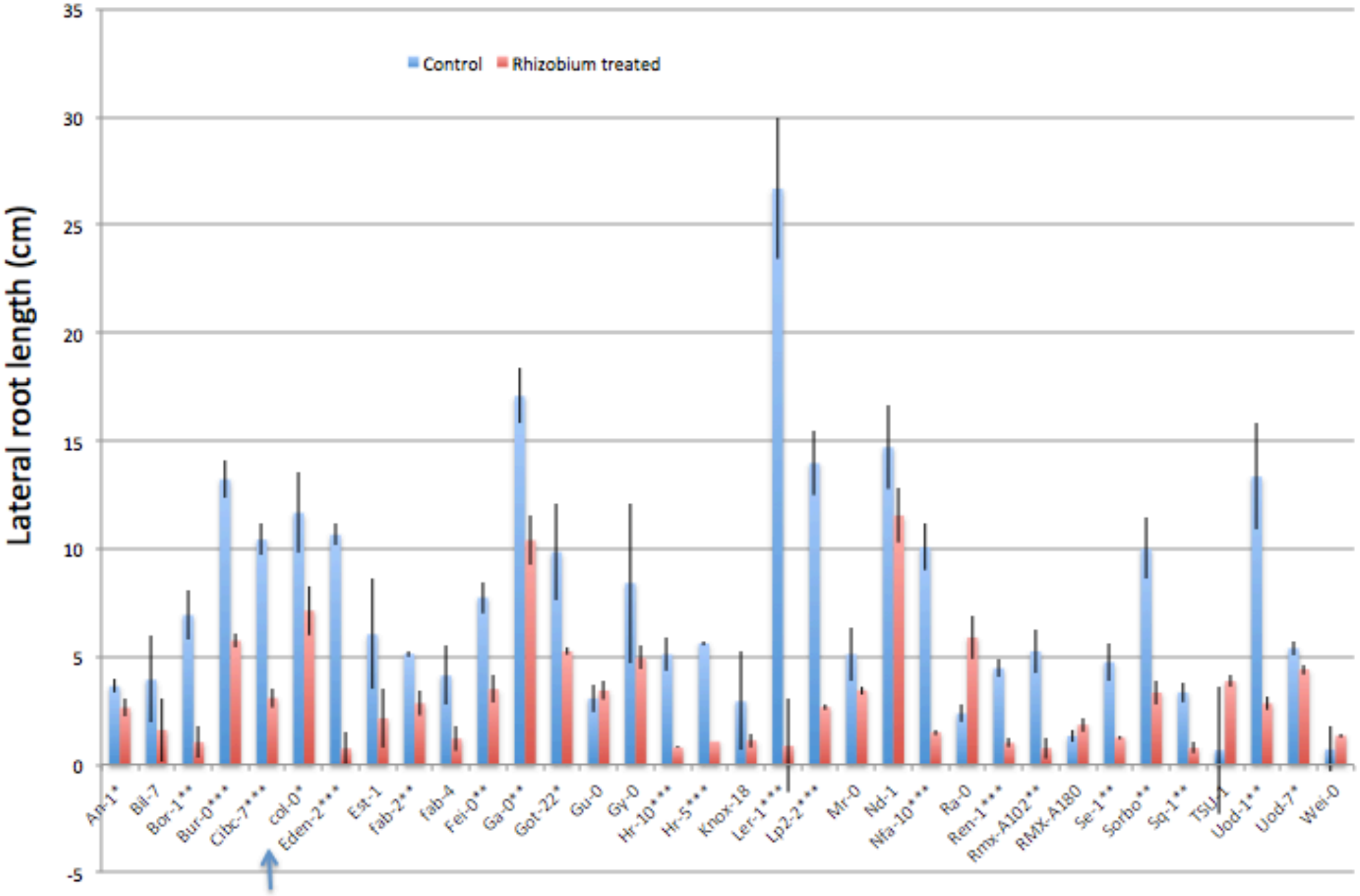
Lateral root length (cm)
Control
Rhizobium treated
35
30
25
20
15
10
5
0
-5
An-1*
Bil-7
Bor-1**
Bur-0***
Cibc-7***
col-0*
Eden-2***
Est-1
fab-2**
fab-4
Fei-0**
Ga-0**
Got-22*
Gu-0
Gy-0
Hr-10***
Hr-5***
Knox-18
Ler-1***
Lp2-2***
Mr-0
Nd-1
Nfa-10***
Ra-0
Ren-1***
Rmx-A102**
RMX-A180
Se-1**
Sorbo**
Sq-1**
TSU-1
Uod-1**
Uod-7*
Wei-0

Table 3.1 Additional measurements for standard inoculated *Arabidopsis* accessions. All lengths measured are in cm. For each ecotype and treatment, measurements were taken from at least three viable seedlings. Plants were grown for 6 days prior to treatment, and measurements taken 6 days after treatment.

	LR number	Average LR length	Total root length	LR density (number of roots/cm of primary root)
An-1	4.0	0.9	11.6	0.5
Bil-7	6.7	0.6	15.0	0.6
Bor-1	6.0	1.2	16.3	0.6
Bur-0	8.0	1.7	24.5	0.7
Cibc-17	6.0	1.7	18.5	0.7
Col-0	9.0	1.3	20.7	1.0
Eden-2	6.3	1.7	20.2	0.7
Est-1	6.7	1.7	16.5	0.6
Fab-2	6.3	0.8	14.9	0.6
Fab-4	5.3	0.8	14.2	0.5
Fei-0	4.7	1.7	16.6	0.5
Ga-0	14.0	1.2	29.6	1.1
Got-22	9.0	1.1	20.5	0.8
Gu-0	5.0	0.6	12.1	0.6
Gy-0	9.0	0.9	18.3	0.9
Hr-10	3.3	1.5	10.3	0.6
Hr-5	3.0	1.9	12.1	0.5
Knox-18	5.0	0.6	14.5	0.4
Ler-1	14.0	1.9	37.6	1.3
Lp2-2	11.0	1.3	22.4	1.3
Mr-0	2.3	2.2	11.5	0.4
Nd-1	11.0	1.3	24.6	1.1
Nfa-10	6.3	1.6	17.4	0.9
Ra-0	4.0	0.6	13.4	0.4
Ren-1	7.7	0.6	15.3	0.7
Rmx-A02	5.7	0.9	15.0	0.6
RMX-A180	2.0	0.7	7.2	0.3
Se-0	5.7	0.8	14.7	0.6
Sorbo	8.0	1.3	17.5	1.1
Sq-1	2.7	1.3	11.9	0.3
TSU-1	1.7	0.4	9.3	0.2
Uod-1	11.3	1.2	25.4	0.9
Uod-7	5.0	1.1	17.1	0.4
Wei-0	1.5	0.7	8.7	0.2

Table 3.2 Additional measurements for *Sinorhizobium* inoculated *Arabidopsis* accessions, All distances measured are in cm. For each ecotype and treatment, measurements were taken from at least three viable seedlings. Plants were grown for six days before treatment, and measurements were taken six days after treatment

	LR number	Average LR length	Total root length	LR density (number of roots/cm of primary root)
An-1	3.7	0.7	9.5	0.5
Bil-7	4.3	0.4	11.9	0.4
Bor-1	2.0	0.5	5.6	0.4
Bur-0	11.0	0.5	11.4	1.9
Cibc-17	6.3	0.5	8.2	1.2
Col-0	9.7	1.2	14.5	1.3
Eden-2	2.3	0.3	6.3	0.4
Est-1	3.3	0.6	13.1	0.3
Fab-2	4.7	0.6	9.0	0.8
Fab-4	3.0	0.4	5.1	0.8
Fei-0	3.3	1.0	9.7	0.5
Ga-0	11.5	0.9	21.2	1.1
Got-22	4.7	1.1	9.2	1.2
Gu-0	7.0	0.5	7.7	1.6
Gy-0	7.3	0.7	13.6	0.8
Hr-10	1.3	0.6	6.0	0.3
Hr-5	3.7	0.3	4.7	1.0
Knox-18	3.3	0.3	8.7	0.4
Ler-1	2.0	0.4	8.0	0.3
Lp2-2	8.3	0.3	8.1	1.5
Mr-0	3.7	0.9	6.7	1.1
Nd-1	11.3	1.0	23.7	0.9
Nfa-10	4.3	0.3	7.4	0.7
Ra-0	8.0	0.7	18.8	0.6
Ren-1	3.0	0.3	10.0	0.3
Rmx-A02	2.7	0.3	6.6	0.5
RMX-A180	3.7	0.5	6.1	0.9
Se-0	1.7	0.8	12.2	0.2
Sorbo	6.3	0.5	7.1	1.7
Sq-1	1.3	0.6	8.0	0.2
TSU-1	5.0	0.8	9.4	0.9
Uod-1	5.3	0.5	7.2	1.2
Uod-7	4.7	0.9	11.9	0.6
Wei-0	7.3	1.0	15.8	0.2

3.4.2.1 Principal component analysis shows importance of all root trait parameters

To gain an insight into which component best explains the difference between treatments, principal component analysis (PCA) was performed on the difference in trait value (measurements) between the control and the treated plants. PCA is a statistical method that uses an orthogonal transformation to convert a set of putatively correlated variables into a set of values of linearly uncorrelated variables denoted as principal components. As the data contains data in multiple dimensions, measurements were scaled before the PCA was carried out. The first three principal components accounted for 96% of the observed variance in the data (Table 3.3), as found elsewhere (Gifford et al., 2013). By plotting the accessions as well as vectors representing the original 6 parameters along the axis of the first two principal components we can carry out a visual appraisal of parameters that are close together (Figure 3.7).

Table 3.3 Percentages of variance contained within each principal component and cumulative percentage explaining the variation in overal root morphology after treatment with *Sinorhizobium meliloti*. Plants were grown for 6 days before treatment, with measurements taken 6 days after treatment.

	PC1	PC2	PC3	PC4	PC5	PC6
Variance explained	0.57376	0.26724	0.12465	0.02805	0.00627	0
Cumulative variance explained	0.57376	0.84101	0.96566	0.99372	1	1

An analysis of the coefficients of the first three principal components can inform our interpretation of the root architecture phenotypes. The first PC accounts for 57% of the variation (Table 3.3) and is primarily defined by total root and lateral root length, these parameters are by definition likely correlated and in this experiment they are the largest component of change (Table 3.4). However, the

difference between the sizes of the coefficients is small, indicating that all of them can potentially be important. This trend suggests that the greatest variation among the differences of traits were correlated changes, i.e. overall size differences.

The second PC is mainly defined by primary root length and lateral root density (Table 3.4), where one is inversely correlated with the other, i.e. a growth in the primary root is predicted to lower the lateral root density and vice versa, since lateral root number does not appear to be a strong component. The second PC also shows an inverse correlation between primary root length and average lateral root length.

Table 3.4 Coefficients of traits corresponding to principal components explaining variation in root morphology after treatment with *Sinorhizobium meliloti*. Plants were grown for 6 days before treatment, with measurements taken 6 days after treatment.

	PC1	PC2	PC3
PR length	0.249981714	-0.581763775	-0.529103116
LR number	0.457341396	0.313688596	-0.363086461
Average LR length	0.370246193	-0.211873181	0.743953334
Total LR length	0.519064344	0.033047001	0.152159341
Total root length	0.517396833	-0.189686417	-0.072708874
LR density	0.232676752	0.693676501	-0.079451272

From the plot (Figure 3.7) it appears that average lateral root length and total root length have similar coefficients and thus one of them might be superfluous.

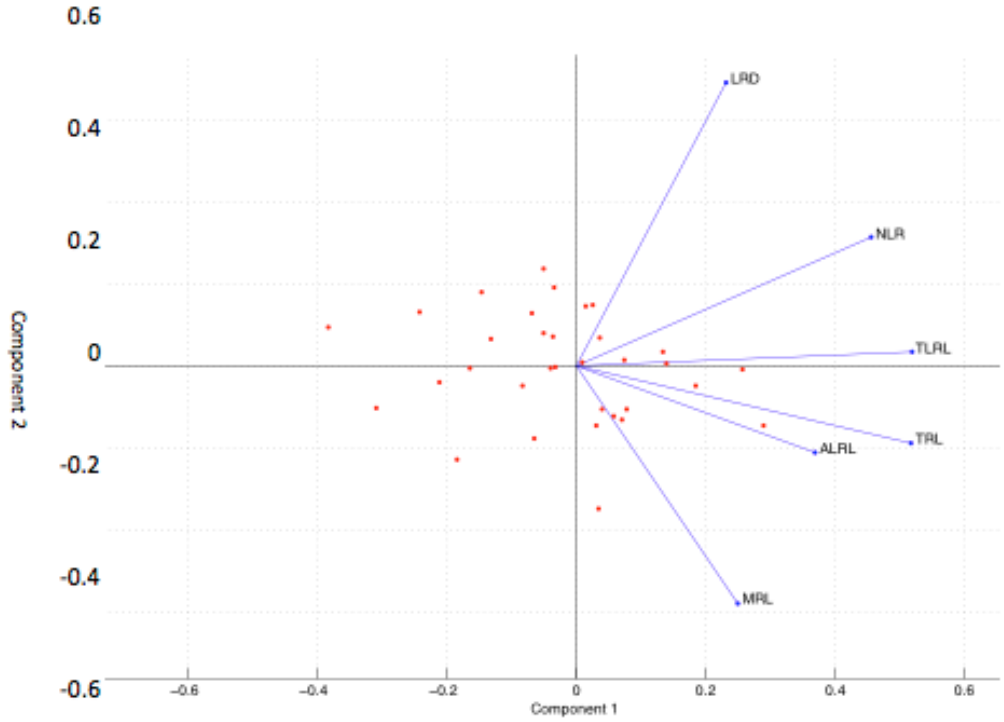

Figure 3.7 2D plot of the first 2 principal component vectors (blue lines) and their relation to the observed change in accessions (red dots). PC1 and PC2 explain 85% of the variance in the data. LRD = lateral root density; NLR = number of lateral roots; TLRL = total lateral root length; TRL = total root length; ALRL = average lateral root length; MRL = Primary root length.

3.4.2.2 Hierarchical clustering of phenotypes gives an indication of the complexity of the response of Arabidopsis roots to Sinorhizobium.

To understand how the individual root trait parameters interact to form overall root system architecture, and how this varies, the dataset created on 34 accessions was clustered (hierarchical clustering, average linkage, Pearson's correlation coefficient, cluster number determined by residual plot) based on the seven root phenotype traits determined earlier, for *S. meliloti* treated as well as standard-treated plants, similar to Gifford et al. (2012) (Figure 3.8). Thus 2 sets of phenotype clusters were obtained, one for each treatment.

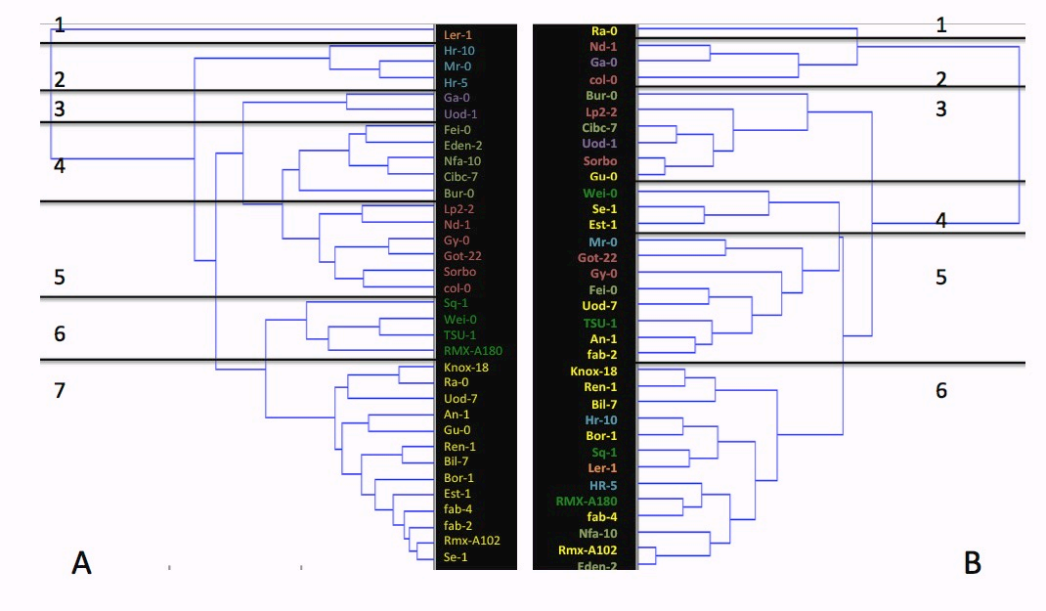

Figure 3.8 Clustering of the *Arabidopsis* accessions for standard (A) and *Sinorhizobium* inoculated plants (B). Seven clusters were determined from the phenotypes in the standard and assigned colour-coded accession name so their relative position in A vs B might be tracked when comparing *Sinorhizobium*-treated and standard-treated cluster assignments. Plants were grown for 6 days before treatment, with measurements taken 6 days after treatment.

In both *S. meliloti* treated and standard treated clusters there was a clear separation of clusters, showing how root parameters might be conserved to form common root architecture types. Most interesting was the reorganisation of the tree topology of the two treatments, as is clear from the shuffling of the positions of the accessions in the clusters from the standard (Figure 3.8A) when they are mapped onto the *S. meliloti* treatment tree (Figure 3.8B). This indicates that sharing a root architecture in one condition does not predict a shared root architecture in another. For example (Figure 3.9 A-D), *Wei-0* and *Est-1* are in separate clusters in the untreated group, the former having few lateral roots, while the latter has many. When treated with *S. meliloti*, both have a similar number of short lateral roots, leading to them clustering together. Also, *Nd-1* clusters together with *Lp2-2* under standard conditions but separately under *S. meliloti* treatment conditions (Figure 3.9 E-F). Both accessions are characterised

by having intermediate to high lateral and primary root lengths in the standard treatment. When treated with *S. meliloti* however, *Lp2-2* has a short primary and lateral root phenotype, whereas in *Nd-1* root lateral root length does not vary compared to standard.

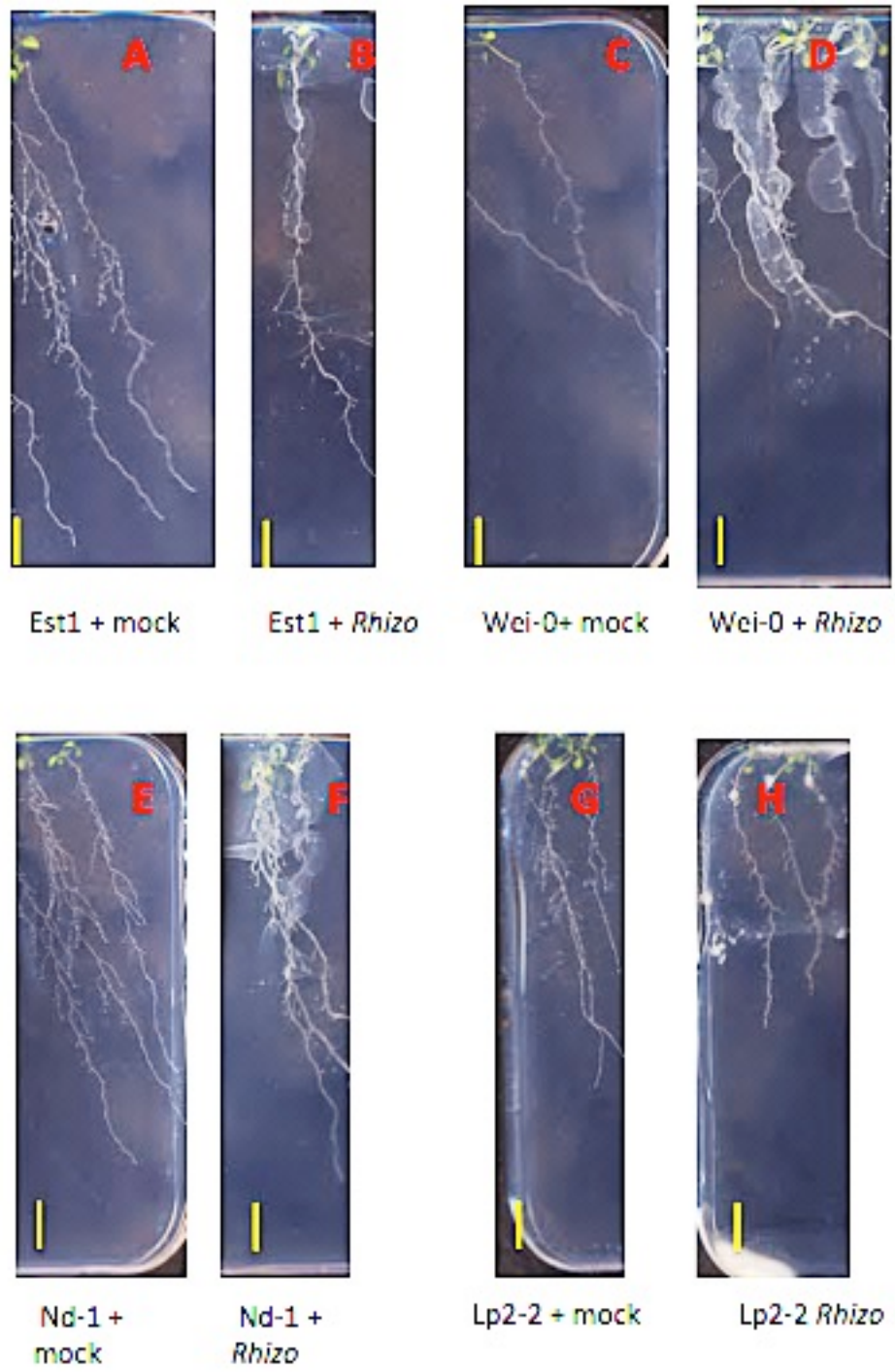

Figure 3.9 Images of different *Arabidopsis* accessions standard and *S. meliloti* treated. Yellow bars represent 1 cm. *Est1* (A-B) and *Wei-0* (C-D) have different phenotypes in the standard treatment, but similar phenotypes when treated with *S. meliloti*. *Nd-1* (E-F) and *Lp2-2* (G-H) have similar phenotypes in the standard treatment but different phenotypes when treated with *S. meliloti*. Plants were grown for 6 days before treatment, with measurements taken 6 days after treatment.

3.5 Discussion

These results suggest that *Sinorhizobium* inoculation specifically represses lateral root elongation (Figure 3.2), but not initiation (Figure 3.4) in *Arabidopsis*. It is not clear whether the LR root shortening phenotype (Figure 3.1 and 3.2) is due to an active interaction between the bacteria and the plant, or due to alterations in the environment mediated by the bacteria, thus acting as indirect effects. Here are a number of hypotheses that can be tested and tentatively discounted: (i) the lack of effect when plants were treated with bacterial culture supernatant suggests that it is not the effect of an exuded molecule in the bacterial solution when the bacteria are grown. (ii) The similarity of lateral root length between low N-grown and *S. meliloti*-inoculated seedlings (Figure 3.2 and 3.10) could suggest that the bacteria is utilising nutrients in the agar plate, adjacent to the plant roots, and thus depleting those nutrients adjacent to the roots. However, *S. meliloti* elicits a very specific effect on lateral root outgrowth, whereas low N (similar to other nutrient depletion) has the strongest effect on primary root length and also on shoot size and chlorophyll content (greening), something not observed with *S. meliloti* inoculation. In addition, the nutrient uptake of *S. meliloti* cultures would be minor compared to the effect of multiple days of growth on low N. However, it is possible that other changes in the plate environment as a result of bacterial inoculation, such as possible changes in pH of the growth medium cause the LR phenotype.

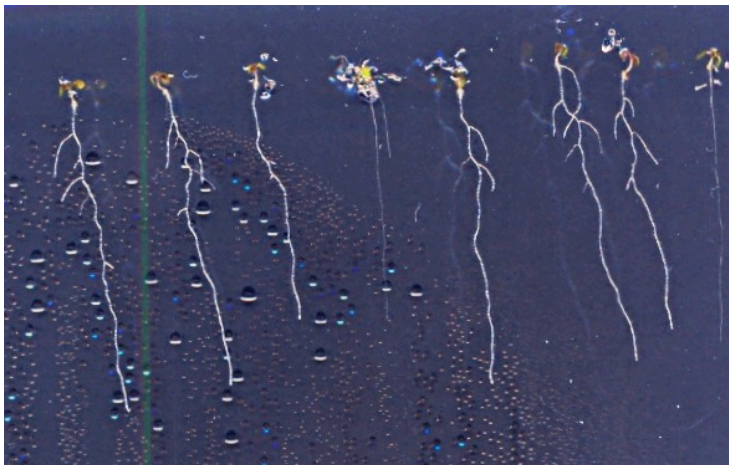

Figure 3.10 12 day old *Arabidopsis* seedlings grown under limiting N (0.3mM KNO_3) conditions. Picture from Gifford (unpublished)

It is important to understand the nature of this *Arabidopsis Sinorhizobium* phenotype compared to other previously published responses to bacteria. For example, there are similarities between observations in this work (Figure 3.2) and previously reported phenotypes in *Arabidopsis* in response to oxylipins, which are produced in response to pathogenic invasion (Vellosillo et al., 2007). They report several different phenotypes, one of which is reduction in lateral root numbers. However there are also differences between the pathogen and *Sinorhizobium* responses. The pathogen response is always associated with a strong exaggerated wavy pattern of root growth, with primary roots growing almost horizontally before changing direction, rather than a more or less straight primary root, something not observed in the phenotype responses *to Sinorhizobium* in this work.

As one mechanism for the environmental regulation of root development, it could be hypothesized that different accessions respond in a uniform way to a particular treatment, increasing or decreasing the size of traits in a connected way. For example, all accessions might have a longer primary root and longer lateral roots in a higher nutrient concentration environment, thus

relative root size between accessions in different environments would be maintained. However instead, we see that traits respond in multiple independent ways to the *Sinorhizobium* inoculation with no connection of architecture in one environment predicting architecture in another (Figure 3.8). This suggests that there are multiple regulating factors controlling the individual aspects of root development and that these regulatory factors work at least partially independently from each other. This confirms earlier findings of Gifford et al. (2013), where root response to different N concentrations is similarly divergent. To help identify putative regulatory mechanisms it would be necessary to carry out expression profiling to identify genes that respond to *Sinorhizobium* inoculation and try to implicate them in the control of different aspects of root architecture, similar to Gifford et al. (2013).

It is tempting to link the reduced LR phenotype observed here to the effect of *Sinorhizobium* on its host *M. truncatula.* Negative regulation of root growth in favour of nodulation in legumes has been described in several genes including miRNA166 (Boualem et al., 2008), CDC16 (Kuppusamy et al., 2009) and *MtCEP1 (*C-terminally encoded peptide). *MtCEP1* is an enhancer of nodulation and is upregulated by low N concentrations (Imin et al., 2013). In *Arabidopsis,* overexpression of ATCEP1 results in a reduction of lateral roots (Ohayama et al., 2008). This suggests that existing LR signaling mechanisms have been modified in legumes to suit the needs of the novel nodulation mechanism.

Profiling of multiple *Arabidopsis* accessions in response to *Sinorhizobium* shows the complexity of the *Sinorhizobium* response (Figure 3.8) although it does not conclusively suggest a direct rather than indirect effect since

the variation in root responses could still be due to perceiving a different environmental factor, altered by the *Sinorhizobium* in different ways.

Chapter 4

Analysis of differentially expressed gene clusters

4.1 Introduction

Individual cell types consist of dramatically different transcriptional programming to enable their distinct functions (Birnbaum et al., 2003; Gifford et al., 2008). For example, cell types that form different developmental structures will need particular transcriptional programs. Furthermore, environmental and stress responses are also influenced by cell identity (Dinneny et al., 2008).

Lateral roots and nodules (in legume plants) initiate from different cell types; pericycle and cortex (Desbrosses et al., 2011). It is therefore of interest to specifically investigate these cell types in their response to various treatments in order to understand how their development is regulated by environmental conditions. In this chapter, gene expression in *Arabidopsis thaliana* (GFP marker lines for either cortex or pericycle cells) (section 2.1) in response to N availability and *Sinorhizobium* inoculation is investigated. All plant lines contained a GFP marker for either pericycle or cortical cells in the root.

4.2 Experimental design

The expression of GFP-marked pericycle and cortical cells was confirmed using confocal microscopy (Figure 2.1). Plants were grown as described in section 2.4. After 12 days of growth on N limiting conditions (0.3 mM NH_4NO_3) (Gifford et al., 2008) in Sanyo growth cabinets under long day (16 hours of artificial light, light intensity at 150 μmol m^{-2}) conditions, plants were removed from plates with

sterilized forceps, rinsed in either dH_2O or *Sinorhizobium* solution and transplanted onto a fresh agar plate with either high (5 mM) or low (0.3 mM) NH_4NO_3. This resulted in six time series, each consisting of three treatments (N, *Sinorhizobium* and a standard) in 2 different *Arabidopsis* GFP lines. Gene expression was measured at 14 time points: 0, 1, 2, 4, 6, 8, 10, 12, 14, 16, 20, 24, 36 and 48 hours post treatment. The 0 hour time point consisted of plants that were sampled without being treated. Every sample was grown on an individual plate.

Table 4.1 Experimental design for time course experiment.

	Rinse with:	*[NH_4NO_3] in agar*
Standard	Water	0.3 mM
N	Water	5 mM
Sinorhizobium	*Sinorhizobium* (OD 0.8)	0.3 mM

Plates were returned to the growth chamber after treatment, with samples taken between 0 and 48 hours (Table 4.1). Samples were processed with FACS to specifically isolate cortex or pericycle cells. mRNA was then extracted, amplified and labeled for microarray hybridisation using Nimblegen whole genome TAIR10 gene expression arrays. Array data was then quality checked and normalized (see Methods). The data set is longitudinal as it reflects a response over time, however there is no connection between samples as each sample represents roots from a different growth plate (destructive sampling). Gene expression was evaluated for statistically significant differential expression.

All arrays for each tissue were normalised together and assessed for quality with a number of methods (see 2.6-2.7). Typically 20% of the arrays were removed for quality issues. Time points with missing replicates were repeated so that each time point had at least 2 replicates, and typically 3. After

filtering there were 236 arrays (110 cortex and 126 pericycle) over the 6 treatments and 14 time points, averaging 2.95 replicates per time point. Genes were assessed as differentially expressed within a treatment using the BATS package (Angelini et al. 2008; section 2.7.3).

4.3 Differential expression of genes between time courses

4.3.1 Results

In the following discussion treatments and cell types will be referred to as CS, CN, CR, standing for 'standard treatment in cortex cells', N treatment in cortex cells' and *'Sinorhizobium* treatment in cortex cells' and the same will be done for PS, PN and PR, for pericycle respectively. Arrays were submitted to the Gene expression omnibus online repository (Barret et al., 2013).

DE of genes was assessed across every time series within a treatment. In cortex cells, 4682 genes were found to be DE across all treatments, apporximately equally distributed between the 3 treatment time series. (Figure 4.1A, Supplemental material S1). Each treatment has a slight majority (just over 50%) of DE genes specific only to that treatment (1852 for standard, 2074 for N and 1963 for *Sinorhizobium*). The DE of 203 genes were common in all three treatment time series (Figure 4.1A).

6702 genes were found to be DE in pericycle cells, with the standard and N treatments making up a significantly larger proportion in comparison to the *Sinorhizobium* treatment (4449 and 3590 vs. 1635 genes respectively). 610 genes were DE in all three treatment time series (Figure 4.1B). For a list of all BATS DE genes, see supplemental materials (S1).

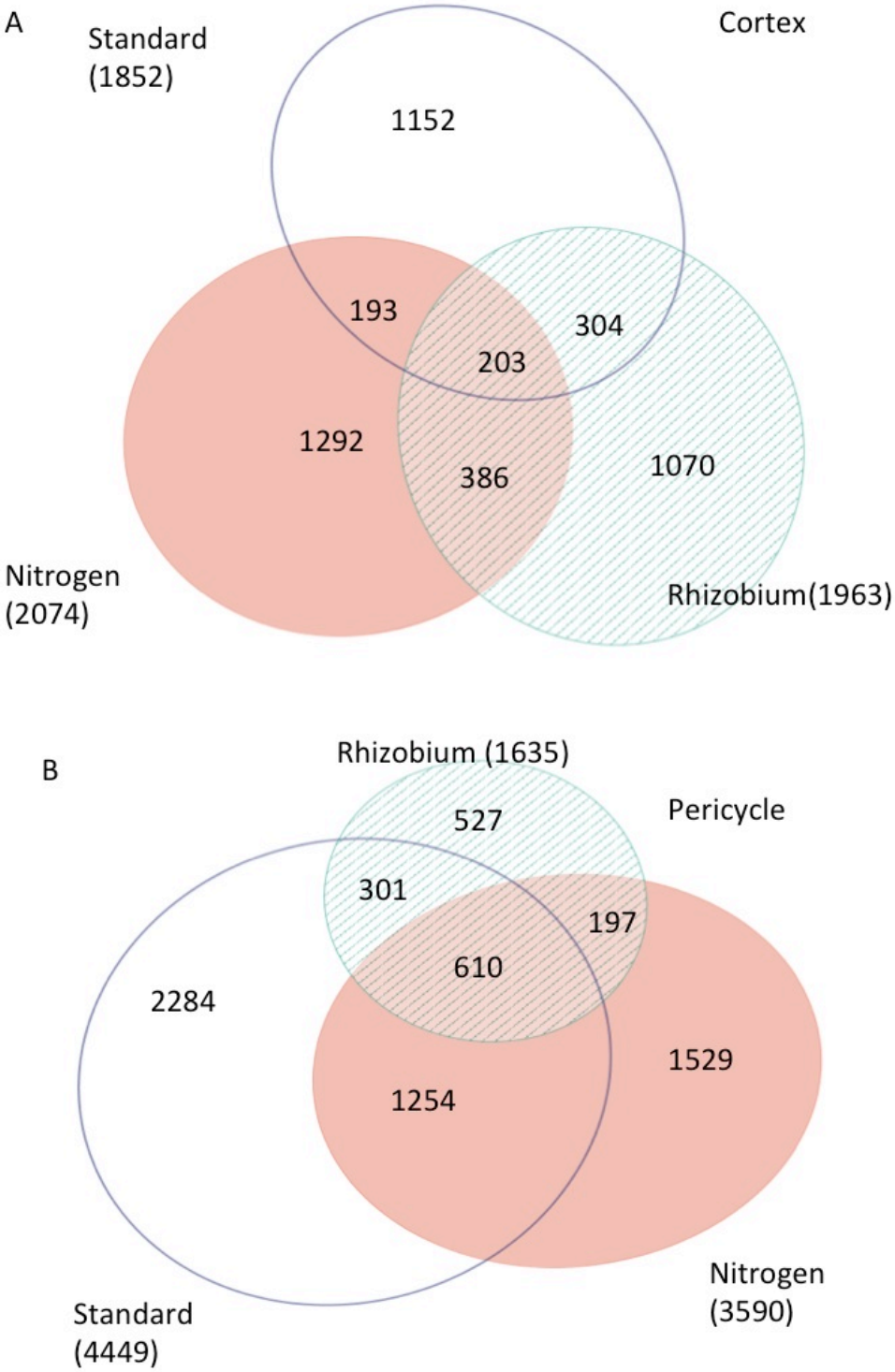

Figure 4.1 Differentially expressed genes over time as determined by BATS in cortex (A) and pericycle (B) cells in response to three different treatments: N, *Sinorhizobium* and standard (mock inoculation and transplantation). At least 2,

and usually 3 biological replicates were analysed for every combination of time point, treatment and cell type.

Overlap between treatments and cell types was small, particularly between cell types, with an overlap of 5-20%, while overlap between any two treatments was between 20-25%. This implies that for each treatment the majority of DE genes are specific to that treatment and cell type. There was a central core of 19 genes that were differentially expressed in all six treatments, comprising five TFs, a higher proportion than in all other cases. Compared to a random model, the pairwise overlaps were higher than expected except for the standard treatments, which was consistent with the random model. However, even against a random model, enrichment was typically only higher by a factor of 2 at most, which is surprising given the expectation that, especially in corresponding tissues, similar processes are being induced.

4.3.2 Comparison of treatment and cell type effects: comparing differential expression over time upon N and rhizobium treatment vs. between cell types

In a time series dataset with a treatment and an untreated standard it is necessary to determine a reliable way of assessing whether a gene that is DE over time within a treatment dataset is also DE compared to the standard dataset, thus really treatment-regulated. This is the case for this dataset, even though there is a 0 h time point (no treatment) standard within each time series. To do this, GP2S (Stegle et al., 2010) was used to assess the difference in expression profiles of genes between treatment and standard time series. GP2S assigns to each gene a BF which indicates the likelyhood of two expression profiles belonging to two different Gaussian processes. As such, genes with a suffciently high BF can be said to be differentially

expressed. Genes with a BF of at least 5 are said to be substantially differentially expressed (Jeffreys, 1961). This analysis is used to identify the proportion of DE genes that exhibit cell specific expression characteristics (i.e. differences between cortical and pericycle cells). All results of the GP2S analysis can be found in the supplemental materials (S2).

In the GP2S comparison between CS and PS, which identifies cell specific expression in untreated (S) conditions, 3264 genes have a different expression profile between the two cell types. Using the same analysis it is possible to test which genes are differentially expressed between a treatment and the control (i.e. CN vs CS and CS, as well as PN vs PS and PR vs PS). When we separately consider which genes are DE upon N or rhizobium treatment vs. standard treatment, in cortical and pericycle cells this is around 10% of the genome, wheras in *Sinorhizobium*-treated cells the number of genes with a different expression profile compared to the standard was significantly lower (3252 for CN vs. 443 for CR and 3775 for PN vs 171 for PR) (Table 4.2). By crossreferencing this list with the genes that exhibit cell specific expression patterns (different between CS and PS), it becomes clear that in CN, CR and PN, approximately one-third of the genes that respond to treatments also exhibit cell type specificity (Table 4.2). *Sinorhizobium* treated genes in pericycle cells form the exception, with only 20 of DE genes between treatments that also exhibit cell type specificity. This emphasizes that the treatment response is highly cell type specific and the analytical strength of analysing cell types separately.

Table 4.2 Number of genes with different expression profiles compared to the standard treatment. Treatment column indicates different treatments and cell identity: Cortex (C) and pericycle (P) treated with nitrate (N) or *Sinorhizobium* (R). The first column indicates how many genes have a different expression profile between the standard treatment and the treatment indicated on the left according to GP2S analysis. Next column indicates the subset of these genes which have different expression profiles between the two cell types in the standard treatment. The third column indicates the amount of genes that are DE between treatments (GP2S) as well as over time (BATS). The final column shows the subset of these genes that also exhibit cell specific expression patterns.

Treatment / cell identity	# DE genes in treatment vs standard	# of cell specific DE genes	# of DE genes that show DE within the time series	# Cell specific DE genes that show DE within the time series
CN	3252	1241	580	203
PN	3775	1486	761	354
CR	443	131	123	37
PR	171	20	8	2

To assess if the degree of DE within a cell type and a treatment over the time series corresponds with DE between the standard and treatment, results from GP2S were combined with results from BATS where differential expression within each time series was analysed (section 4.3.1). The intersect of genes that are DE between treatments (from GP2S) and DE within the time series (from BATS) shows how many genes are changing over time within a treatment while also changing compared to the standard treatment (Table 4.2). This shows that genes that the majority of genes with DE between the treatment and the standard do not show DE over time. Finally it is possible to analyse which of the genes that exhibit DE over time as well as between treatments can be thought to exhibit cell specific

expression patterns, by crossreferencing them with the 3264 genes with differential expression between CS and PS (Table 4.2).

While both methods for assessing DE yielded usable and reliable data, continuing analysis on the dataset of genes that were determined to be DE both by BATS and GP2S is very stringent, and would miss information needed to create reliable and informative clusters (see section 4.4). For further cluster analysis, genes that were DE along a time series (as determined by BATS) were considered in order to include within clusters all genes with similar dynamics.

4.3.3 Validation of expression data

Comparing expression data to existing datasets can give an indication of the validity of the DE dataset. Canales et al. (2014) have created a 'consensus' nitrate responsive set of 50 genes that can be thought of as core N response genes. These 50 genes were determined based on an analysis of 27 datasets of *A. thaliana* root gene expression data. No single gene was DE in every dataset, genes from the consensus nitrate responsive group were induced in at least 10 out of 27 experiments, with the most induced gene being *HRS1 (At1g13300)*, a G2-like TF family protein, being induced in 20 out of 27. On average, ~50% of the consensus genes were induced per dataset.

The list of 50 consensus genes was compared to the list of DE genes in N treated plants, not counting those genes that were also DE in plants that were standard treated. This yielded in 8 matches in DE genes from N treated cortex cells and 10 matches in DE genes from N treated pericycle cells, with two cases of genes being present in both, resulting in 16 out of 50 (32%) consensus nitrate responsive genes being found DE in the dataset here presented. With 3252 DE

genes in the combined cortex and N group, the expected frequency, had this group been randomly sampled, would be ~5 out of 50, given that the total number of genes in the *A. thaliana* genome is 33602 (TAIR 10, Lamesch et al., 2012). Thus we can conclude that there is a clear N response in the cortex and pericycle samples. At 32%, the number of nitrate responsive genes is lower than the average score of datasets used to create the consensus nitrate responsive gene list in Canales et al. (2014). However, our data show that the N response can be highly cell specific, with only of the 2 core genes in common between cortex and pericycle. Thus, by limiting the available data to just two cell types in the root, DE of core nitrate responsive genes in epidermal cells may not be identified

It also necessary to assess the cell identity of cortex and pericycle cells used in this study. Datasets with cell identity marker genes for cortex and pericycle cells were obtained from data provided by Brady et al. (2007). Cortex and pericycle marker genes are found DE between the CS and PS treatments (Table 4.3). When gene expression over time is analysed, more cortex marker genes are found, both in cortex and pericycle. This suggests the pericycle has a less defined cell identity and is consistent with findings of pericycle cell dedifferentiation during the initiation of LR growth (Malamy et al., 1997) and tissue regeneration (Sugimoto et al., 2010). This is not necessarily a problem for the analysis, as GFP-expression in plant lines was repeatedly validated with confocal microscopy for the duration of the experiments, and GFP-expression was typically very stable and limited to the intended cell types.

Table 4.3 Number of marker genes (Brady et al., 2007) for cell types present as differentially expressed genes in time series datasets. First column shows the number of marker genes that exhibit DE between CS and PS, second and third column show the number of marker genes found in CS and PS DE genes over time.

	DE between CS and PS	DE in CS over time	DE in PS over time
Number of cortex marker genes found	22	37	31
Number of pericycle marker genes found	39	9	9

Finally it is necessary to assess the reproducibility the array data. To do this, arrays within a treatment/cell type combination (cortex cells, standard treatment) were clustered (Figure 4.2, euclidian distance, complete linkage). This analysis shows how overall, arrays from biological replicates, as well as arrays from subsequent timepoints tend to cluster together (Figure 4.2). However this is not always the case, highlighting the need for multiple biological replicates per sample.

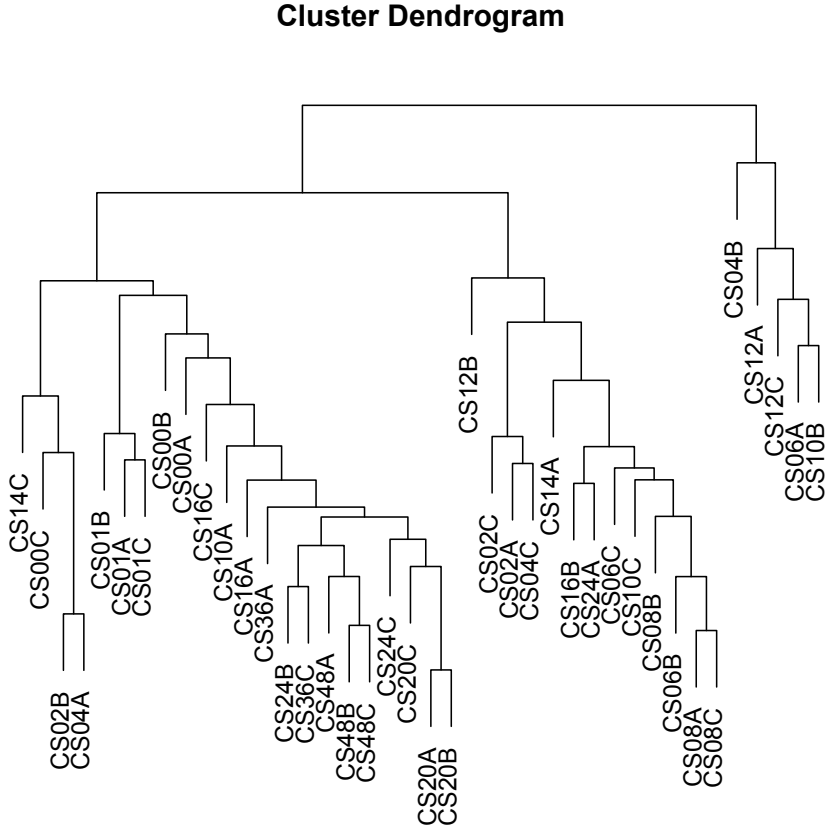

Figure 4.2 Cluster dendrogram (Euclidean distance, complete linkage) of all arrays in the cortex standard treatment. Arrays with similar expression profiles will cluster together.

4.4 Clustering of DE gene expression profiles reveals coexpression of functionally related genes

Following the hypothesis that genes involved in similar processes should be regulated in the same way across a time series of gene expression measurement, an effective way to identify processes and overall responses is to analyse clusters of genes whose expression is similar over the course of the time series. In order to do this, DE genes were clustered using the Splinecluster algorithm (Heard et al., 2005) on the basis of their expression patterns during the different treatments. Each time series was clustered independently. The mean expression value of all biological replicates per gene was used to determine cluster identity. For each

time series, these clusters represent groups of genes that were differentially expressed during the treatment.

Depending on treatment and tissue, this gave 61-95 clusters for cortex and 49-106 clusters for pericycle, with cluster size ranging from 3 to ~100 genes. The clusters show a wave-like activation and inhibition pattern in all experiments, particularly at early time points where successive waves of activation and inhibition can be tracked through successive genes. This wave pattern is indicative of regulatory activation/inhibition and can be seen within 1 hour of treatment, whereas other clusters show more subtle changes over the time course. An overview of all clusters is shown in Figures 4.3-4.8. A list of all clusters and gene ontology enrichment analysis can be retrieved from supplemental data S3 (CN), S4 (CR), S5 (PN) and S6 (PR),

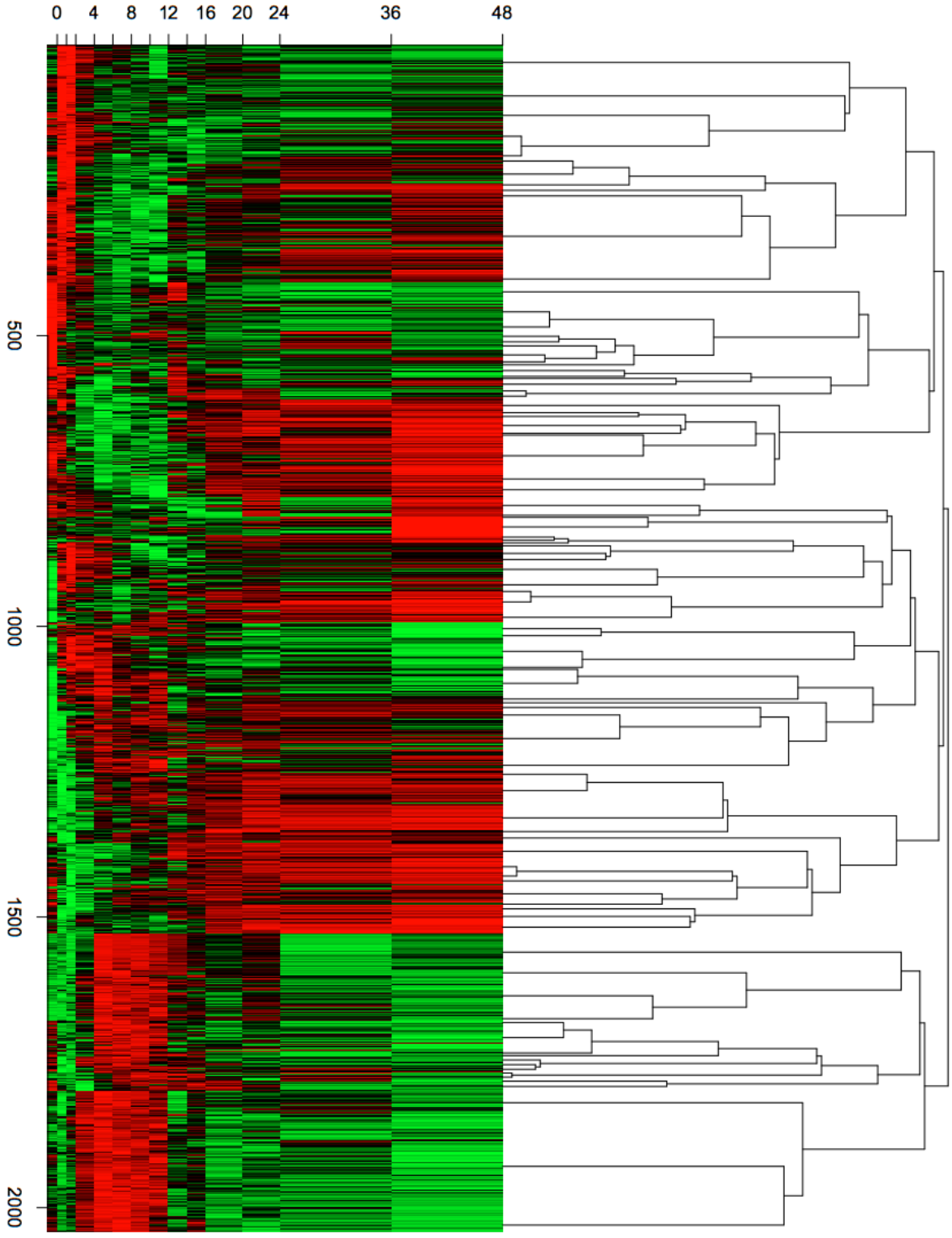

Figure 4.3 Cluster dendrogram for individual genes in the CS time course based on similarity of expression patterns. Genes were clustered using hierarchical clustering with colours indicating high levels of expression (red) vs. low levels of expression (green). Genes are plotted on the Y-axis, time (h) is plotted on the x-axis.

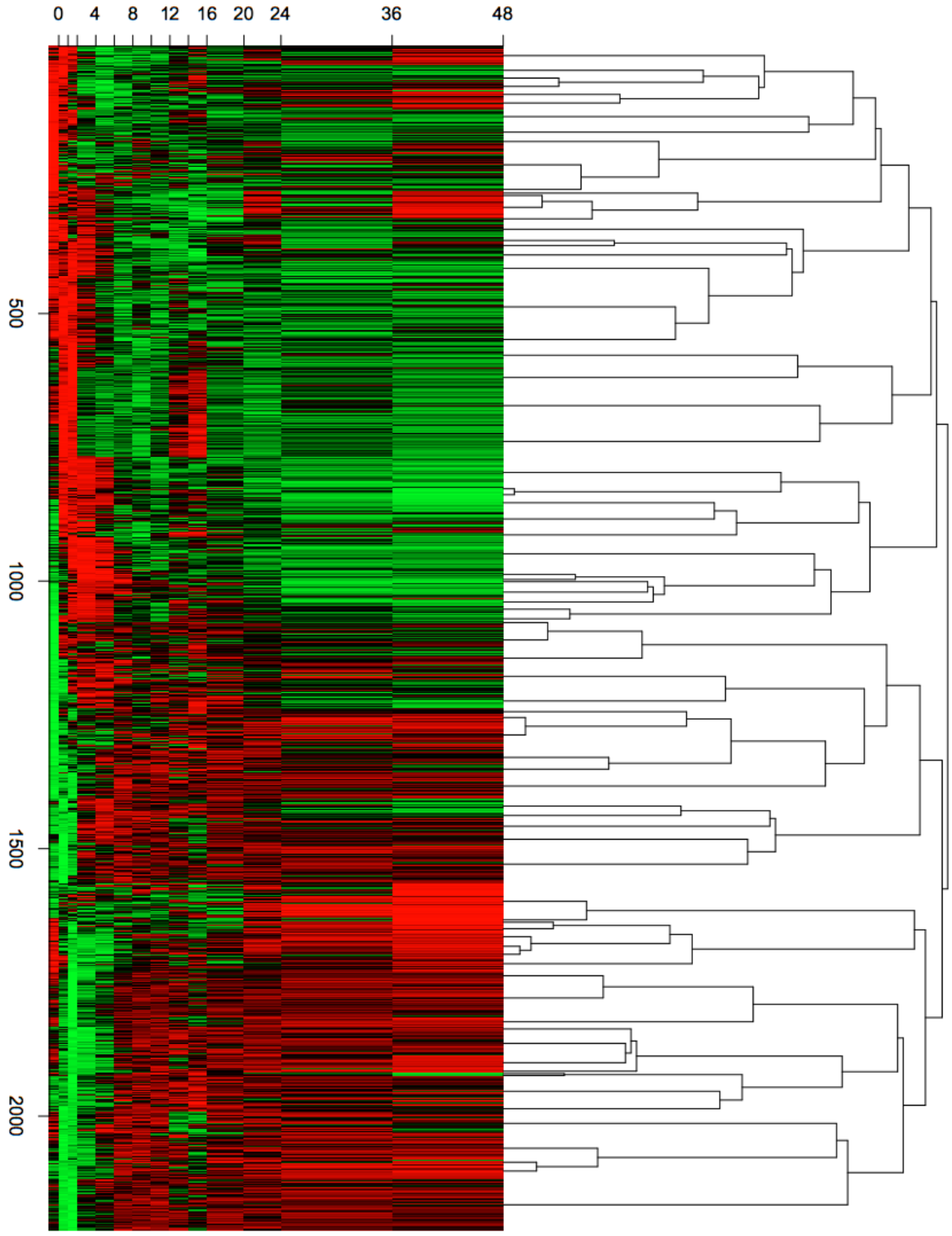

Figure 4.4 Cluster dendrogram for individual genes in the CN time course based on similarity of expression patterns. Genes were clustered using hierarchical clustering with colours indicating high levels of expression (red) vs. low levels of expression (green). Genes are plotted on the Y-axis, time (h) is plotted on the x-axis.

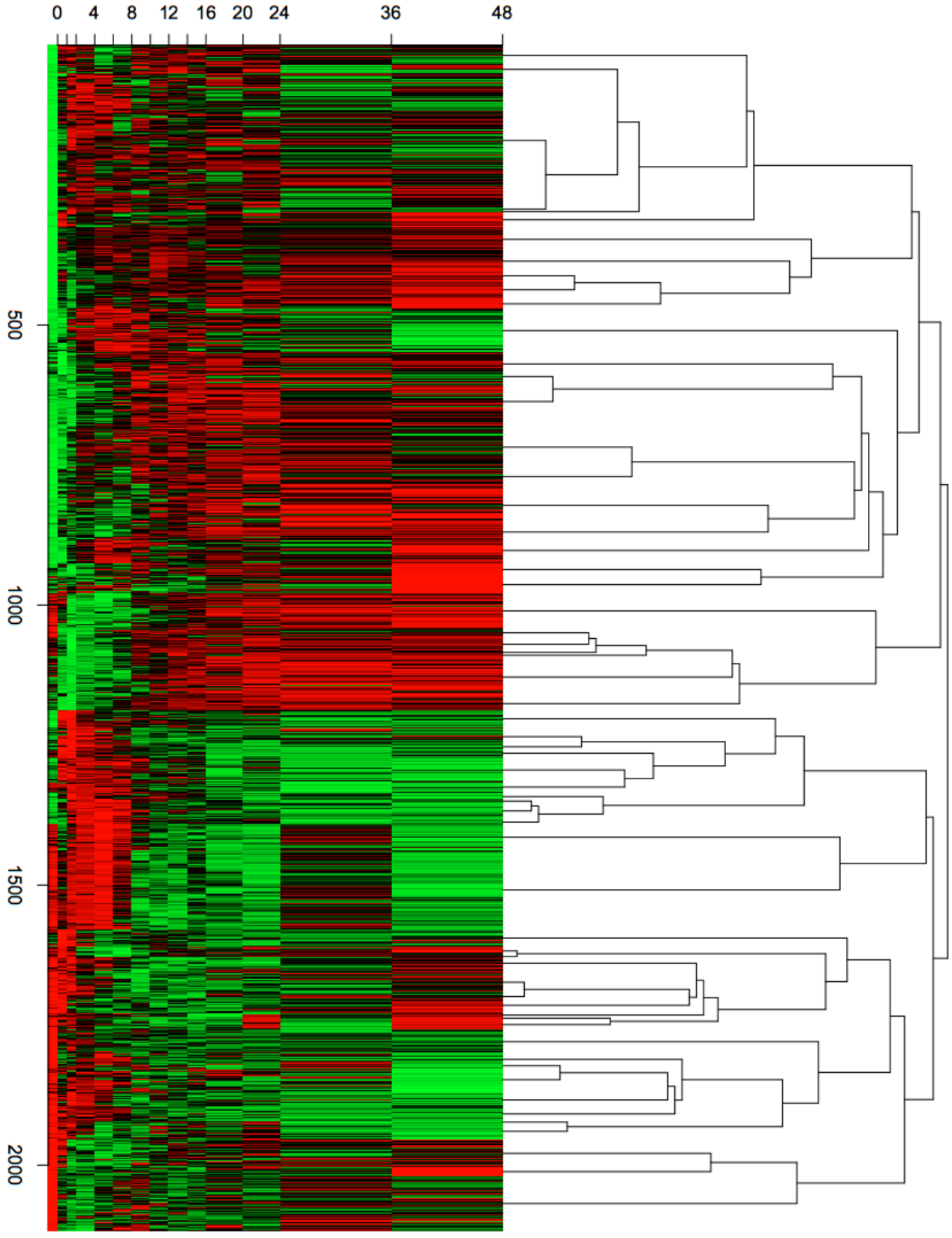

Figure 4.5 Cluster dendrogram for individual genes in the CR time course based on similarity of expression patterns. Genes were clustered using hierarchical clustering with colours indicating high levels of expression (red) vs. low levels of expression (green). Genes are plotted on the Y-axis, time (h) is plotted on the x-axis.

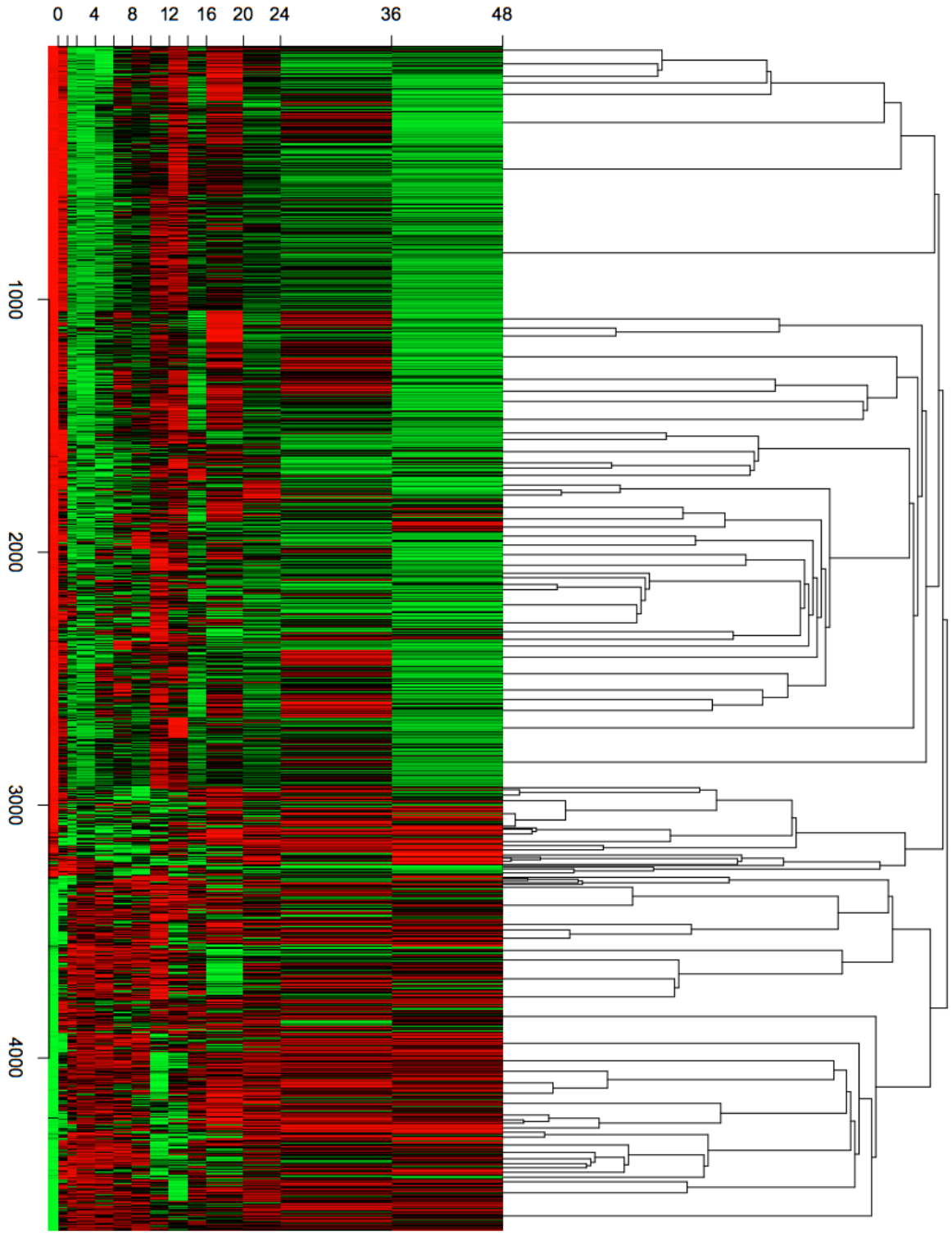

Figure 4.6 Cluster dendrogram for individual genes in the PS time course based on similarity of expression patterns. Genes were clustered using hierarchical clustering with colours indicating high levels of expression (red) vs. low levels of expression (green). Genes are plotted on the Y-axis, time (h) is plotted on the x-axis.

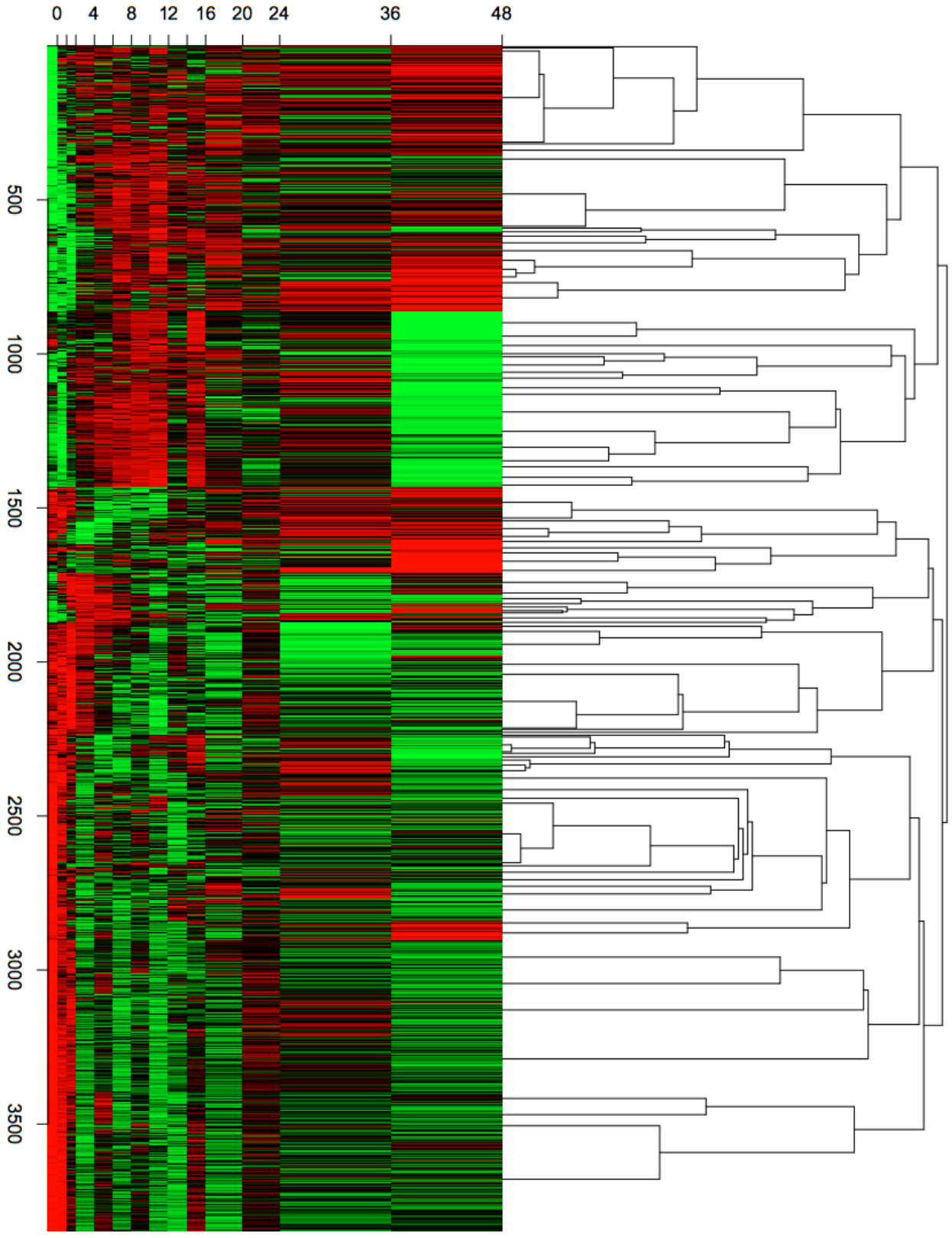

Figure 4.7 Cluster dendrogram for individual genes in the PN time course based on similarity of expression patterns. Genes were clustered using hierarchical clustering with colours indicating high levels of expression (red) vs. low levels of expression (green). Genes are plotted on the Y-axis, time (h) is plotted on the x-axis.

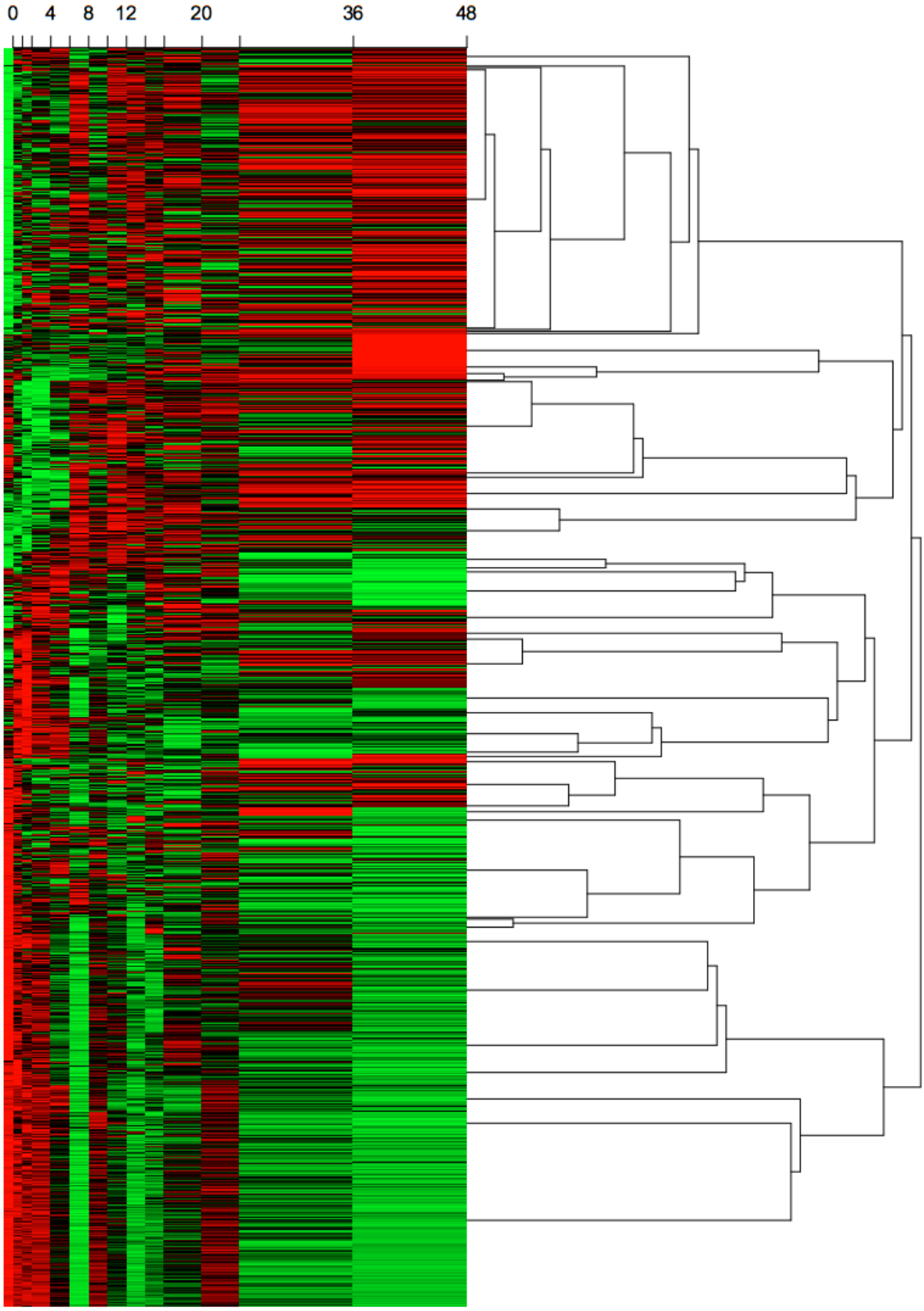

Figure 4.8 Cluster dendrogram for individual genes in the PR time course based on similarity of expression patterns. Genes were clustered using hierarchical clustering with colours indicating high levels of expression (red) vs. low levels of expression (green). Genes are plotted on the Y-axis, time (h) is plotted on the x-axis.

An effective way of validating the expression data and these clusters is to investigate whether genes that are expected to have DE and be coexpressed are also clustered together. The *Arabidopsis* circadian clock is a very well understood and tightly regulated system with very specific repetitive expression patterns. *LHY*, *CCA1* and *PRR9* are expected to exhibit a high degree of coexpression (McClung, 2006; Pokhilko et al., 2012). These genes were in the same cluster in five out of six treatment time series (Table 4.3 and Figure 4.9), the one exception being PR (see * in table 4.3), although PR clusters 26 and 33 are reasonably similar shaped. This approach shows the validity of the splineclustering approach as well as the consistency of the clusters between treatments.

Table 4.3: Cluster numbers of coexpressed circadian genes per treatment. Selected circadian genes were always found in the same cluster per treatment, with the exception of *LHY*, which was in a different cluster from *CCA1* and *PRR9* in the PR treatment.

	PR	PN	PS	CR	CN	CS
LHY	26*	44	64	51	14	37
CCA1	33	44	64	51	14	37
PRR9	33	44	64	51	14	37

A

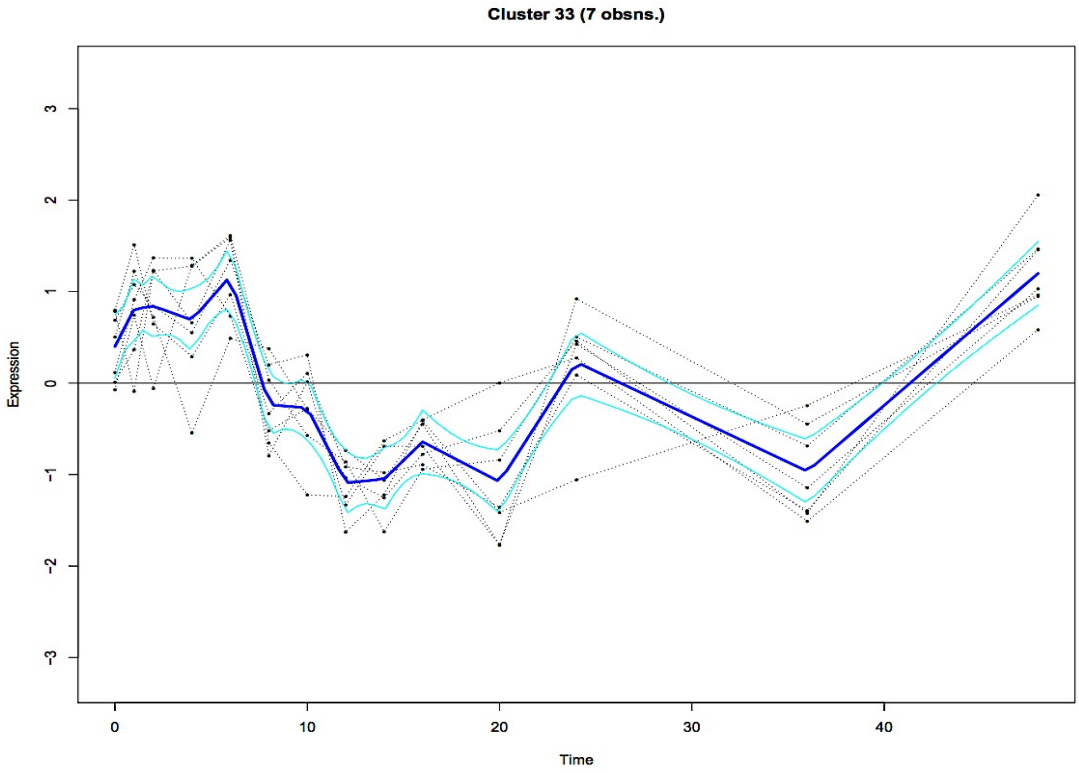
Cluster 33 (7 obsns.)
Expression
Time
3
2
1
0
−1
−2
−3
0
10
20
30
40

B

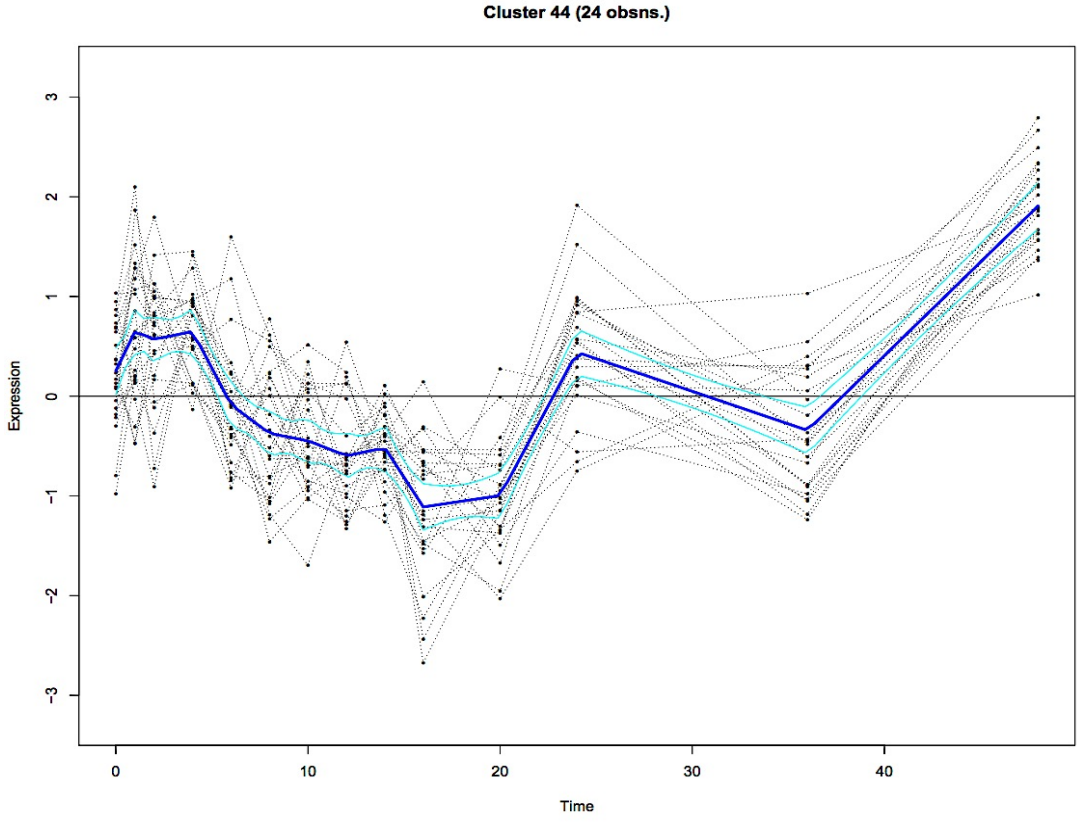
Cluster 44 (24 obsns.)
Expression
Time
3
2
1
0
−1
−2
−3
0
10
20
30
40

C

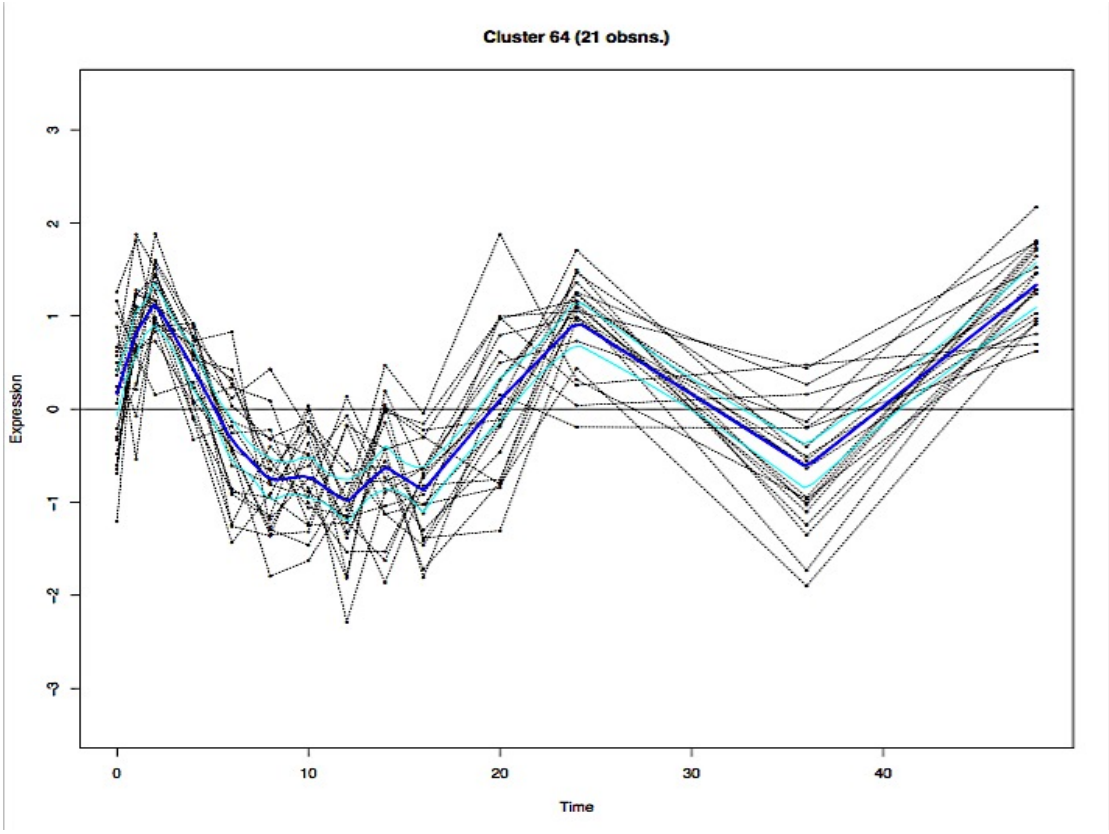
Cluster 64 (21 obsns.)
Expression
Time
3
2
1
0
-1
-2
-3
0
10
20
30
40

D

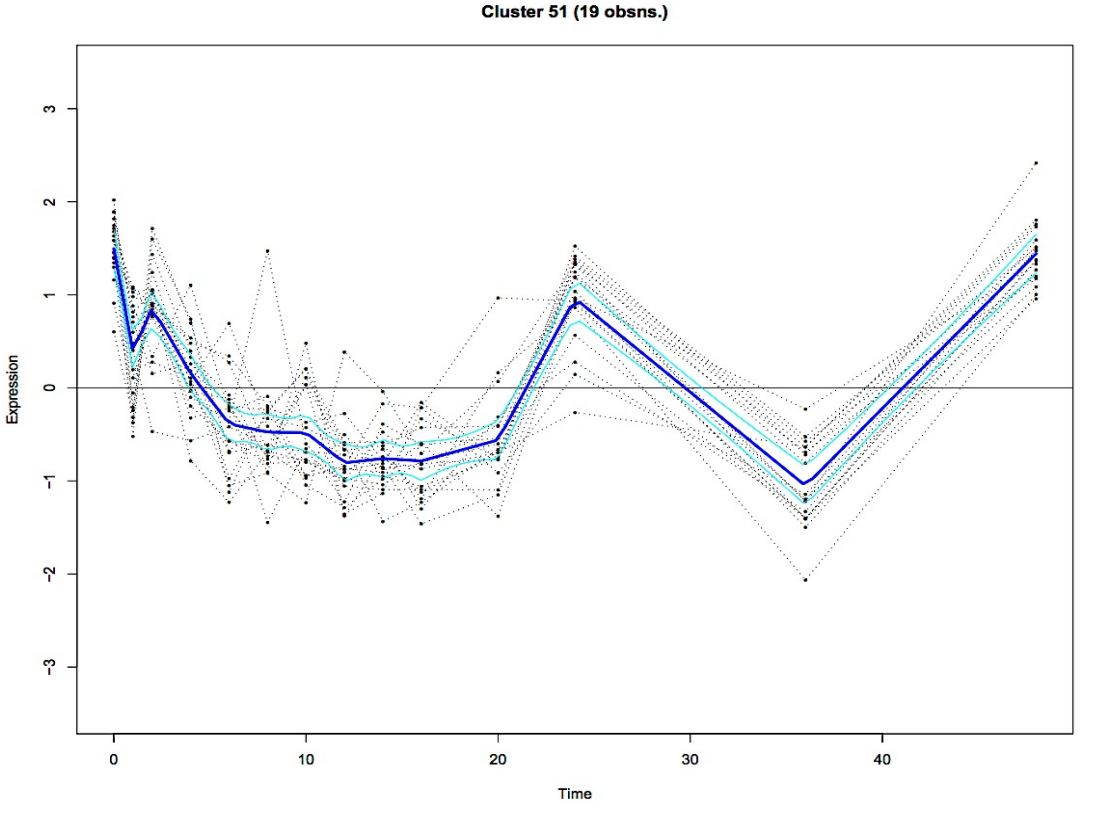
Cluster 51 (19 obsns.)
Expression
Time
3
2
1
0
-1
-2
-3
0
10
20
30
40

E

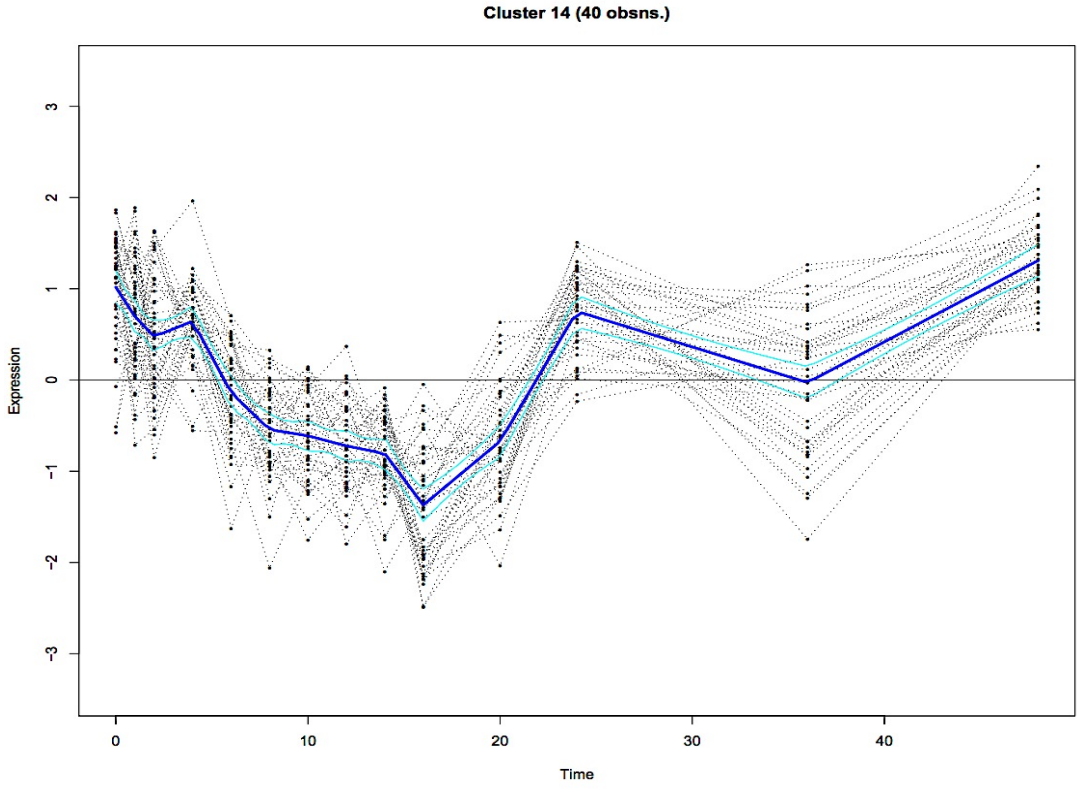
Cluster 14 (40 obsns.)
Expression
Time
3
2
1
0
−1
−2
−3
0
10
20
30
40

F

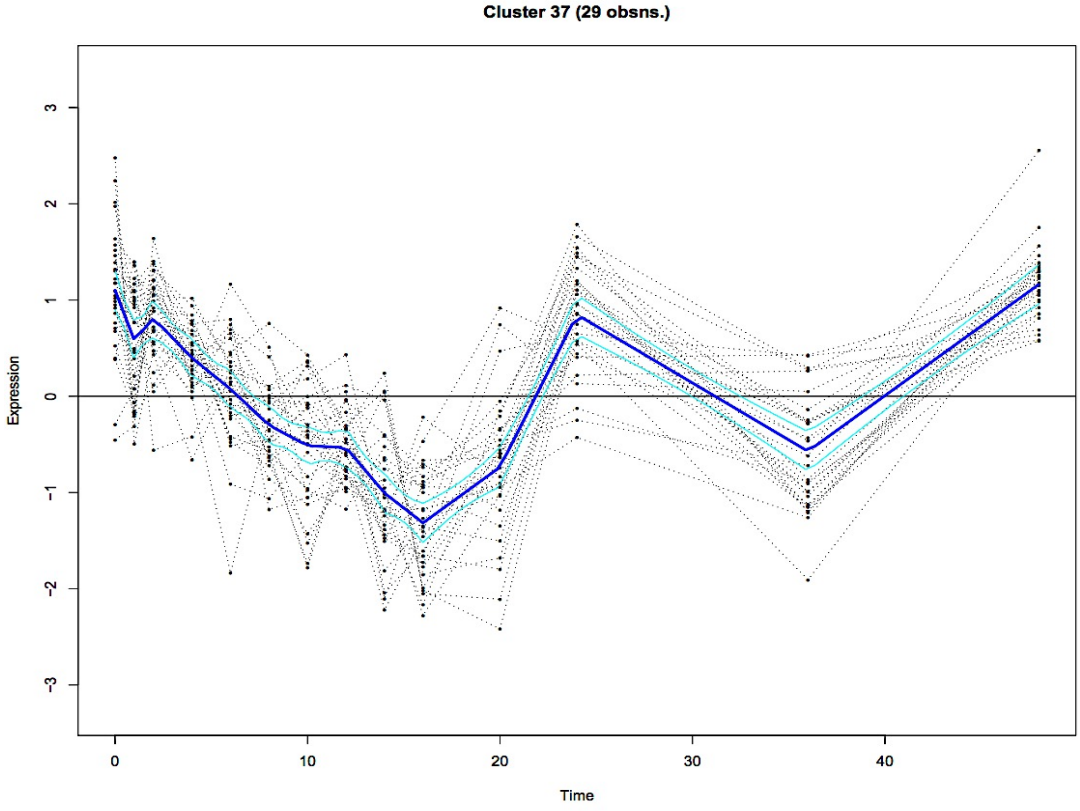
Cluster 37 (29 obsns.)
Expression
Time
3
2
1
0
−1
−2
−3
0
10
20
30
40

Figure 4.9 (continued) Plots with gene expression of clusters containing core circadian genes in different cell types and treatments. (A) *Sinorhizobium* treatment pericycle (7 genes) (B) N treatment pericycle (24 genes) (C) standard treatment pericycle (21 genes) (D) *Sinorhizobium* treatment cortex (19 genes) (E) N treatment cortex (40 genes) (F) Standard treatment cortex (29 genes). The dashed blue lines indicate the mean ± 1 SD of the cluster Time is plotted in hours on X-axis, Y-axis indicate log2 expression normalized on a per gene basis. Clustering was performed using Splinecluster (Heard et al., 2006).

4.4.1 Chronology of the responses to N or *Sinorhizobium* treatment

Identification of biological processes that change in the response to N or *Sinorhizobium* was carried out by analysing clusters of coexpressed genes for overexpressed gene ontologies. Analysis of overrepresented gene ontologies was carried out using GOstats (Gentleman et al., 2007) on the DE genes in each cluster. To avoid the effect of circadian rhythm on the analysis of clusters of DE genes, for each cell type seperately, all DE genes in N and *Sinorhizobium* treatment that were DE as well in the standard treatment were filtered out after clustering. As clusters of DE genes reflect possible common regulatory elements, the clustering was performed on all DE genes. To then identify the treatment-specific effects, genes that were also DE in the standard treatment were filtered out prior to gene ontology enrichment analysis.

Selected gene ontologies (GO) of interest are discussed here and analysed in more detail in the sections below. Gene ontologies of special interest were hormone-related GO terms, pathogenesis and general stress response, response to N, root morphology and development related GO terms and ontologies related to plant growth or defense such as cell wall biosynthesis.

Clusters were ordered chronologically, with the time of differential expression determined through comparison with similar genes in the standard treatment. This allowed for a rudimentary time-based sorting of relevant biological events. Typically early in the treatments clusters enriched with genes

for hormone-associated GO terms are found, in the N response treatment, clusters enriched with genes for responses to auxin and JA were observed within the first 6 hours in both cortex and pericycle cells (Figure 4.10). In the *Sinorhizobium* response there is similarly a cluster enriched with genes for response to auxin GO terms found (Figure 4.27). Clusters enriched with genes for root development GO terms are found in the N treatment with differential expression starting 4 hours after treatment.

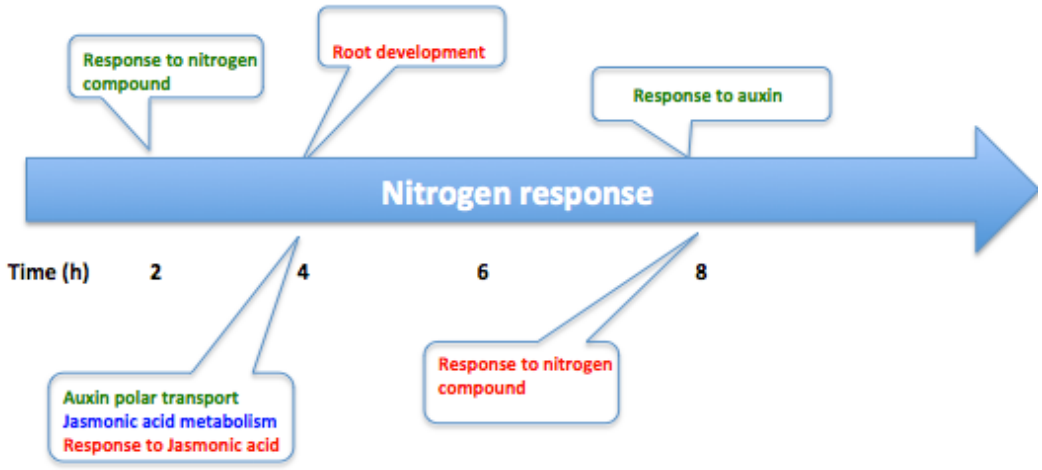

Figure 4.10 Overview of discussed enriched GO terms found in different clusters over the duration of the N response. GO terms below the blue arrow of time represent clusters with decreasing levels of gene expression whereas GO terms above the blue arrow of time represent clusters with increasing levels of gene expression. Green terms refer to GO's in cortex clusters, red terms refer to GO's in pericycle clusters and blue terms refer to GO's in both.

4.4.2 Root cell transcriptional responses to N

4.4.2.1 Genes associated with root development in response to high N

Genes belonging to clusters enriched for GO's associated with lateral root development are found differentially expressed early (4 h) in pericycle cells (Figure 4.11: PN cluster 31, $P = 0.00619$; Figure 4.12: PN cluster 50, $P = 5.4 \times 10^{-6}$). *WRKY75* (*At5g13080*) (PN cluster 50) is strongly upregulated early after N

treatment. It has previously been shown to be involved in the mediation of phosphate stress, as well as having an effect on root hair and lateral root number, independent of the phosphate status of the plant (Devaiah et al., 2007). It is possible that an increase in N concentration within the plant leads to an increased metabolic turnover, which is a possible cause for P-deficiency. *NRP1* (*At1g74560*) (PN cluster 31, figure 4.11) expression is induced by auxin (Huang et al., 2008) and plays a critical role in ensuring correct genome transcription in the maintenance of root growth (Zhu et al., 2007). Here it is upregulated in pericycle and cortex cells in the N treatment, while it is downregulated in *Sinorhizobium*-treated cortex cells.

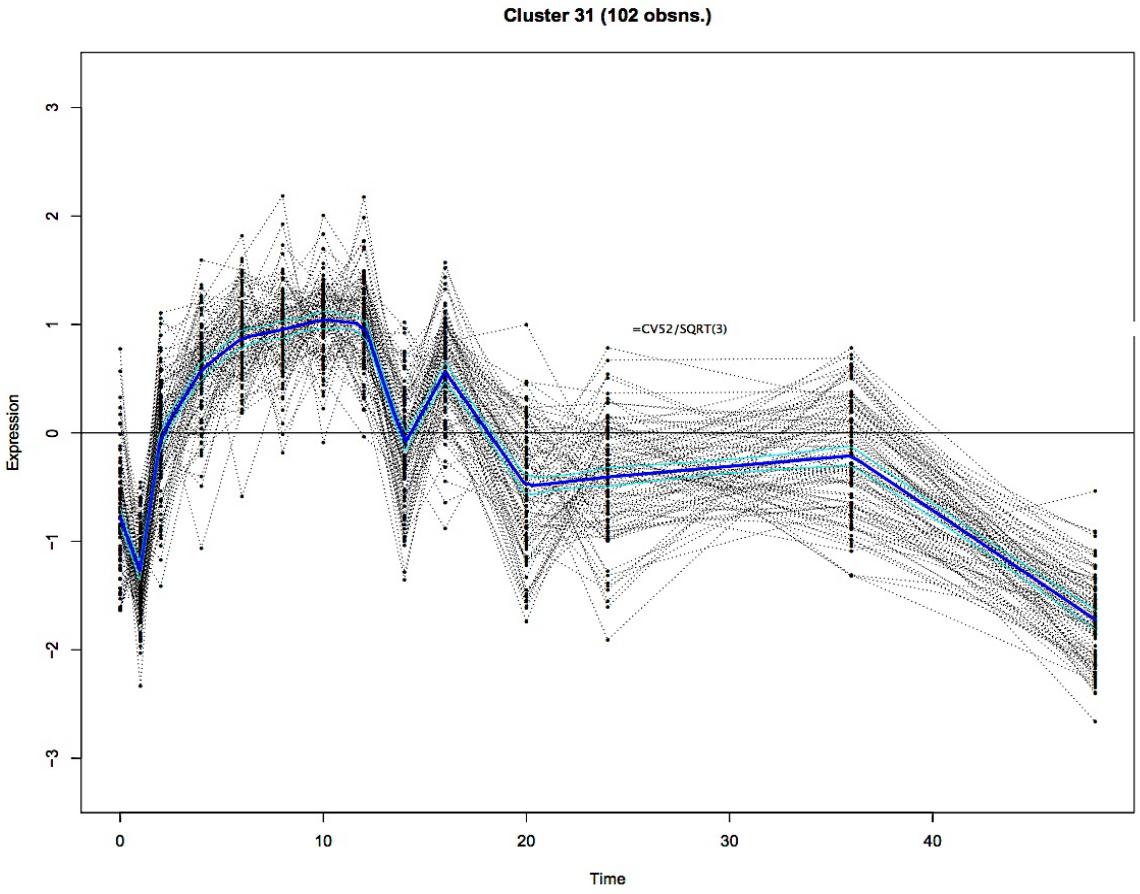

Figure 4.11 PN cluster 31, enriched for genes with root development GO terms (*P*=0.00619). Individual gene profiles are shown as grey lines with the mean expression profile in blue. The dashed blue lines indicate the mean ± 1 SD of the cluster. The Y-axis indicates log2 expression normalized on a per gene basis. The X-axis indicates time in hours. Clustering was performed using Splinecluster

(Heard et al., 2006), Gene ontology analysis was performed with Gostats (Gentleman et al., 2005).

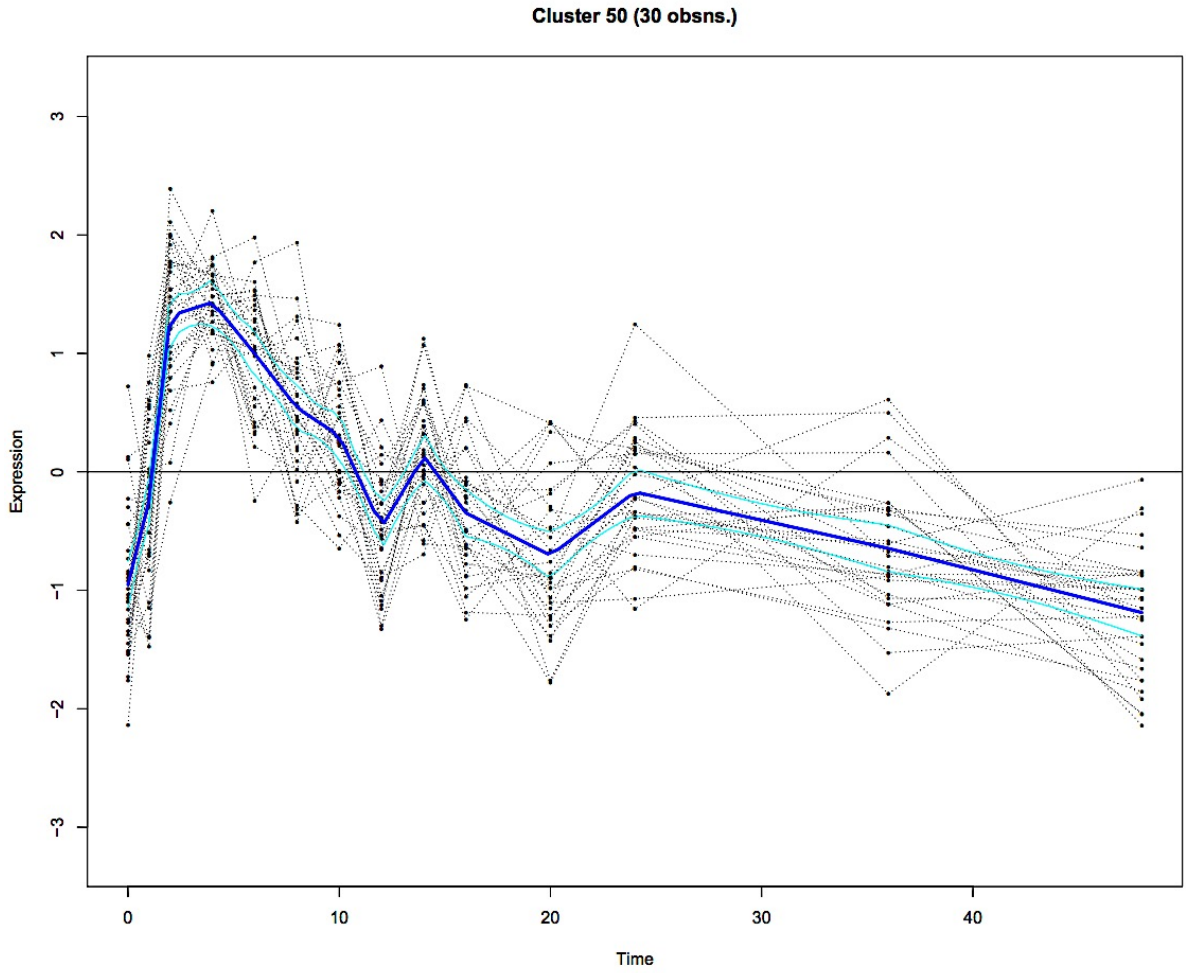

Figure 4.12 PN cluster 50, enriched for genes with root development GO terms (P=5.4 x 10^{-6}). Individual gene profiles are shown as grey lines with the mean expression profile in blue. The dashed blue lines indicate the mean ± 1 SD of the cluster. The Y-axis indicates log2 expression normalized on a per gene basis. The X-axis indicates time in hours. Clustering was performed using Splinecluster (Heard et al., 2006), Gene ontology analysis was performed with Gostats (Gentleman et al., 2005).

4.4.2.3 Genes associated with N metabolism in response to high N

A large number of genes associated with the formation and metabolism of N-containing compounds are strongly upregulated within 2 h of N treatment, and remain at an elevated expression level for the duration of the experiment, both in

pericycle and cortex cells. This gives an indication of the speed with which *Arabidopsis* can adapt its transcriptome to adapt to a changing environment.

A cortex cluster enriched with genes associated with GO terms for response to N compound contained several key N transporter genes (Figure 4.13: CN cluster 27, P = 3.72 x 10^{-10}). This cluster contains, among others, three nitrate transporter genes: *NRT1.1* (*At1g12110*), *NRT2.1 (At1g08090)* and *NRT3.1 (At5g50200*) with a peak in expression 2 hours after N treatment. *NRT1.1*, as already discussed in (section 1.1.2) is a nitrate transceptor (both signaler and transporter) expressed in lateral roots that acts mostly as a signaling protein for nitrate availability in the soil (Krouk et al., 2009; Glass et al., 2013). It directs lateral root growth to patches of high N in soil (Remans et al., 2006) and acts as a regulator for *NRT2.1* (Munos et al., 2004). NRT2.1 forms a N-transporting complex with NRT3.1 (Yong et al., 2010, Kotur et al., 2012). *NRT2.1* is a high affinity nitratre transporter specifically associated with cortical cells in the root (Gifford et al., 2008) and has been shown to act in response to rescue from N starvation, preparing the plant to start acquiring N again (Yong et al., 2010). The time series data suggests that internal N transport is upregulated in the recovery period after starvation via transient increase of the expression levels of N transport genes.

NRT3.1 was also found in pericycle cluster 59, which was also enriched for genes associated with response to N compound (Figure 4.14, *P* = 3.7 x 10^{-16}). Genes in this cluster typically are downregulated compared to the standard treatment in both pericycle and cortex cells from 8h after treatment onwards.

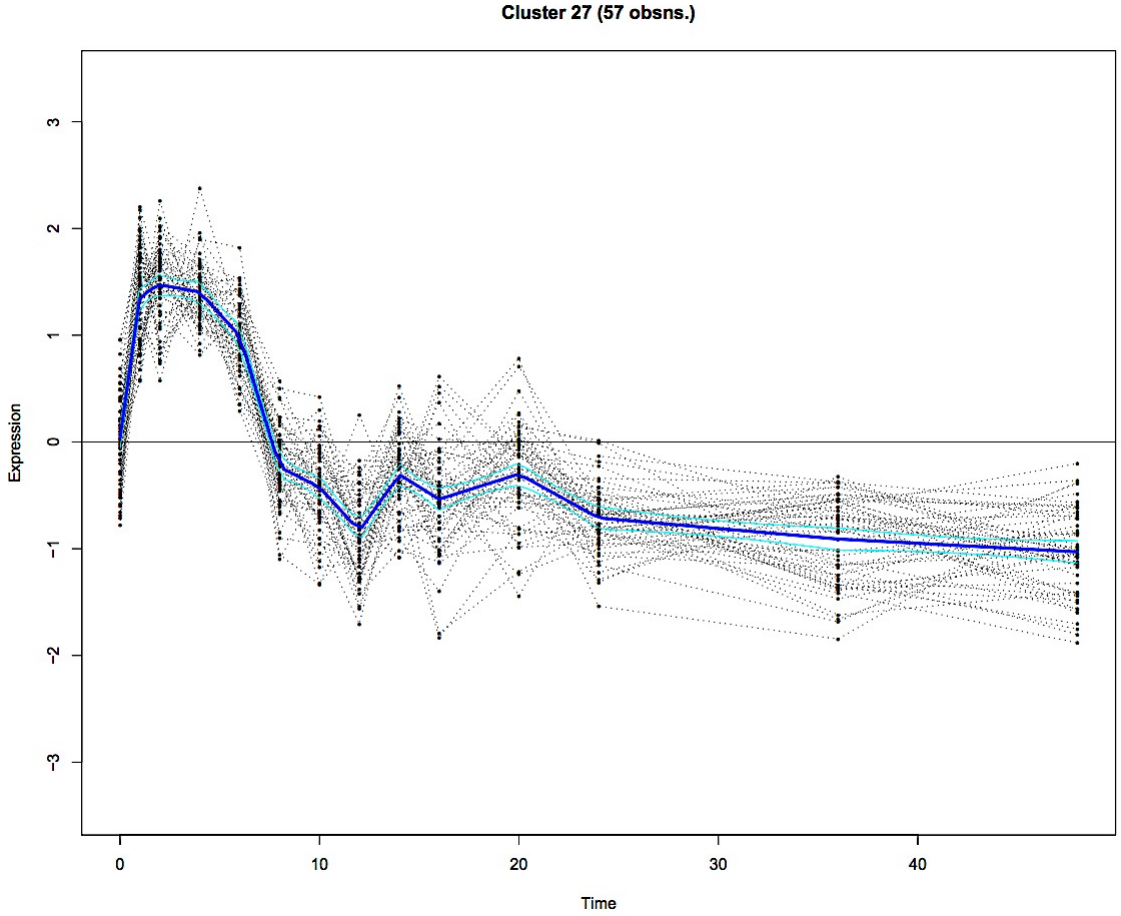

Figure 4.13 CN cluster 27, enriched for genes with response to N compound GO terms (P = 3.72 x 10^{-10}). Individual gene profiles are shown as grey lines with the mean expression profile in blue. The dashed blue lines indicate the mean ± 1 SD of the cluster. The Y-axis indicates log2 expression normalized on a per gene basis. The X-axis indicates time in hours. Clustering was performed using Splinecluster (Heard et al., 2006), Gene ontology analysis was performed with Gostats (Gentleman et al., 2005).

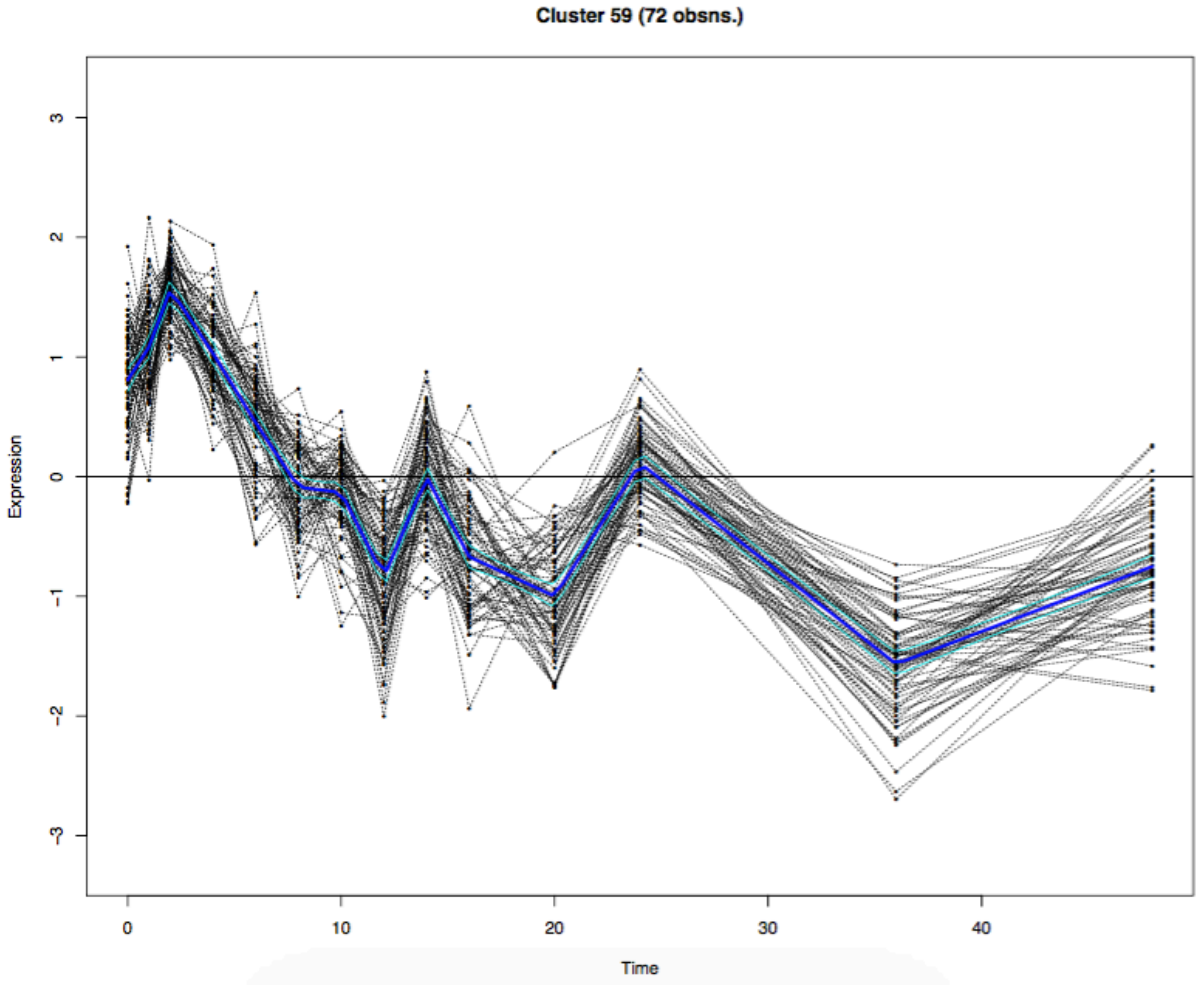

Figure 4.14 PN cluster 59, enriched for genes with response to N compound GO terms (P = 3.7 x 10^{-16}). Individual gene profiles are shown as grey lines with the mean expression profile in blue. The dashed blue lines indicate the mean ± 1 SD of the cluster. The Y-axis indicates log2 expression normalized on a per gene basis. The X-axis indicates time in hours. Clustering was performed using Splinecluster (Heard et al., 2006), Gene ontology analysis was performed with Gostats (Gentleman et al., 2005).

4.4.2.4 Mitochondrial chromosome genes in response to high N

In pericycle cells we find two clusters (Figures 4.15 and 4.16) with similar expression patterns (drop in expression levels at 4 h and 20 h) that contain an unusually high number of mitochondrial chromosome genes, four out of seven and six out of eight respectively. Given that there are only 146 known genes in the mitochondrial chromosome (Lamesch et al., 2012), the expected frequency in

case of random selection would be 0.5%, rather than the 57% and 80% observed in these groups. Earlier studies have shown that genes that are in close physical proximity in the genome are also more likely to be coexpressed in *Arabidopsis* (Williams et al., 2004) and in other eukaryotes (Lee et al., 2000; Boutanaev et al., 2002), however the genes picked in our clusters appear to be evenly distributed along the mitochondrial chromosome. The genes in these clusters typically have lower expression levels in N and *Sinorhizobium* treatments than in the standard treatment. Genes include NADH dehydrogenases *NAD2A (AtMg00285)* and *NAD5 (AtMg00060)*.

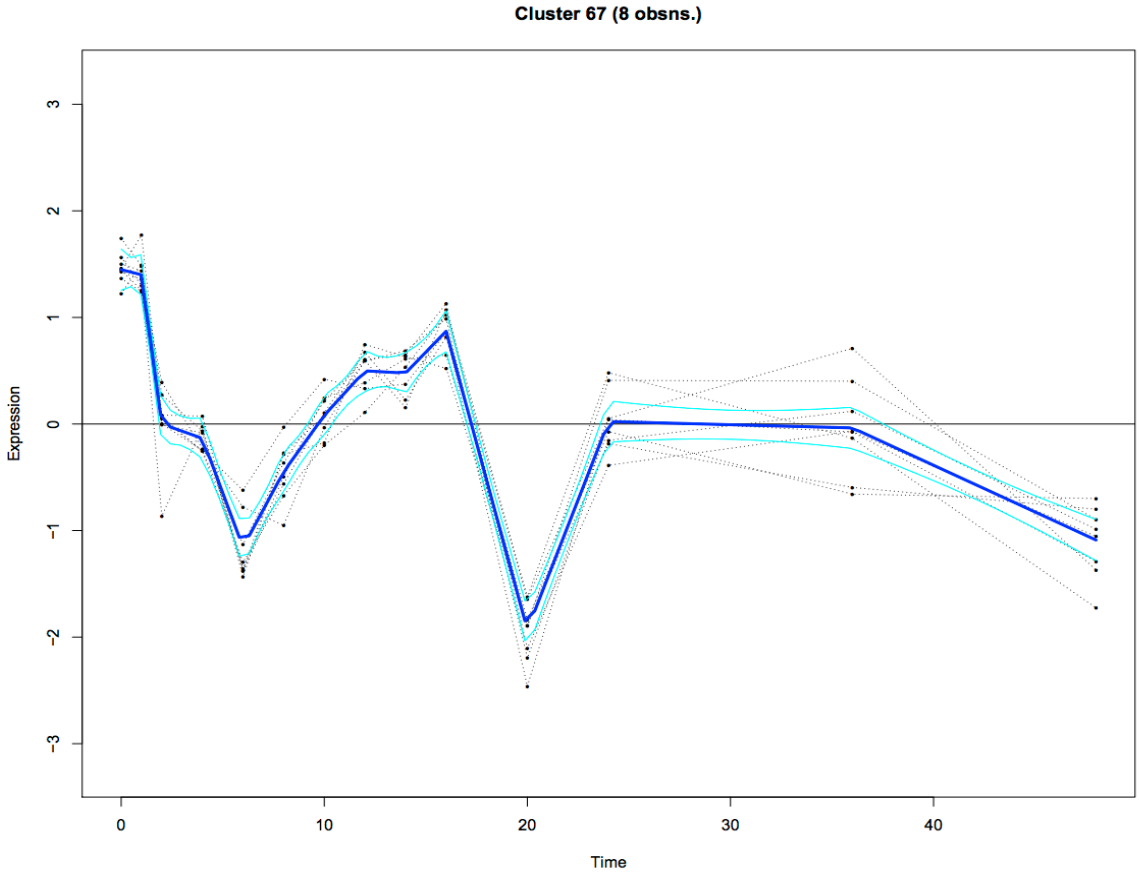

Figure 4.15 PN cluster 67 consisting of seven genes, four of which are mitochondrial chromosome genes. Individual gene profiles are shown as grey lines with the mean expression profile in blue. The dashed blue lines indicate the mean ± 1 SD of the cluster. The Y-axis indicates log2 expression normalized on a per gene basis. The X-axis indicates time in hours. Clustering was performed using Splinecluster (Heard et al., 2006).

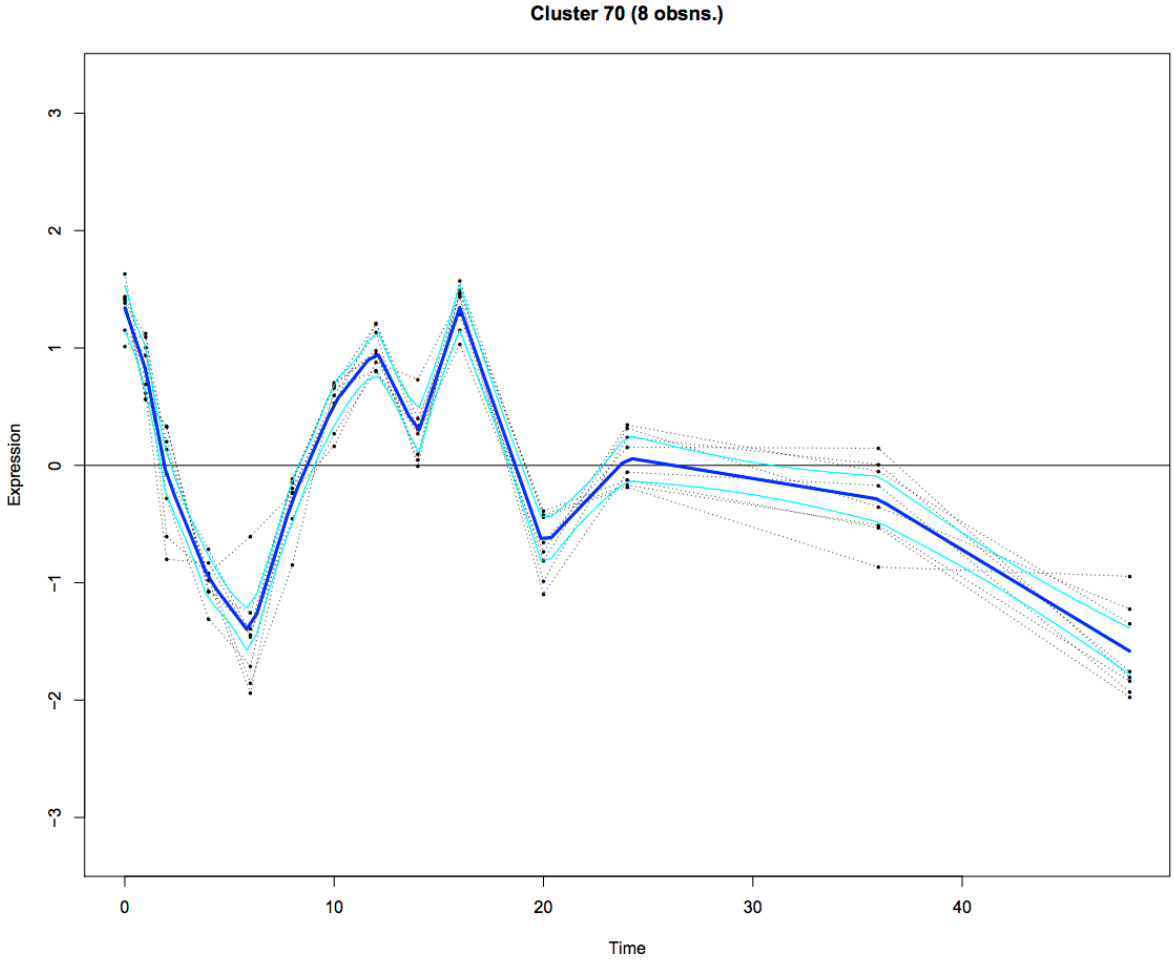

Figure 4.16 PN cluster 70 consisting of eight genes, six of which are mitochondrial chromosome genes. Individual gene profiles are shown as grey lines with the mean expression profile in blue. The dashed blue lines indicate the mean ± 1 SD of the cluster. The Y-axis indicates log2 expression normalized on a per gene basis. The X-axis indicates time in hours. Clustering was performed using Splinecluster (Heard et al., 2006).

4.4.2.5 Genes associated with auxin GO terms in response to high N

Plant hormones play a major role in the response to N, investigating them can provide a useful timeline for their synthesis and/or action (Kiba et al., 2011; Krouk et al., 2011,). There is considerable evidence linking different hormones to N status in the plant. ABA insensitive and deficient mutants are less sensitive to the inhibitory effect of high nitrate concentrations on root growth (Signora et al., 2011). Cytokinin acts as a communicator of N availability to shoots (Takei et

al., 2002) and available N is known to increase transcript levels of IPT3 (Wang et al 2004), a key cytokinin biosynthesis enzyme (Takei et al., 2004). Auxin is a central hormone in the development of lateral roots (Overvoorde et al, 2011). Transfer from high to low nitrate media has been shown to increase auxin content in roots, resulting in lateral root outgrowth in *Arabidopsis* (Walch-Liu et al., 2006). *NRT1.1*, the dual affinity nitrate transceptor, functions as a transporter of auxin as well as nitrates (Krouk et al., 2010).

Auxin is a plant hormone controlling many aspects of plant development, including the development of primary and lateral roots (Casimiro et al., 2001; Blilou et al., 2005; Overvoorde et al., 2010), apical meristem development (Jiang et al., 2005), and cell division in root primordia (Ullah et al., 2003; Campanoni et al., 2005).

CN cluster 70 is enriched with genes associated with GO terms for auxin response (Figure 4.17: CN cluster 70, $P = 0.0041$). In this cluster, several cell-cycle or cell wall related auxin responsive genes first decrease in expression and then increase at about 10 h after treatment. Genes here are typically upregulated compared to standard treated plants from 8 h after treatments onwards. *EXT (At2g06850)* is an auxin-responsive protein that is part of a member of environment-driven cell wall modifying enzymes (Xu et al, 1996, Eklof et al., 2010). *AIR9* (*At2g34680*) is another auxin responsive gene from this cluster that is strongly associated with initiation of cell division.

Cortex cluster 18 is enriched with genes associated with GO terms for auxin transport (Figure 4.18, $P = 3.8 \times 10^{-4}$), here 2 auxin efflux carriers are downregulated compared to the standard treatment. Interestingly, they appear to be downregulated in the *Sinorhizobium* treatment as well. *PILS3* (*At1g76520*), is

a putative auxin carrier regulating cellular homeostasis in plants (Barbez et al., 2012) and ZIFL1 (*At5g13750*) has been shown to modulate auxin transport (Remy et al., 2013). This indicates a possible role for these genes in modulating auxin concentrations in cortex cells in response to N availability.

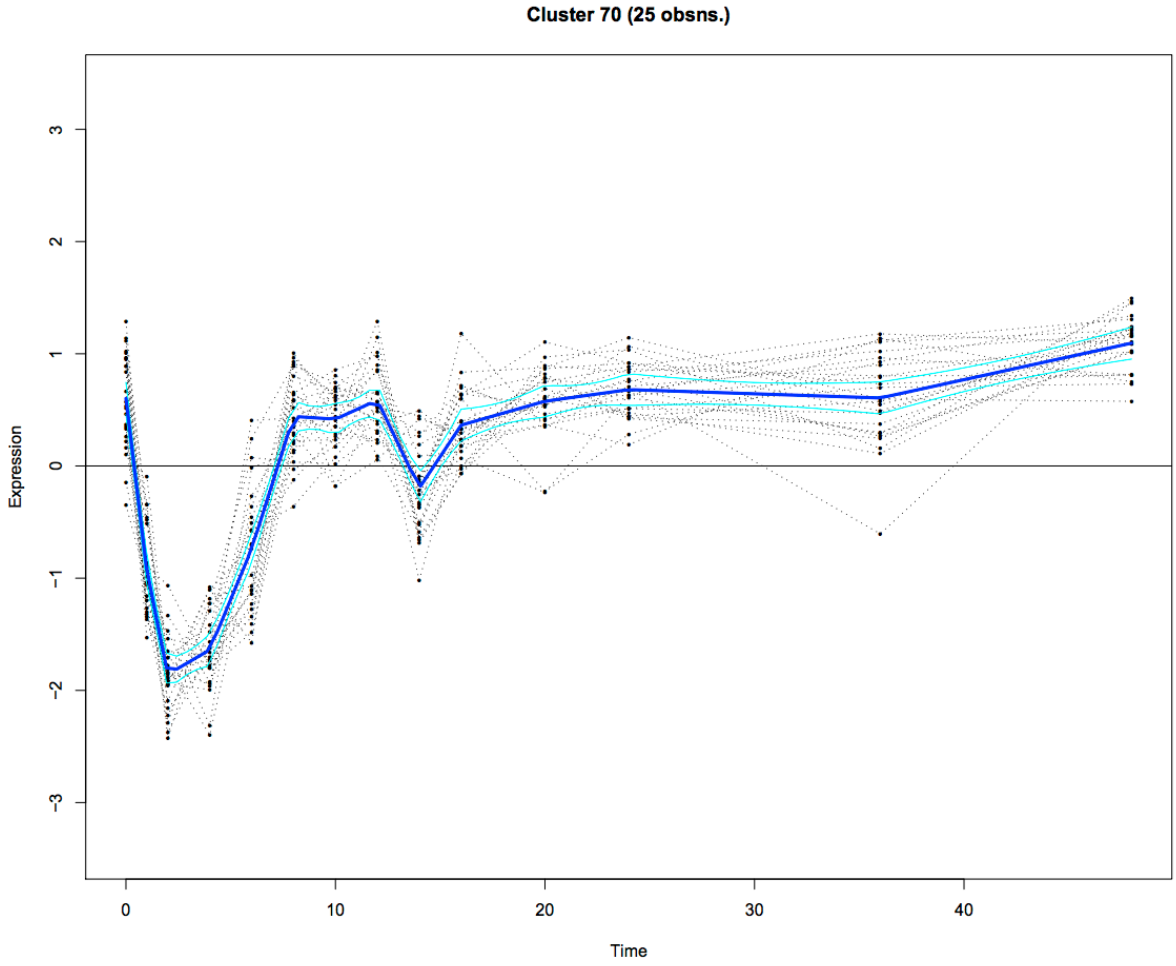

Figure 4.17 CN cluster 70, enriched for genes with response to auxin stimulus GO terms (*P = 0.0041).* Individual gene profiles are shown as grey lines with the mean expression profile in blue. The dashed blue lines indicate the mean ± 1 SD of the cluster. The Y-axis indicates log2 expression normalized on a per gene basis. The X-axis indicates time in hours. Clustering was performed using Splinecluster (Heard et al., 2006), Gene ontology analysis was performed with Gostats (Gentleman et al., 2005).

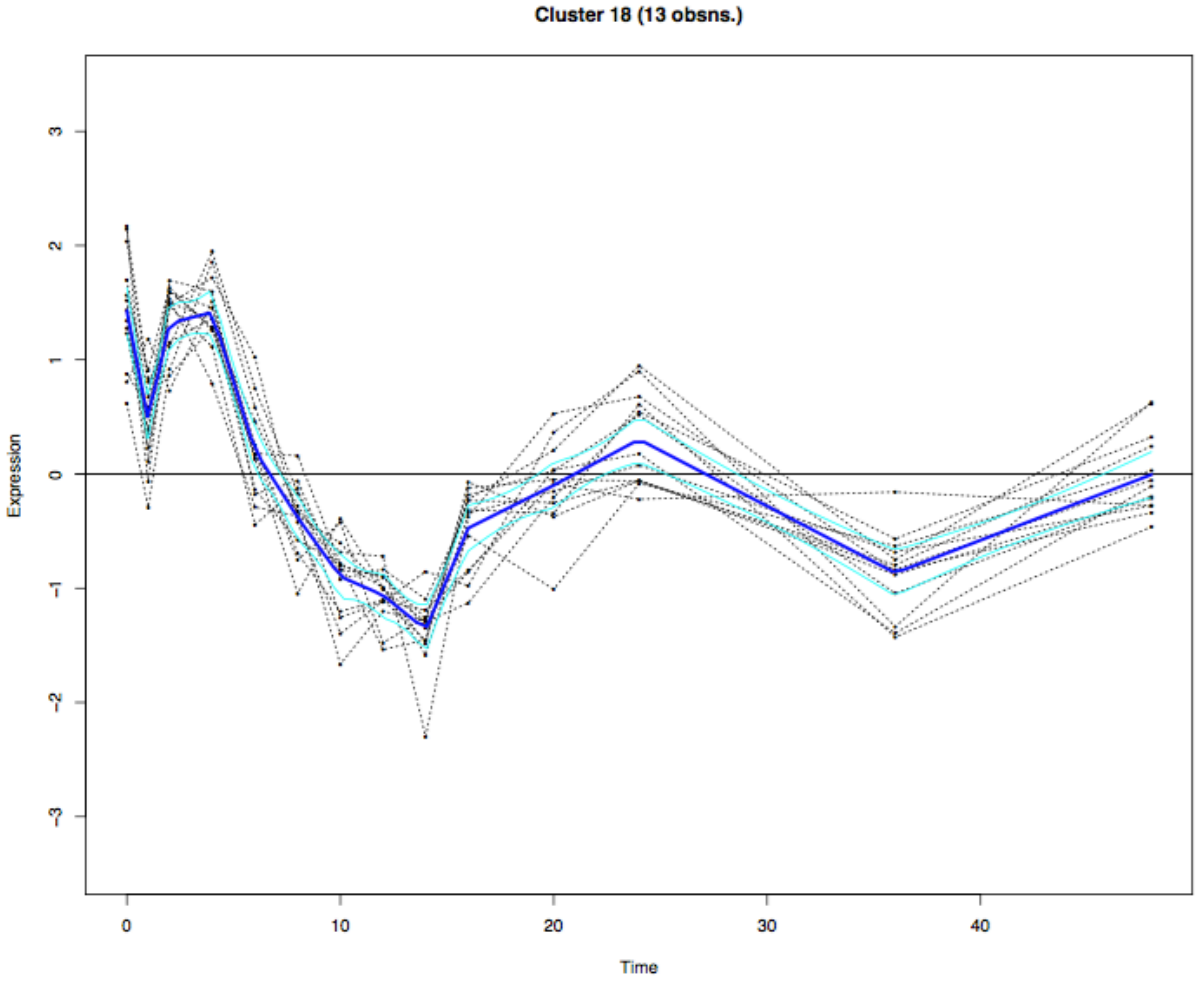

Figure 4.18 CN cluster 18, enriched for genes with auxin transport GO terms (*P* = 3.8 x 10^{-4}). Individual gene profiles are shown as grey lines with the mean expression profile in blue. The dashed blue lines indicate the mean ± 1 SD of the cluster. The Y-axis indicates log2 expression normalized on a per gene basis. The X-axis indicates time in hours. Clustering was performed using Splinecluster (Heard et al., 2006), Gene ontology analysis was performed with Gostats (Gentleman et al., 2005).

4.4.2.6 Genes associated with jasmonic acid GO terms in response to high N

In pericycle cells there are two large clusters enriched with genes associated with GO terms for response to JA (Figure 4.19: PN cluster 59, *P*=1.05 x 10^{-12}) and JA metabolism (Figure 4.20: PN cluster 60, *P* = 3.49 x 10^{-13}). These show downregulation from 4 h after treatment compared to standard and *Sinorhizobium* treated plants. Most of these genes are downregulated in cortex cells as well, but in slightly different expression patterns and thus not clustered

together. These include *PEPR1* (*At1g73080*) and *PEPR2 (At1g17750)*, leucine-rich receptor kinases which have recently been shown to regulate root growth (Krol et al., 2010; Ma et al., 2014). Another interesting group of downregulated genes in these clusters are a group of *JAZ* (jasmonate-ZIM domain) genes: *JAZ1 (At1g19180), JAZ3 (AT3G17860) and JAZ7 (At2g34600)*. This is a group of JA signaling regulators that are targeted for degradation in response to JA. *NAC3 (At3g15500)* is also found in PN cluster 59 and is a putative regulator of JA-associated defense response (Bu et al., 2008). *NAC3* is downregulated in the N treatment compared to the standard treatment.

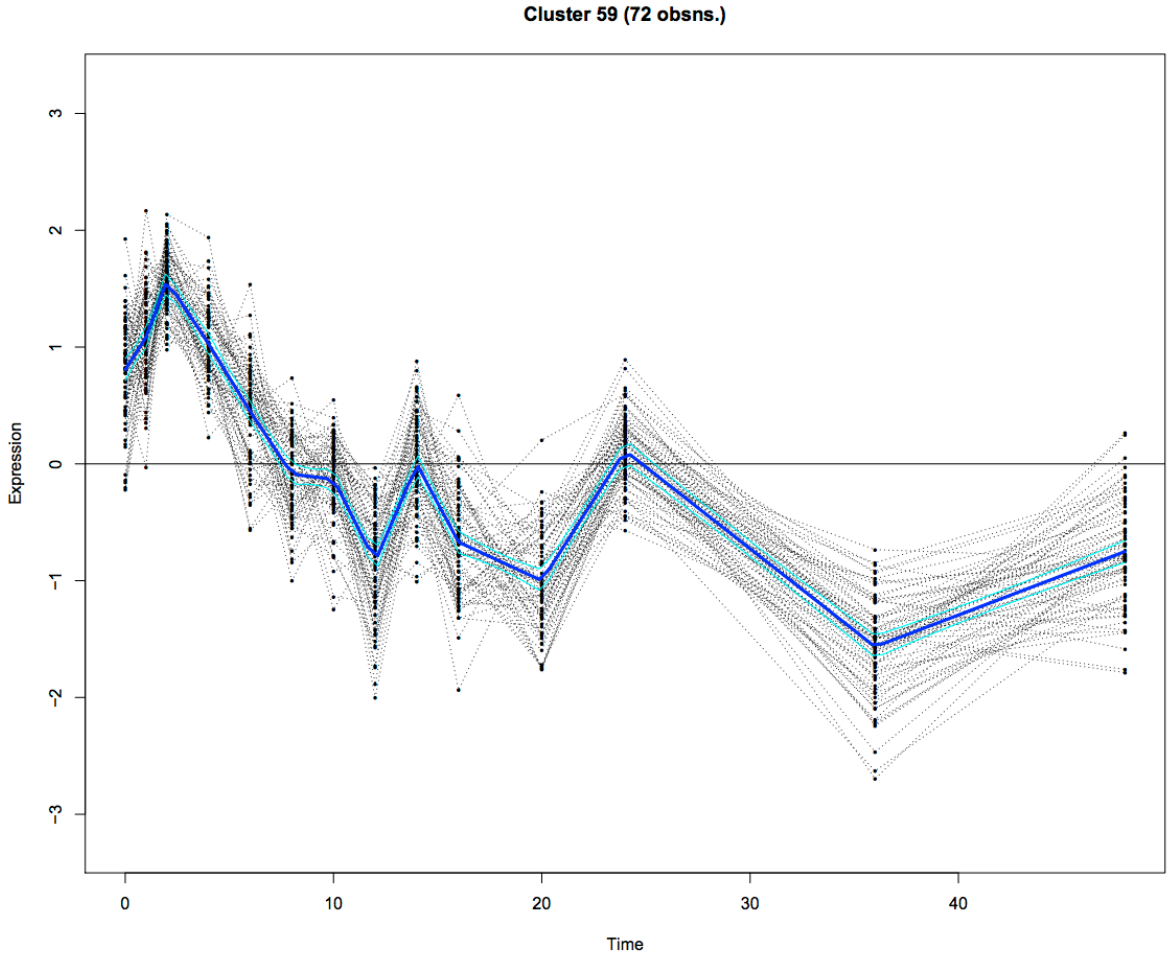

Figure 4.19 PN cluster 59, enriched for genes with JA metabolism GO terms (*P* = 1.05 x 10^{-12}). Individual gene profiles are shown as grey lines with the mean expression profile in blue. The dashed blue lines indicate the mean ± 1 SD of the cluster. The Y-axis indicates log2 expression normalized on a per gene basis. The

X-axis indicates time in hours. Clustering was performed using Splinecluster (Heard et al., 2006), Gene ontology analysis was performed with Gostats (Gentleman et al., 2005).

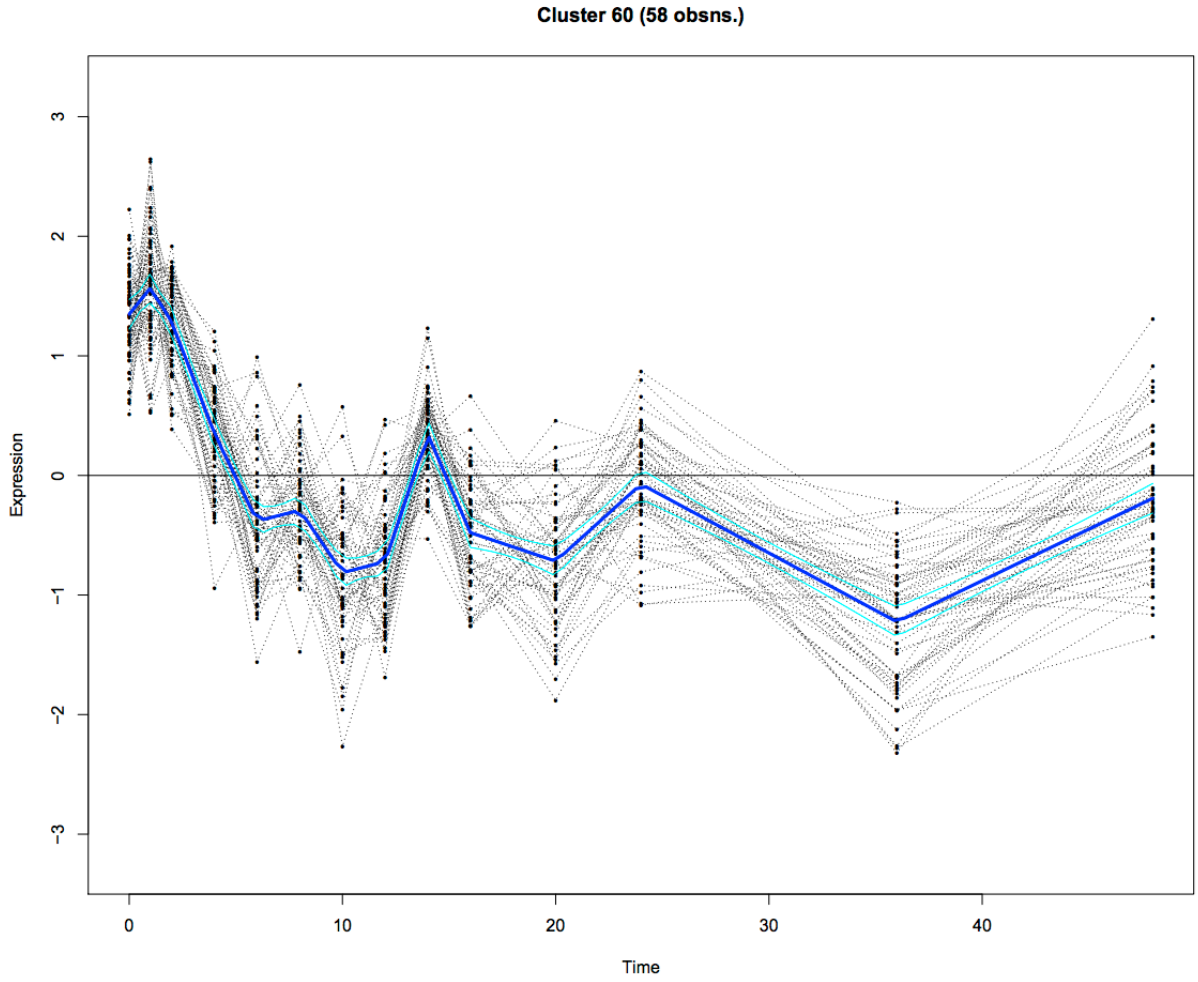

Figure 4.20 PN cluster 60, enriched for genes with JA metabolism GO terms (P = 1.05 x 10^{-13}). Individual gene profiles are shown as grey lines with the mean expression profile in blue. The dashed blue lines indicate the mean ± 1 SD of the cluster. The Y-axis indicates log2 expression normalized on a per gene basis. The X-axis indicates time in hours. Clustering was performed using Splinecluster (Heard et al., 2006), Gene ontology analysis was performed with Gostats (Gentleman et al., 2005).

In cortex clusters we find a cluster enriched with genes associated with GO terms for JA metabolism. CN cluster 21 (Figure 4.21, P = 9.8 x 10^{-8}) is enriched with genes associated with JA metabolism and shows lowered expression levels compared to standard treated plants. Here another JAZ family gene is found to have reduced expression levels compared to the standard: *JAZ10 (At5g13220).* *JAZ1* and *JAZ7* (from PN cluster 59) and *JAZ10* (from CN cluster 21) have been

described as regulators of plant growth, specifically cambium growth, with jaz10-mutants having an enlarged cambium phenotype as well as being specifically expressed in the root tip (Sehr et al., 2010; Sheard et al., 2010).

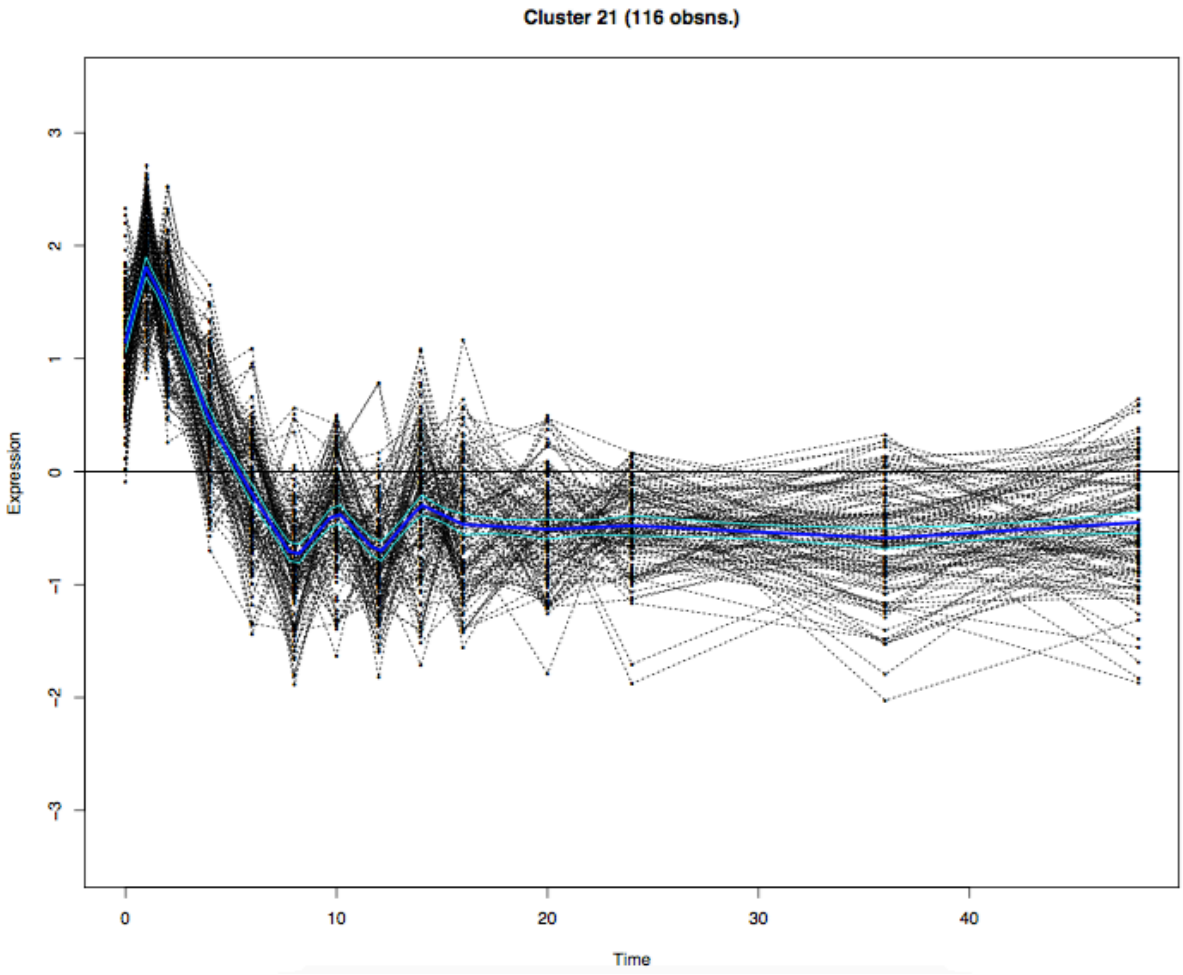

Figure 4.21 CN cluster 21, enriched for genes with JA metabolism GO terms (*P* = 9.8 x 10^{-9}). Individual gene profiles are shown as grey lines with the mean expression profile in blue. The dashed blue lines indicate the mean ± 1 SD of the cluster. The Y-axis indicates log2 expression normalized on a per gene basis. The X-axis indicates time in hours. Clustering was performed using Splinecluster (Heard et al., 2006), Gene ontology analysis was performed with Gostats (Gentleman et al., 2005).

4.4.3 Root cell transcriptional response to *Sinorhizobium*

Arabidopsis exposed to *Sinorhizobium* should not display any transcriptomic characteristics of symbiotic interaction, as no symbiotic interactions have been observed. However, from the phenotypic assays in Chapter 3 it is known that inoculation with *Sinorhizobium* will give rise to a

specific short lateral root phenotype. Other studies have also shown that Nod-factors, secreted by *Rhizobia*, can trigger the production of reactive oxygen species (Wang et al., 2014) and suppression of the immune response (Liang et al., 2013). In this analysis, interactions between *Arabidopsis* and *Sinorhizobium* are studied, as well as hormonal signaling and general responses to bacteria, in order to get an overview of early signaling in *Arabidopsis* in response to *Sinorhizobium* (Figure 4.22). In the *Sinorhizobium* treatment several clusters are enriched for various stress responses: There are clusters enriched for genes specific to defense response, chitin (a component of bacterial cell walls), and for hypersensitivity response (HR), typically these clusters are differentially expressed early, between 2 and 6 hours after treatment.

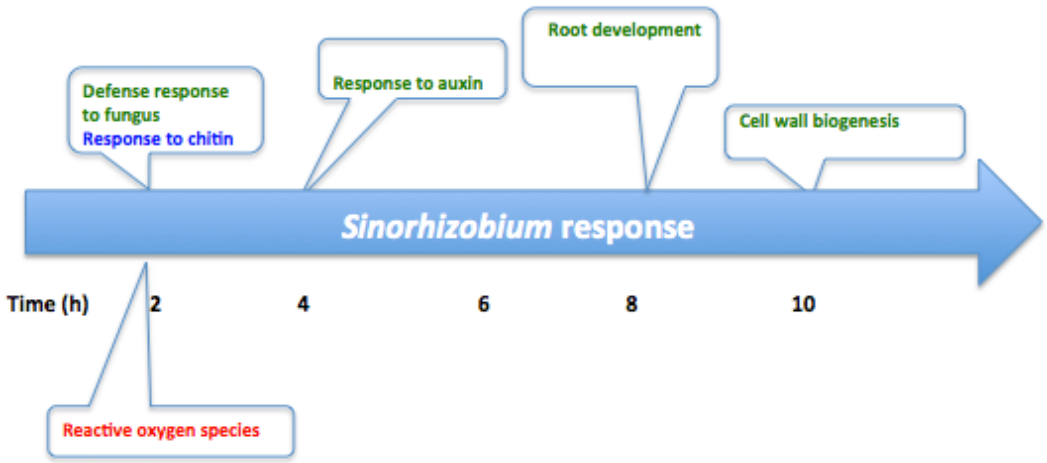

Figure 4.22 Overview of selected enriched GO terms found in different clusters over the duration of the *Sinorhizobium* response. GO terms below the blue arrow of time represent clusters with decreasing levels of gene expression whereas GO terms above the blue arrow of time represent clusters with increasing levels of gene expression. Green terms refer to cortex clusters, red terms refer to pericycle clusters, blue terms can be found in both cortex and pericycle clusters.

4.4.3.1 Genes associated with general defense response GO terms in response to Sinorhizobium

In cortex cells there is one cluster enriched with genes associated with GO terms for defense response to fungus (Figure 4.23, CR cluster 3, $P = 7.8 \times 10^{-5}$). Genes in this cluster are typically found to be upregulated, both in *Sinorhizobium* and N treated plants when compared to the standard treatment. Upregulation of genes was limited to cortex cells. The group of defense genes contains one TF, TGA3 *(At1g22070)*, which is linked to defense against the necrotrophic pathogen *Botrytis cinerea* (Windram et al., 2012). In addition *GXRS13* (*At1g22070*) is found in this group as well. *GXRS13* is a facilitator of *Botrytis cinerea* infection (La Camera et al., 2011).

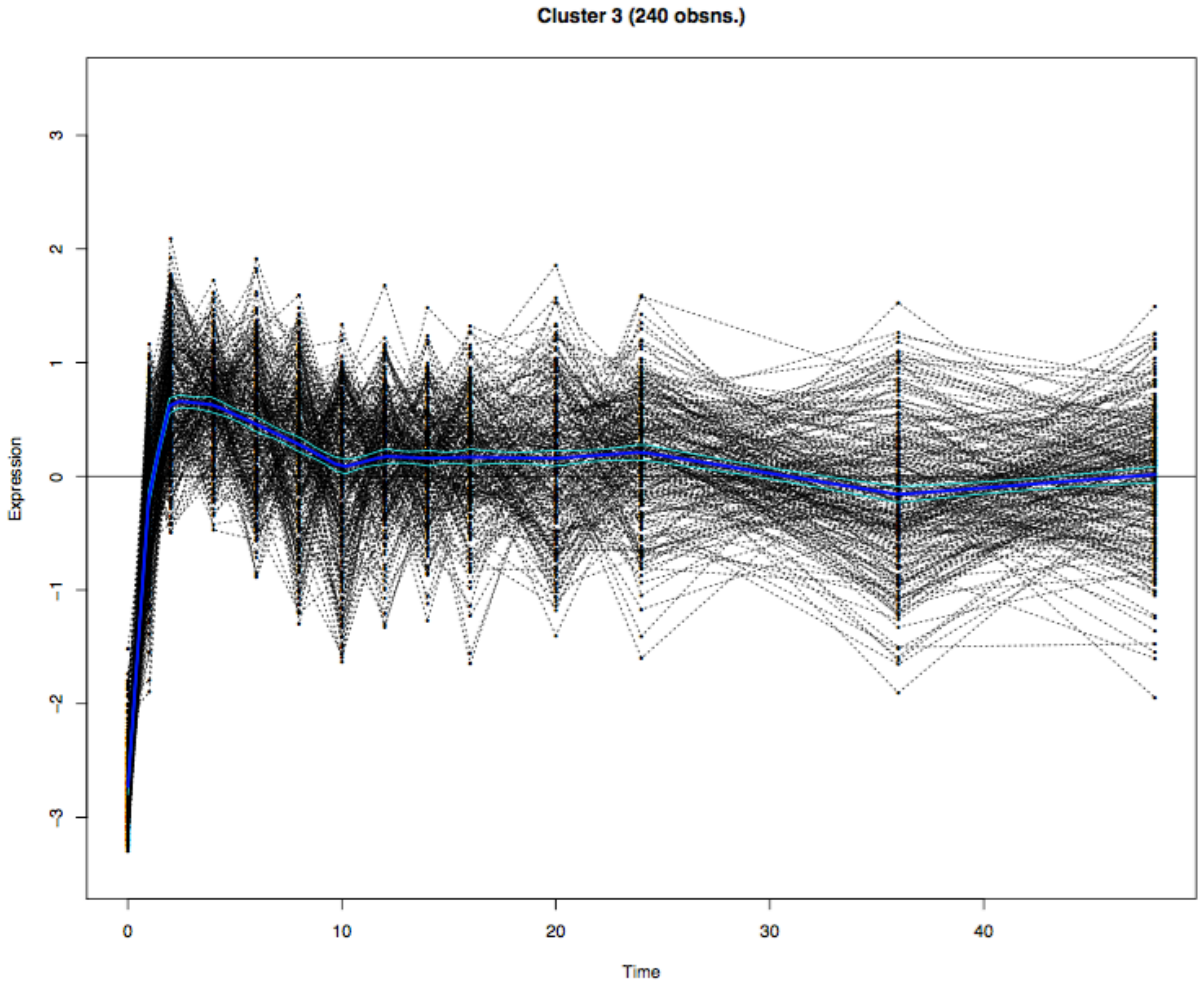

Figure 4.23 CR cluster 3, enriched for genes with defense against fungus GO terms (P = 7.8 x 10^{-5}). Individual gene profiles are shown as grey lines with the mean expression profile in blue. The dashed blue lines indicate the mean ± 1 SD of the cluster. The Y-axis indicates log2 expression normalized on a per gene basis. The X-axis indicates time in hours. Clustering was performed using Splinecluster (Heard et al., 2006), Gene ontology analysis was performed with Gostats (Gentleman et al., 2005).

4.4.3.2 Chitin-response associated genes in response to Sinorhizobium

Multiple clusters of DE cortex genes are enriched with genes associated with GO terms for the response to chitin. Chitin is a long chain polymer of N-acetylglucosamine and a major component of the cell walls of fungi. Chitin is an interesting GO to investigate as there is considerable structural similarity between chitin and Nod-factors, and Nod-factor receptors are thought to have evolved from chitin-responsive receptors (Liang et al., 2014). Two clusters of

cortex cell genes are strongly enriched for genes associated with chitin response GO terms, with the relevant genes showing increased expression levels compared to standard treatment (Figure 4.24: CR cluster 6, $P = 5.4 \times 10^{-5}$; Figure 4.25: CR cluster 7, $P = 1.5 \times 10^{-6}$). Both clusters are characterized by a rise in gene expression immediately (1-2h) after treatment followed by a constitutively high expression level compared to the standard treatment until the end of the experiment. In the standard and N treatments, genes in this cluster typically have a similar rise in expression but lack the prolonged increased expression levels beyond 2 h.

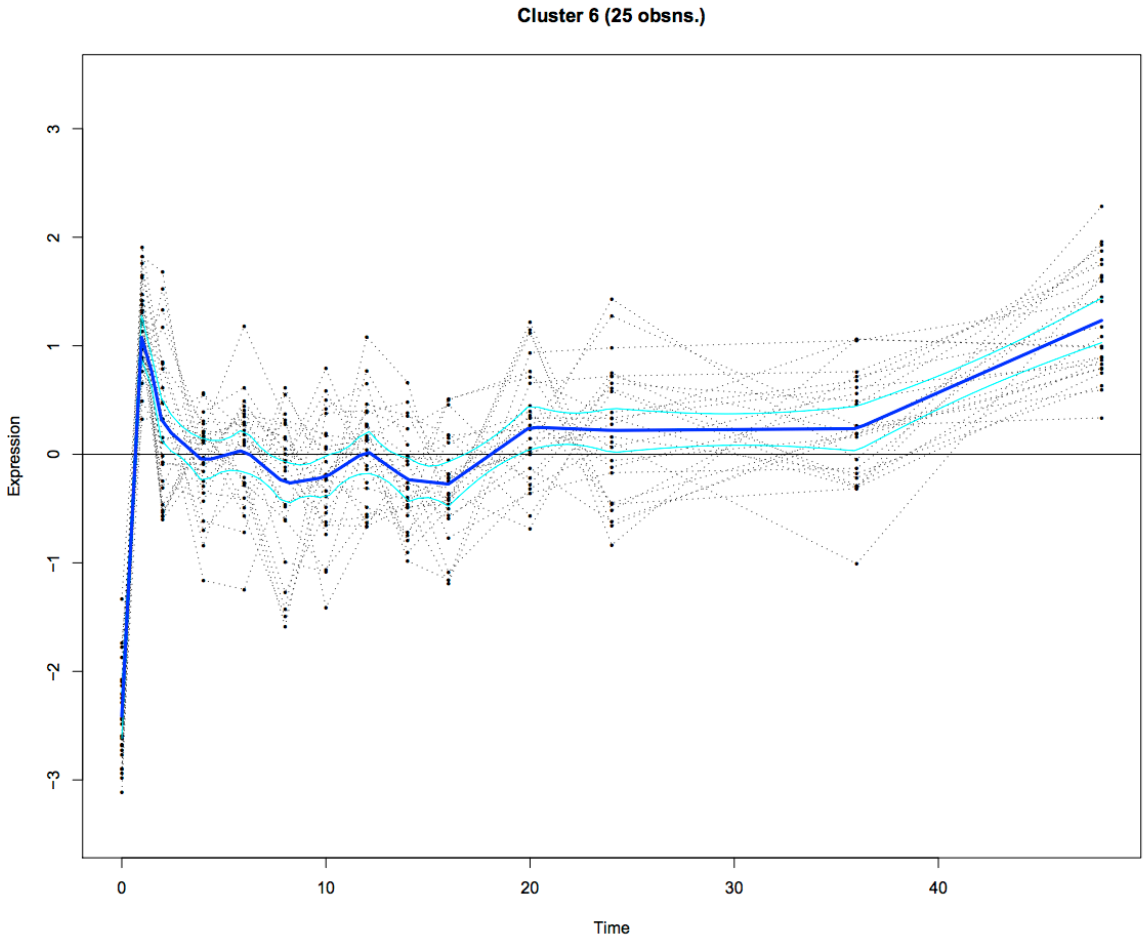

Figure 4.24 CR cluster 6, enriched for genes with response to chitin GO terms ($P = 5.4 \times 10^{-5}$). Individual gene profiles are shown as grey lines with the mean expression profile in blue. The dashed blue lines indicate the mean ± 1 SD of the cluster. The Y-axis indicates log2 expression normalized on a per gene basis. The X-axis indicates time in hours. Clustering was performed using Splinecluster

(Heard et al., 2006), Gene ontology analysis was performed with Gostats (Gentleman et al., 2005).

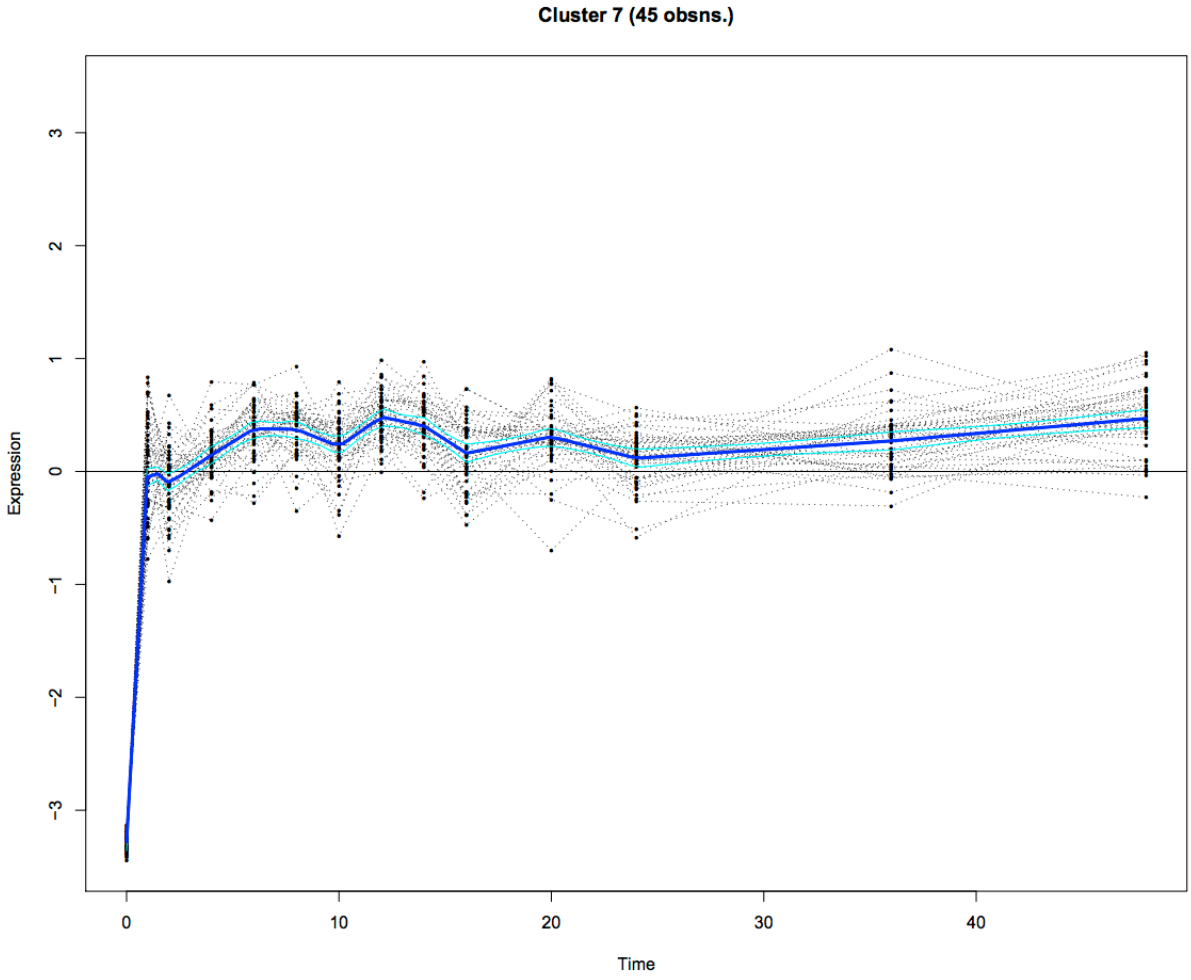

Figure 4.25 CR cluster 7, enriched for genes with response to chitin GO terms (*P* = 1.5 x 10^{-5}). Individual gene profiles are shown as grey lines with the mean expression profile in blue. The dashed blue lines indicate the mean ± 1 SD of the cluster. The Y-axis indicates log2 expression normalized on a per gene basis. The X-axis indicates time in hours. Clustering was performed using Splinecluster (Heard et al., 2006), Gene ontology analysis was performed with Gostats (Gentleman et al., 2005).

Among the chitin responsive genes are several TFs, *ERF11* (*At1g28370*) (CR cluster 6) and *WRKY48* (*At5g49520*) and *MYB44 (At5g67300)* (CR cluster 7). *WRKY48* is a known repressor of the plants basal defense genes (Xing et al., 2008). *MYB44* is a positive regulator of SA-associated defense responses and a negative regulator of JA-associated defense response (Shim et al., 2012; Shim et

al., 2013). These genes are all characterized by having their differential expression limited to cortical cells.

Interestingly, there is one pericycle cluster (PR cluster 21, $P = 3.8 \times 10^{-5}$, Figure 4.26) strongly enriched with genes for response to chitin GO terms, but with a different expression pattern. In PR Cluster 21, gene expression rises sharply in the first 2 h after treatment and then gradually decreases. This cluster contains a different set of genes to the cortex clusters. Interesting is that it again contains a WRKY and an ERF gene, *WRKY46 (At2g46400)* and *ERF105 (At5g51190)*. Both these genes are characterized by having elevated gene expression levels compared to the standard treatment early in the experiment (2 - 6 h), whereafter the expression drops back to the level of the standard treatment. *WRKY46* is a known activator of plant defense genes (Hu et al., 2012) and has specifically been linked to SA-associated plant defense, of which MYB44, expressed in a cortex cluster associated with chitin was an activator (Hu et al., 2012).

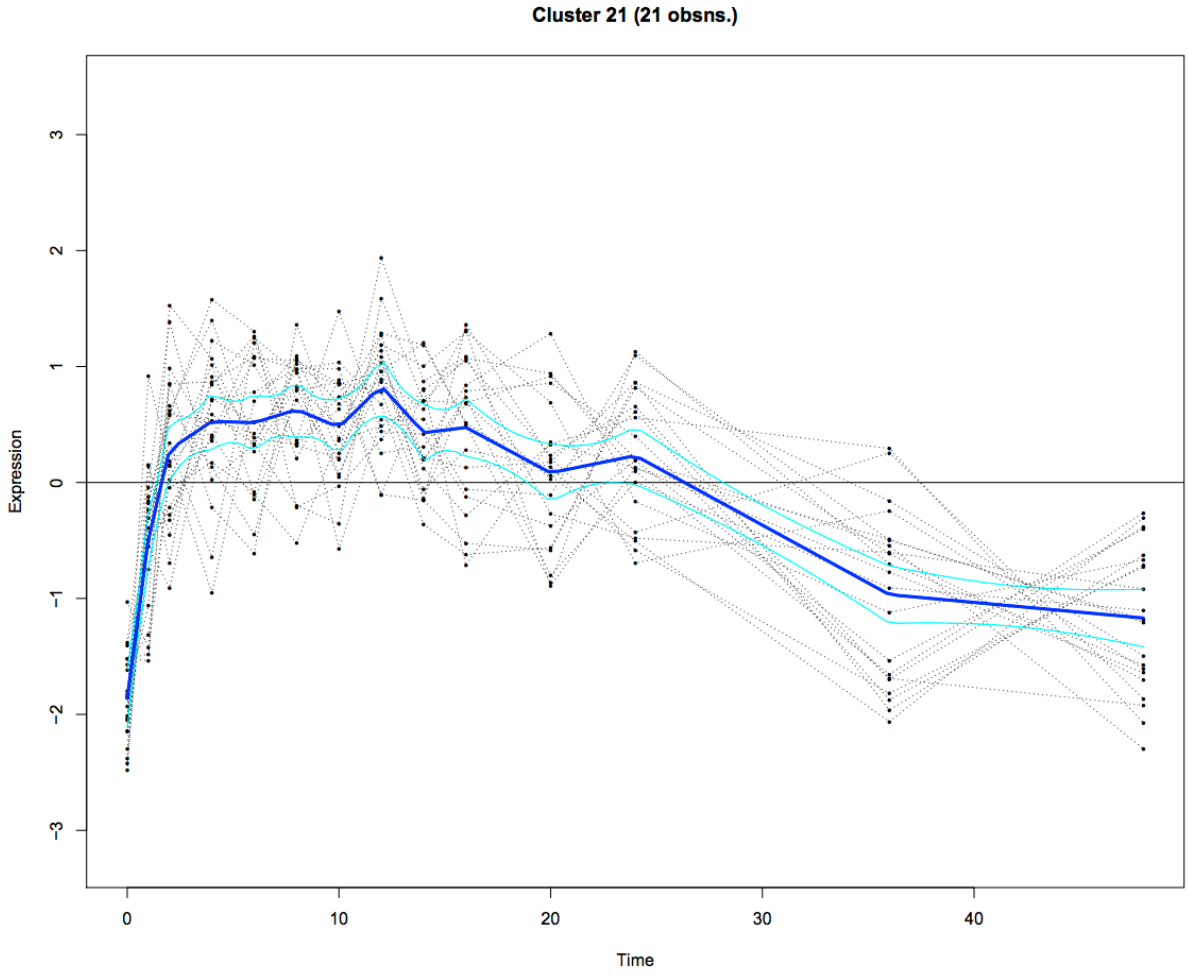

Figure 4.26 PR cluster 21, enriched for genes with response to chitin GO terms (*P* = 3.8 x 10^{-5}). Individual gene profiles are shown as grey lines with the mean expression profile in blue. The dashed blue lines indicate the mean ± 1 SD of the cluster. The Y-axis indicates log2 expression normalized on a per gene basis. The X-axis indicates time in hours. Clustering was performed using Splinecluster (Heard et al., 2006), Gene ontology analysis was performed with Gostats (Gentleman et al., 2005).

4.4.3.3 Genes associated with Auxin GO terms in response to Sinorhizobium

CR cluster 12 is enriched with genes associated with response to auxin GO terms (Figure 4.27: CR cluster 12, *P* = 6.9 x 10^{-5}), with an increase in gene expression at 4 hours followed by a gradual decline at 8-10 hours after treatment. Genes in this group typically upregulated both in N and *Sinorhizobium* treatments

compared to the standard treatment and do not exhibit DE in pericycle cells. This cluster includes the auxin-synthesis associated gene *GH3.4 (At1g59500)*, suggesting the possibility that auxin synthesis is induced in response to *Sinorhizobium* treatment. This group also contains *NAC2 (At5g39610)*, an auxin-responsive TF with a role in lateral root development (He et al., 2005).

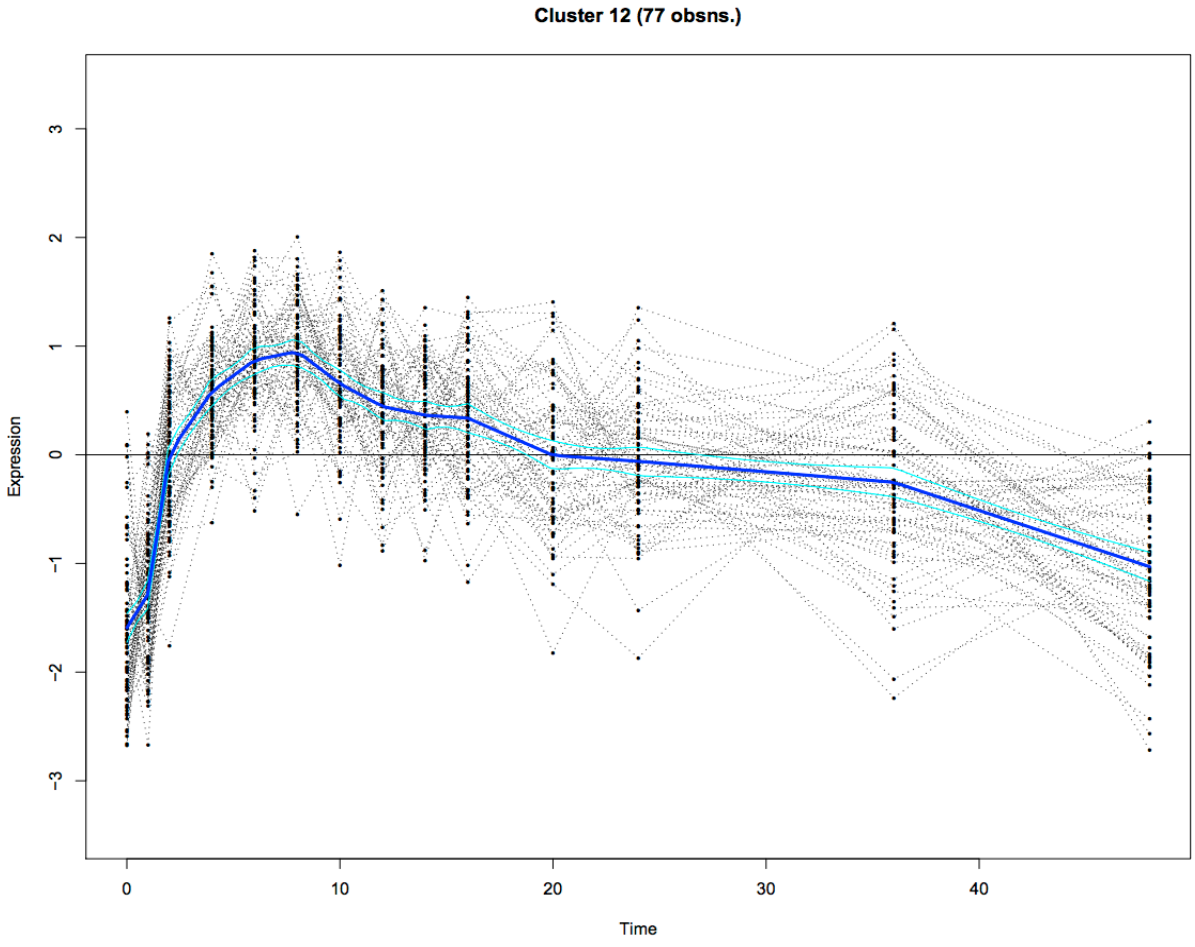

Figure 4.27 CR cluster 12, enriched for genes with auxin response GO terms (*P*=6.9 x 10^{-5}). Individual gene profiles are shown as grey lines with the mean expression profile in blue. The dashed blue lines indicate the mean ± 1 SD of the cluster. The Y-axis indicates log2 expression normalized on a per gene basis. The X-axis indicates time in hours. Clustering was performed using Splinecluster (Heard et al., 2006), Gene ontology analysis was performed with Gostats (Gentleman et al., 2005).

4.4.3.5 Genes associated with reactive oxygen species GO terms in response to **Sinorhizobium**

Reactive oxygen can be an indicator of plant stress and can be purposefully generated by plants during pathogen defense responses (Apel and Hirt, 2004). Several clusters for cortex cells are enriched with genes associated with reactive oxygen species GO terms. The most significantly enriched are clusters 52 (Figure 4.28; P = 5.5 x 10^{-7}) and 56 (Figure 4.29; P = 2.6 x 10^{-13}). Both are characterized by a drop in expression levels upon treatment and, in the case of cluster 56, a secondary peak of expression at 4-6 h. In both clusters, genes expression levels are lower compared to standard treatment, yet similar to levels in the N treatment, it is not clear why this should be the case. Cluster CR 52 contains seven ROS-linked genes, six of which are heat shock proteins: *HSP70b (At1g16030), HSP70T-2 (AT2G32120), HSP23.6 (At4g25200)* or members of a heat shock like superfamily (*At1g52560, At4g10250, At5g37670*), while the sixth gene, *BAG6* (*At2g46240*), has been shown to be induced by another heat shock TF, *HSFA2* (Nishizawa-Yokoi et al., 2009).

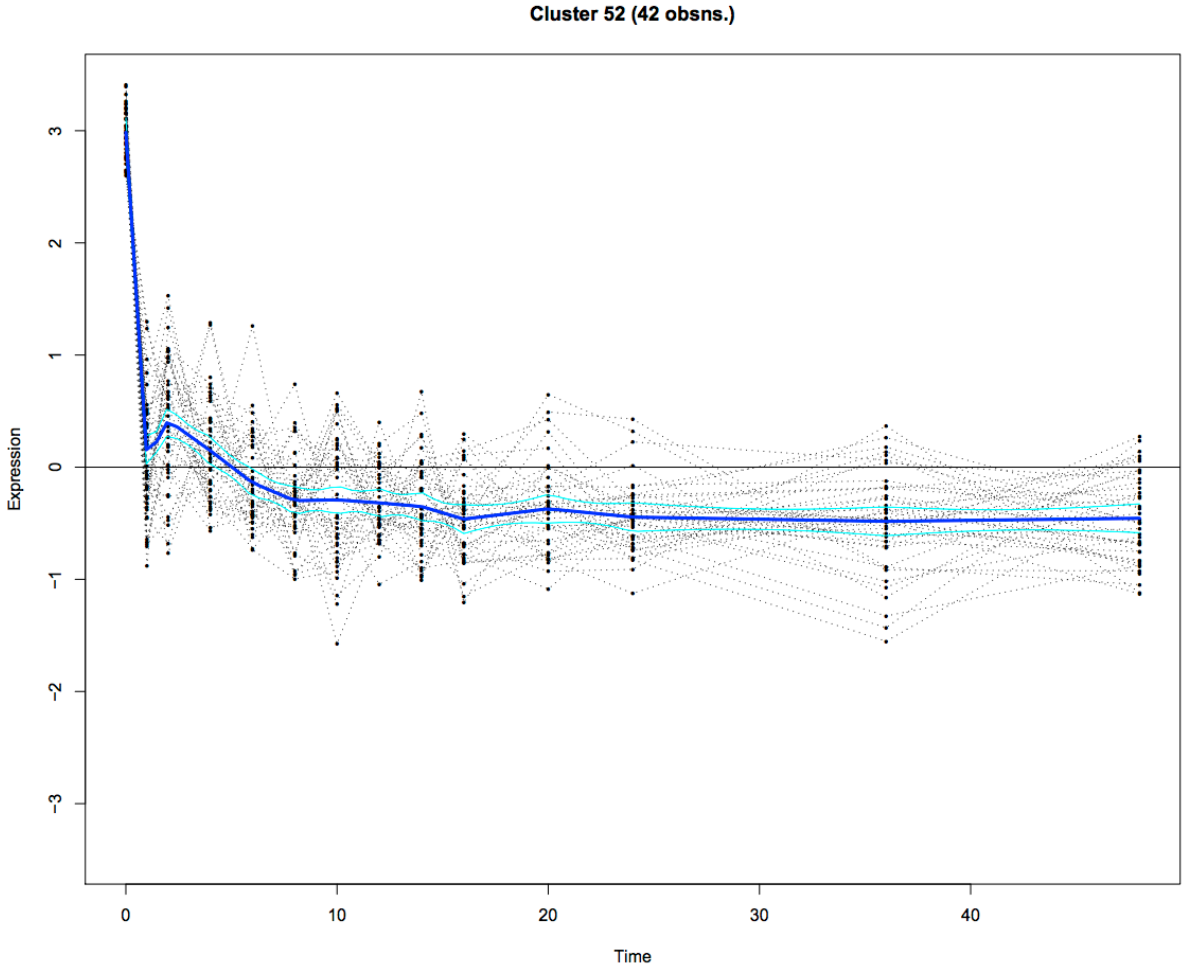

Figure 4.28 CR cluster 52, enriched for genes with reactive oxygen species GO terms (P = 5.5 x 10^{-7}). Individual gene profiles are shown as grey lines with the mean expression profile in blue. The dashed blue lines indicate the mean ± 1 SD of the cluster. The Y-axis indicates log2 expression normalized on a per gene basis. The X-axis indicates time in hours. Clustering was performed using Splinecluster (Heard et al., 2006), Gene ontology analysis was performed with Gostats (Gentleman et al., 2005).

In cluster 56, several genes were associated with reactive oxygen species, with eight out of ten coding for heat shock proteins: *HSA32 (At4g21320), FES1A (At3g09350) HSP17.6A (At5g12030), HSP17.6B* (*At5g12020*) and *TMS1 (At3g08970),* (Charng et al., 2006; Zhang et al., 2010; Wehmeyer and Vierling, 2000; Yang et al., 2009) or proteins associated with heat shock: *At2g20560, TPR10 (At3g04710), HOP2 (At1g62740)* (Busch et al., 2005; Prasad et al., 2010). It is not clear why these genes have similar expression levels in both the

Sinorhizobium and N treatment. It could be related to a lowering of environmental stress, which would certainly make sense in the N treatment.

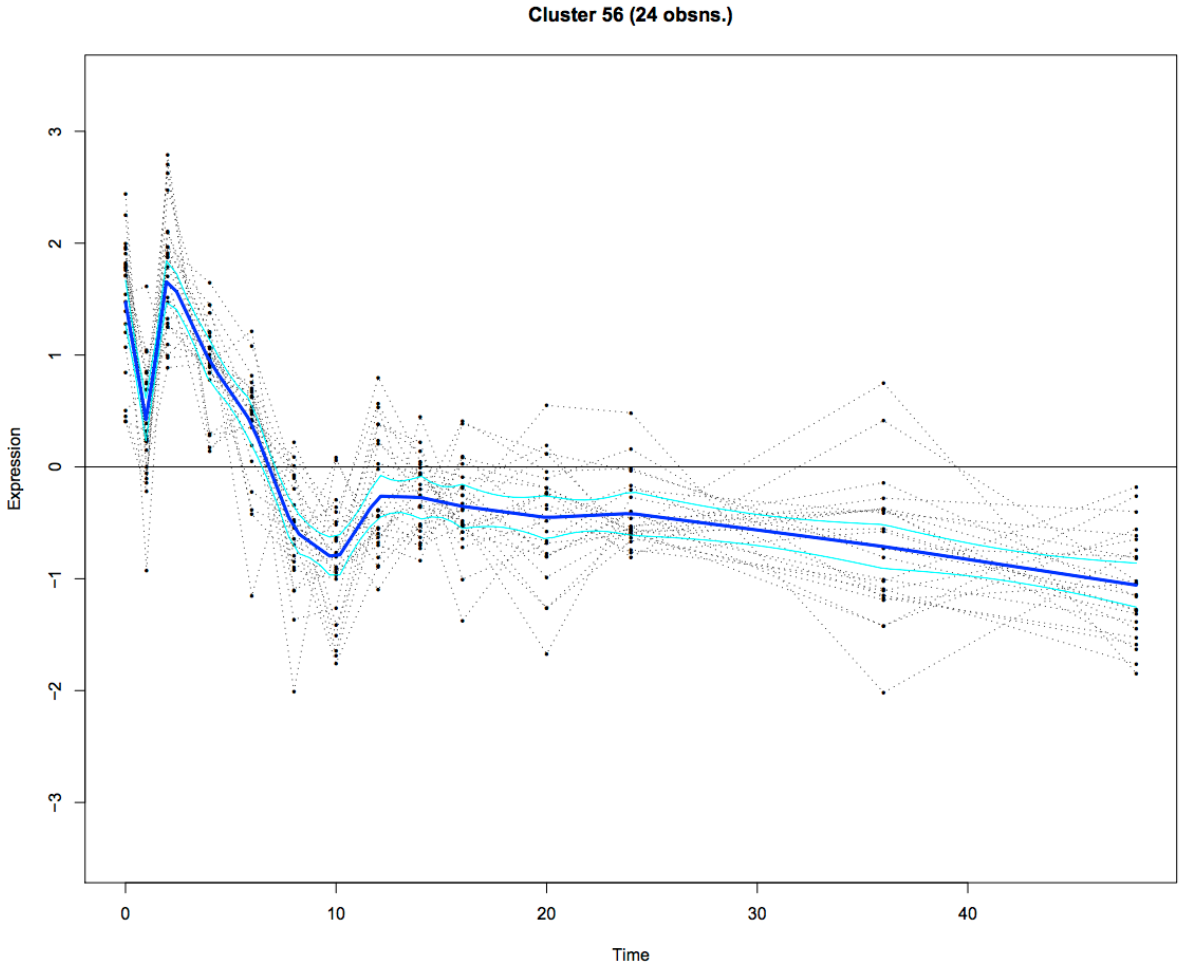

Figure 4.29 PR cluster 56, enriched for genes with reactive oxygens species GO terms (P = 2.6 x 10^{-13}). Individual gene profiles are shown as grey lines with the mean expression profile in blue. The dashed blue lines indicate the mean ± 1 SD of the cluster. The Y-axis indicates log2 expression normalized on a per gene basis. The X-axis indicates time in hours. Clustering was performed using Splinecluster (Heard et al., 2006), Gene ontology analysis was performed with Gostats (Gentleman et al., 2005).

4.4.3.6 Genes associated with cell wall modification GO terms in response to **Sinorhizobium**

CR cluster 15 is enriched with genes associated with cell wall biogenesis GO terms (Figure 4.30, P = 5.68 x 10^{-5}). Genes in this cluster are typically only differentially expressed in cortical cells, with levels of expression in the cortex

consistently elevated in the *Sinorhizobium* treatment compared to the N and standard treatment, the difference being the most pronounced at 12 h+ after treatment. Several genes in this cluster are directly linked to synthesis of components of the cell wall. *GXMT* (*AT1G33800*) is a methyltransferase with a role in the production of xylan, a cell wall component (Lee et al., 2012), and *CESA3* (*AT5G05170*) and *CSI1* both have a role in the production of cellulose (Daras et al., 2009; Gu et al., 2010), where *CESA3* has been shown to be root specific (Pysh et al., 2012).

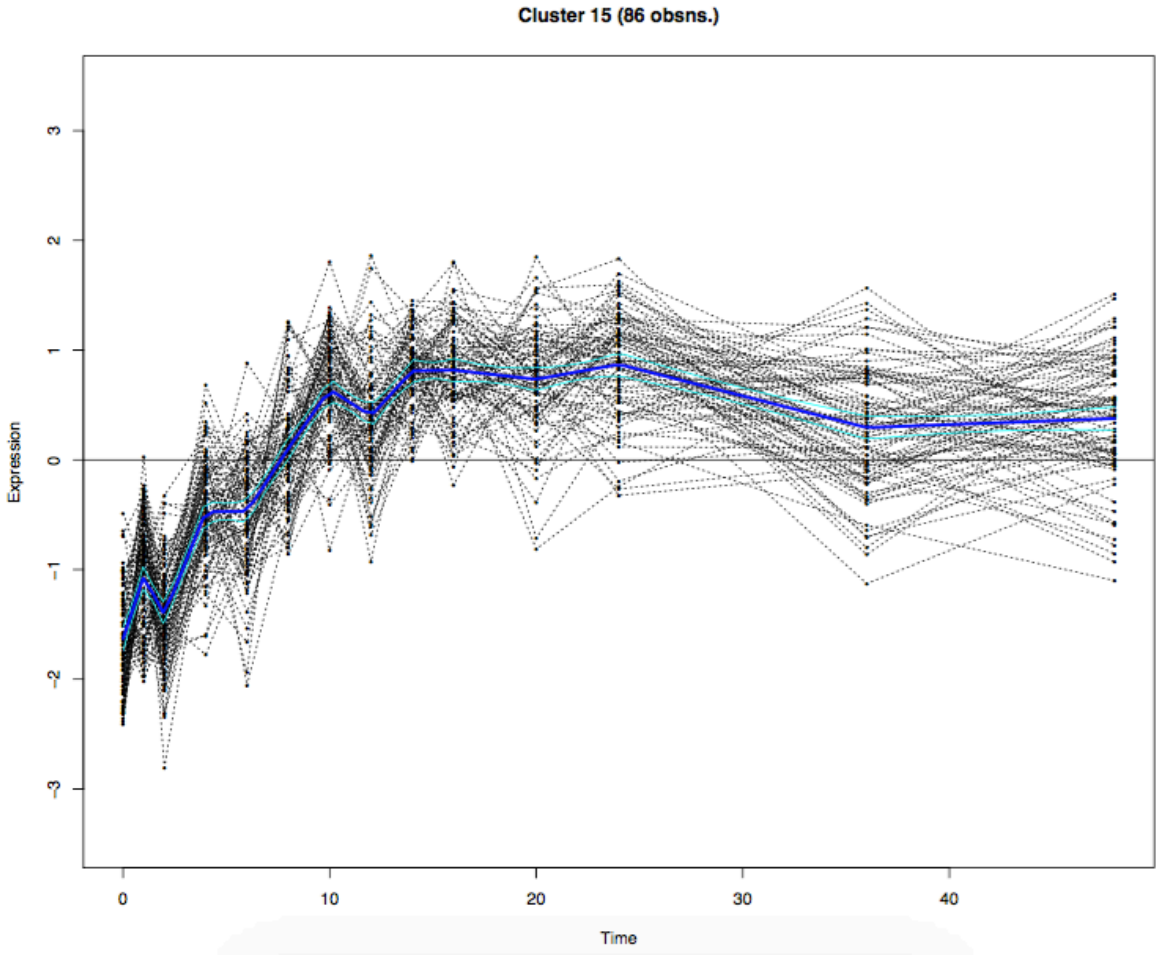

Figure 4.30 CR cluster 15, enriched for genes with cell wall biogenesis GO terms (*P* = 5.68 x 10^{-5}). Individual gene profiles are shown as grey lines with the mean expression profile in blue. The dashed blue lines indicate the mean ± 1 SD of the cluster. The Y-axis indicates log2 expression normalized on a per gene basis. The X-axis indicates time in hours. Clustering was performed using Splinecluster (Heard et al., 2006), Gene ontology analysis was performed with Gostats (Gentleman et al., 2005).

4.4.3.7 Genes associated with root GO terms in response to Sinorhizobium

One cluster of cortex cells was found to be enriched with genes specifically associated with root development GO terms. (Figure 4.31, CR cluster 28, P = 0.00069). Genes in this cluster are upregulated in cortex cells compared to the standard treatment. *PIP5K* (*At1g77740*) and *ABCB1* (*AT2G36910*) are both thought to mediate root tropism through directed transport of auxin (Mei et al., 2013; Wang et al., 2013).

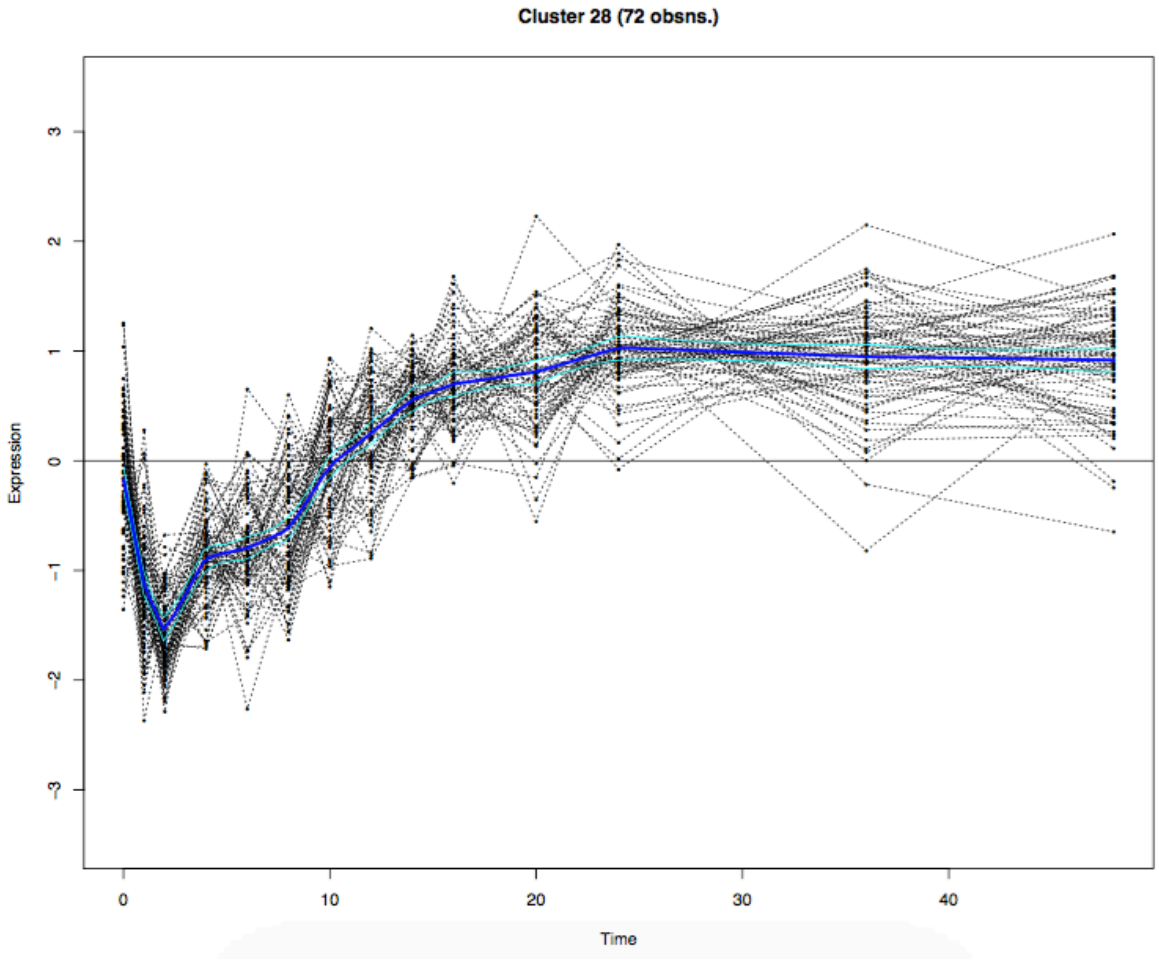

Figure 4.31 CR cluster 28, enriched for genes with root development GO terms (*P* = 0.00069). Individual gene profiles are shown as grey lines with the mean expression profile in blue. The dashed blue lines indicate the mean ± 1 SD of the cluster. The Y-axis indicates log2 expression normalized on a per gene basis. The X-axis indicates time in hours. Clustering was performed using Splinecluster (Heard et al., 2006), Gene ontology analysis was performed with Gostats (Gentleman et al., 2005).

4.5 Comparative analysis of time series data

Changing the available N concentration and inoculation with a nonpathogenic bacteria are very different experimental conditions, but as has been observed in the previous discussion, we occasionally see expression features where Sinorhizobium treated plants will have an expression pattern that is intermediate between the standard and N treated plants. Therefore, it is very informative to test how different the treatments are from each other. In a first analysis, all treatment-cell type combinations were clustered (Euclidean distance, complete linkage) based similarites of gene expression profiles (Figure 4.32). This shows clearly how expression profiles are predominantly dominated by cell identity, with the first split in the hierarchical tree splitting the expression profiles in two groups, one of which is mostly expression profiles from cortical cells, whereas the other is mostly expression profiles from pericycle cells. In the second split, 4 early time points are clustered together (CN2, CN1, PS1, PR1 and PN1), indicating a common element driving gene expression, most likely the removal of the samples from the growth cabinet and administering the different treatments. Within the both cell type clusters, cluster identity is predominantly driven by treatment, i.e. with the groups of the cortex and pericycle clusters, the different treatments largely cluster together. This indicates how the cell type is the most important determinant of gene activity, again highlighting the strength of the cell type-specific analysis of gene expression.

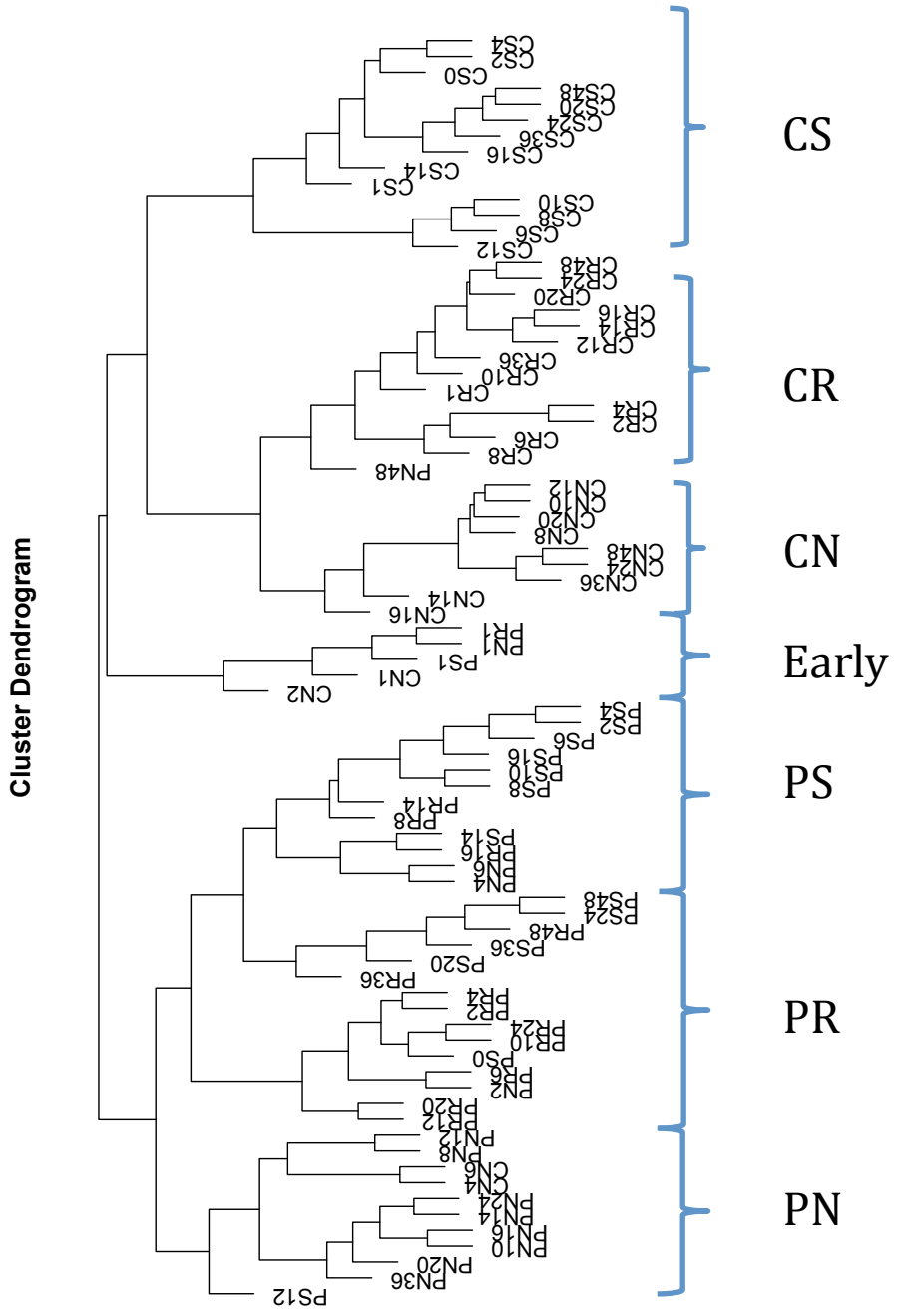

Figure 4.32 Cluster dendrogram (Euclidean distance, complete linkage) of all treatment - cell type combinations. On the right the most identifiying element of the 7 major groups is identified. CS, CN, CR, PS, PN and PR identify the cell type and treatment as before, whereas 'Early' denotes a group of treatment – cell type combination that clustered together, with the common element of being early samples.

Overlapping genes that are DE within the four time series (cortex N and *Sinorhizobium*, pericycle N and *Sinorhizobium*) were identified (Figure 4.33).

The majority of genes were DE in one cell type and treatment only, however there was still a considerable amount of shared DE genes between treatments and between cell types.

GO term enrichment analysis was applied to each set of genes to identify potentially informative pathways and functions common or specific between the responses and cell types. Selected overrepresented GO terms for each group that are unique to DE in one time series only were identified (Figure 4.33). The PR gene sets contained no overrepresented GO terms. This suggests that the response in PR was more functionally dispersed than in the cortex. In most of the other groups, there was significant overlap in overrepresented GO terms between groups. GO terms responding to different plant hormones are overrepresented in all categories, emphasizing the role these hormones play in regulating the response to changing environmental signals.

Immune and defense responses are observed across both cell types and treatments, but they differ in their specificity. Genes associated with chitin responses are only seen in cortex cells treated with *Sinorhizobium* in this analysis. Genes common between N treatment in cortex and pericycle cells have several cell-death related ontologies overrepresented, including cell death induced by a symbiont.

GO terms involved in the organization of the cell wall are overrepresented mostly in the CN group, possibly indicating how the plant has to increase the output of these genes to keep up with the increased root growth following an increase in available N.

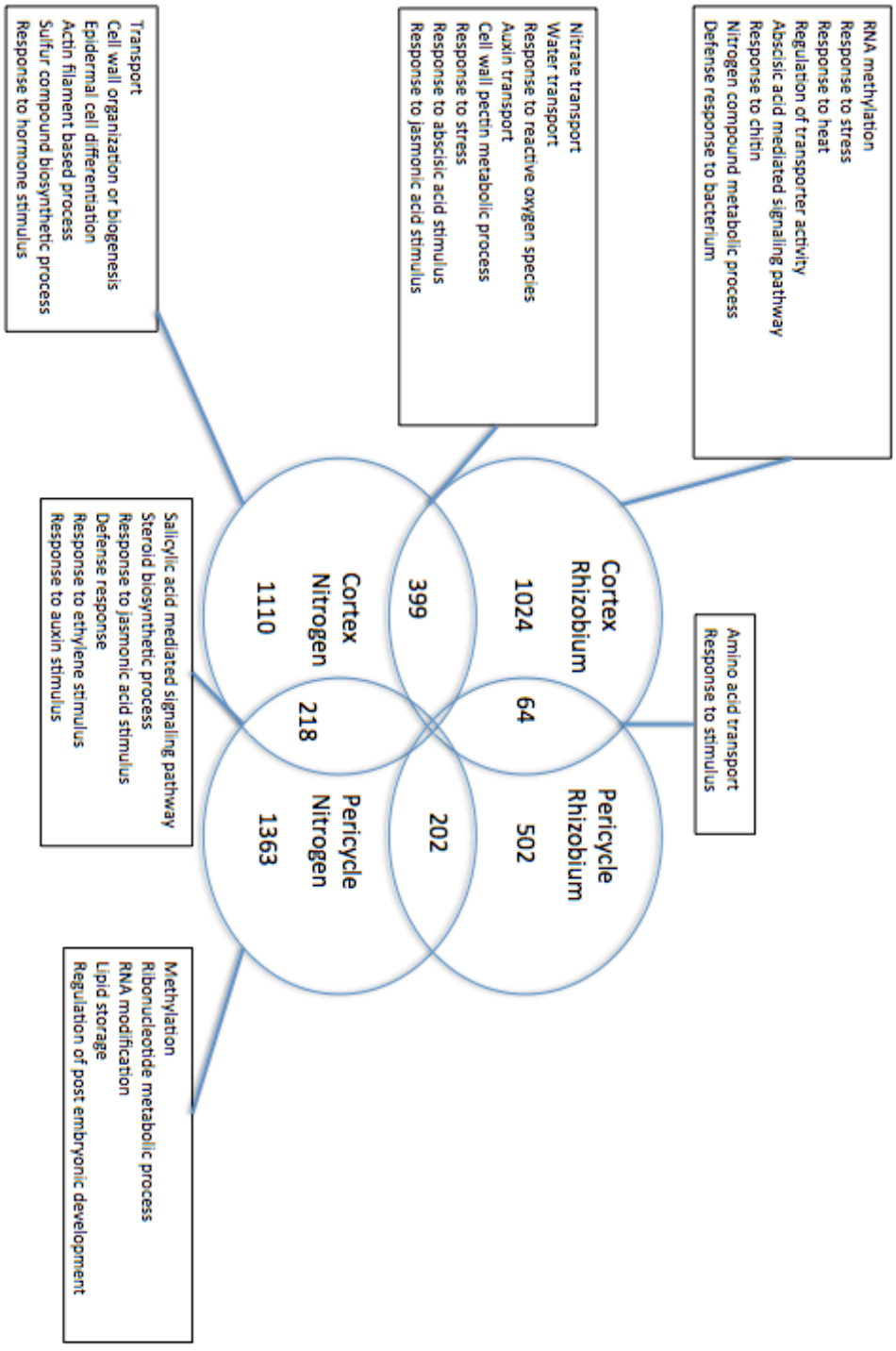

Figure 4.33 Number of genes differentially expressed and selected overrepresented GO terms associated with these genes. Data was obtained by gene ontology enrichment analysis of total DE genes in each treatment/cell type combination, omitting those genes that were also DE in the standard treatment.

4.6 Discussion

This chapter has investigated differential gene expression in N-starved plants in response to either a treatment with N or *Sinorhizobium* in two distinct cell types, cortex and pericycle. Analysis of the transcriptome in these cells over a time series treatment has shown that less than 10% of the genome was differentially expressed in either cell type. We found the overlap between treatments, typically 20-25% (Figure 4.1), to be larger than the overlap between cell types, which was 5-20%. Similarly, we found that clustering of gene expression profiles by treatment and cell type showed that similar cell types tend to cluster together more than similar treatments (Figure 4.32). This highlights the importance of the cell type specific approach used in this study for capturing environmental responses.

Gene expression was characterized by large changes very early after treatment, most changes in gene expression were observed within the first 6 h. Clusters of DE genes show a wave-like activation and inhibition pattern, which is indicative of regulatory pathways being activated (Tyson et al., 2003).

In contrast to the specialization of most gene expression patterns, circadian regulation of key clock genes over time was shown to be very consistent, validating the robustness of the data. A core of circadian genes (*LHY, CCA1* and *PRR9*) was always found in the same cluster (with one exception in the PR time series), as well as having very similar cluster patterns across cell types and treatments.

4.6.1 Overrepresented GO terms in N treated plants suggest regulation of root development

Analysis of clusters of DE genes for enriched GO terms helps to illustrate which biological events are happening in the plant tissues. All pericycle clusters significantly enriched for root development GO terms are characterized by an early change in expression levels (Fig 4.11 and 4.12), indicating the speed with which plants change their developmental response to changes in the environment (Lynch et al., 1995).

N transporter genes of the *NRT2* family show elevated expression levels in cortex followed by a drop in expression later in the time series (Figure 4.13). This response to rescue from N starvation is consistent with their role as N inducible high affinity transporters and has been previously described (Remans et al., 2006). What is more surprising is that the primary low affinity transporter (*NRT1.1*) follows the same expression pattern: it can be assumed that expression of *NRT2.1* is reduced by increasing N concentration in the cytosol (Remans et al., 2006; Miller et al., 2008), but *NRT1.1*, as encoding a low affinity nitrate transporter, would be expected to have consistently high expression levels in the presence of an abundant nitrate source.

The finding of two pericycle clusters: PN cluster 67 (Figure 4.15) and PN cluster 70 (Figure 4.16) with an exceptionally high proportion of mitochondrial chromosome genes can be interpreted as a result of stress response during N starvation and the subsequent alleviation of that stress. It is likely that the number of mitochondria is reduced under N stress (Giegé et al., 2005). When the stress is subsequently alleviated there is regulation of a coordinated effort to re-establish the number of mitochondria in its cells. Evidence for this was shown

in (Giegé et al., 2005), where following a reduction in the number of mitochondria after sucrose starvation, genes involved in the biogenesis of mitochondria were shown to be coordinated at the posttranscriptional level. Giegé et al. (2005) were unable to find evidence for coordination at the transcriptional level as be suggested by our results. However it is possible that the higher temporal and spatial resolution of our data can account for finding evidence for transcriptional coordination.

Plant hormone associated GO terms showed a wide variety in regulation. CN cluster 18 (Figure 4.18) contains two auxin transporter genes that are both downregulated in the N and *Sinorhizobium* treatment. ZIFL is a known promoter of polar auxin transport, facilitating auxin transport from root to shoot (Remy et al., 2013). A reduction of polar auxin transport through a reduction of expression as observed here can be the result of an increase in N availability in the environment, necessitating the promotion of root growth to make maximal use of this. Mechanisms in which nitrate inhibits cell-to-cell auxin transport have been described for *NRT1.1* (Krouk et al., 2010).

The finding of a decrease in expression levels in clusters of genes enriched for JA GO terms (Figure 4.19, Figure 4.20 and Figure 4.21) is consistent with findings in literature where JA genes are upregulated during nutrient starvation and quickly downregulated after resupply (Armengaud et al., 2004)

4.6.2 Overrepresented GO terms in the Rhizobial response suggest a high level of stress and hormonal regulation

Several clusters of cortex and pericycle genes that increase their expression early in the time series are enriched with genes for chitin response GO terms (Figure

4.24, 4.25 and 4.26). The pericycle cluster (4.26) has a delayed activation compared to the cortex clusters (4.24 and 4.25), this is potentially explained by the closer proximity of cortex cells to the outer layers of the plant, placing them in closer contact to rhizobia. Chitin has a strong structural resemblance to Nod factor (Figure 1.4) and it has been hypothesized that the Nod/Myc factor signaling in bacterial symbiosis in plants has evolved through co-opting of PAMP-recognition signaling by symbiotic bacteria (Liang et al., 2014). Therefore it is tempting to use the enrichment of chitin receptive genes in *Arabidopsis* here as an indicator of the veracity of this theory, rather than as a general response to PAMPs. Further studies where chitin responsive genes are analyzed in detail between treatments with *Sinorhizobium* and various pathogenic bacteria, as well as AM are necessary to answer this question.

In a cluster of cortex genes that increases expression early in the time series (Figure 4.22), genes associated with fungal defense GO terms are enriched. This suggests that *Arabidopsis* responds to *Sinorhizobium* as if it is a pathogen. Rhizobia are known to use pathogen-like effector proteins to be able to distinguish between compatible and non-compatible potential symbionts (Kambara et al., 2009; Deakin and Broughton, 2009).

Two clusters (Figure 4.28 and 4.29) show a repression of the expression of several heat shock proteins (HSP) family members immediately upon treatment. HSP are indicators of a stress response and their drop in expression seems to indicate the alleviation of a stress, which is paradoxical, given the concurrent observation of a increase in pathogen stress-related genes. It is possible that plants reprioritize their stress signaling when going from mild N

starvation into potential pathogen stress, and the DE of different stress associated genes therefore could be what was observed here.

Auxin-response genes follow a different activation pattern, with a slow increase in expression (Figure 4.27), starting at 2 h, peaking at 8 h and declining afterwards. This decrease is consistent with analysis of the root phenotype in response to *Sinorhizobium* inoculation in Chapter 3 (Figure 3.1 and 3.2), where lateral root growth was arrested in 6 day old *Arabidopsis* seedlings. Free-living rhizobia have the ability to synthesize auxin (Badendoch-Jones et al., 1982), a process which has been shown to have a direct effect of nodulation in *M. truncatula* (Pii et al., 2007). Thus, further research is needed in the role of auxin in response to *Sinorhizobium* inoculation.

A cluster of genes in cortex cells that increase their expression gradually during the time series is enriched with GO terms for cell wall modification processes (Figure 4.30). The role of cell wall modifications in the process of root growth is well known. Mutants of cell wall synthase genes have reduced root and hypocotyl growth (Arioli et al., 1998; Fagard et al., 2000). On the other hand, cell wall modifications can be a defense response to invasive pathogens (Sanchez-Rodriguez et al., 2009; Bellincampi et al., 2014). Genes in this cluster have increased expression levels compared to the standard treatement, making the latter explanation more likely.

4.6.3 Analysis of similarities between enriched GO terms

Analysis of enriched GO terms for all DE genes shows how pericycle cells have distinct environmental response characteristics from cortex (Figure 4.32 and 4.33). In PR, no enriched ontologies could be detected, suggesting that in the PR response there is a large number of functionally diverse processes

active, making it difficult to detect particular whole processes being regulated through use of GO enrichment analysis.

Defense response is a GO that is found enriched everywhere, not restricted to either cell type or treatment. Certain aspects of defense response however are more specific: CR is enriched for stress response and response to chitin.

The PN time course was unique in the sense that all overrepresented GO terms here were unique to this time course, whereas in other groups there was overlap in overrepresented GO terms between time courses. In PN we observed regulation of methylation and RNA modification, suggesting a role for epigenetic modification in response to N stress.

In this analysis, responses to different hormones were found enriched in different time courses. Response to auxin stimulus was enriched in the group with overlapping genes between PN and CN, whereas auxin transport and auxin biosynthesis was enriched in the overlapping group between CN and CR. It appears in our data that genes regulating transport and biosynthesis of auxin are restricted to cortex cells, whereas regulation through auxin is a process that is found in pericycle cells as well (Deinum et al., 2012).

4.7 Conclusion

These analyses have yielded several interesting conclusions that merit further in-depth analysis through additional experiments. It has shown considerable differences between treatments and even larger differences between cell types, emphasizing the importance of tissue specific analysis of gene expression. In N treatment, major observations are DE of N transporter and root development

genes, potential hormonal regulation through auxin and JA, and an unexpected link to the mitochondrial chromosome. In the *Sinorhizobium* treatment major observations include a rapid increase in stress and bacterial defense genes, several clusters specifically overrepresented for chitin response genes and potential regulation through auxin.

A 'meta analysis' of all DE genes together further emphasized how there is more similarity between treatments than between tissue types, as pericycle cells were found to be functionally almost unrelated to cortex cells in terms of their responses and more similarities were found between differently treated cortex cells than between cortex and pericycle cells, similar to what was previously found in Gifford et al. (2008).

Chapter 5

Gene regulatory network inference

Examining overrepresented ontologies in clusters of genes provides a timeline of processes that change, but has limited power at characterizing regulatory interactions between genes. However, time series expression data enables analysis of regulation since it can be used to infer the topology of biological regulatory networks. Using network inference methods it becomes possible to make predictions on regulatory interactions and how they are influenced by different treatments or under different conditions (Hecker et al., 2009; Emmert-Streib et al., 2012). Furthermore, these networks can enable prediction of the effect of genetic perturbations (Krouk et al., 2013).

5.1 Experimental design

Given the number of genes differentially expressed in the time series data (1635-4449 per time series), we limited our interaction model to only allow interactions starting with known or putative TFs. Genes were designated as TFs by a synthesis of functional annotations (Gene Ontology) and gene family annotations (TAIR), with data from NCBI Conserved Domains database indicating presence of conserved protein domains indicative of DNA binding combined with gene annotations indicative of regulatory effect.

As described in more detail in section 2.10, the bioconductor package GRENITS (Morrissey, 2013) was used for gene regulatory network inference, with the mean expression levels from all replicates of each gene at a time point as the input. NIACS (Network interference analysis and correction software,

Wang et al., 2014) was used to correct for regulator interference (the effect where two regulators with similar dynamics mutually suppress the probability of regulating a target in the model as well as the link strength). The GRENITS method (see 2.10.1) requires the time series time spacing to be conductive with transcriptional time scales, thus we limited ourselves to time points 0, 1, 2, 4, 6, 8, 10, 12, 14 and 16. GRENITS gave the posterior probability of each directed link between two genes. If a link probability exceeded a threshold of 0.4, this link was considered to exist in the network. Six networks were generated, one per cell type for each treatment, including the standard time series. Within the networks, nodes represent genes and edges represent regulatory interactions, either activating or inhibiting (Figures 5.2-5.7).

5.2 Results

5.2.1 Cell type regulatory network topology

Networks covered all temporal patterns observed in cluster analysis (see section 4.3), only missing out a small number of clusters, so the overall dynamics of the transcriptional response was accurately represented (Figure 5.1). All network data can be found in the supplemental materials (S7).

The cortex networks (Figure 5.2-5.4), along with PR (Figure 5.7) have between 785 and 981 nodes and 1099 to 1347 edges. PN (Figure 5.6) and PS (Figure 5.5) have a larger number of nodes and interactions, 1557 and 1651 nodes and 2017 and 1973 edges respectively. This reflects the larger number of differentially expressed genes in these networks. Between 37 and 48 % of DE from the dataset were incorporated into the networks (Table 5.1), with an average of 6.3 targets per TF.

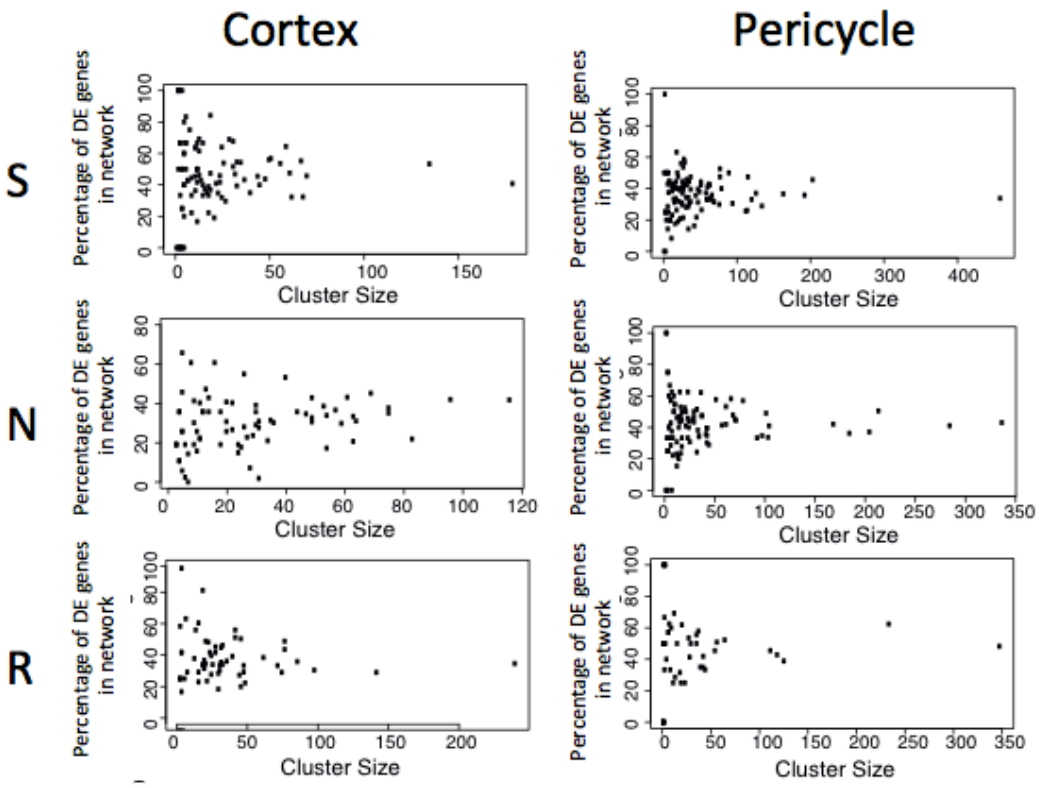

Figure 5.1 Decomposition of DE gene regulatory clusters by presence in the inferred network. Scatter plot shows the proportion of genes in a given cluster that are in the network plotted against the cluster size. Clusters were generated with GRENITS (Morrissey, 2013). Six treatments/tissues shown (Pericycle and Cortex cells, treated with N, rhizobium and standard).

The edge-to-node ratio is similar for all six networks, with 1.2 to 1.4 edges per node. One striking difference between cortex and pericycle networks was the edge count of top hub genes. Hub genes are defined as highly connected genes in the network (Fuller et al., 2007), here we define major hubs as TFs with more than seven targets: In cortex networks the top hub genes typically have half as many edges as the top hub genes in pericycle networks (~30 vs. ~75), (Tables 5.2 and 5.3). There are only a couple of major TF hubs present in more than one network, *BHLH093* (*At5g65640)* is present in all except PS and *LHY* (*At1g01060*) is present in six experiments and a major hub in four. Most of the hubs present in multiple networks are tissue specific: *HD2A (At3g44750*), *ARR17* (*At3g56380*) and *NF-YA10* (*At5g06510*) are in all three cortex conditions and

NTL9 (At4g35580) and *ING2* (*At1g54390*) are in all 3 pericycle networks. There is little overlap between targets of any of the common hubs. Hub *TGA1* (*At5g65210*) has two common targets in the CS and PN networks: *At5g27395* and *NOP56 (At1g56110*).

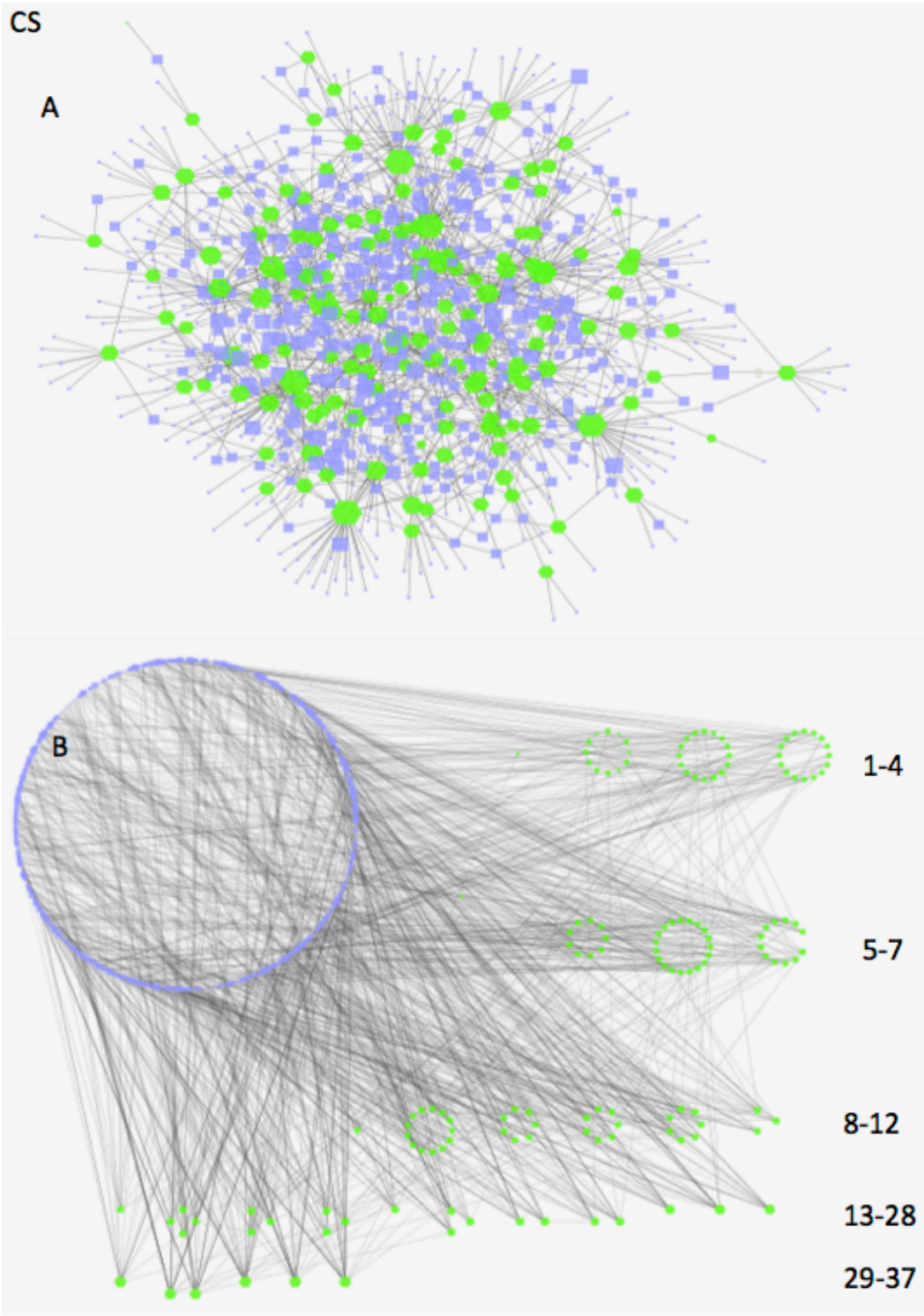

Figure 5.2 CS Inferred regulatory network using the GRENITS (Morrissey, 2013) algorithm. Green nodes are TFs, blue nodes are regular genes. Size of nodes is correlated with number of inferred regulatory interactions (i.e. big nodes regulate more) (A) General representation of the network (B) TFs grouped by number of regulatory interactions, each group of TFs has the same predicted number of regulatory interactions (edges) within the group. TFs with the lowest (1-4) number of predicted interactions are at the top, TFs with the highest (29-37) number of predicted interactions are at the bottom.

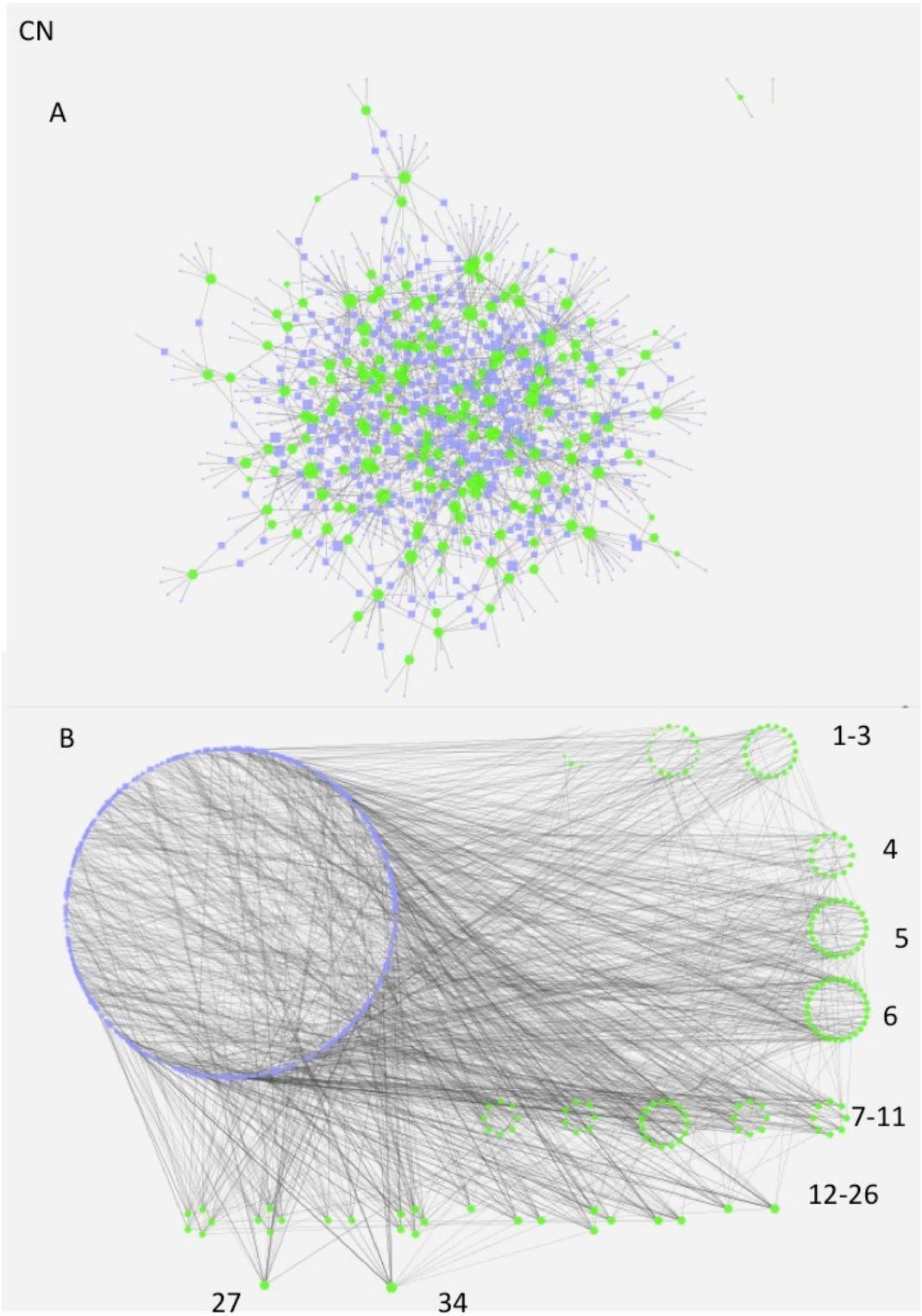

Figure 5.3 CN Inferred regulatory network using the GRENITS (Morrissey, 2013) algorithm. Green nodes are TFs, blue nodes are regular genes. Size of nodes is correlated with number of inferred regulatory interactions (i.e. big nodes regulate more) (A) General representation of the network (B) TFs grouped by number of regulatory interactions, each group of TFs has the same predicted number of regulatory interactions (edges) within the group. TFs with the lowest (1-3) number of predicted interactions are at the top, TFs with the highest (12-26) number of predicted interactions are at the bottom.

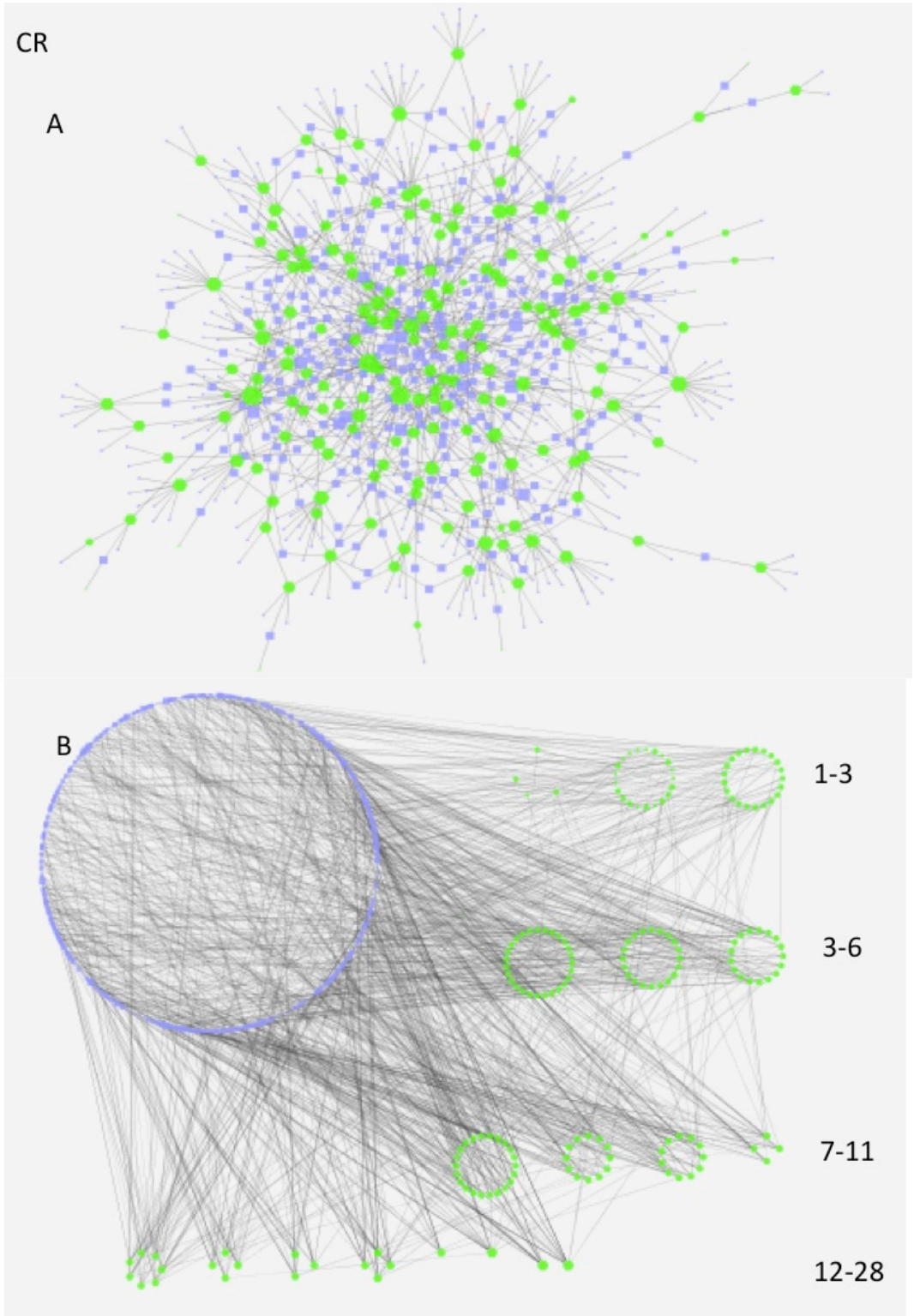

Figure 5.4 CR Inferred regulatory network using the GRENITS (Morrissey, 2013) algorithm. Green nodes are TFs, blue nodes are regular genes. Size of nodes is correlated with number of inferred regulatory interactions (i.e. big nodes regulate more) (A) General representation of the network (B) TFs grouped by number of regulatory interactions, each group of TFs has the same predicted number of regulatory interactions (edges) within the group. TFs with the lowest (1-3) number of predicted interactions are at the top, TFs with the highest (12-28) number of predicted interactions are at the bottom.

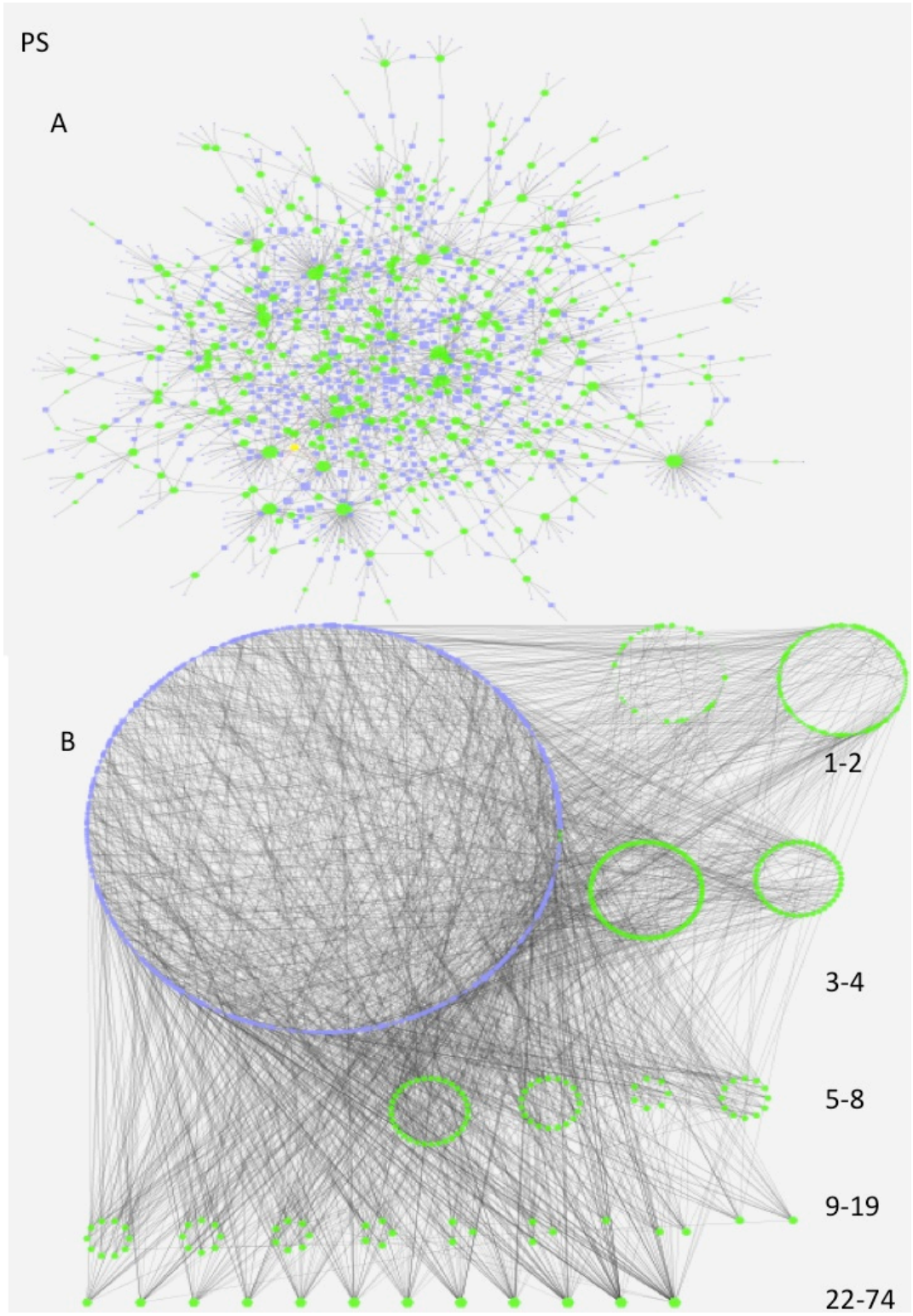

Figure 5.5 PS Inferred regulatory network using the GRENITS (Morrissey, 2013) algorithm. Green nodes are TFs, blue nodes are regular genes. Size of nodes is correlated with number of inferred regulatory interactions (i.e. big nodes regulate more) (A) General representation of the network (B) TFs grouped by number of regulatory interactions, each group of TFs has the same predicted number of regulatory interactions (edges) within the group. TFs with the lowest (1-2) number of predicted interactions are at the top, TFs with the highest (22-74) number of predicted interactions are at the bottom.

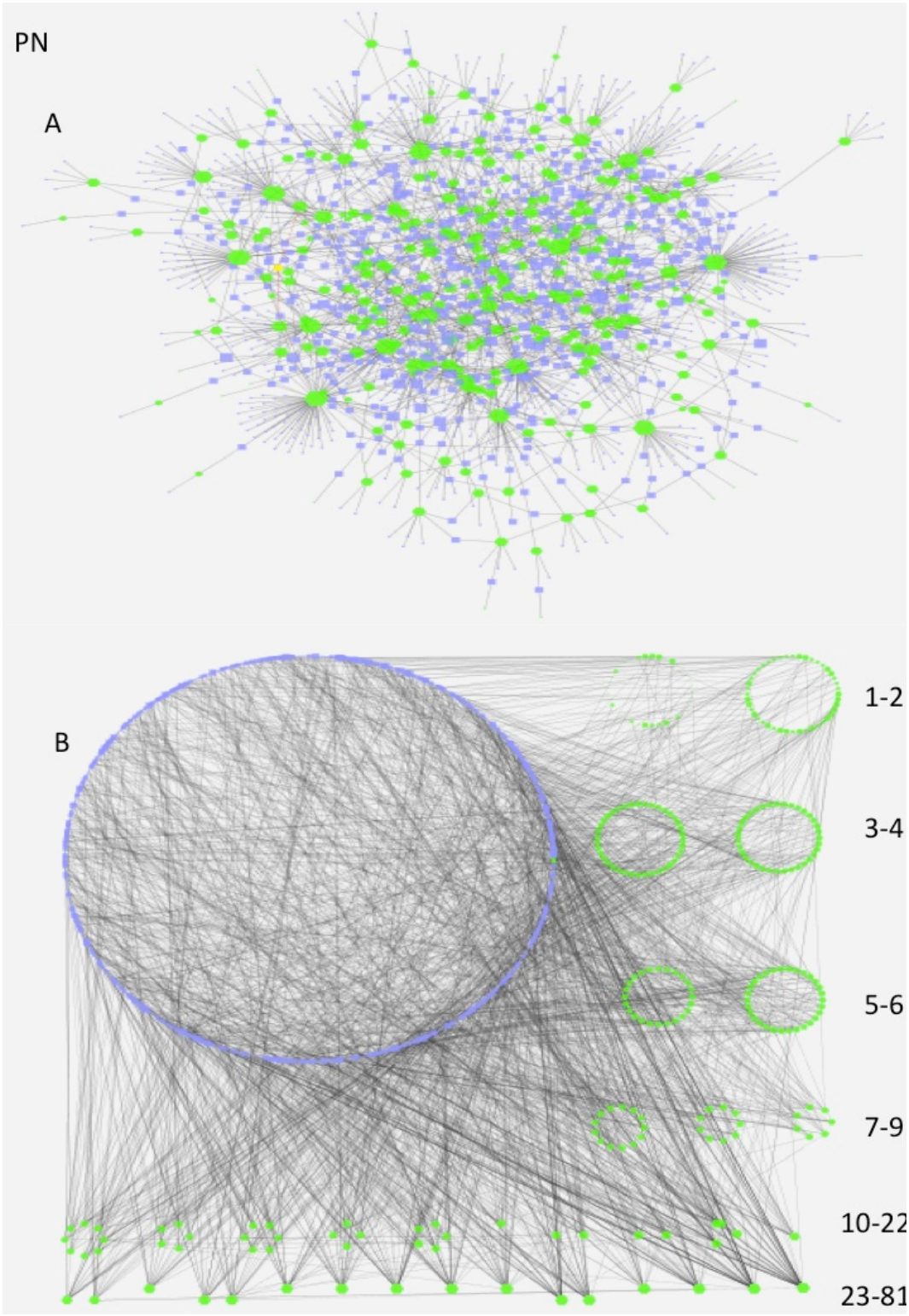

Figure 5.6 PN Inferred regulatory network using the GRENITS (Morrissey, 2013) algorithm. Green nodes are TFs, blue nodes are regular genes. Size of nodes is correlated with number of inferred regulatory interactions (i.e. big nodes regulate more) (A) General representation of the network (B) TFs grouped by number of regulatory interactions, each group of TFs has the same predicted number of regulatory interactions (edges) within the group. TFs with the lowest (1-2) number of predicted interactions are at the top, TFs with the highest (23-81) number of predicted interactions are at the bottom.

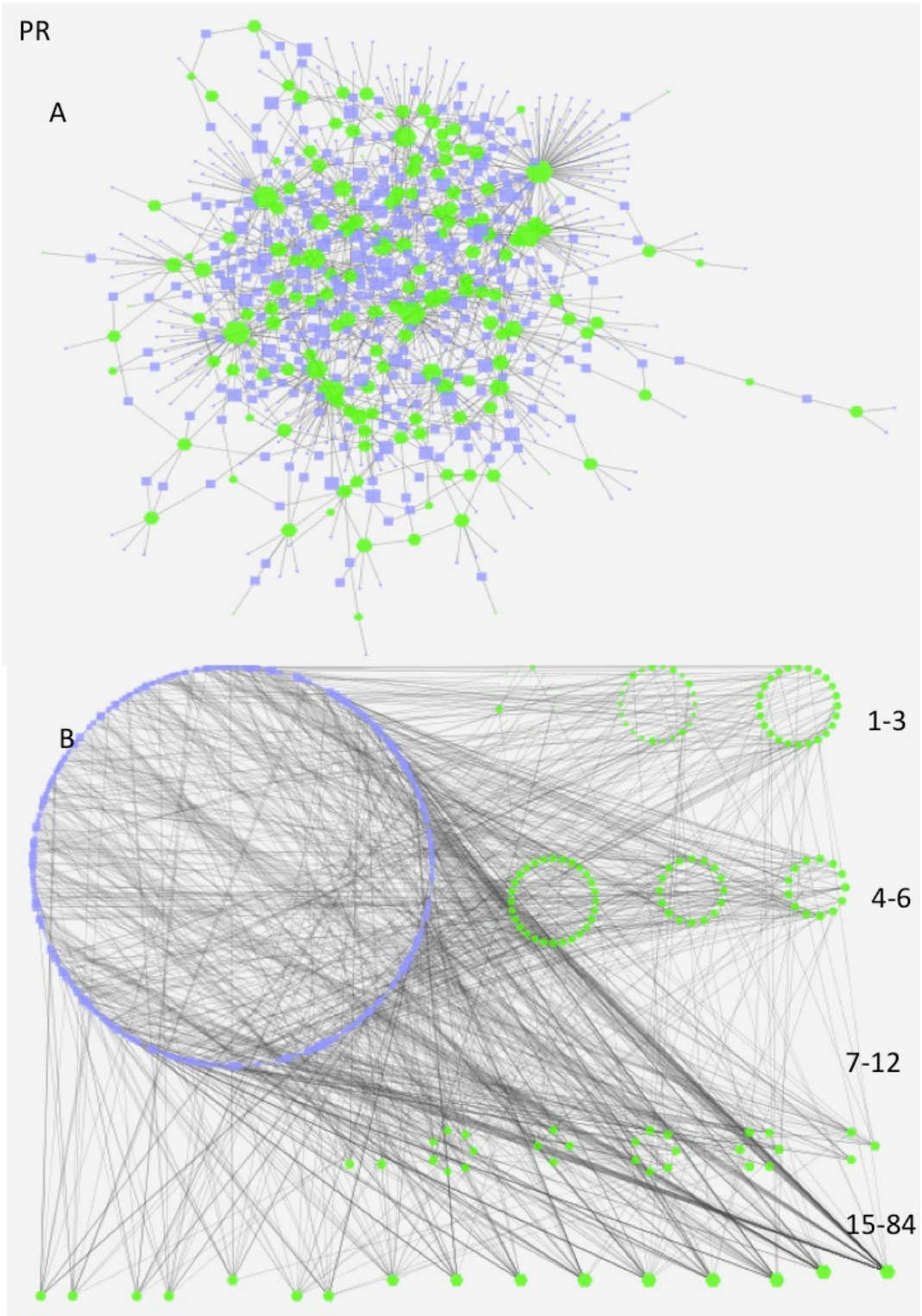

Figure 5.7 PR Inferred regulatory network using the GRENITS (Morrissey, 2013) algorithm. Green nodes are TFs, blue nodes are regular genes. Size of nodes is correlated with number of inferred regulatory interactions (i.e. big nodes regulate more) (A) General representation of the network (B) TFs grouped by number of regulatory interactions, each group of TFs has the same predicted number of regulatory interactions (edges) within the group. TFs with the lowest number (1-3) of predicted interactions are at the top, TFs with the highest number (15-84) of predicted interactions are at the bottom.

Table 5.1 Properties for regulatory inference networks based on differentially expressed genes during 6 treatments. Table shows amount of nodes (genes) and edges (interactions) fore every network, the amount and percentage of DE genes found in the network, and the node-to-edge ratio. Networks were generated using Grenits (Morrissey, 2013).

	Nodes	Edges	Differentially expressed genes in seed set (percentage of genes present in network)	Node/Edge ratio
Cortex standard	898	1271	1852 (48%)	0.71
Cortex N	981	1347	2074 (47%)	0.73
Cortex *Sinorhizobium*	892	1147	1963 (45%)	0.78
Pericycle Standard	1651	1973	4449 (37%)	0.84
Pericycle N	1557	2017	3590 (43%)	0.77
Pericycle *Sinorhizobium*	785	1099	1635 (48%)	0.71

Table 5.2 Top five hub genes (genes with the highest number of outgoing edges) in cortex networks with number of edges shown in brackets. Networks were generated using Grenits (Morrissey, 2013).

Cortex Standard		Cortex N		Cortex *Sinorhizobium*	
Arabidopsis gene ID	Gene name or description	*Arabidopsis* gene ID	Gene name or description	*Arabidopsis* gene ID	Gene name or description
At5g65640 (37)	*BHLH093*	*At5g61270 (34)*	*PIF7*	*At5g63700 (28)*	*Zinc ion binding*
At2g47210 (36)	*MYB-like TF*	*At5g25190 (27)*	*Integrase-type DNA BP*	*At5g25220 (28)*	*KNAT3*
At3g23050 (35)	*AXR2/IAA7*	*At5g06510 (26)*	*NFYA10*	*At5g65670 (24)*	*IAA9*
At3g16870 (34)	*GATA17*	*At5g67480 (23)*	*BT4*	*At2g47190 (17)*	*MYB2*
At5g65210 (34)	*TGA1*	*At4g30980 (23)*	*LRL2*	*At3g15210 (15)*	*ERF4*

Table 5.3 Top hub genes (genes with the highest number of outgoing edges) in pericycle networks with number of edges shown in brackets. Networks were generated using Grenits (Morrissey, 2013).

Pericycle Standard		Pericycle N		Pericycle *Sinorhizobium*	
Arabidopsis gene ID	Gene name or description	*Arabidopsis* gene ID	Gene name or description	*Arabidopsis* gene ID	Gene name or description
At1g45249 (72)	*ABF2*	*At1g31760 (77)*	*MDM2 domain protein*	*At5g60120 (84)*	*TOE2*
At1g07980 (66)	*NFYC10*	*At5g13960 (75)*	*SUVH4*	*At1g13300 (45)*	*HRS1 (MYB-l)*
At5g56110 (54)	*MYB103*	*At5g57410 (51)*	*Alpha-actinin BP*	*At3g47500 (39)*	*CDF3*
At4g00610 (43)	/	*At5g41020 (44)*	*MYB family TF*	*At4g18170 (36)*	*WRKY28*
At1g27740 (37)	*RSL4*	*At3g10000 (42)*	*EDA31*	*At1g22590 (34)*	*AGL87*

5.2.2 Validation of regulatory interactions

Regulatory networks, inferred from gene expression data are powerful computational tools for analyzing biological relationships, however the regulatory edges are predictions, not fact. To assess the biological relevance of the links predicted by our network we compared a subset of predicted regulatory edges to known regulatory interactions (for computational reasons it was not possible to compare the full networks). Edges between nodes that are common between all interaction networks in a cell type were selected as a test. This test subset of the network was analyzed by searching for evidence of known cis-acting TF-family binding sites in the promoters of target genes, predicted to be regulated by known TFs. Data on the presence of predicted *cis*-acting TF-family binding sites in the 3-kb upstream region (likely promoter) of target genes was obtained from the VirtualPlant platform (Katari et al., 2010), which contains a database of predicted binding sites for TF families for every gene (Nero et al., 2009). Out of the 26 edges predicted by our model in cortex networks, 10 were corroborated as representing known putative TF binding sites (Table 5.4). The same method was applied to pericycle networks, where 20 out of 66 edges were corroborated (Table 5.5). This validation method was also used to test edges from randomized networks with a similar topology and node/edge distribution to our networks. Randomized networks were created by taking an identical number of node genes, with identical distribution of source and target nodes (i.e. all source nodes were TFs), and creating a number of random edges between these sources and targets, the number of edges was again identical to the number of edges in the networks predicted based on gene expression data. This was repeated 10 times for both cortex and pericycle networks. These random

networks of TFs regulating target genes were analysed with the same dataset as the predicted network. The interactions predicted by network inference in this chapter consistently outperformed the randomized networks by a factor of 2 (average of 2.7 for cortex and 2.5 for pericycle). It should be noted here that the presence of a binding element does not necessarily validate the existence of a regulatory interaction, rather it indicates the presence of a binding site at a target gene for genes from the respective source TF family.

Table 5.4 Corroborated interactions in cortex networks based on the presence of cis-acting TF family binding sites. Data derived from Nero et al. (2009). Source contains TFs that interact with a putative regulated gene (Target). Type of interaction (activation/inhibition) is shown.

Source	Target	Network	Activation/Inhibition
CCA1	*At4g31890*	CS	Inhibition
WRKY46	*MLP34*	CN	Inhibition
WRKY46	*At1g33790*	CS	Activation
BHLH93	*MDHAR*	CS	Inhibition
FQR1	*At1g49560*	CS	Inhibition
At3g25790	*MDHAR*	CN	Inhibition
WRKY46	*ZAT10*	CN	Inhibition
PRR9	*BHLH118*	CN	Activation
LHY	*RVE8*	CR	Activation
ESE3	*GATA17*	CN	Inhibition

Table 5.5 Corroborated interactions in pericycle networks based on the presence of cis-acting TF family binding sites. Data derived from Nero et al. (2009). Source contains TFs that interact with a putative regulated gene (Target). Type of interaction (activation/inhibition) is shown.

Source	Target	Network	Activation/Inhibition
LHY	*At5g04460*	PR	Activation
ABF2	*At4g06479*	PS	Inhibition
CGA1	*LHY1*	PN	Activation
LHY	*At2g16190*	PS	Inhibition
BHLH093	*At2g29780*	PN	Inhibition
BHLH093	*At5g57410*	PN	Activation
at2g43140	*NAC035*	PR	Activation
AGL104	*At2g20280*	PN	Inhibition
NTL9	*NAC035*	PR	Inhibition
AGL1	*At5g57410*	PN	Inhibition
BHLH134	*At5g13380*	PS	Activation
WRKY34	*AIRP3*	PR	Inhibition
BHLH093	*At1g26350*	PN	Inhibition
TRFL6	*At2g29780*	PS	Inhibition
At1g29950	*NAC035*	PN	Inhibition
AGL1	*At1g30160*	PN	Activation
TRFL6	*FRS1*	PS	Activation
WRKY34	*At3g54390*	PN	Activation
LHY	*At2g43140*	PR	Activation
NAC368	*DIN3*	PN	Activation

5.2.3 Analysis of top hubs in the networks

A first method to explore these networks for information is to assess which TFs regulate the largest number of genes (Table 5.2 and 5.3), and thus act as regulatory hubs to co-ordinate gene expression in the different treatments and cell types.

5.2.3.1 Rhizobial regulatory interactions in the cortex

In the CR network the top hub gene is *KNAT3* (*At5g25220*) (Table 5.2), A member of class II knotted1-like homeobox gene family with 28 putative downstream genes. It is a HOMEOBOX gene that has been found to regulate development of seedlings and germination (Kim et al., 2013). It is specifically expressed along the longitudinal axis of the root, especially in cortex and

pericycle cells (Truernit and Haseloff, 2006), although it is not yet known what the relevance of this cell type specific pattern is for function. In the gene expression datasets in chapter 4, no differential expression compared to the standard was observed in pericycle cells. According to our network, *KNAT3* is a regulator for two meristem growth related genes: *RML1 (Root meristem less 1, At4g23100),* a glutamate-cysteine ligase, mutants of which have a stunted root meristem growth in the absence of glutathione (Reichheld et al., 2007) and *AGP9* (*Arabinogalactanprotein 9, At2g14890*), which has been linked to meristem growth through computational analysis (Heyndrickx and Vandepoele, 2012).

KNAT3 also regulates two cell wall growth genes. *CSLA9 (Cellulose synthase like A9, At5g03760),* a beta-mannan synthase gene which is specifically expressed in the root elongation zone, and *CESA1 (At4g23410),* which is a cellulose synthase, have both been shown to be critical for cell wall formation (Holland et al., 2000; Burn et al., 2002; Heyndrickx and Vandepoele, 2012).

Another large hub (Table 5.2) is the auxin-inducible TF *IAA9 (Indole 3 acetic acid inducible 9, At5g65670)* with 24 regulatory interactions. *IAA9* is predicted by our model to negatively regulate *CPK11 (Calcium-dependent protein kinase 2*, *At4g11280)*, which is a positive regulator of ABA signaling (Lynch et al., 2012), as well as being required in the pep-immunity activation pathway (Boudsocq et al., 2010; Ma et al., 2013). *IAA9* itself is predicted in the inference network to be activated by *ERF11 (Ethylene response factor 11, AT1G28370),* which is involved in a wide range of hormonal and defense-associated responses, most closely with ABA-mediated control of ethylene synthesis (Li et al., 2011).

5.2.3.2 Nitrogen regulatory interactions in the cortex

The largest hub in the CN network model is *PIF7 (Phytochrome interacting factor 7, At5g61270)*, a member of a basic helix-loop-helix-type TF family that has recently been linked to transcriptional activation leading to a rapid growth response (Li et al., 2012). In the network model it is predicted to regulate 34 downstream genes. Strikingly 75% of these 34 edges are repressive interactions, compared to 50% of the full CN network edges being repressive. Nine of the *PIF7*-repressed genes are stress or plant defense related, including *SCZ (Schizoria, At1g46264)*, a heat-shock protein that regulates cell division in several root tissues: epidermis, cortex, endodermis (Hove et al., 2010; Begum et al., 2012).

5.2.3.3 Nitrogen regulatory interactions in the pericycle

The top regulatory hub TF in the PN network, with 77 regulatory targets (Table 5.3), is *At1g31760*, an unknown member of the *SWIB/MDM2* domain superfamily. It regulates a putative negative feedback loop by inhibiting the TF *BRC1 (Branched 1, At3g18550)*, a shoot-branching associated gene (Poza-Carrion et al., 2007), as well as one of its own activation targets.

The second largest hub-TF is *SUVH4* (Table 5.3) *(Suvar homolog 4, At5g13960)*, a methyltransferase involved in the maintenance of DNA methylation. The group of 75 putative targets is very strongly enriched (22 genes, $P = 7 \times 10^{-20}$) for genes associated with methylation GO terms. However, most of these genes appear to be known as modifiers of RNA, rather than DNA (RNA methylation has a P-value of 4.2×10^{-26}). This would suggest that posttranscriptional modifications play a crucial role in the regulation of the response to N in the pericycle. In the inference network *SUVH4* also inhibits

RHA1 (RAB homolog 1, At5g45130), while simultaneously activating two of RHA1's predicted targets, *At4g05400* and *At5g27850*, both of which have unknown functions. *RHA1* is thought to be involved in the general response of roots to auxin, with mutants exhibiting defective gravitropism and auxin physiology (Fortunati et al., 2007).

5.2.3.4 Rhizobial regulatory interactions in the pericycle

TOE2 (Table 5.5) (*Target of early activation tagged 2, AT5G60120*) is a TF predicted to have 84 regulatory targets (Table 5.3), the largest number of putative targets of any network. *TOE2* is known as a target for miRNA directed gene silencing during development (Aukerman et al., 2003), but not much is known about its regulatory functions. TOE2 in pericycle cells from plants treated with *Sinorhizobium* is downregulated compared with pericycle cells from the standard treatment, suggesting that there might be miRNA directed silencing of *TOE2* in response to treatment with *Rhizobium.* In the PR network model, several development-associated genes are predicted to be regulated by *TOE2. SRF8 (Strubbelig receptor family 8, At4g22130),* a protein kinase and *LMI1* (*Late meristem identity 1, At5g03790*), a homeobox gene, are both associated with meristem growth (Xu et al., 2010; Heyndricks et al., 2012), with *LMI1*, here inhibited by *TOE2*, a key regulatory enzyme in plant development, directing meristem identity (Saddic et al., 2006).

HRS1 (Table 5.3) *(Hypersensitivity to root shortening 1, At1g13300)* is the second largest hub gene in the PN network, with 44 regulated genes. It is a member of a small G2-like TF-family (Liu et al., 2009), with a role in seed germination (Wu et al., 2011) and salt stress response, specifically as a regulator of the ABA-signaling (Mito et al., 2011).

LTP2 (Table 5.3) *(Lipid transfer protein 2, At2g38530)* is the third largest PR TF-hub gene and is thought to play a role in various stress responses, particularly programmed cell death (Kim et al., 2007) and water deprivation (Chae et al., 2010).

5.2.4 Analysis of TF families with several hub members

In addition to analyzing the top hub genes separately, it can be informative to look at families of TFs, especially families with multiple members among the top hub genes. TF families often have specific functions associated with them, e.g.: The *WRKY* family and stress and disease responses (Bakshi et al., 2014), *bZIP* family genes which are primarily associated with abiotic stress and plant development (Jacobi et al., 2002) or the smaller GRF family, associated with leaf and cotyledon growth (Kim et al., 2003)

5.2.4.1 MYB gene family

Among the top predicted regulatory TFs for all networks are several *MYB* genes. The *MYB* TF family function in a variety of processes, including in the control of development, metabolism and stress responses (for an overview, see (Dubos et al., 2010)). Four *MYB* or *MYB*-like TFs in each of the CR, PR, and PN networks and one in the CN network were identified. Due to the high number of genes regulated by MYB TFs gene ontology enrichment analysis was used to interpret the role of MYB genes in the CR network. The strongest recurring ontology for their predicted targets was salt stress ($P = 3.7 \times 10^{-09}$), (Figure 5.8). Three out of 4 regulatory MYB genes in the CR network are known to be associated with salt stress responses (Yanhui et al., 2006). Interestingly, 10 out of 12 salt stress genes regulated by the *MYB* TFs are predicted to be activated (rather than repressed), and both inhibited salt stress genes are TFs *WRKY33 (At2g38470)* and *MYB44*

(*At5g67300*), possibly indicating a negative feedback mechanism. *MYB2* is a known regulator of dehydration responsive genes (Urao et al., 1993; Yanhui et al., 2005), corroborating the finding here of its induction of *RD21B (Response to dehydration, At5g43060)* expression, which is induced in response to dehydration stress (Jiang et al., 2006).

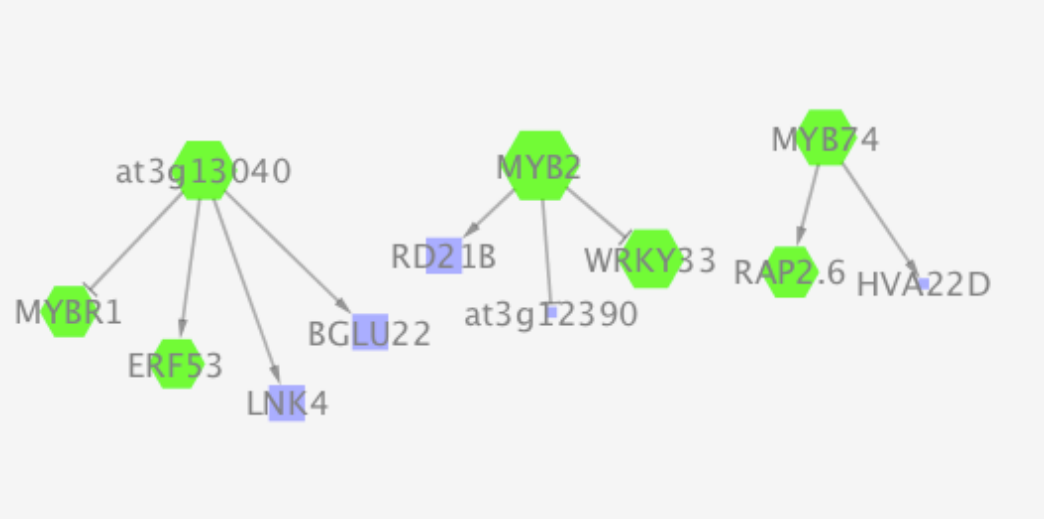

Figure 5.8 Subsection of the CR network representing salt stress responsive genes activated by MYB TFs. Green hexagons represent TF genes, blue squares are non-TF genes. Only salt stress-associated genes are shown. Arrows indicate activating regulatory interaction, T-bars indicate an inhibitory regulatory interaction. Gene inference networks were generated by GRENITS (Morrisssey, 2013).

In the PR network, two out of four MYB TFs are predicted to be controlled by *WRKY46 (At2g46400)* (Figure 5.9), a chitin responsive TF. *DUO1* (*At3g60460*) is a MYB-like protein which is predicted to be inhibited by *WRKY46*, while *MYB48 (AT3G46130)* is predicted to be indirectly inhibited *WRKY46*. *WRKY46* shares four regulatory targets with *HRS1* (another MYB-like TF), the former inhibiting the four targets, while the latter functions as an activator (see Figure 5.9). These results suggest a possible role for *WRKY46* as a central regulator for a *MYB* TF-family driven response in pericycle cell response to *Sinorhizobium*. In a recent network inference study on WRKY genes, Choura

et al. (2015) show how *WRKY46* is a potential major controller of WRKY-gene associated gene regulation.

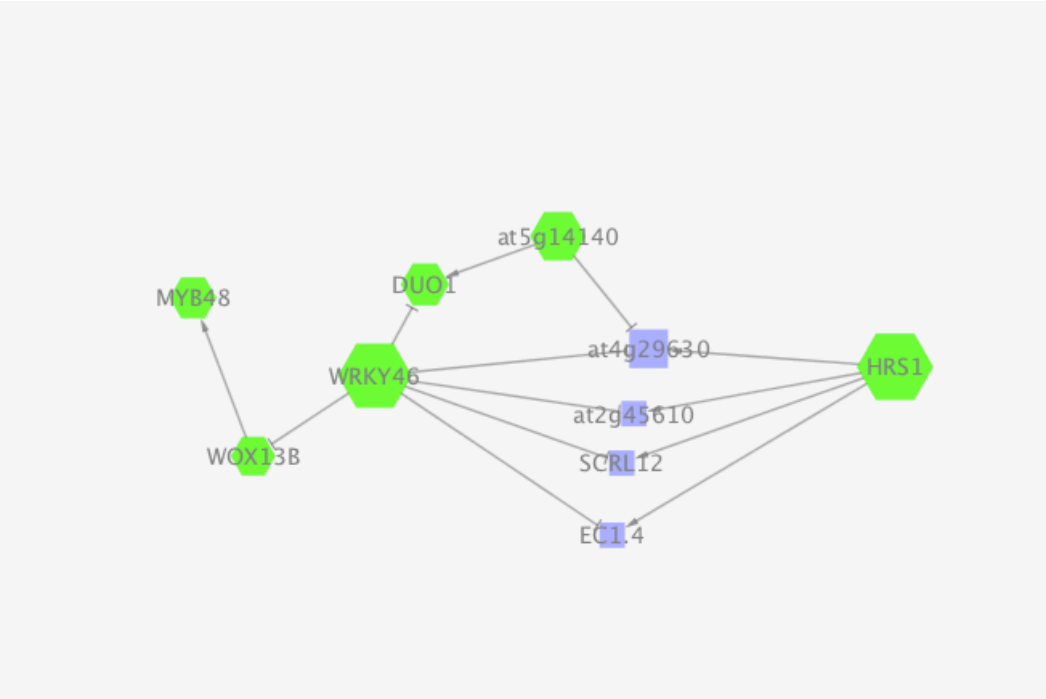

Figure 5.9 Subsection of the PR network, representing WRKY46 regulation. Green hexagons represent TF genes, blue squares represent non-TF genes. Arrows indicate activating regulatory interaction, T-bars indicate an inhibitory regulatory interaction. Gene inference networks were generated by GRENITS (Morrisssey, 2013).

5.2.4.2 WRKY gene family

In both *Sinorhizobium* networks there are major hub *WRKY* TFs: *WRKY3 (At2g03340)* and *WRKY33* in CR and *WRKY28 (At4g18170)* and *WRKY46* (Figure 5.9, section 5.2.4.1) *(At4g46400)* in PR. Among the genes that are predicted to be regulated by *WRKY* genes in the cortex network, ontologies for salt stress and salicylic acid are among the top overrepresented ontologies, with six and five genes respectively. The large number of *WRKY*s in the list of top hub TFs in the *Sinorhizobium* response suggests a central role for WRYK-family TFs in the response to *Sinorhizobium*, which is absent in the N response.

5.2.4.3 Type A ARR gene family

Cytokinin signaling in *Arabidopsis* utilizes a multistep phosphorelay two-component signaling system, comprised of histidine kinases and response regulators (*ARRs*) (Ren et al., 2009). Several type A *ARR*-family genes are among the top regulatory TFs controlling a large group of genes in cortical networks. In the model presented here, *ARR15 (At1g74890), ARR16 (At2g40670)* and *ARR17 (At3g56380)* regulate 26 genes in CR and 32 genes in CN. Type A ARRs have a high degree of functional redundancy and because of this their specific roles in plant development are generally not well understood. *ARR15* however is known to be auxin responsive and involved in establishment of the root stem cell specification (Müller and Sheen, 2008).

In the CR network, 16 of the 26 genes predicted to be regulated by AAR-family genes were found to be specific to N compound metabolism (P = 8.8 x 10^{-5}). Other overrepresented GOs in this group of genes are response to ethylene stimulus (P = 4e x 10^{-5}) and response to JA stimulus (P = 4 x 10^{-4}). In the CN network *ARR15* is predicted to be a negative regulator of *NRP1*, linking the enriched hormonal GO terms to regulation of lateral root growth. Enrichment analysis of CN *ARRs* suggests a link to hormonal response stimulus (P=2 x 10^{-4}), highlighting the potential role of *ARRs* as transducers of hormonal signaling.

5.3 Discussion

5.3.1 Network modeling enables predictions of regulatory interactions

In chapter 4 gene ontology enrichment analysis was used to elucidate the chronology of biological processes in response to treatments with N and *Sinorhizobium*. The wave-like activation/inhibition pattern observed in clusters

(Figures 4.2-4.7) is an indicator of major transcriptional reprogramming in response to environmental cues. Time series data can be used to predict a gene regulatory network that can help in identifying key regulatory components of the response to N/*Sinorhizobium*. One major shortcoming of this approach is that we eliminate posttranscriptional and posttranslational regulation, which play major roles in various *Arabidopsis* regulatory systems (Harms et al., 2004; Mazzucotelli et al., 2008).

Six regulatory networks were generated, all networks had a similar amount of DE genes represented in them (37-48%) and similar node/edge ratios (0.71-0.84). Differences were observed between hub genes in the networks, with pericycle networks typically having twice the number of genes connecting to top hub genes compared to cortex. This result was independent of the amount of genes used to create the networks: The PR DE gene set was the smallest, with 1635 DE genes identified, yet the PR network contained the largest network hub gene, *TOE2*, predicted to regulate 84 genes.

Network validation was done on two subsets of genes DE between all networks in a tissue type. Known TF family binding sites were retrieved from VirtualPlant and these corroborated 10 out of 26 interactions (38%) in the cortex networks and 20 out of 66 (30%) interactions in the pericycle networks, a twofold improvement over random networks generated with similar network topology.

Validation of network data is a complex undertaking. Many published network inference methods use biological databases to validate their predictions, comparing the proportion of interactions found in the network and the database (Altay et al., 2013). However, this assumes the networks are static and do not

change between phenotypes or treatments, which can limit the usefulness of using this validation method (Altay et al., 2013; Olsen et al., 2014). Chromatine immunoprecipitation sequencing (Chip-seq) or yeast-1-hybrid (Y1H) assays can be used to confirm regulatory interactions between genes and TFs, but carry a risk of false negatives and false positives. For example, Y1H assays cannot detect interactions with obligatory heterodimers, resulting in false negatives. Y1H interactions can occur when a chromatin binding site is available in the context of yeast chromatin, but not in the organism from which the DNA fragment was cloned (Walhout, 2012). This approach has been demonstrated in a large scale approach using network perturbation of the mammalian transcriptional network in response to pathogens (Amit et al., 2009). Marbach et al. (2012) suggest integrating multiple inference networks derived from multiple methods, thus leading to a superior 'consensus' network which can then be experimentally validated. Given several putative core regulator genes RNA interference can be used to silence the TF allowing for study of the effect of network perturbations on the network. Olsen et al. (2014) suggest an iterative gene knockdown method, combined with genomic data and prior networks, to compute the inferred network's performance.

It would be interesting to see if knockouts of the hub genes in the *Sinorhizobium* networks can have an influence on the phenotypes observed in chapter 3. Furthermore it would be relevant to test wether this effect would be different between cell specific and whole-genome knockouts. Smaller sub-networks such as the WRKY33-regulation discussed in this chapter can be studied more in detail directed knockout such as described by Olsen et al. (2014) or through other other methods (Y1H and chip-seq).

5.3.2 Top N hubs reveal a potential role for histone modification

PIF7 is the top hub regulator in CN networks, it is associated with growth regulation (Li et al., 2012). *PIF7* is a regulator for 34 genes, 25 are repressed and nine are activated. Eleven out of 25 repressed genes are found in CN cluster 80, which is enriched for genes associated with histone methylation ($P = 3.1 \times 10^{-4}$). Out of five genes associated with the GO term in the cluster, two are predicted to be regulated by *PIF7,* including *FIE (Fertilization independent endosperm, At3g20740)*, traditionally associated with seed development and flowering (Bouyer et al., 2011), but data from Brady et al. (2007) suggest that it has elevated expression levels in root cortex cells, suggesting a role for *PIF7* in the suppression of histone modification.

Given this potential suppression of posttranslational modification by *PIF7*, and the already (section 5.2.3.3) described role of the top regulatory gene in PN networks as a methyltransferase gene (*SUVH4*), it appears that there could be a central role for posttranslational modifications in *Arabidopsis* response to N treatment. The link between histone modification and nutrient depletion has already been described in various organisms such as *Arabidopsis* (Arnholdt-Schmitt, 2004) and animals (McCabe et all., 2005). The finding of *PIF7* and *SUVH4* as key regulatory genes in the plant response after recovery from nutrient depletion could be a novel regulatory pathway of posttranslational regulation.

5.3.3 Top *Sinorhizobium* treatment regulatory genes are associated with root meristem development

KNAT3, the top regulatory gene in the CR network, and TOE2, top regulator of the PR network both are predicted to regulate several genes associated with meristem growth. In lateral root growth, this is where the priming of the lateral

root occurs (Dubrovsky et al., 2008), this could suggest that phenotypic effects described in chapter 3 might be better understood by specific analysis of meristematic cells, rather than cortex or pericycle.

5.3.4 Analysis of TF families with multiple top hubs reveals interplay of *MYB* and *WRKY* families in *Sinorhizobium* networks

Analysis of major regulatory hubs of MYB and WRKY family genes reveals that they are closely linked and might be part of another core regulatory motif integrating hormonal responses (specifically salicylic acid) with stress response and/or pathogen defense. The absence of *WRKY* TFs among top regulatory hubs in the N response indicates the important role of this family in regulating the response to *Sinorhizobium. WRKY* TFs have been shown to play a critical role in plant defense (Dong et al., 2003; Rushton et al., 2010), but also in the establishment of symbiotic interactions between plants and AM (Gallou et al., 2012). Previous research suggests that *WRKY33* is a key regulator of hormonal and metabolic responses in response to *Botrytis cinerea* infection (Birkenbihl et al., 2012). Our finding of a central regulatory role for *WRKY33* specifically in the more outward lying cortical tissue (rather than in the pericycle) supports the function of this gene as a primary inducer of the defense response since this is closer to the likely site of chitin perception by the root.

5.4 Conclusion

Analysis of gene regulatory networks has generated novel insights in addition to analyses of clusters of DE genes (chapter 4). In the *Sinorhizobium* treatment, both top regulatory genes are shown to regulate root meristem identity genes, potentially explaining how regulatory mechanisms regulate the root phenotype

seen when plants are treated with *Sinorhizobium*. Analysis of families of hub genes revealed a link between regulation of *MYB* and *WRKY* family genes in *Sinorhizobium* networks, which is of special interest given the role *WRKY* genes play in the establishing of symbiosis in the interaction of plants with AM (Gallou et al., 2012).

Chapter 6

Differential gene expression in response to pathogen treatment

6.1 Motivation

In the previous chapters changes in gene expression in response to N and treatment with *Sinorhizobium* are analyzed. There are strong indications of similarities between the transcriptional response to *Sinorhizobium* and the general transcriptional response to pathogenic bacteria, as seen in clusters that were enriched for genes with defence response GO terms (section 4.4.3.1). Therefore, it would be informative to be able to compare differential gene expression in response to the presumed non-pathogen *Sinorhizobium meliloti* to gene expression in response to bacteria known to be pathogenic to the host *Arabidopsis thaliana*.

In order to compare as closely related responses as possible to *Sinorhizobium,* which colonizes root nodules in host plants (Oldroyd et al., 2011; Oldroyd et al., 2013), a root-tissue-specific pathogen was chosen. *Ralstonia solanacearum* is a tropical pathogen that colonizes the xylem through openings in the epidermis, caused by wounding or emergence of lateral roots (Denny et al., 2006). *Ralstonia* causes bacterial wilt in a wide range of host plants, primarily through blocking of vascular tissues leading to a lack of water in leaves and other plant organs.

The aim of this chapter is to investigate which genes and processes are specific to treatment with *Sinorhizobium* or *Ralstonia* or N, as well as those that are common between them.

6.2 Experimental design

A similar experimental approach to the one used in the time course dataset (Chapter 4) was used to analyze responses to *Ralstonia solanacearum* (methods). Plants were grown on low N (0.3 mM NH_4NO_3) for 6 days after which they were removed from the plate and submerged in a diluted solution of *R. solanacearum* (section 2.4.2). Plants were then placed on a fresh low N plate and returned to the incubator. Root samples were taken at 2 and 6 hours after incubation with *Ralstonia*, then protoplast generation carried out and cortical cells were isolated using FACS, with RNA extraction and microarray analysis preparation as described in sections 2.5.

The 2 and 6 h time points were chosen to capture the early responses to bacterial inoculation, as it is during this period that significant changes in in gene expression in the *Sinorhizobium* experiments were observed. No high-resolution time series experiment in 2 cell types was set up for this experiment as it was not financially feasible to increase the amount of arrays analysed by another 25%. Cortex tissue was investigated rather than pericycle, as it is closer to the outer layer of the root, representing a more relevant response site for interaction between the plant and bacterial infection. These root cortical *Ralstonia* response cell samples were analyzed in combination with samples taken during the time course experiment previously described (Chapter 4), giving a total of four

treatments (*Ralstonia*, *Sinorhizobium*, N and standard) and 2 time points (2 and 6 hours).

Prior to their use in treatments, *Ralstonia* cultures were confirmed to be virulent by growing them on tetrazolium chloride medium. Virulent colonies were confirmed since they were white with a pink center (whereas nonvirulent colonies would have been uniform dark red) (Champoiseau et al., 2009). When roots were inoculated with *Ralstonia,* root growth typically halted within 1 to 2 days post-inoculation, with complete wilting of the seedlings at around 5 to 6 days post-inoculation (Figure 6.1).

Figure 6.1 Wilting of *Arabidopsis Col-0* seedlings 5 days after inoculation with *Ralstonia solanacearum* (OD600 0.8). Yellow bar = 1 cm.

RNA extraction, microarray preparation and normalization were performed as in the time course experiments (section 2.6-2.7.2). BATS (section 2.7.3) could not be used for determining DE in this experiment, as it is not a time course experiment. The 2 and 6 hour time points were treated independently and analyzed using the Limma package (Smyth, 2005) in R. For every time point DE was determined by comparing one of the treatments (*Ralstonia, Sinorhizobium*, N) to the standard treatment. Gene ontology enrichment analysis was performed using Agrigo (Du et al., 2010), with yekutieli correction for multiple testing (Benjamini and Yekutieli, 2001) and a cutoff of FDR < 0.05.

All experiments were carried out in replicate, with 2 or 3 replicates per treatment and time point. Nineteen arrays were analyzed in total: 4 new arrays treated with *Ralstonia,* and 15 previously analyzed arrays treated with standard/N/*Sinorhizobium.* Lists of DE genes can be retrieved from Supplemental data S8.

Differential expression was determined using Limma analysis implemented in R. Analysis for DE was different here from chapter 4 as there is no time series dataset and thus it is not informative to use either BATS or GP2s to test for DE genes. Limma uses a linear model approach where it fits a linear model to the data and then uses an empirical Bayes method to determine differential expression (Smyth, 2005). In this experiment genes from all three treatments were compared pairwise to the control to assess whether a gene was differentially expressed in a treatment. The 2 and 6 hour time points were analyzed independently. The cutoff for differential expression was set at a *P*-value < 0.005.

6.3 Results

6.3.1 The cortical response to *Ralstonia solanacearum* inoculation is larger in magnitude than the response to *Sinorhizobium* or N treatment.

Results from analysis of DE in R solanacearum treated plants can be found in the supplemental materials (S8).

In total, 2198 genes were DE at 2 h across all treatments (1081 downregulated and 1136 upregulated) in cortical cells (Figure 6.2 a-b), with *Ralstonia* regulating the largest number of genes (1891 DE genes), followed by N (337) and *Sinorhizobium* (193). At 6 h 3087 genes were DE across all

treatments (1422 downregulated and 1665 upregulated) (Figure 6.2 c-d), with *Ralstonia* again regulating the largest number of gene (2519), followed by N (736) and *Sinorhizobium* (635). In the *Ralstonia* DE group, 216 genes were upregulated at both time points and 204 were downregulated at both time points, for N eight genes were upregulated and 15 downregulated at both time points and for *Sinorhizobium* seven genes were upregulated and 14 downregulated at both time points. Across all treatments, 17 genes are commonly downregulated and four upregulated at 2 h after treatments, while 127 are downregulated and 90 are upregulated at 6 h after treatments.

The amount of DE genes appears to increase with time in all three treatments. The much larger effect of the *Ralstonia* treatment on gene expression is expected given the destructive nature of *Ralstonia* infections.

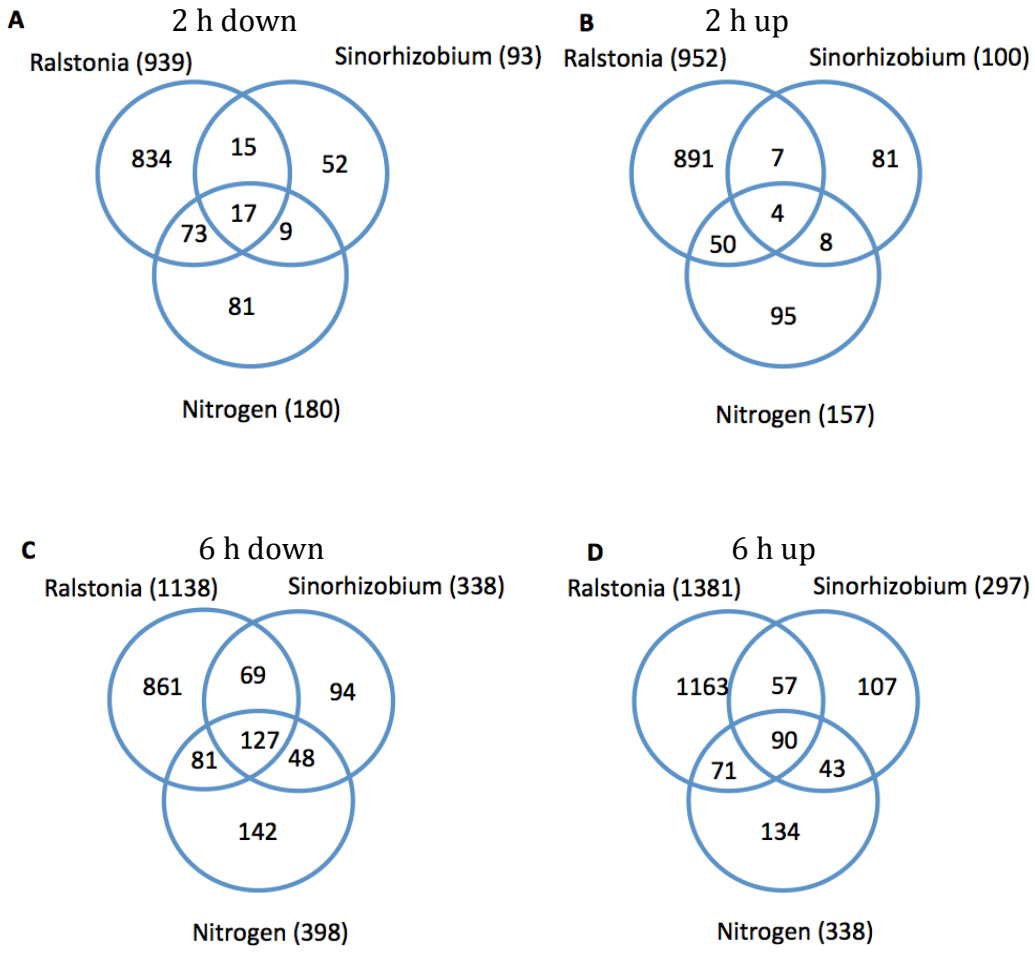

Figure 6.2 Differentially expressed genes at 2 h (A-B) and 6 h (C-D) in cortical cells in response to three different treatments: N, *Sinorhizobium* and *Ralstonia*. Total number of differentially expressed genes are shown in brackets, with overlap shown on the Venn-diagrams. (A) downregulated genes at 2 h, (B) upregulated genes at 2 h, (C) downregulated genes at 6 h, (D) upregulated genes at 6 h.

6.3.2 Analysis of processes affected by *Ralstonia* inoculation using GO term overrepresentation analysis: overall trends

Gene ontology enrichment analysis was used to identify processes regulated by the different treatments. DE expressed genes were separately analyzed for up and downregulated genes (compared to standard treatment). At 2 h post treatment (Figure 6.3) with *Ralstonia*, no GO's are overrepresented in downregulated genes. Upregulated genes are enriched for metabolic processes GO terms Metabolism associated processes are largely linked to photosynthesis (P = 7.1 x 10^{-17}) and other photosynthesis-related ontologies, such as photosystem II assembly (P = 5.5 x 10^{-10}).

At 6 h post-treatment (Figure 6.4) with *Ralstonia* there is a strong enrichment for genes associated with stress responses GOs, both in up-and downregulated genes. Heat stress (P = 4.2 x 10^{-25}), oxidative stress (P = 1.8 x 10^{-12}) and high light intensity (P = 3 x 10^{-20}) are among the most overrepresented GO terms in DE genes with lower expression levels compared to the standard treatment. Among DE genes with higher expression levels compared to the standard treatment, overrepresented GO's are associated with osmotic stress (P = 1.2 x 10^{-8}) as well as auxin response (P = 8.3 x 10^{-6}).

At first glance, GO terms differ strongly between 2 and 6 h time points, with only 4 hours between sampling. However, when the common genes (216 upregulated DE genes and 204 downregulated DE genes) between both *Ralstonia* time points were analyzed for GO enrichment together, heat response was again one of the strongest enriched ontologies in downregulated genes (P = 4.7 x 10^{-7}), with about half of the heat response-associated genes from the 6 h time point being DE in the 2 h time point as well, indicating that this effect is maintained. In

upregulated genes, one of the most overrepresented GO's is anthocyanin biosynthesis (P = 7.0 x 10^{-6}). Anthocyanins have been associated with hydrogen peroxide regulation in *Arabidopsis* (Vanderauwera et al., 2005; Page et al., 2012), which could explain the regulation of this category. Hydrogen peroxides are a common feature of pathogen response in plants (Neill et al., 2002), explaining their presence here.

6.3.3 Comparison of pathogen-regulated processes to those regulated by the non-pathogen *Sinorhizobium* and N treatment

By comparing genes DE expressed in *Ralstonia* treated plants to DE genes in *Sinorhizobium* treated plants we can gain an insight into the processes that underlie pathogenic vs. non-pathogenic plant responses. At the 2 hour time point (Figure 6.3) there are interesting differences in overrepresented GO terms. In the *Ralstonia* treatment at both time points there was no overrepresentation of genes with GO associated with bacterial infection. However, amongst the *Sinorhizobium* DE genes at 2 h after infection, the group of downregulated DE genes is enriched with genes with immune system GO terms (P = 1.1 x 10^{-11}), as well as more specific processes such as, callose deposition during defense response (P = 9.0 x 10^{-8}) and response to chitin (P = 1.6 x 10^{-8}). These defense associated genes are absent in the intersection of DE between *Ralstonia* and *Sinorhizobium* DE genes at this time point. When only the genes DE in the *Sinorhizobium* treatment are analyzed, further overrepresented defense-related GO terms are found among downregulated genes: systemic acquired resistance (P = 4.8 x 10^{-6}), as well as SA-biosynthesis (P = 6.2 x 10^{-6}). There were few genes DE in common between *Ralstonia* and *Sinorhizobium*/N treatments at this time point (32 genes downregulated and 11 genes upregulated), and analysis of

enriched GO's yielded no significant results in this group or in the group of upregulated genes *Sinorhizobium* treated cells.

At 6 h (Figure 6.4) there is a large overlap between enriched GO terms from common DE genes between *Sinorhizobium* and *Ralstonia* treated plants. The most highly enriched GO among downregulated genes in this group is heat stress ($P = 3.8 \times 10^{-40}$), with related ontologies such as high light intensity ($P = 1.8 \times 10^{-36}$), as well as oxidative stress such as response to hydrogen peroxide ($P = 1.4 \times 10^{-31}$). In the upregulated DE genes common to *Sinorhizobium* and *Ralstonia* treated plants, the response to auxin stimulus is the most overrepresented GO ($P = 7.0 \times 10^{-8}$). No overrepresented GO's were found in upregulated genes specific to *Sinorhizobium* treatment at 6 h. Among downregulated genes specific to the *Sinorhizobium* treatment at 6 h, RNA elongation ($P = 9.2 \times 10^{-12}$) and photosynthesis ($P=4.1 \times 10^{-7}$) were among the overrepresented GO terms.

In genes upregulated 2 h after N treatment, the most enriched GO in upregulated genes was photosynthesis ($P = 3.2 \times 10^{-8}$). In the group of downregulated genes at 2 h post treatment, no GO was overrepresented.

At 6 hours post treatment there are strong similarities between the *Ralstonia* and N treatments in downregulated genes, with heat response as the strongest enriched GO ($P = 3.0 \times 10^{-30}$), followed closely by high light intensity ($P = 2.3 \times 10^{-24}$) and hydrogen peroxide ($P = 2.4 \times 10^{-21}$). At 6 h, upregulated genes common between Ralstonia and N treated plants were enriched for GO's including osmotic stress ($P = 6.3 \times 10^{-10}$) and auxin stimulus ($P = 2.4 \times 10^{-7}$). Downregulated genes were again enriched for GO's for general stress responses including heat ($P = 1.9 \times 10^{-36}$) and oxidative stress ($P = 1.9 \times 10^{-18}$).

6.3.4 Common responses to non-pathogen and pathogen conditions

Analyzing the treatments as separate effects gave some insight into the individual responses, but to get a complete understanding of root responses to pathogen vs. non-pathogen conditions it is critical to analyze DE genes in common between treatments. At 2 hours there were 23 genes in common between all treatments, with no significantly enriched GO terms (Figure 6.3). In the group of 23 DE genes were 2 TFs, TAF7 and IAA3. IAA3 is a TF that is negatively regulated by auxin, with reduced lateral root phenotypes in both gain and loss of function mutations of the TF (Goh et al., 2012) (Table 6.1). TAF7 is a TF binding protein with no strong functional annotations (Heyndrickx and Vandepoel, 2012).

Table 6.1 Fold changes in response to treatment, comparison between treatment and standard. Positive fold change implies higher expression levels in treatment vs. standard.

Gene ID	*Ralstonia*	*Sinorhizobium*	N
TAF7	-3.5	-3.4	-2.9
IAA3	-2	1.4	1.6

At the 6 h time point we find 218 genes DE common between the three treatments, with the overrepresented ontologies here mostly similar to those already discussed for the treatments separately (Figure 6.3). These included GO terms for response to heat ($P = 8 \times 10^{-32}$), high light intensity ($P = 5.7 \times 10^{-27}$) and hydrogen peroxide ($P = 9.6 \times 10^{-23}$) among the most highly overrepresented. Interestingly we find that of the common genes between treatments, 11 upregulated genes are annotated for the response to auxin stimulus ($P = 0.00058$). Among these are three SAUR-family genes (Small AUxin Upregulated), members of a large family of genes that are most strongly expressed in epidermal and cortical cells and are typically induced by auxin. SAUR genes are

characterized by having mRNA that is both short and short-lived (Hagen and Guilfoyle, 2002), but their functions are largely unknown.

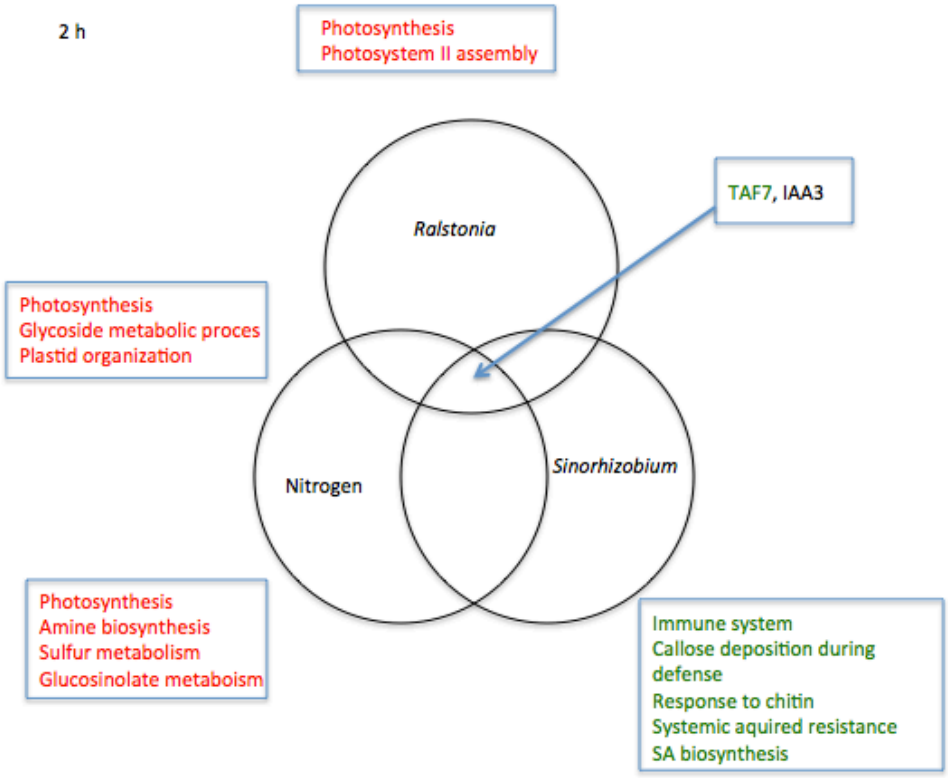

Figure 6.3 Overview of GO terms enriched in DE genes at 2 h in N, *Sinorhizobium* and standard treatments. GO's from groups of upregulated genes are shown in red, GO's from groups of downregulated genes are shown in green. GO analysis was performed in AGRIGO on sets of genes DE from the standard treatment. IAA3 was up or downregulated depending on the treatment (Table 6.1)

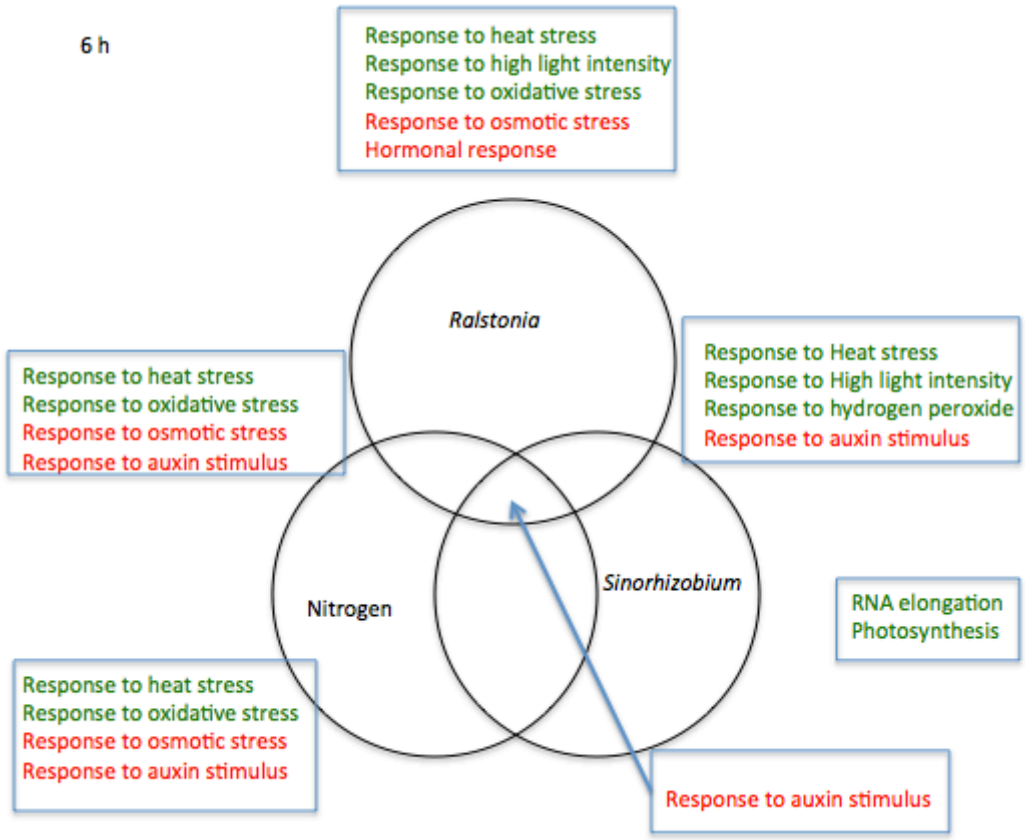

Figure 6.4 Overview of GO terms enriched in DE genes at 6 h in N, *Sinorhizobium* and standard treatments. GO's from groups of upregulated genes are shown in red, GO's from groups of downregulated genes are shown in green. GO analysis was performed in AGRIGO on sets of genes DE from the standard treatment.

6.4 Discussion

Overall, there are large differences in DE genes between *Ralstonia* and *Sinorhizobium* treated plants. The number of DE genes in response to *Ralstonia* was an order of magnitude larger in number than either DE genes in response to N or *Sinorhizobium* (Figure 6.2). This could be a consequence of the large reprogramming effect of the pathogenic invasion. Alternatively it may be an experimental artifact due to the fact that the data gathering for the *Ralstonia* treated plants was carried out at a much later stage. One element to consider in future work is that even though inoculations with both *Ralstonia* and *Sinorhizobium* bacterial cultures were carried out at similar concentrations of

bacteria (determined by OD), the two species might very well have a different growth rate. This is relevant since the influence of bacterial growth rate, and the speed with which they can transition through different growth phases (lag to exponential to declining growth) has been demonstrated to influence the degree of gene expression in the fungus *Botrytis cinerea* (Windram et al., 2012).

One interpretation of the overrepresentation of genes associated with photosynthesis GO terms in N and *Ralstonia* treated plants (Figure 6.3) is an effect of down-regulation of photosyntetic genes, since dawn begins 3 hours prior to the treatments. However if this were the case we would also expect to see a similar effect in the control group, and thus no DE genes would be observed. Reduction of photosynthesis as a response to macronutrient starvation has been well documented (Geider et al., 1993; Plaxton and Carswell, 1999) and the upregulation of photosynthesis genes here observed is more likely interpreted as a reversal of this starvation effect. However, photosynthesis is usually reduced in response to pathogen invasion (Windram et al., 2012), which leaves the problem at least partially unexplained.

The strong core response of stress-related genes that are DE in all three treatments at 6 h after treatment (Figure 6.4) is intriguing, and could suggest a common response that is observed in the cortex upon any environmental change. It is unclear why some stress GO terms such as heat and high light intensity are found enriched in downregulated genes while other stress GO terms such as water and osmotic stress are found enriched in upregulated genes. In the same group of core DE genes there are also several genes associated with auxin responsive GO-terms upregulated in all treatments. Auxin is not traditionally linked to pathogen defense or bacterial response, but interactions between

pathogens and auxin physiology have been observed in *Pseudomonas syringae* (Chen et al., 2007; Cui et al., 2013).

The absence of an enrichment of defense response GO-terms in plants treated with a pathogen, while plants treated with *Sinorhizobium*, a presumably non-pathogenic bacteria, do have an enrichment of defense response GO terms in downregulated genes might seem contradictory at first. However if this cultivar of *Ralstonia* has a compatible interaction with *Arabidopsis*, it by definition is able to bypass the early defense response and might not trigger any early defense-associated genes.

The downregulation of genes associated with defense response GO terms (Figure 6.3) in *Sinorhizobium* plants is intriguing. Different Rhizobia species are known to effectively suppress plant defense in compatible symbiotic plants from the very first stages of the infection process (Aslam et al., 2008; Lopez-Gomez et al., 2012; Gourion et al., 2015). Of particular interest here, given the earlier observed lateral root phenotype (Chapter 3) of *Arabidopsis* inoculated with *Sinorhizobium,* is the defense associated gene *ASA1* (*Athranalite synthase alpha*) *(At5g05730*) (Buell and Somerville, 1995; Heyndrickx and Vandepoele, 2012), which is downregulated in the *Sinorhizobium* treated plants at 2 h post treatment. *ASA1* has been described as a link between JA and auxin in the regulation of LR formation and null mutants for this gene are known to have severely impaired LR formation in the absence of JA (Sun et al., 2009).

Chapter 7 Discussion and conclusions

With the increasing constraints put on agriculture worldwide, N use and the inefficiency of the N cycle in agriculture are becoming critical problems that need to be addressed. There are 2 broad ways of tackling this problem - either natural N uptake capacity in plants is improved or the ability to form a mutual symbiosis between N fixing bacteria and legumes is transformed to other crop plants. To be able to do either, a better understanding of plant responses to N as well as the response to N fixing bacteria in non-symbiotic plants is necessary. This work aims to determine cell type specific responses in the root to N and *Sinorhizobium*. This will help to identify key regulatory networks regulating both response pathways in *Arabidopsis*, and understand how these underlie effects on lateral root development to alter root architecture.

Transcriptomic analysis through the use of expression profiling with microarrays is a well-established technique in life science research (Schaffer et al., 2000; Birnbaum et al., 2006). Recent advances have shown how gene expression in organisms is highly tissue-dependent (Birnbaum et al., 2003; Brady et al., 2007), thus it is critical to carry out expression profiling in cell types where the most relevant changes are thought to occur. Given the two primary systems studied (N and *Sinorhizobium*) and the context (root formation), pericycle and cortical cells were selected for analysis. Pericycle cells are the site of lateral root initiation (Dubrovsky et al., 2010), whereas in legumes nodules initiate from cell divisions in cortical cells (Desbrosses et al., 2011). Microarrays were used to quantify the expression of genes from FACS sorted cells. This generated six time

series transcriptomic datasets detailing the changes in gene expression in pericycle and cortex cells in response to N and *Sinorhizobium* treatments. These data were then used to infer regulatory networks based on the differentially expressed genes, which allowed for identification of regulatory genes that could be controlling plant responses to either changes of N in the environment or a response to *Sinorhizobium meliloti*.

Information on gene expression was analyzed in the context of results from phenotypic assays. The root phenotype effect of *Sinorhizobium* inoculation on *Arabidopsis* was analyzed, as well as the difference in effect between *Arabidopsis* accessions.

Finally, in order to better understand the response to *Sinorhizobium*, specifically to discover the context in which *Arabidopsis* roots react to it (neutral, pathogen or symbiont), gene expression at two early time points to gene expression in response to the pathogenic bacterium *Ralstonia solanacearum* were compared.

7.1 Sinorhizobium inoculation affects lateral root elongation in *Arabidopsis*

The phenotype of *Arabidopsis* in response to different N concentrations has been well-documented in Col-0 (the most commonly studied *Arabidopsis thaliana* accession) (Malamy et al., 2001; Casimiro et al., 2003, Walch-liu et al., 2006) and various accessions (Gifford et al., 2013). Therefore, analysis of *Arabidopsis* responses to *Sinorhizobium* were studied. Seedlings grown in the presence of *Sinorhizobium* had a short lateral root phenotype (Figure 3.1 and 3.2), similar but not identical to *Arabidopsis* seedlings grown in N-starvation

conditions (Walch-liu et al., 2006). Further experiments with developing seedlings showed no difference in lateral root development between different stages of lateral root development (Figure 3.4), indicating that the observed phenotype is a restriction of lateral root elongation, rather than lateral root initiation.

Sinorhizobium is known to be able to influence LR initiation in *M. truncatula. MtCEP1,* a N-responsive promotor of nodulation and simultaneously an inhibitor of LR formation (Imin et al., 2013). In *Arabidopsis,* overexpression of the homolog *AtCEP1* inhibits LR elongation (Ohayama et al., 2008), suggesting that the function of *CEP1* was co-opted in the evolution of nodulation to create a promotor for nodule growth. Interestingly, in the pericycle cells *Arabidopsis* plants treated with *S. meliloti* time series (Chapter 4), *CEP1* is upregulated compared to the standard between 2 and 8 h after treatment.

In a separate experiment a set of 34 *Arabidopsis thaliana* accessions were phenotypically characterized and then clustered based on 6 root traits capturing root size in two environments, inoculation with *Sinorhizobium* compared to standard inoculated (Figure 3.8). There was a clear rearrangement of cluster dendrogram tree topology in the two environments, which indicates that sharing a phenotype in one environment does not predict similarity in another environment. This suggests there are multiple factors controlling lateral root development and that these regulate development in different ways in different environments, at least partially independently from each other. This finding was consistent with earlier findings of Gifford et al. (2013), which showed that the N response of LRs was similarly dependent on multiple factors. Gifford et al. were able to use genome wide association study and gene

expression analysis to map this plasticity and further link genetic defects in identified genes to predicted phenotypic variation.

7.2 Networks and clusters provide insights into regulatory mechanisms underlying phenotypic changes

Analysis of DE genes shows how different treatments within a cell type are more similar in gene expression that the same treatment across different cell types (Figure 4.32). This highlights the importance of the cell type specific approach used in this study, as well as how the choice of cell types can influence the results obtained when performing gene expression analysis (See also Birnbaum et al., 2003; Brady et al., 2007; Gifford et al., 2008). Had different cell types been chosen, the results, including the identification of top regulatory genes in networks, are likely to have been different. This should be taken into consideration where it might be tempting to declare a certain regulatory interaction a 'major regulatory hub' (Table 5.2 and 5.3). To develop truly comprehensive regulatory networks, either transduction of regulatory signals through cell types should be studied or an effort should be made to integrate regulatory data from different cell types (Birnbaum et al., 2003; Brady et al., Gifford et al., 2008) into one regulatory network.

Analysis of clusters of DE genes shows different GO terms are enriched, and thus different processes being regulated at different time points over the N and *Sinorhizobium* treatments. The time course of response to *Sinorhizobium* treatment (Figure 4.22) is predominantly characterized by very early (DE starting at 1-2 h) clusters with stress/chitin/defense-associated genes DE in cortex cells. In contrast, the N treatment (Figure 4.10) encompasses a more diverse response,

both in time and biological functions, with root development, N transport and metabolism, as well as auxin and JA-associated responses.

Network inference provided insight into the regulatory connections of the N and *Sinorhizobium* responses. In networks of DE genes from *Sinorhizobium* treated roots, some of the top regulatory genes were associated with growth and development processes (Figure 5.4 and 5.7): *KNAT3* and *TOE2*. Further research on these might provide additional insight into the short lateral root phenotype observed in Chapter 3. GO terms in *Sinorhizobium* treated plants might be linked to the interplay of the hub WRKY and MYB genes. WRKY46, upregulated in *Sinorhizobium* treated compared to standard treated pericycle cells, is known to be responsive to chitin (Libault et al., 2007) and is predicted to be a strong regulatory hub in pericycle cells (section 5.2.4.1). It is placed in PR cluster 21 (Figure 4.26), which appears to be a stress responsive cluster. WRKY46 is also known to be a regulator of several biological processes such as stomatal movement, osmotic stress (Ding et al., 2014) and basal resistance against *Pseudomonas syringae* (Hu et al., 2012).

7.3 The *Arabidopsis* transcriptional response to *Ralstonia* and *Sinorhizobium* is partially overlapping

A comparative analysis of DE genes between *Ralstonia*/*Sinorhizobium*/N treated plants shows considerable differences in the functional response to the two bacteria. Paradoxically it is the response to *Sinorhizobium*, not *Ralstonia* that is enriched for bacterial defense genes. One explanation could be that because *Ralstonia* is able to infect *Arabidopsis,* it is able to bypass the early defense response, whereas *Sinorhizobium* is triggering it. However there is a much

greater transcriptional response to *Ralstonia* compared to *Sinorhizobium* in terms of the number of differentially expressed genes, even at just 2 hours after *Ralstonia* inoculation (Figure 6.2). This could suggest that the plant does not detect *Ralstonia* and that *Ralstonia* rapidly infects roots, causing rapid reprogramming of the transcriptome as it is infected.

Analysis of common DE genes between treatments found 11 upregulated auxin responsive genes to be similarly upregulated in *Ralstonia*, *Sinorhizobium* as well as N treatments. This is reminiscent of the response to the pathogenic bacterium *Pseudomonas syringae* which is known to induce virulence by using its type III secretion system to deliver a specific effector (*AvrRpt2*) into cells. This stimulates auxin turnover by binding to auxin transcription repressors and degrading them (Deakin and Broughton, 2009; Cui et al., 2013). The type III secretion system has also been shown to be co-opted in nodulation, as a delivery mechanism for Nod-factors into plant cells (Marie et al., 2001; Okazaki et al., 2013). The potential link between auxin responses and methods of microbial entry are worthy of further experiments.

7.4 Future perspectives

Up until now the interaction between *Sinorhizobium* and *Arabidopsis* has not been analyzed to the level of detail presented in this work. This study shows that *Sinorhizobium* can cause a reprogramming of the *Arabidopsis* transcriptome and opens the door to future research. For example it would be interesting to profile the *Sinorhizobium* response in other cell types such as the epidermis, or even more specifically in epidermal root hair cells, since that is the primary site of contact between legumes and *Sinorhizobium* (Esseling et al., 2004). However,

rather than specific cells it might be of more interest to investigate specific zones in the root, such as the root elongation zone or the apical meristem.

The information content in the dataset generated in this project is vast and there is much further scope for its analysis. For example, the gene ontology and network analysis of chapters 4 and 5 were mostly restricted to the first 16 h of treatment, since the network inference required regularly spaced time points. This meant we could not analyze regulatory interactions later than 16 h, leaving an untapped resource of data from 20 to 48 h. Furthermore, the generated gene networks present a vast amount of data and additional experiments to test hypotheses generated by this study will be necessary.

7.5 Summary

This study used a comprehensive phenotypic analysis of the response of *Arabidopsis thaliana* roots to *Sinorhizobium* inoculation, as well as a transcriptomic analysis of FACS sorted cells to gain insight into the different regulatory pathways potentially controlling the response to N or *Sinorhizobium.* Network inference was used to identify key regulatory genes coordinating specific responses.

A *Sinorhizobium*-associatied short lateral root phenotype was discovered and analysis of clusters of DE genes as well as regulatory networks has provided clues as to how this phenotype could arise. Several putative key regulatory hubs (*WRKY46, TOE2, PIF7, KNAT3, IAA9* and *SUVH4)* with a role in root development which potentially influence plant development or plant stress responses were identified. These hubs provide opportunities for further studies. *Arabidopsis thaliana* was shown to have a distinct transcriptional

response to *Rhizobium* that is distinct from a response to the pathogen *Ralstonia solanacearum*.

Bibliography

Akkermans, A.D.L., Abdulkadir, S. and Trinick, M.J. (1978). N_2-fixing root nodules in Ulmaceae: *Parasponia* or (and)*Trema* spp.? *Plant and Soil*, 49 (3): 711-715.

Almagro, A., Lin, S.H. and Tsay, Y.F. (2008). Characterization of the *Arabidopsis* nitrate transporter NRT1.6 reveals a role of nitrate in early embryo development. *The Plant Cell*, 20 (12): 3289-3299.

Altay, G., Altay, N., Neal, D. (2013). Global assessment of network inference algorithms based on available literature of gene/protein interactions. *Turkish Journal of Biology*, 37 (5): 547–555

Álvarez, B., López, M.M. and Biosca, E.G. (2008). Survival strategies and pathogenicity of Ralstonia solanacearum phylotype II subjected to prolonged starvation in environmental water microcosms. *Microbiology*, 154 (11): 3590-3598.

Amit, I., Garber, M., Chevrier, N., Leite, A. P., Donner, Y., Eisenhaure, T. and Regev, A. (2009). Unbiased reconstruction of a mammalian transcriptional network mediating pathogen responses. *Science*, 326 (5950): 257-263.

Amor, B.B., Shaw, S.L., Oldroyd, G.E.D., Maillet, F., Penmetsa, R. V., Cook, D., Long, S.R., Denarie, J. and Gough, C. (2003). The NFP locus of *Medicago truncatula* controls an early step of Nod factor signal transduction upstream of a rapid calcium flux and root hair deformation. *The Plant Journal*, 34 (4): 495-506.

Angelini, C., Cutillo, L., De Canditiis, D., Mutarelli, M., and Pensky, M. (2008). BATS: a Bayesian user-friendly software for analyzing time series microarray experiments. *BMC Bioinformatics,* 9 (1): 415.

Apel, K. and Hirt, H. (2004). Reactive oxygen species: metabolism, oxidative stress, and signal transduction. *Annual Review of Plant Biology*, 55: 373-399.

Arioli, T., Peng, L., Betzner, A. S., Burn, J., Wittke, W., Herth, W. and Williamson, R. E. (1998). Molecular analysis of cellulose biosynthesis in *Arabidopsis*. *Science*, (5351): 717-720.

Armengaud, P., Breitling, R. and Amtmann, A. (2004). The potassium-dependent transcriptome of *Arabidopsis* reveals a prominent role of jasmonic acid in nutrient signaling. *Plant Physiology*, 136 (1): 2556-2576.

Arnholdt-Schmitt, B. (2004). Stress-induced cell reprogramming. A role for global genome regulation? *Plant Physiology*, 136 (1): 2579-2586.

Arrighi, J.F., Barre, A., Ben Amor, B., Bersoult, A., Soriano, L.S., Mirabella, R., de Carvalho-Niebel, F., Journet, E.P. Gherardi, M., Huguet, T., Geurts, R., Denarie, J., Rouge, P. and Cough, C. (2006). The *Medicago truncatula* lysine motif-receptor-like kinase gene family includes NFP and new nodule-expressed genes. *Plant Physiology*, 142 (1): 265-279.

Aslam, S.N., Newman, M.A., Erbs, G., Morrissey, K.L., Chinchilla, D., Boller, T. and Cooper, R. M. (2008). Bacterial polysaccharides suppress induced innate immunity by calcium chelation. *Current Biology*, 18 (14): 1078-1083.

Attaway, S. (2013). Matlab. Butterworth-Heinemann, Oxford.

Aukerman, M. J. and Sakai, H. (2003). Regulation of flowering time and floral organ identity by a microRNA and its APETALA2-like target genes. *The Plant Cell,* 15 (11): 2730-2741.

Babiychuk, E., Kushnir, S., Belles-Boix, E., Van Montagu, M. and Inzé, D. (1995). *Arabidopsis thaliana* NADPH oxidoreductase homologs confer tolerance of yeasts toward the thiol-oxidizing drug diamide. *Journal of Biological Chemistry*, 270 (44): 26224-26231.

Badenoch-Jones, J., Summons, R. E., Djordjevic, M. A., Shine, J., Letham, D. S. and Rolfe, B. G. (1982). Mass spectrometric quantification of indole-3-acetic acid in *Rhizobium* culture supernatants: relation to root hair curling and nodule initiation. *Applied and Environmental Microbiology*, 44 (2): 275-280.

Bakshi, M. and Oelmüller, R. (2014). WRKY transcription factor: Jack of many trades in plants. *Plant Signaling & Behavio*r, 9 (1): e27700.

Barbez, E., Kubeš, M., Rolčík, J., Béziat, C., Pěnčík, A., Wang, B. and Rosquete M. (2012). A novel putative auxin carrier family regulates intracellular auxin homeostasis in plants. *Nature,* 485 (7396): 119-122.

Barrett, T., Wilhite, S.E., Ledoux, P., Evangelista, C., Kim, I.F., Tomashevsky, M., Marshall, K.A., Phillippy, K.H., Sherman P.M., Holko, M., Yefanov, A., Lee, H., Zhang, N., Robertson, C.L., Serova, N., Davis, S., Soboleva, A. (2013). NCBI GEO: archive for functional genomics data sets--update. *Nucleic Acids Research.* 41: 991-995.

Bellincampi, D., Cervone, F. and Lionetti, V. (2014). Plant cell wall dynamics and wall-related susceptibility in plant–pathogen interactions. *Frontiers in Plant Science*, 5 (228).

Ben, C., Toueni, M., Montanari, S., Tardin, M.C., Fervel, M., Negahi, A., Saint-Pierre, L., Mathieu, G., Gras, M.C., Noel, D., Prosperi, J.M., Pilet-Nayel, M.L., Baranger, A., Huguet, T., Julier, B., Rickauer, M. and Gentzbittel, L. (2013). Natural diversity in the model legume *Medicago truncatula* allows identifying distinct genetic mechanisms conferring partial resistance to *Verticillium* wilt. *Journal of Experimental Botany,* 64 (1): 317-332.

Benfey, P.N. and Mitchell-Olds, T. (2008). From genotype to phenotype: Systems biology meets natural variation. *Science*, 320 (5): 495-497.

Benjamini, Y. and Hochberg, Y. (1995). Controlling the false discovery rate: a practical and powerful approach to multiple testing. *Journal of the royal statistical society.* 57 (1): 289-300.

Benjamini, Y. and Yekutieli, D. (2001). The control of the false discovery rate in

multiple testing under dependency. *Annals of statistics,* 29 (4):1165-1188.

Bi, Y.M., Wang, R.L., Zhu, T., and Rothstein, S. J. (2007). Global transcription profiling reveals differential responses to chronic nitrogen stress and putative nitrogen regulatory components in *Arabidopsis*. *BMC Genomics*, 8 (1): 281-294.

Birnbaum, K., Shasha, D.E., Wang, J.Y., Jung, J.W., Lambert, G.M., Galbraith, D.W. and Benfey, P.N. (2003). A gene expression map of the *Arabidopsis* root. *Science*, 302 (5652): 1956-1960.

Blilou, I., Xu, J., Wildwater, M., Willemsen, V., Paponov, I., Friml, J., Heidstra, R., Aida, M., Palme, K. and Scheres, B. (2005). The PIN auxin efflux facilitator network controls growth and patterning in *Arabidopsis* roots. *Nature*, 433 (7021): 39-44.

Boller, T. and Felix, G. (2009). A renaissance of elicitors: Perception of microbe-associated molecular patterns and danger signals by pattern-recognition receptors. *Annual Review of Plant Biology*, 60 (1): 379-406.

Bongaarts, J. (2009). Human population growth and the demographic transition. *Philosophical Transactions of the Royal Society B: Biological Sciences,* 364 (1532): 2985-2990.

Boualem, A., Laporte, P., Jovanovic, M., Laffont, C., Plet, J., Combier, J. P. and Frugier, F. (2008). MicroRNA166 controls root and nodule development in *Medicago truncatula*. *The Plant Journal*, 54 (5): 876-887.

Boudsocq, M., Willmann, M.R., McCormack, M., Lee, H., Shan, L., He, P., Bush, J., Cheng, S-H. and Sheen, J. (2010). Differential innate immune signalling via $Ca^{(2+)}$ sensor protein kinases. *Nature,* 464 (7287): 418-422.

Boutanaev, A.M., Kalmykova, A.I., Shevelyov, Y.Y., and Nurminsky, D.I. (2002). Large clusters of co-expressed genes in the Drosophila genome. *Nature*, 420 (6916): 666-669.

Bouyer, D., Roudier, F., Heese, M., Andersen, E.D., Gey, D., Nowack, M.K., Goodrich, J., Renou, J.P., Grini, P.E., Colot, V. and Schnittger, A. (2011). Polycomb repressive complex 2 controls the embryo-to-seedling phase transition. *PLoS Genetics*, 7 (3): e1002014.

Brady, S.M., Orlando, D.A., Lee, J.Y., Wang, J.Y., Koch, J., Dinneny, J.R., Mace, D., Ohler, U. and Benfey, P.N. (2007). A high-resolution root spatiotemporal map reveals dominant expression patterns. *Science*, 318 (5851): 801-806.

Brotman, Y., Landau, U., Pnini, S., Lisec, J., Balazadeh, S., Mueller-Roeber, B., Zilberstein, A., Willmitzer, L., Chet, I. and Viterbo, A. (2012). The LysM receptor-like kinase LysM RLK1 is required to activate defense and abiotic-stress responses induced by overexpression of fungal chitinases in *Arabidopsis* plants. *Molecular Plant,* 5 (5): 1113-1124.

Bruex, A., Kainkaryam, R.M., Wieckowski, Y., Kang, Y.H., Bernhardt, C., Xia, Y., Zheng, X., Wang, J.Y., Lee, M.M., Benfey, P., Woolf, P.J. and Schiefelbein, J.

(2012). A gene regulatory network for root epidermis cell differentiation in *Arabidopsis*. *PLoS genetics,* 8 (1): e1002446.

Bu, Q., Jiang, H., Li, C.B., Zhai, Q., Zhang, J., Wu, X., Sun, J., Xie, Q. and Li, C. (2008). Role of the *Arabidopsis thaliana* NAC transcription factors ANAC019 and ANAC055 in regulating jasmonic acid-signaled defense responses. *Cell Research*, 18 (7): 756-767.

Buchanan-Wollaston, V., Page, T., Harrison, E., Breeze, E., Lim, P.O., Nam, H.G., Lin, J.F., Wu, S.H., Swidzinski, J., Ishizaki, K. and Leaver, C.J. (2005). Comparative transcriptome analysis reveals significant differences in gene expression and signalling pathways between developmental and dark/starvation-induced senescence in *Arabidopsis*. *The Plant Journal*, 42 (4): 567-585.

Buell, C.R. and Somerville, S.C. (1995). Expression of defense-related and putative signaling genes during tolerant and susceptible interactions of *Arabidopsis* with *Xanthomonas campestris* pv. *Molecular Plant Microbe Interactions,* 8 (3): 435-443.

Burn, J. E., Hocart, C.H., Birch, R.J., Cork, A.C. and Williamson, R.E. (2002). Functional analysis of the cellulose synthase genes *CesA1, CesA2*, and *CesA3* in *Arabidopsis*. *Plant Physiology*, 129 (2): 797-807.

Busch, W., Wunderlich, M., and Schöffl, F. (2005). Identification of novel heat shock factor dependent genes and biochemical pathways in *Arabidopsis thaliana*. *The Plant Journal,* 41 (1): 1-14.

Cain, M. L., Subler, S., Evans, J. P. and Fortin, M. J. (1999). Sampling spatial and temporal variation in soil nitrogen availability. *Oecologia*, 118 (4): 397-404.

Campanoni, P. and Nick, P. (2005). Auxin-dependent cell division and cell elongation. 1-Naphthaleneacetic acid and 2, 4-dichlorophenoxyacetic acid activate different pathways. *Plant Physiology*, 137 (3): 939-948.

Canales, J., Moyano, T. C., Villarroel, E. and Gutiérrez, R. A. (2014). Systems analysis of transcriptome data provides new hypotheses about *Arabidopsis* root response to nitrate treatments. *Frontiers in plant science*, 5 (22).

Carter, A.D., Bonyadi, R. and Gifford, M.L. (2013). The use of fluorescence-activated cell sorting in studying plant development and environmental responses. *International Journal of Developmental Biology*, 57 (6): 545-552.

Carvalho, B.S. and Irizarry, R.A. (2010). A framework for oligonucleotide microarray preprocessing. *Bioinformatics*. 26 (19):1367-4803.

Casimiro, I., Marchant, A., Bhalerao, R.P., Beeckman, T., Dhooge, S., Swarup, R., Graham, N., Inze, D., Sandberg, G., Casero, P.J. and Bennett, M. (2001). Auxin transport promotes *Arabidopsis* lateral root initiation. *The Plant Cell,* 13 (4): 843-852.

Castaings, L., Marchive, C., Meyer, C. and Krapp, A. (2011). Nitrogen signalling in *Arabidopsis*: how to obtain insights into a complex signalling network. *Journal*

of Experimental Botany, 62 (4): 1391-1397.

Cerezo, M., Tillard, P., Filleur, S., Munos, S., Daniel-Vedele, F. and Gojon, A. (2001) Major alterations of the regulation of root NO^{3-} uptake are associated with the Mutation of *Nrt2.1* and *Nrt2.2* Genes in *Arabidopsis*. *Plant Physiology*, 127 (1): 262-271.

Chabaud, M., Genre, A., Sieberer, B.J., Faccio, A., Fournier, J., Novero, M., Barker, D.G. and Bonfante, P. (2011). Arbuscular mycorrhizal hyphopodia and germinated spore exudates trigger Ca^{2+} spiking in the legume and nonlegume root epidermis. *The New Phytologist*, 189 (1): 347-355.

Chae, K., Gonong, B.J., Kim, S.C., Kieslich, C.A., Morikis, D., Balasubramanian, S. and Lord, E.M. (2010). A multifaceted study of stigma/style cysteine-rich adhesin (SCA)-like *Arabidopsis* lipid transfer proteins (LTPs) suggests diversified roles for these LTPs in plant growth and reproduction. *Journal of Experimental Botany,* 61 (15): 4277-4290.

Champoiseau, P., Jones, J. and Allen, C. (2009). *Ralstonia solanacearum* race 3 biovar 2 causes tropical losses and temperate anxieties. *Plant Health Progress,* 10: 1-10.

Charng, Y.Y., Liu, H. C., Liu, N.Y., Hsu, F.C., and Ko, S.S. (2006). *Arabidopsis* Hsa32, a novel heat shock protein, is essential for acquired thermotolerance during long recovery after acclimation. *Plant Physiology*, 140 (4): 1297-1305.

Charpentier, M., Bredemeier, R., Wanner, G., Takeda, N., Schleiff, E., & Parniske, M. (2008). *Lotus japonicus* CASTOR and POLLUX are ion channels essential for perinuclear calcium spiking in legume root endosymbiosis. *The Plant Cell*, *20* (12): 3467-3479.

Chen, Z., Agnew, J.L., Cohen, J.D., He. P., Shan, L., Sheen, J. and Kunkel, B.N. (2007). *Pseudomonas syringae* type III effector AvrRpt2 alters *Arabidopsis thaliana* auxin physiology. *Proceedings of the National Academy of Sciences*, 104 (50): 20131-20136.

Chew, Y.H., Wenden, B., Flis, A., Mengin, V., Taylor, J., Davey, C.L., Tindal, C., Thomas, H., Ougham, H.J., de Reffye, P., Stitt, M., Williams, M., Muetzefeldt, R., Halliday, K.J. and Millar, A. J. (2014). Multiscale digital *Arabidopsi*s predicts individual organ and whole-organism growth. *Proceedings of the National Academy of Sciences*, 111 (39): E4127-E4136.

Chiu, W.H., Chandler, J., Cnops, G., Van Lijsebettens, M., and Werr, W. (2007). Mutations in the *TORNADO2* gene affect cellular decisions in the peripheral zone of the shoot apical meristem of *Arabidopsis thaliana*. *Plant Molecular Biology*, 63 (6): 731-744.

Crawford, N.M. and Glass, A.D.M. (1998). Molecular and physiological aspects of nitrate uptake in plants. *Trends in Plant Science,* 3 (10): 389-395.

Cui, F., Wu, S., Sun, W., Coaker, G., Kunkel, B., He, P. and Shan, L. (2013). The Pseudomonas syringae type III effector AvrRpt2 promotes pathogen virulence via stimulating *Arabidopsis* auxin/indole acetic acid protein turnover. *Plant*

Physiology, 162 (2): 1018-1029.

Daras, G., Rigas, S., Penning, B., Milioni, D., McCann, M. C., Carpita, N. C. and Hatzopoulos, P. (2009). The thanatos mutation in *Arabidopsis thaliana* cellulose synthase 3 (AtCesA3) has a dominant-negative effect on cellulose synthesis and plant growth. *New Phytologist*, 184 (1): 114-126.

Deakin, W.J. and Broughton, W.J. (2009). Symbiotic use of pathogenic strategies: rhizobial protein secretion systems. *Nature Reviews Microbiology*, 7 (4): 312-320.

Deinum, E.E., Geurts, R., Bisseling, T. and Mulder, B.M. (2012). Modeling a cortical auxin maximum for nodulation: different signatures of potential strategies. *Frontiers in Plant Science*, 3 (96).

De Jonge, R., Peter van Esse, H., Kombrink, A., Shinya, T., Desaki, Y., Bours, R., van der Krol, S., Shibuya, N., Joosten, M.H.A.J. and Thomma, B.P.H.J. (2010). Conserved fungal LysM effector Ecp6 prevents chitin-triggered immunity in plants. *Science,* 329 (5994): 953-955.

De Lange, O., Schreiber, T., Schandry, N., Radeck, J., Braun, K.H., Koszinowski, J., Heuer, H., Strauß, A. and Lahaye, T. (2013). Breaking the DNA-binding code of *Ralstonia solanacearum* TAL effectors provides new possibilities to generate plant resistance genes against bacterial wilt disease. *The New Phytologist*, 199 (3): 773-786.

De Lucas, M. and Brady, S.M. (2013) Gene regulatory networks in the *Arabidopsis* root. *Current Opinion in Plant Biology*, 16 (1): 50-55.

Denny, T. (2006) Plant pathogenic *Ralstonia* species. In: Plant-associated bacteria. Springer, Netherlands. pp. 573-644.

Desbrosses, G.J. and Stougaard, J. (2011). Root nodulation: A paradigm for how Plant-microbe symbiosis influences host developmental pathways. *Cell Host & Microbe*, 10 (4): 348-358.

Deslandes, L. and Genin, S. (2014). Opening the *Ralstonia solanacearum* type III effector tool box: insights into host cell subversion mechanisms. *Current Opinion in Plant Biolo*gy, 20: 110-117.

De Smet, I., Tetsumura, T., De Rybel, B., dit Frey, N. F., Laplaze, L., Casimiro, I., Swarup, R., Naudts, M., Vanneste, S., Audenaert, D., Inzé, D., Bennett., M.J. and Beeckman, T. (2007). Auxin-dependent regulation of lateral root positioning in the basal meristem of *Arabidopsis*. *Development*, 134 (4): 681-690.

De Smet, I., White, P.J., Bengough, A.G., Dupuy, L., Parizot, B., Casimiro, I., Heidstrag, R., Laskowskih, M., Lepetit, M., Hochholdinger, F., Draye, X., Zhang, H., Broadlea, M., Péret, B., Hammond, J., Fukaki, H., Mooney S., Lynch, J., Nacry, P., Schurr, U., Laplazet, L., Benfey, P., Beeckman, T. and Bennett, M. (2012). Analyzing lateral root development: how to move forward. *The Plant Cell*, 24 (1): 15-20.

Devaiah, B.N., Karthikeyan, A.S. and Raghothama, K.G. (2007). WRKY75 transcription factor is a modulator of phosphate acquisition and root development in *Arabidopsis*. *Plant Physiology*, 143 (4): 1789-1801.

Dinneny, J.R., Long, T.A., Wang, J.Y., Jung, J.W., Mace, D., Pointer, S., Barron, C., Brady, S.M., Schiefelbein, J. and Benfey, P. N. (2008). Cell identity mediates the response of *Arabidopsis* roots to abiotic stress. *Science*, 320 (5878): 942-945.

Ding, Z.J., Yan, J. Y., Xu, X.Y., Yu, D.Q., Li, G.X., Zhang, S.Q. and Zheng, S.J. (2014). Transcription factor WRKY46 regulates osmotic stress responses and stomatal movement independently in *Arabidopsis*. *The Plant Journal*, 7 (1): 13-27.

Dong, J., Chen, C. and Chen, Z. (2003). Expression profiles of the *Arabidopsis WRKY* gene superfamily during plant defense response. *Plant Molecular Biology,* 51 (1): 21-37.

Downie, H., Holden, N., Otten, W., Spiers, A.J., Valentine, T.A. and Dupuy, L.X. (2012) Transparent Soil for Imaging the Rhizosphere Bennett. *PLoS One*, 7 (9): e44276.

Downie, J.A. (2014). Legume nodulation. *Current Biology*, 24 (5): 184-190.

Doyle, J.J. (2011) Phylogenetic perspectives on the origins of nodulation. *Molecular Plant-Microbe Interactions*, 24 (11): 1289-1295.

Doyle, E.L., Stoddard, B.L., Voytas, D.F. and Bogdanove, A.J. (2013). TAL effectors: highly adaptable phytobacterial virulence factors and readily engineered DNA-targeting proteins. *Trends in Cell Biology*, 23 (8): 390-398.

Du, Z., Zhou, X., Ling, Y., Zhang, Z. and Su, S. (2010). agriGO: a GO analysis toolkit for the agricultural community. *Nucleic Acids Research,* 38 (2): 64-70.

Dubos, C., Stracke, R., Grotewold, E., Weisshaar, B., Martin, C. and Lepiniec, L. (2010). MYB transcription factors in *Arabidopsis*. *Trends in Plant Science*, 15 (10): 573-581.

Dubrovsky, J. G., Doerner, P. W., Colón-Carmona, A., and Rost, T. L. (2000). Pericycle cell proliferation and lateral root initiation in *Arabidopsis*. *Plant Physiology*, 124 (4): 1648-1657.

Dubrovsky, J.G., Sauer, M., Napsucialy-Mendivil, S., Ivanchenko, M.G., Friml, J., Shishkova, S., Celenza, J. and Benková, E. (2008). Auxin acts as a local morphogenetic trigger to specify lateral root founder cells. *Proceedings of the National Academy of Sciences of the USA,* 105 (25): 8790-8794.

Ehrhardt, D.W., Wais, R., and Long, S.R. (1996). Calcium spiking in plant root hairs responding to *Rhizobium* nodulation signals. *Cell*, 85 (5): 673-681.

Eklöf, J.M. and Brumer, H. (2010). The XTH gene family: an update on enzyme structure, function, and phylogeny in xyloglucan remodeling. *Plant Physiology*, 153 (2): 456-466.

Ellis, C.M., Nagpal, P., Young, J.C., Hagen, G., Guilfoyle, T.J. and Reed, J.W. (2005). AUXIN RESPONSE FACTOR1 and AUXIN RESPONSE FACTOR2 regulate senescence and floral organ abscission in *Arabidopsis thaliana. Development*, 132 (20): 4563-4574.

Emmert-Streib, F., Glazko, G. and De Matos Simoes, R. (2012). Statistical inference and reverse engineering of gene regulatory networks from observational expression data. *Frontiers in Genetics*, 3 (8): 1-15.

Endre, G., Kereszt, A., Kevei, Z., Mihacea, S., Kaló, P. and Kiss, G.B. (2002). A receptor kinase gene regulating symbiotic nodule development. *Nature*, *417*(6892): 962-966.

Erisman, J. W., Sutton, M. A., Galloway, J., Klimont, Z. and Winiwarter, W. (2008). How a century of ammonia synthesis changed the world. *Nature Geoscience*, 1 (10): 636-639.

Esseling, J.J., Lhuissier, F.G. and Emons, A.M.C. (2004). A nonsymbiotic root hair tip growth phenotype in NORK-mutated legumes: implications for nodulation factor-induced signaling and formation of a multifaceted root hair pocket for bacteria. *The Plant Cell*, 16 (4): 933-944.

Fagard, M., Desnos, T., Desprez, T., Goubet, F., Refregier, G., Mouille, G., Höfte, H. (2000). PROCUSTE1 encodes a cellulose synthase required for normal cell elongation specifically in roots and dark-grown hypocotyls of *Arabidopsis*. *The Plant Cell*, 12 (12): 2409-2423.

Falcon S., Carey B., Settles M. and Beuf K.D. (2007). pdInfoBuilder: Platform Design Information Package Builder. R package version 1.28.0.

Fan, S.C., Lin, C.S., Hsu, P.K., Lin, S.H. and Tsay, Y.F. (2009). The *Arabidopsis* nitrate transporter NRT1.7, expressed in phloem, is responsible for source-to-sink remobilization of nitrate. *The Plant Cell*, 21 (9): 2750-2761.

Fortunati, A., Piconese, S., Tassone, P., Ferrari, S. and Migliaccio, F. (2007). A new mutant of *Arabidopsis* disturbed in its roots, right-handed slanting, and gravitropism defines a gene that encodes a heat-shock factor. *Journal of Experimental Botany,* 59 (6): 1363-1374.

Fuller, T.F., Ghazalpour, A., Aten, J.E., Drake, T.A., Lusis, A.J. and Horvath, S. (2007). Weighted gene coexpression network analysis strategies applied to mouse weight. *Mammalian Genome*, 18 (6): 463-472.

Galbraith, D.W. and Birnbaum, K. (2006). Global studies of cell type-specific gene expression in plants. *Annual Reviews of Plant Biology*, 57: 451-475.

Gallou, A., Declerck, S. and Cranenbrouck, S. (2012). Transcriptional regulation of defence genes and involvement of the WRKY transcription factor in arbuscular mycorrhizal potato root colonization. *Functional & Integrative Genomics,* 12 (1): 183-198.

Galloway, J. N. (1998). The global nitrogen cycle: changes and consequences.

Environmental Pollution, 102 (1): 15-24.

Geider, R.J., Roche, J., Greene, R.M. and Olalzola, M. (1993). Response of the photosynthetic apparatus of *Phaedactylum triconutum* (Bacillariophycae) to nitrate, phosphate, or iron starvation. *Journal of Phycology* 29 (6): 755-766.

Genin, S. and Denny, T.P. (2012). Pathogenomics of the *Ralstonia solanacearum* species complex. *Annual Review of Phytopathology,* 50 (1): 67-89.

Genre, A., Chabaud, M., Balzergue, C., Puech‐Pagès, V., Novero, M., Rey, T. and Barker, D. G. (2013). Short‐chain chitin oligomers from arbuscular mycorrhizal fungi trigger nuclear Ca^{2+} spiking in *Medicago truncatula* roots and their production is enhanced by strigolactone. *New Phytologist*, 198 (1): 190-202.

Gentleman, R. and Falcon, S. (2005). Gostats: Tools for manipulating go and microarrays. *R package version*, 1 (3).

Giegé, P., Sweetlove, L.J., Cognat, V. and Leaver, C.J. (2005). Coordination of nuclear and mitochondrial genome expression during mitochondrial biogenesis in *Arabidopsis*. *The Plant Cell*, 17 (5): 1497-1512.

Gifford, M.L., Dean, A., Gutierrez, R.A., Coruzzi, G.M. and Birnbaum, K.D. (2008) Cell-specific nitrogen responses mediate developmental plasticity. *Proceedings of the National Acadamy of Sciences of the USA*, 105 (2): 803-808.

Gifford, M.L., Banta, J., Katari, M. S., Hulsmans, J., Chen, L., Ristova, D. and Birnbaum, K. D. (2013) Natural variation reveals modular plasticity of root traits in different nitrogen environments. *PLoS Genetics.* 9 (9): e1003760.

Girin, T., Lejay, L., Wirth, J., Widiez, T., Palenchar, P.M., Nazoa, P., Touraine, B., Gojon, A. and Lepetit, M. (2007). Identification of a 150 bp *cis*-acting element of the *AtNRT2.1* promoter involved in the regulation of gene expression by the N and C status of the plant. *Plant, Cell & Environment*, 30 (11): 1366-1380.

Glass, A.D. and Kotur, Z. (2013). A reevaluation of the role of *Arabidopsis* NRT1. 1 in high-affinity nitrate transport. *Plant Physiology*, 163 (3): 1103-1106.

Goh, T., Kasahara, H., Mimura, T., Kamiya, Y. and Fukaki, H. (2012). Multiple AUX/IAA-ARF modules regulate lateral root formation: the role of *Arabidopsis* SHY2/IAA3-mediated auxin signalling. *Philosophical Transactions of the Royal Society of Biological Sciences*, 367 (1595): 1461-1468.

Gojon, A., Krouk, G. and Perrine-Walker, F. (2011) Nitrate transceptor(s) in plants. *Journal of experimental botany,* 62 (7): 2299-2308.

Gourion, B., Berrabah, F., Ratet, P. and Stacey, G. (2015). *Rhizobium*-legume symbioses: the crucial role of plant immunity. *Trends in Plant Science*, 20 (3): 186-194.

Grønlund, J.T., Eyres, A., Kumar, S., Buchanan-Wollaston, V. and Gifford, M.L. (2012). Cell specific analysis of *Arabidopsis* leaves using fluorescence activated

cell sorting. *Journal of Visualized Experiments*, 68: 4241.

Gu, Y., Kaplinsky, N., Bringmann, M., Cobb, A., Carroll, A., Sampathkumar, A. and Somerville, C.R. (2010). Identification of a cellulose synthase-associated protein required for cellulose biosynthesis. *Proceedings of the National Academy of Sciences of the USA*, 107 (29): 12866-12871.

Guo, W.J. and Ho, T.H.D. (2008). An abscisic acid-induced protein, HVA22, inhibits gibberellin-mediated programmed cell death in cereal aleurone cells. *Plant Physiology,* 147 (4): 1710-1722.

Guo, Y., Cai, Z. and Gan, S. (2004) Transcriptome of *Arabidopsis* leaf senescence. *Plant, Cell & Environment,* 27 (5): 521-549.

Gust, A.A., Willmann, R. andDesaki, Y. (2012). Plant LysM proteins: modules mediating symbiosis and immunity. *Trends in Plant Science,* 17 (8): 495-502.

Gutiérrez, R.A., Stokes, T.L., Thum, K., Xu, X., Obertello, M., Katari, M. S., Tanurdzic, M., Dean, A., Nero, D.C., McClung, R. and Coruzzi, G. M. (2008). Systems approach identifies an organic nitrogen-responsive gene network that is regulated by the master clock control gene *CCA1*. *Proceedings of the National Academy of Sciences of the USA,* 105 (12): 4939-4944.

Gutiérrez, R.A. (2012) Systems Biology for Enhanced Plant Nitrogen Nutrition. *Science*, 336 (6): 1673-1675.

Hagen, G. and Guilfoyle, T. (2002). Auxin-responsive gene expression: genes, promoters and regulatory factors. *Plant Molecular Biology*, 49 (3): 373-385.

Harms, E., Kivimäe, S., Young, M.W. and Saez, L. (2004). Posttranscriptional and posttranslational regulation of clock genes. *Journal of Biological Rhythms,* 19 (5): 361-373.

He, X.J., Mu, R.L., Cao, W.H., Zhang, Z.G., Zhang, J.S. and Chen, S.Y. (2005). AtNAC2, a transcription factor downstream of ethylene and auxin signaling pathways, is involved in salt stress response and lateral root development. *The Plant Journal*, 44 (6): 903-916.

Heard N.A., Holmes C.C. and Stephens D.A. (2006). A quantitative study of gene regulation involved in the immune response of anopheline mosquitoes: An application of Bayesian hierarchical clustering of curves. *Journal of the American Stastical Association,* 101 (473): 18-29.

Hecker, M., Lambeck, S., Toepfer, S., Van Someren, E. and Guthke, R. (2009). Gene regulatory network inference: data integration in dynamic models - a review. *Biosystems*, 96 (1): 86-103.

Heckmann, A. B., Lombardo, F., Miwa, H., Perry, J. A., Bunnewell, S., Parniske, M., and Downie, J. A. (2006). *Lotus japonicus* nodulation requires two GRAS domain regulators, one of which is functionally conserved in a non-legume. *Plant Physiology*, 142 (4): 1739-1750.

Heidstra, R., Welch, D. and Scheres, B. (2004). Mosaic analyses using marked activation and deletion clones dissect *Arabidopsis* SCARECROW action in asymmetric cell division. *Genes & Development*, 18 (16): 1964-1969.

Heyndrickx, K.S. and Vandepoele, K. (2012). Systematic identification of functional plant modules through the integration of complementary data sources. *Plant Physiology,* 159 (3): 884-901.

Ho, C.H., Lin, S.H., Hu, H.C. and Tsay, Y.F. (2008). CHL1 functions as a nitrate sensor in plants. *Cell*, 138 (6): 1184-1194.

Hodge, A., Robinson, D., Griffiths, B.S. and Fitter, A.H. (1999). Why plants bother: root proliferation results in increased nitrogen capture from an organic patch when two grasses compete. *Plant Cell and Environment* 22 (7): 811-820

Hoeffding, W. (1948). A class of statistics with asymptotically normal distribution. *The Annals of Mathematical Statistics*, 293-325.

Holland, N., Holland, D., Helentjaris, T., Dhugga, K. S., Xoconostle-Cazares, B. and Delmer, D.P. (2000). A comparative analysis of the plant cellulose synthase (*CesA*) gene family. *Plant Physiology*, 123 (4): 1313-1324.

Hove, C.A., Willemsen, V., de Vries, W.J., van Dijken, A., Scheres, B. and Heidstra, R. (2010). *Schizoria* encodes a nuclear factor regulating asymmetry of stem cell divisions in the *Arabidopsis* root. *Current Biology,* 20 (5): 452-457.

Hsu, P.K. and Tsay, Y.F. (2013) Two phloem nitrate transporters, NRT1.11 and NRT1.12, are important for redistributing xylem-borne nitrate to enhance plant growth. *Plant Physiology*, 163 (2): 844-856.

Hu, H.C., Wang, Y.Y., and Tsay, Y.F. (2009). AtCIPK8, a CBL-interacting protein kinase, regulates the low-affinity phase of the primary nitrate response. *The Plant Journal*, 57 (2): 264-278.

Hu, J., Barlet, X., Deslandes, L., Hirsch, J., Feng, D. X., Somssich, I., and Marco, Y. (2008). Transcriptional responses of *Arabidopsis thaliana* during wilt disease caused by the soil-borne phytopathogenic bacterium, *Ralstonia solanacearum*. *PLoS One*, *3* (7): e2589.

Hu, Y., Dong, Q. and Yu, D. (2012). *Arabidopsis* WRKY46 coordinates with WRKY70 and WRKY53 in basal resistance against pathogen *Pseudomonas syringae*. *Plant Science*, 185: 288-297.

Huang, Y.C., Chang, Y.L., Hsu, J.J. and Chuang, H.W. (2008). Transcriptome analysis of auxin-regulated genes of *Arabidopsis thaliana*. *Gene*, 420 (2): 118-124.

Imin, N., Mohd-Radzman, N. A., Ogilvie, H. A., and Djordjevic, M. A. (2013). The peptide-encoding CEP1 gene modulates lateral root and nodule numbers in Medicago truncatula. *Journal of Experimental Botany*, 64 (17): 5395-5409.

Jakoby, M., Weisshaar, B., Dröge-Laser, W., Vicente-Carbajosa, J., Tiedemann, J.,

Kroj, T. and Parcy, F. (2002). bZIP transcription factors in *Arabidopsis*. *Trends in Plant Science,* 7 (3): 106-111.

Jeffreys, H. (1961). The Theory of Probability (3 ed.). OUP, Oxford. p. 432.

Jiang, K. and Feldman, L.J. (2005). Regulation of root apical meristem development. *Annual Reviews of Cell and Developmental Biololgy,* 21: 485-509.

Jiang, Y., Yang, B., Harris, N. S., & Deyholos, M. K. (2006) Comparative proteomic analysis of NaCl stress-responsive proteins in *Arabidopsis* roots. *Journal of Experimental Botany*, 58 (13): 3591-3607

Jiao, Y., Yang, H., Ma, L., Sun, N., Yu, H., Liu, T., Gao, H. and Deng, X. W. (2003). A genome-wide analysis of blue-light regulation of *Arabidopsis* transcription factor gene expression during seedling development. *Plant Physiology,* 133 (4): 1480-1493.

Jones, J. and Dangl, J.L. (2006). The plant immune system. *Nature*, 444 (7117): 323-329

Journet, E.P., Pichon, M. and Dedieu, A. (1994) *Rhizobium meliloti* Nod factors elicit cell-specific transcription of the ENOD12 gene in transgenic alfalfa. *The Plant Journal for Cell and Molecular Biology*, 6 (2): 241-249.

Jung, J. K., & McCouch, S. (2013). Getting to the roots of it: genetic and hormonal control of root architecture. *Frontiers in Plant Science*, 4: 186.

Kambara, K., Ardissone, S., Kobayashi, H., Saad, M.M., Schumpp, O., Broughton, W. J. and Deakin, W.J. (2009). Rhizobia utilize pathogenlike effector proteins during symbiosis. *Molecular Microbiology*, 71 (1): 92-106.

Katari, M.S., Nowicki, S.D., Aceituno, F.F., Nero, D., Kelfer, J., Thompson, L.P., Cabello, J.M., Davidson, R.S., Goldberg, A.P. Shasha, D.E., Coruzzi, G.M. and Gutiérrez, M. (2010). VirtualPlant: a software platform to support systems biology research. *Plant Physiology*, 152 (2): 500-515.

Kauffmann, A., Gentleman, R. and Huber, W. (2009). arrayQualityMetrics - a bioconductor package for quality assessment of microarray data. *Bioinformatics*, 25 (3): 415-416.

Kiba, T., Kudo, T., Kojima, M. and Sakakibara, H. (2011). Hormonal control of nitrogen acquisition: roles of auxin, abscisic acid, and cytokinin. *Journal of Experimental Botany,* 62 (4): 1399-1409.

Kiba, T., Feria-Bourrellier, A.B., Lafouge, F., Lezhneva, L., Boutet-Mercey, S., Orsel, M., Bréhaut, V., Miller, A., Daniel-Vedele, F., Sakakibara, H., and Krapp, A. (2012). The *Arabidopsis* nitrate transporter NRT2.4 plays a double role in roots and shoots of nitrogen-starved plants. *The Plant Cell,* 24 (1): 245-258.

Kim, D., Cho, Y.H., Ryu, H., Kim, Y., Kim, T.-H. and Hwang, I. (2013) BLH1 and KNAT3 modulate ABA responses during germination and early seedling development in *Arabidopsis*. *The Plant Journal*, 75 (5): 755-766.

Kim, J. H., Choi, D. and Kende, H. (2003). The AtGRF family of putative transcription factors is involved in leaf and cotyledon growth in *Arabidopsis*. *The Plant Journal*, 36 (1): 94-104.

Kim, K.M., Jun, D.Y., Kim, S.K., Kim, C.K., Kim, B.O., Kim, Y.H., Park, W., Sohn, J.K., Hirata, A., Kawai-Yamada, M.,Uchimiya, H., Kim, D.H. and Sul, I.W. (2007). Identification of novel mitochondrial membrane protein (Cdf 3) from *Arabidopsis thaliana* and its functional analysis in a yeast system. *Journal of Microbiology and Biotechnology,* 17 (6): 891-896.

Kiyosue, T., Abe, H., Yamaguchi-Shinozaki, K. and Shinozaki, K. (1998). ERD6, a cDNA clone for an early dehydration-induced gene of *Arabidopsis*, encodes a putative sugar transporter. *Biochimica et Biophysica Acta - Biomembranes,* 1370 (2): 187-191.

Kong, Y., Zhou, G., Yin, Y., Xu, Y., Pattathil, S. and Hahn, M. G. (2011). Molecular analysis of a family of *Arabidopsis* genes related to galacturonosyltransferases. *Plant Physiology,* 155 (4): 1791-1805.

Konishi, M. and Yanagisawa, S. (2013) *Arabidopsis* NIN-like transcription factors have a central role in nitrate signalling. *Nature Communications,* 4: 1617.

Kosuta, S., Hazledine, S., Sun, J., Miwa, H., Morris., R.J. Downie. J.A. and Oldroyd, G.E.D. (2008) Differential and chaotic calcium signatures in the symbiosis signaling pathway of legumes. *Proceedings of the National Academy of Sciences,* 105 (28): 9823-9828.

Kotur, Z., Mackenzie, N., Ramesh, S., Tyerman, S.D., Kaiser, B.N. and Glass, A.D.M (2012). Nitrate transport capacity of the *Arabidopsis thaliana* NRT2 family members and their interactions with AtNAR2.1. *New Phytologist*, 194 (3): 724-731.

Krapp, A., David, L.C., Chardin, C., Girin, T., Marmagne, A., Leprince, A.-S., Chailou, S., Ferrario-Méry, S., Meyer, C. and Daniel-Vedele, F. (2014). Nitrate transport and signalling in *Arabidopsis*. *Journal of Experimental Botany,* 65 (3): 789-798.

Kreps, J.A., Wu, Y., Chang, H.S., Zhu, T., Wang, X. and Harper, J.F. (2002). Transcriptome changes for *Arabidopsis* in response to salt, osmotic, and cold stress. *Plant Physiology*, 130 (4): 2129-2141.

Krol, E., Mentzel, T., Chinchilla, D., Boller, T., Felix, G., Kemmerling, B., Postel, S., Arents, M., Jeworutzki, E., Al-Rasheid, K.A.S., Becker. D. and Hedrich, R. (2010). Perception of the *Arabidopsis* danger signal peptide 1 involves the pattern recognition receptor AtPEPR1 and its close homologue AtPEPR2. *Journal of Biological Chemistry*, 285 (18): 13471-13479.

Krouk, G., Lacombe, B., Bielach, A., Perrine-Walker, F., Malinska, K., Mounier, E., Hoyerova, K., Tillard, P., Leon, S., Ljung, K., Zazimalova, E., Benkova, E., Nacry, P. and Gojon, A. (2010). Nitrate-regulated auxin transport by NRT1.1 defines a mechanism for nutrient sensing in plants. *Developmental Cell*, 18 (6): 927-937.

Krouk, G., Ruffel, S., Gutiérrez, R. A., Gojon, A., Crawford, N. M., Coruzzi, G. M. and Lacombe, B. (2011). A framework integrating plant growth with hormones and nutrients. *Trends in Plant Science*, 16 (4): 178-182.

Krouk, G., Lingeman, J., Colon, A.M., Coruzzi, G. and Shasha, D. (2013). Gene regulatory networks in plants: learning causality from time and perturbation. *Genome biology,* 14 (6): 123.

Kuppusamy, K. T., Ivashuta, S., Bucciarelli, B., Vance, C. P., Gantt, J. S. and VandenBosch, K. A. (2009). Knockdown of CELL DIVISION CYCLE16 reveals an inverse relationship between lateral root and nodule numbers and a link to auxin in Medicago truncatula. *Plant Physiology*, 151 (3): 1155-1166.

Kurkela, S. and Borg-Franck, M. (1992). Structure and expression of *kin2*, one of two cold-and ABA-induced genes of *Arabidopsis thaliana*. *Plant Molecular Biology,* 19 (4): 689-692.

La Camera, S., L'Haridon, F., Astier, J., Zander, M., Mansour, E., Page, G. and Lamotte, O. (2011). The glutaredoxin ATGRXS13 is required to facilitate Botrytis cinerea infection of Arabidopsis thaliana plants. *The Plant Journal*, 68 (3): 507-519.

Lamesch, P., Berardini, T.Z., Li, D., Swarbreck, D., Wilks, C., Sasidharan, R., Muller, R., Dreher, K., Alexander, D.L., Garcia-Hernandez, M., Karthikeyan, A.S., Lee, C.H., Nelson, W.D., Ploets, L., Singh, S., Wensel, A. and Huala, E. (2012). The *Arabidopsis* Information Resource (TAIR): improved gene annotation and new tools. *Nucleic Acids Research,* 40 (1): D1202-D1210.

Lee, C., Teng, Q., Zhong, R., Yuan, Y., Haghighat, M. and Ye, Z. H. (2012). Three Arabidopsis DUF579 domain-containing GXM proteins are methyltransferases catalyzing 4-O-methylation of glucuronic acid on xylan. *Plant and Cell Physiology*, 53 (11): 1934-1949.

Lee, T.I. and Young, R.A. (2000). Transcription of eukaryotic protein-coding genes. *Annual Review of Genetics*, 34 (1): 77-137.

Lejay, L., Tillard, P., Lepetit, M., Olive, F.D., Filleur, S., Daniel-Vedele, F. and Gojon, A. (1999) Molecular and functional regulation of two NO^{3-} uptake systems by N- and C-status of *Arabidopsis* plants. *The Plant Journal,* 18 (5): 509-519.

Léran, S., Varala, K., Boyer, J.C., Chiurazzi, M., Crawford, N., Daniel-Vedele, F., David, L., Dikckstein, R., Fernandez, E., Forde, B., Gassmann, W., Geiger, D., Gojon, A., Gong, J.M., Halkier, B.A., Harris, J.M., Hedrich, R., Limami, A.M. Rentsch, D., Seo, M., Tsay, Y.F., Zhang, M., Coruzzi, G. and Lacombe, B. (2014). A unified nomenclature of NITRATE TRANSPORTER 1/PEPTIDE TRANSPORTER family members in plants. *Trends in Plant Science,* 19 (1): 5-9.

Less, H., Angelovici, R., Tzin, V. and Galili, G. (2011) Coordinated gene networks regulating *Arabidopsis* plant metabolism in response to various stresses and nutritional cues. *The Plant Cell,* 23 (4): 1264-1271.

Lévy, J., Bres, C., Geurts, R., Chalhoub, B., Kulikova, O., Duc, G. and Debellé, F. (2004). A putative Ca^{2+} and calmodulin-dependent protein kinase required for bacterial and fungal symbioses. *Science*, *303* (5662): 1361-1364.

Lewis, D. R., Miller, N. D., Splitt, B. L., Wu, G. and Spalding, E. P. (2007). Separating the roles of acropetal and basipetal auxin transport on gravitropism with mutations in two *Arabidopsis* multidrug resistance-like ABC transporter genes. *The Plant Cell,* 19 (6): 1838-1850.

Li, H., Johnson, P., Stepanova, A., Alonso, J.M. and Ecker, J.R. (2004). Convergence of Signaling Pathways in the Control of Differential Cell Growth in *Arabidopsis*. *Developmental Cell*, 7 (2): 193-204.

Li, J.Y., Fu, Y.L., Pike, S.M., Bao, J., Tian, W., Zhang, Y., Chen, C.Z., Li, H.M., Huang, Jing., Li, L.G., Schroeder, J.I. Gassman, W. and Gong, J.M. (2010). The *Arabidopsis* Nitrate Transporter NRT1.8 Functions in Nitrate Removal from the Xylem Sap and Mediates Cadmium Tolerance. *The Plant Cell,* 22 (5): 1633-1646.

Li, L., Kim, B.G., Cheong, Y.H., Pandey, G.K. and Luan, S. (2006). A $Ca^{(2)+}$ signaling pathway regulates a $K^{(+)}$ channel for low-K response in *Arabidopsis*. *Proceedings of the National Academy of Sciences of the USA*, 103 (33): 12625-12630.

Li, L., Ljung, K., Breton, G., Schmitz, R.J., Pruneda-Paz, J., Cowing-Zitron, C., Cole, B.J., Ivans, L.J., Pedmale, U.V., Jung, H.S., Ecker, J.R., Kay, S.A. and Chory, J. (2012). Linking photoreceptor excitation to changes in plant architecture. *Genes & Development,* 26 (8): 785-790.

Li, W., Wang, Y., Okamoto, M., Crawford, N.M., Siddiqi, M.Y. and Glass, A.D.M. (2007). Dissection of the *AtNRT2.1:AtNRT2.2* Inducible High-Affinity Nitrate Transporter Gene Cluster. *Plant Physiology*, 143 (1): 425-433.

Li, Z., Zhang, L., Yu, Y., Quan, R., Zhang, Z., Zhang, H. and Huang, R. (2011). The ethylene response factor AtERF11 that is transcriptionally modulated by the bZIP transcription factor HY5 is a crucial repressor for ethylene biosynthesis in *Arabidopsis*. *The Plant Journal*, 68 (1): 88-99.

Liang, Y., Cao, Y., Tanaka, K., Thibivilliers, S., Wan, J., Choi, J., Kang, C.H., Qiu, J. and Stacey, G. (2013). Nonlegumes respond to rhizobial Nod factors by suppressing the innate immune response. *Science*, 341 (6152): 1384-1387.

Liang, Y., Tóth, K., Cao, Y., Tanaka, K., Espinoza, C. and Stacey, G. (2014). Lipochitooligosaccharide recognition: an ancient story. *The New Phytologist,* 204 (2): 289-296.

Libault, M., Wan, J., Czechowski, T., Udvardi, M., & Stacey, G. (2007). Identification of 118 *Arabidopsis* transcription factor and 30 ubiquitin-ligase genes responding to chitin, a plant-defense elicitor. *Molecular Plant-Microbe Interactions*, 20 (8): 900-911.

Lilliefors, H., W. (1967). On the Kolmogorov-Smirnov test for normality with mean and variance unknown. *Journal of the American Statistical Association*, 62

(318): 399-402.

Lin, R. and Wang, H. (2005). Two homologous ATP-binding cassette transporter proteins, AtMDR1 and AtPGP1, regulate *Arabidopsis* photomorphogenesis and root development by mediating polar auxin transport. *Plant Physiology,* 138 (2): 949-964.

Lin, S.H., Kuo, H.F., Canivenc, G., Lin, C.S. Lepetit, M., Hsu, P.K., Tillard, P., Lin, H.L., Wang, Y.Y., Tsai, C.B., Gojon, A. and Tsay, Y.F. (2008). Mutation of the *Arabidopsis* NRT1.5 Nitrate Transporter Causes Defective Root-to-Shoot Nitrate Transport. *The Plant Cell,* 20 (9): 2514-2528.

Little, D.Y., Rao, H., Oliva, S., Daniel-Vedele, F., Krapp, A. and Malamy, J.E. (2005). The putative high-affinity nitrate transporter NRT2.1 represses lateral root initiation in response to nutritional cues. *Proceedings of the National Academy of Sciences of the USA,* 102 (38): 13693-13698.

Liu, B., Li, J.F., Ao, Y., Qu, J., Li, Z., Su, J., Zhang, Y., Liu, J., Feng, D., Qi, K., He, Y., Wang, J. and Wang, H.-B. (2012). Lysin motif-containing proteins LYP4 and LYP6 play dual roles in peptidoglycan and chitin perception in rice innate immunity. *The Plant Cell,* 24 (8): 3406-3419.

Liu, K.H., Huang, C.Y. and Tsay, Y.F. (1999) CHL1 is a dual-affinity nitrate transporter of *Arabidopsis* involved in multiple phases of nitrate uptake. *The Plant Cell,* 11 (5): 865-874.

Liu, K.H. and Tsay, Y.F. (2003). Switching between the two action modes of the dual-affinity nitrate transporter CHL1 by phosphorylation. *The EMBO journal,* 22 (5): 1005-1013.

Liu, H., Yang, H., Wu, C., Feng, J., Liu, X., Qin, H. and Wang, D. (2009). Overexpressing HRS1 confers hypersensitivity to low phosphate-elicited inhibition of primary root growth in *Arabidopsis thaliana*. *Journal of Integrative Plant Biology,* 51 (4): 382-392.

Lodwig, E. and Poole, P. (2003). Metabolism of *rhizobium* bacteroids. *Critical Reviews in Plant Sciences*, 22 (1): 37-78.

Lopez-Gomez, M., Sandal, N., Stougaard, J., and Boller, T. (2011). Interplay of flg22-induced defence responses and nodulation in *Lotus japonicus*. *Journal of Experimental Botany*, 63 (1): 393-401.

Luhua, S., Hegie, A., Suzuki, N., Shulaev, E., Luo, X., Cenariu, D., Ma, V., Kao, S., Lim, J., Gunay, M.B., Oosumi, T., Lee, S.C., Harper, J., Cushman, J., Gollery, M., Girke, T., Bailey-Serres, J., Stevenson, R.A., Zhu, J.-K. and Mittler, R. (2013). Linking genes of unknown function with abiotic stress responses by high‐throughput phenotype screening. *Physiologia Plantarum,* 148 (3): 322-333.

Lynch, J. (1995). Root architecture and plant productivity. *Plant Physiology,* 109 (1): 7-13.

Lynch, T., Erickson, B.J. and Finkelstein, R.R. (2012). Direct interactions of ABA-insensitive(ABI)-clade protein phosphatase(PP)2Cs with calcium-dependent protein kinases and ABA response element-binding bZIPs may contribute to turning off ABA response. *Plant Molecular Biology*, 80 (6): 647-658.

Ma, C., Guo, J., Kang, Y., Doman, K., Bryan, A.C., Tax, F. E., Yamaguchi, Y. and Qi, Z. (2014). AtPEPTIDE RECEPTOR2 mediates the AtPEPTIDE1 induced cytosolic Ca^{2+} rise, which is required for the suppression of Glutamine Dumper gene expression in *Arabidopsis* roots. *Journal of Integrative Plant Biology.* 56 (7): 684-694.

Ma, Y., Zhao, Y., Walker, R.K. and Berkowitz, G.A. (2013). Molecular steps in the immune signaling pathway evoked by plant elicitor peptides: Ca^{2+}-dependent protein kinases, nitric oxide, and reactive oxygen species are downstream from the early Ca^{2+} signal. *Plant Physiology*, 163 (3): 1459-1471.

Maathuis, F.J. (2009). Physiological functions of mineral macronutrients. *Current Opinion in Plant Biology*, 12 (3): 250-258.

Macchiavelli, R.E. and Brelles-Mariño, G. (2004). Nod factor-treated *Medicago truncatula* roots and seeds show an increased number of nodules when inoculated with a limiting population of *Sinorhizobium meliloti*. *Journal of Experimental Botany,* 55 (408): 2635-2640.

Madsen, E.B., Madsen, L.H., Radutoiu, S., Olbryt, M., Rakwalska, M., Szczyglowski, K., Sato, S., Kaneko, T., Tabata, S., Sandal, N. and Stougaard, J. (2003). A receptor kinase gene of the LysM type is involved in legume perception of rhizobial signals. *Nature*, 425 (6958): 637-640.

Maekawa, S., Sato, T., Asada, Y., Yasuda, S., Yoshida, M., Chiba, Y. and Yamaguchi, J. (2012). The *Arabidopsis* ubiquitin ligases ATL31 and ATL6 control the defense response as well as the carbon/nitrogen response. *Plant Molecular Biology*, 79 (3): 217-227.

Maillet, F., Poinsot, V., André, O., Puech-Pages, V., Haouy, A., Gueunier, M., Cromer, L., Giraudet, D., Formey, D., Niebel, A., Martinez, E.A., Driguez, H., Bécard, G. and Dénarié, J. (2011). Fungal lipochitooligosaccharide symbiotic signals in arbuscular mycorrhiza. *Nature*, 469 (7328): 58-63.

Mairhofer, S., Zappala, S., Tracy, S.R., Sturrock, C., Bennet, M., Mooney, S.J. and Pridmore, T. (2012). RooTrak: automated recovery of three-dimensional plant root architecture in soil from X-ray microcomputed tomography images using visual tracking. *Plant Physiology,* 158 (2): 561-569.

Malamy, J.E. and Benfey, P.N. (1997). Down and out in *Arabidopsis*: the formation of lateral roots. *Trends in Plant Science,* 2 (10): 390-396.

Malamy, J. E., & Ryan, K. S. (2001). Environmental regulation of lateral root initiation in *Arabidopsis*. *Plant Physiology,* 127 (3): 899-909.

Malamy, J.E. (2005). Intrinsic and environmental response pathways that regulate root system architecture. *Plant, Cell and Environment*, 28 (1): 67-77.

Marbach, D., Costello, J.C., Küffner, R., Vega, N.M., Prill, R.J., Camacho, D. and Allison, K. Wisdom of crowds for robust gene network inference. *Nature Methods* 9 (8): 796-804.

Marchive, C., Roudier, F., Castaings, L., Bréhaut, V., Blondet, E., Colot, V., Meyer, C. and Krapp, A. (2013). Nuclear retention of the transcription factor NLP7 orchestrates the early response to nitrate in plants. *Nature Communications,* 4: 1713.

Marie, C., Broughton, W.J. and Deakin, W.J. (2001). *Rhizobium* type III secretion systems: legume charmers or alarmers? *Current Opinion in Plant Biology,* 4 (4): 336-342.

Markmann, K. and Parniske, M. (2009). Evolution of root endosymbiosis with bacteria: how novel are nodules? *Trends in Plant Science,* 14 (2): 77-86.

Martinez-Abarca, F., Herrera-Cervera, J.A., Bueno, P., Sanjuan, J., Bisseling, T. and Olivares, J. (1998). Involvement of salicylic acid in the establishment of the *Sinorhizobium meliloti* - alfalfa symbiosis. *Molecular Plant - Microbe Interactions,* 11 (2): 153-155.

Masucci, J.D. and Schiefelbein, J.W. (1994). The *rhd6* mutation of *Arabidopsis thaliana* alters root-hair initiation through an auxin-and ethylene-associated process. *Plant Physiology,* 106 (4): 1335-1346.

Mazzucotelli, E., Mastrangelo, A.M., Crosatti, C., Guerra, D., Stanca, A.M. and Cattivelli, L. (2008). Abiotic stress response in plants: When post-transcriptional and post-translational regulations control transcription. *Plant Science,* 174 (4): 420-431.

McCabe, D.C. and Caudill, M. A. (2005). DNA methylation, genomic silencing, and links to nutrition and cancer. *Nutrition Reviews*, 63 (6): 183-195.

McClung, C.R. (2006). Plant circadian rhythms. *The Plant Cell,* 18 (4): 792-803.

McClung, C.R. and Gutiérrez, R.A. (2010). Network news: prime time for systems biology of the plant circadian clock. *Current Opinion in Genetics & Development*, 20 (6): 588-598.

McCully, M. E. (1999). Roots in soil: unearthing the complexities of roots and their rhizospheres. *Annual Review of Plant Biology*, *50* (1): 695-718.

Mei, Y., Jia, W.J., Chu, Y.J. and Xue, H.W. (2012). *Arabidopsis* phosphatidylinositol monophosphate 5-kinase 2 is involved in root gravitropism through regulation of polar auxin transport by affecting the cycling of PIN proteins. *Cell Research*, 22 (3): 581-597.

Mentlak, T.A., Kombrink, A., Shinya, T., Ryder, L.S., Otomo, I., Saitoh, h., Terauchi, R., Nishizawa, Y., Shibuya, N., Thomma, B.P.H.J and Talbot, N. (2012). Effector-Mediated Suppression of Chitin-Triggered Immunity by Magnaporthe oryzae Is Necessary for Rice Blast Disease. *The Plant Cell,* 24 (1): 322-335.

Miller, A.J., Fan, X., Orsel, M., Smith, S.J. and Wells, D. (2007). Nitrate transport and signalling. *Journal of Experimental Botany*, 58 (9): 2297-2306.

Miller, A.J. and Smith, S. J. (2008). Cytosolic nitrate ion homeostasis: could it have a role in sensing nitrogen status?. *Annals of Botany,* 101 (4): 485-489.

Mito, T.T., Seki, M.M., Shinozaki, K.K., Ohme-Takagi, M. and Matsui, K. (2011). Generation of chimeric repressors that confer salt tolerance in *Arabidopsis* and rice. *Plant Biotechnology Journal,* 9 (7): 736-746.

Miya, A., Albert, P., Shinya, T., Desaki, Y., Ichimura, K., Shirasu, K., Narusaka, Y., Kawakami, N., Kaku, H. and Shibuya, N. (2007). CERK1, a LysM receptor kinase, is essential for chitin elicitor signaling in *Arabidopsis*. *Proceedings of the National Academy of Sciences,* 104 (49): 19613-19618.

Morrissey, E.R. (2013). GRENITS: Gene regulatory network inference using time series. *R package.*

Müller, B. and Sheen, J. (2008). Cytokinin and auxin interaction in root stem-cell specification during early embryogenesis. *Nature*, 453 (7198): 1094-1097.

Muños, S., Cazettes, C., Fizames, C., Gaymard, F., Tillard, P., Lepetit, M., Lejay, L. and Gojon, A. (2004). Transcript profiling in the *chl1-5* mutant of *Arabidopsis* reveals a role of the nitrate transporter NRT1.1 in the regulation of another nitrate transporter, NRT2.1. *The Plant Cell,* 16 (9): 2433-2447.

Murphy, A.S., Hoogner, K.R., Peer, W.A. and Taiz, L. (2002). Identification, purification, and molecular cloning of N-1-naphthylphthalmic acid-binding plasma membrane-associated aminopeptidases from *Arabidopsis*. *Plant Physiology,* 128 (3): 935-950.

Murray, J.D., Karas, B.J., Sato, S., Tabata, S., Amyot, L. and Szczyglowski, K. (2007). A cytokinin perception mutant colonized by *Rhizobium* in the absence of nodule organogenesis. *Science*, 315 (5808): 101-104.

Neill, S., Desikan, R. and Hancock, J. (2002). Hydrogen peroxide signalling. *Current Opinion in Plant Biology,* 5 (5): 388-395.

Nero, D., Katari, M.S., Kelfer, J., Tranchina, D. and Coruzzi, G.M. (2009). In silico evaluation of predicted regulatory interactions in *Arabidopsis thaliana*. *BMC bioinformatics*, 10 (1): 435.

Nishizawa-Yokoi, A., Yoshida, E., Yabuta, Y. and Shigeoka, S. (2009). Analysis of the regulation of target genes by an *Arabidopsis* heat shock transcription factor, HsfA2. *Bioscience, Biotechnology, and Biochemistry*, 73 (4): 890-895.

Okazaki, S., Kaneko, T., Sato, S. and Saeki, K. (2013). Hijacking of leguminous nodulation signaling by the rhizobial type III secretion system. *Proceedings of the National Academy of Sciences of the USA,* 110 (42): 17131-17136.

Okushima, Y., Mitina, I., Quach, H.L. and Theologis, A. (2005). AUXIN RESPONSE FACTOR 2 (ARF2): a pleiotropic developmental regulator. *The Plant*

Journal, 43 (1): 29-46.

Oldroyd, G.E.D, and Downie, J.A. (2008). Coordinating nodule morphogenesis with rhizobial infection in legumes. *Annual Review of Plant Biology*. 59: 519-546.

Oldroyd, G.E.D., Murray, J.D., Poole, P.S. and Downie, J.A. (2011). The rules of engagement in the legume-rhizobial symbiosis. *Annual Review of Genetics*, 45: 119-144.

Oldroyd, G.E.D. (2013). Speak, friend, and enter: signalling systems that promote beneficial symbiotic associations in plants. *Nature Reviews: Microbiology,* 11 (4): 252-263

Olsen, C., Fleming, K., Prendergast, N., Rubio, R., Emmert-Streib, F., Bontempi, G., Haibe-Kains, B. and Quackenbush, J. (2014). Inference and validation of predictive gene networks from biomedical literature and gene expression data. *Genomics*, 103 (5): 329-336.

Op den Camp, R., Streng, A., De Mita, S., Cao, Q., Polone, E., Liu, W., Ammiraju, J.S.S., Kurdna, D., Wing, R., Untergasser, A., Bisseling, T. and Geurts, R. (2011). LysM-type mycorrhizal receptor recruited for Rhizobium symbiosis in nonlegume Parasponia. *Science Signalling*, 331 (6019): 909-912.

Orsel, M., Chopin, F., Leleu, O., Smith, S.J., Krapp, A., Daniel-Vedele, F. and Miller, A.J. (2006) Characterization of a two-component high-affinity nitrate uptake system in *Arabidopsis*. Physiology and Protein-Protein Interaction. *Plant Physiology*, 142 (3): 1304-1317.

Osmont, K.S., Sibout, R. and Hardtke, C.S., (2007) Hidden branches: developments in root system architecture. *Annual Reviews Plant Biology,* 58: 93-113.

Ouellet, F., Overvoorde, P.J. and Theologis, A. (2001). *IAA17/AXR3*: biochemical insight into an auxin mutant phenotype. *The Plant Cell,*13 (4): 829-841.

Overvoorde, P., Fukaki, H. and Beeckman, T. (2010). Auxin control of root development. *Cold Spring Harbor Perspectives in Biology,* 2 (6): a001537.

Page, M., Sultana, N., Paszkiewicz, K., Florance, H. and Smirnoff, N. (2012). The influence of ascorbate on anthocyanin accumulation during high light acclimation in *Arabidopsis thaliana*: further evidence for redox control of anthocyanin synthesis. *Plant, Cell & Environment,* 35 (2): 388-404.

Painter, H. A. (1970). A review of literature on inorganic nitrogen metabolism in microorganisms. *Water Research*, 4 (6): 393-450.

Pajoro, A., Biewers, S., Dougali, E., Valentim, F.L., Mendes, M.A., Porri, A., Coupland, G., Van de Peer, Y., van Dijk, A.D.J., Colombo, L., Davies, B. and Angenent, G.C. (2014). The (r) evolution of gene regulatory networks controlling *Arabidopsis* plant reproduction: a two-decade history. *Journal of Experimental Botany,* 65 (17): 4731-4745.

Pandey, G.K., Grant, J.J., Cheong, Y.H., Kim, B.G., Li, L. and Luan, S. (2005). ABR1,

an APETALA2-domain transcription factor that functions as a repressor of ABA response in *Arabidopsis*. *Plant Physiology,* 139 (3): 1185-1193.

Pant, B. D., Musialak-Lange, M., Nuc, P., May, P., Buhtz, A., Kehr, J. and Scheible, W. R. (2009). Identification of nutrient-responsive *Arabidopsis* and rapeseed microRNAs by comprehensive real-time polymerase chain reaction profiling and small RNA sequencing. *Plant Physiology*, 150 (3): 1541-1555.

Parniske, M. (2008) Arbuscular mycorrhiza: the mother of plant root endosymbioses. *Nature Reviews: Microbiology,* 6 (10): 763-775.

Perruc, E., Charpenteau, M., Ramirez, B. C., Jauneau, A., Galaud, J.P., Ranjeva, R. and Ranty, B. (2004). A novel calmodulin binding protein functions as a negative regulator of osmotic stress tolerance in *Arabidopsis thaliana* seedlings. *The Plant Journal,* 38 (3): 410-420.

Peeters, N., Carrère, S., Anisimova, M., Piener, L., Cazale, A.-C. and Genin, S. (2012). Repertoire, unified nomenclature and evolution of the Type III effector gene set in the *Ralstonia solanacearum* species complex. *BMC genomics,* 14 (1): 859-859.

Pidwirny, M. (2006). The Nitrogen Cycle. *Fundamentals of Physical Geography,* 4.

Pieterse, C.M., Van der Does, D., Zamioudis, C., Leon-Reyes, A. and Van Wees, S.C. (2012). Hormonal modulation of plant immunity. *Annual Review of Cell and Developmental Biology,* 28: 489-521.

Pii, Y., Crimi, M., Cremonese, G., Spena, A. and Pandolfini, T. (2007). Auxin and nitric oxide control indeterminate nodule formation. *BMC Plant Biology*, 7 (1): 21.

Plaxton, W. C., & Carswell, M. C. (1999). Metabolic aspects of the phosphate starvation response in plants. Plant responses to environmental: from phytohormones to genome reorganization. Marcel Dekker, New York, 349-372.

Plet, J., Wasson, A., Ariel, F., Le Signor, C., Baker, D., Mathesius, U., and Frugier, F. (2011). MtCRE1 dependent cytokinin signaling integrates bacterial and plant cues to coordinate symbiotic nodule organogenesis in *Medicago truncatula*. *The Plant Journal*, 65 (4): 622-633.

Pokhilko, A., Fernández, A.P., Edwards, K.D., Southern, M.M., Halliday, K.J. and Millar, A.J. (2012). The clock gene circuit in *Arabidopsis* includes a repressilator with additional feedback loops. *Molecular Systems Biology*, 8 (1): 574.

Poza-Carrión, C., Aguilar-Martínez, J.A. and Cubas, P. (2007). Role of TCP gene BRANCHED1 in the control of shoot branching in *Arabidopsis*. *Plant Signal Behaviour,* 2 (6): 551-552.

Prasad, B. D., Goel, S., & Krishna, P. (2010). In silico identification of carboxylate clamp type tetratricopeptide repeat proteins in *Arabidopsis* and rice as putative co-chaperones of Hsp90/Hsp70. *PLoS One*, 5 (9): e12761.

Preston, K (2004). Phenotypic Integration : Studying the Ecology and Evolution of

Complex Phenotypes. OUP, Oxford.

Punja, Z.K. and Zhang, Y.Y. (1993). Plant chitinases and their roles in resistance to fungal diseases. *Journal of Nematology*, 25 (4): 526-540.

Pysh, L., Alexander, N., Swatzyna, L. and Harbert, R. (2012). Four alleles of AtCESA3 form an allelic series with respect to root phenotype in *Arabidopsis* thaliana. *Physiologia plantarum*, 144 (4): 369-381.

Rasband, W. S. (2013). ImageJ 1.47 v. *US National Institutes of Health: Bethesda, MD, USA*.

Redecker, D., Kodner, R. and Graham, L.E. (2000). Glomalean fungi from the Ordovician. *Science*, 289 (5486): 1920-1921.

Reichheld, J.P., Khafif, M., Riondet, C., Droux, M., Bonnard, G. and Meyer, Y. (2007). Inactivation of thioredoxin reductases reveals a complex interplay between thioredoxin and glutathione pathways in *Arabidopsis* development. *The Plant Cell*, 19 (6): 1851-1865.

Reiter, W.D., Chapple, C. and Somerville, C.R. (1997). Mutants of *Arabidopsis thaliana* with altered cell wall polysaccharide composition. *The Plant Journal for Cell and Molecular Biology,* 12 (2): 335-345.

Remans, T., Nacry, P., Pervent, M., Filleur, S., Diatloff, E., Mounier, E., Tillard, P., Forde, B.G. and Gojon, A. (2006). The *Arabidopsis* NRT1.1 transporter participates in the signaling pathway triggering root colonization of nitrate-rich patches. *Proceedings of the National Academy of Sciences,* 103 (50): 19206-19211.

Remans, T., Nacry, P., Pervent, M., Girin, T., Tillard, P., Lepetit, M. and Gojon, A. (2006). A Central Role for the Nitrate Transporter NRT2.1 in the Integrated Morphological and Physiological Responses of the Root System to Nitrogen Limitation in *Arabidopsis*. *Plant Physiology,* 140 (3): 909-921.

Remigi, P., Anisimova, M., Guidot, A., Genin, S. Peeters, N. (2011). Functional diversification of the GALA type III effector family contributes to Ralstonia solanacearum adaptation on different plant hosts. *New Phytologist,* 192 (4): 976-987.

Remy, E., Cabrito, T. R., Baster, P., Batista, R. A., Teixeira, M. C., Friml, J. and Duque, P. (2013). A major facilitator superfamily transporter plays a dual role in polar auxin transport and drought stress tolerance in Arabidopsis. *The Plant Cell*, 25 (3): 901-926.

Ren, B., Liang, Y., Deng, Y., Chen, Q., Zhang, J., Yang, X. and Zuo, J. (2009). Genome-wide comparative analysis of type-A *Arabidopsis* response regulator genes by overexpression studies reveals their diverse roles and regulatory mechanisms in cytokinin signaling. *Cell Research,* 19 (10): 1178-1190.

Robert-Seilaniantz, A., Grant, M. and Jones, J.D. (2011). Hormone crosstalk in plant disease and defense: more than just jasmonate-salicylate antagonism. *Annual*

Review of Phytopathology, 49: 317-343.

Robinson, D., Hodge, A., Griffiths, B.S. and Fitter A.H. (1999). Plant root proliferation in nitrogen-rich patches confers competitive advantage. *Proceedings of the Royal Society of London Biological Sciences,* 266 (1418): 431-435.

Rubin, G., Tohge, T., Matsuda, F., Saito, K., Scheible, W.R. (2009). Members of the LBD family of transcription factors repress anthocyanin synthesis and affect additional nitrogen responses in *Arabidopsis*. *The Plant Cell*, 21 (11): 3567-3584.

Rushton, P.J., Somssich, I.E., Ringler, P. and Shen, Q.J. (2010). WRKY transcription factors. *Trends in Plant Science,* 15 (5): 247-258.

Růžička, K., Strader, L.C., Bailly, A., Yang, H., Blakeslee, J., Łangowski, Ł., Nejedla, E., Fujita, H., Itoh, H., Syono, K., Hejatko, J., Gray, W.M., Martinoia, E. Geisler, M., Bartel, B., Murphy, A.SS and Friml, J. (2010). *Arabidopsis* PIS1 encodes the ABCG37 transporter of auxinic compounds including the auxin precursor indole-3-butyric acid. *Proceedings of the National Academy of Sciences,* 107 (23): 10749-10753.

Saddic, L.A., Huvermann, B., Bezhani, S., Su, Y., Winter, C. M., Kwon, C. S., Collum, R.P. and Wagner, D. (2006). The LEAFY target LMI1 is a meristem identity regulator and acts together with LEAFY to regulate expression of CAULIFLOWER. *Development,* 133 (9): 1673-1682.

Saito, K., Yoshikawa, M., Yano, K., Miwa, H., Uchida, H., Asamizu, E. and Kawaguchi, M. (2007). NUCLEOPORIN85 is required for calcium spiking, fungal and bacterial symbioses, and seed production in *Lotus japonicus*. *The Plant Cell*, 19 (2): 610-624.

Sánchez-Rodríguez, C., Estévez, J. M., Llorente, F., Hernández-Blanco, C., Jordá, L., Pagán, I. and Molina, A. (2009). The ERECTA receptor-like kinase regulates cell wall-mediated resistance to pathogens in Arabidopsis thaliana. *Molecular Plant-Microbe Interactions*, 22 (8): 953-963.

Schaffer, R., Landgraf, J., Pérez-Amador, M. and Wisman, E. (2000). Monitoring genome-wide expression in plants. *Current Opinion in Biotechnology,* 11 (2): 162-167.

Schauser, L., Roussis, A., Stiller, J. and Stougaard, J. (1999). A plant regulator controlling development of symbiotic root nodules. *Nature*, 402 (6758): 191-195.

Schneider, C.A., Rasband, W.S. and Eliceiri, K.W. (2012). NIH Image to ImageJ: 25 years of image analysis. *Nature Methods,* 9 (7): 671-675.

Segonzac, C., Boyer, J.C., Ipotesi, E., Szponarski, W., Tillard, P., Touraine, B., Sommerer, N., Rossignol, M. and Gibrat, R. (2007). Nitrate efflux at the root plasma membrane: identification of an *Arabidopsis* excretion transporter. *The Plant Cell,* 19 (11): 3760-3777.

Sehr, E.M., Agusti, J., Lehner, R., Farmer, E.E., Schwarz, M. and Greb, T. (2010).

Analysis of secondary growth in the *Arabidopsis* shoot reveals a positive role of jasmonate signalling in cambium formation. *The Plant Journal,* 63 (5): 811-822.

Sheard, L. B., Tan, X., Mao, H., Withers, J., Ben-Nissan, G., Hinds, T. R. and Zheng, N. (2010). Jasmonate perception by inositol-phosphate-potentiated COI1-JAZ co-receptor. *Nature*, 468 (7322): 400-405.

Shibuya, N. and Minami, E. (2001) Oligosaccharide signalling for defence responses in plant. *Physiological and Molecular Plant Pathology,* 59 (5): 223-233.

Shim, J. S., Jung, C., Lee, S., Min, K., Lee, Y.W., Choi, Y., Lee, J.S., Song, J.T., Kim, J.K. and Choi, Y.D. (2012). AtMYB44 regulates *WRKY70* expression and modulates antagonistic interaction between salicylic acid and jasmonic acid signaling. *The Plant Journal,* 73 (3): 483-495.

Shim, J.S. and Choi, Y.D. (2013). Direct regulation of WRKY70 by AtMYB44 in plant defense responses. *Plant Signal and Behaviour,* 8 (6): e20783.

Shimizu, T., Nakano, T., Takamizawa, D., Desaki, Y., Ishii-Minami, N., Nishizawa, Y., Minami, E., Okada, K., Yamane, H., Kaku, H. and Shibuya, N. (2010). Two LysM receptor molecules, CEBiP and OsCERK1, cooperatively regulate chitin elicitor signaling in rice. *The Plant Journal*, 64 (2): 204-214.

Shimoda, Y., Han, L., Yamazaki, T., Suzuki, R., Hayashi, M. and Imaizumi-Anraku, H. (2012). Rhizobial and fungal symbioses show different requirements for calmodulin binding to calcium calmodulin–dependent protein kinase in *Lotus japonicus. The Plant Cell*, 24 (1): 304-321.

Shin, R., Berg, R.H. and Schachtman, D.P. (2005). Reactive oxygen species and root hairs in *Arabidopsis* root response to nitrogen, phosphorus and potassium deficiency. *Plant and Cell Physiology*, 46 (8): 1350-1357.

Sieberer, B.J., Chabaud, M., Timmers, A.C., Monin, A., Fournier, J. and Barker, D.G. (2009). A nuclear-targeted cameleon demonstrates intranuclear Ca^{2+} spiking in Medicago truncatula root hairs in response to rhizobial nodulation factors. *Plant Physiology*, 151 (3): 1197-1206.

Sieberer, B.J., Chabaud, M., Fournier, J., Timmers, A.C.J. and Barker, D.G. (2012). A switch in Ca^{2+} spiking signature is concomitant with endosymbiotic microbe entry into cortical root cells of Medicago truncatula. *The Plant Journal,* 69 (5): 822-830.

Signora, L., De Smet, I., Foyer, C.H. and Zhang, H. (2001). ABA plays a central role in mediating the regulatory effects of nitrate on root branching in *Arabidopsis*. *The Plant Journal,* 28 (6): 655-662.

Smit, P., Raedts, J., Portyanko, V., Debellé, F., Gough, C., Bisseling, T. and Geurts, R. (2005). NSP1 of the GRAS protein family is essential for rhizobial Nod factor-induced transcription. *Science*, 308 (5729): 1789-1791.

Smyth, G. K. (2005). Limma: linear models for microarray data. Bioinformatics and computational biology solutions using R and Bioconductor (pp. 397-420).

Springer, New York.

Soltis, D.E., Soltis, P.S., Morgan, D.R., Swensen, S.M., Mullin, B.C., Dowd, J.M. and Martin, P.G. (1995). Chloroplast gene sequence data suggest a single origin of the predisposition for symbiotic nitrogen fixation in angiosperms. *Proceedings of the National Academy of Sciences of the USA,* 92 (7): 2647-2651.

Stacey, G. and Shibuya, N. (1997). Chitin recognition in rice and legumes. *Plant and Soil,* 194 (1-2): 161-169.

Staswick, P.E., Serban, B., Rowe, M., Tiryaki, I., Maldonado, M.T., Maldonado, M.C. and Suza, W. (2005). Characterization of an *Arabidopsis* enzyme family that conjugates amino acids to indole-3-acetic acid. *The Plant Cell*, 17 (2): 616-627.

Stegle, O., Denby, K.J., Cooke, E.J., Wild, D.L., Ghahramani, Z. and Borgwardt, K.M. (2010). A robust Bayesian two-sample test for detecting intervals of differential gene expression in microarray time series. *Journal of Computational Biology*, 17 (3): 355-367.

Stracke, S., Kistner, C., Yoshida, S., Mulder, L., Sato, S., Kaneko, T. and Parniske, M. (2002). A plant receptor-like kinase required for both bacterial and fungal symbiosis. *Nature*, 417 (6892): 959-962.

Sugimoto, K., Gordon, S. P. and Meyerowitz, E. M. (2011). Regeneration in plants and animals: dedifferentiation, transdifferentiation, or just differentiation?. *Trends in cell biology*, 21 (4): 212-218.

Sun, J., Xu, Y., Ye, S., Jiang, H., Chen, Q., Liu, F., Zhou, W., Chen, R., Li, X., Tietz, O., Wu, X., Cohen, J.D., Palme, K. and Li, C. (2009). *Arabidopsis* ASA1 is important for jasmonate-mediated regulation of auxin biosynthesis and transport during lateral root formation. *The Plant Cell,* 21 (5): 1495-1511.

Swarup, R., Kargul, J., Marchant, A., Zadik, D., Rahman, A., Mills, R., Yemm, A., May, S., Williams, L., Millner, P., Tsurumi, S., Moore, I., Napier, R., Kerr, I.D. and Bennett, M.J. (2004). Structure-function analysis of the presumptive *Arabidopsis* auxin permease AUX1. *The Plant Cell,* 16 (11): 3069-3083.

Takei, K., Takahashi, T., Sugiyama, T., Yamaya, H. and Sakakibara, H. (2002). Multiple routes communicating nitrogen availability from roots to shoots: a signal transduction pathway mediated by cytokinin. *Journal of Experimental Botany*, 53 (370): 971-977

Takei, K., Ueda, K., Aoki, T., Kuromori, T., Hirayama, K., Shinozaki, T., Yamaya, H. and Sakakibara, H. (2004) AtIPT3 is a key determinant of nitrate-dependent cytokinin biosynthesis in *Arabidopsis*. *Plant Cell Physiology*, 45 (8): 1053-1062.

Thomma, B.P., Eggermont, K., Penninckx, I.A., Mauch-Mani, B., Vogelsang, R., Cammue, B.P. and Broekaert, W.F. (1998). Separate jasmonate-dependent and salicylate-dependent defense-response pathways in *Arabidopsis* are essential for resistance to distinct microbial pathogens. *Proceedings of the National Academy of Sciences of the USA*, 95 (25): 15107-15111.

Tilman, D., Balzer, C., Hill, J. and Befort, L. (2011). Global food demand and the sustainable intensification of agriculture. *Proceedings of the National Academy of Sciences*, 108 (50): 20260-20264.

Tirichine, L., Imaizumi-Anraku, H., Yoshida, S., Murakami, Y., Madsen, L. H., Miwa, H. and Stougaard, J. (2006). Deregulation of a Ca2+/calmodulin-dependent kinase leads to spontaneous nodule development. *Nature*, 441 (7097): 1153-1156.

Truernit, E. and Haseloff, J. (2006) A Role for KNAT Class II Genes in Root Development. *Plant Signaling & Behavior*, 2 (1): 10-12.

Tyson, J.J., Chen, K.C. and Novak, B. (2003). Sniffers, buzzers, toggles and blinkers: dynamics of regulatory and signaling pathways in the cell. *Current Opinion in Cell Biology,* 15 (2): 221-231.

Ullah, H., Chen, J.G., Temple, B., Boyes, D.C., Alonso, J.M., Davis, K.R., Ecker, J.R. and Jones, A. M. (2003). The β-subunit of the *Arabidopsis* G protein negatively regulates auxin-induced cell division and affects multiple developmental processes. *The Plant Cell,* 15 (2): 393-409.

Urao, T., Yamaguchi-Shinozaki, K., Urao, S. and Shinozaki, K. (1993). An *Arabidopsis myb* homolog is induced by dehydration stress and its gene product binds to the conserved MYB recognition sequence. *The Plant Cell,* 5 (11): 1529-1539.

Vance, C.P. (2001). Symbiotic nitrogen fixation and phosphorus acquisition. Plant nutrition in a world of declining renewable resources. *Plant Physiology,* 127 (2): 390-397

Vanderauwera, S., Zimmermann, P., Rombauts, S., Vandenabeele, S., Langebartels, C., Gruissem, W., Inze, D. and Van Breusegem, F. (2005). Genome-wide analysis of hydrogen peroxide-regulated gene expression in *Arabidopsis* reveals a high light-induced transcriptional cluster involved in anthocyanin biosynthesis. *Plant Physiology,* 139 (2): 806-821.

Vellosillo, T., Martínez, M., López, M.A., Vicente, J., Cascon, T., Dolan, L., Hamberg, M. and Castresana, C. (2007). Oxylipins produced by the 9-lipoxygenase pathway in *Arabidopsis* regulate lateral root development and defense responses through a specific signaling cascade. *The Plant Cell*, 19 (3): 831-846.

Vidal, E. A., Araus, V., Lu, C., Parry, G., Green, P. J., Coruzzi, G. M., & Gutiérrez, R. A. (2010). Nitrate-responsive miR393/AFB3 regulatory module controls root system architecture in *Arabidopsis thaliana*. *Proceedings of the National Academy of Sciences*, 107 (9): 4477-4482.

Walch-Liu, P., Ivanov, I. I., Filleur, S., Gan, Y., Remans, T. and Forde, B. G. (2006). Nitrogen regulation of root branching. *Annals of Botany,* 97 (5): 875-881.

Wan, J., Zhang, S. and Stacey, G. (2004). Activation of a mitogen-activated protein kinase pathway in *Arabidopsis* by chitin. *Molecular Plant Pathology*, 5 (2): 125-135.

Wan, J., Zhang, X.C., Neece, D., Ramonell, K.M. Clough, S., Kim, S.Y. Stacey, M.G. and Stacey, G. (2008). A LysM receptor-like kinase plays a critical role in chitin signaling and fungal resistance in *Arabidopsis*. *The Plant Cell*, 20 (2): 471-481.

Wang, B., Bailly, A., Zwiewka, M., Henrichs, S., Azzarello, E., Mancuso, S. and Geisler, M. (2013). *Arabidopsis* TWISTED DWARF1 functionally interacts with auxin exporter ABCB1 on the root plasma membrane. *The Plant Cell*, 25 (1): 202-214.

Wang, L., Tsuda, K., Truman, W., Sato, M., Nguyen, L.V., Katagiri, F. and Glazebrook, J. (2011). CBP60g and SARD1 play partially redundant critical roles in salicylic acid signaling. *The Plant Journal,* 67 (6): 1029-1041.

Wang, R., Tischner, R., Gutiérrez, R., Hoffman, M., Xing, X., Chen, M., Coruzzi, G. and Crawford, N.M. (2004). Genomic analysis of the nitrate response using a nitrate reductase-null mutant of *Arabidopsis. Plant Physiology* 136: 2512-2522

Wang, W., Xie, Z.P. and Staehelin, C. (2014) Functional analysis of chimeric lysin motif domain receptors mediating Nod factor-induced defense signaling in *Arabidopsis thaliana* and chitin-induced nodulation signaling in *Lotus japonicus*. *The Plant Journal,* 78 (1): 56-69.

Wang, Y., Penfold, C.A., Hodgson, D.A., Gifford, M. L., & Burroughs, N. J. (2014). Correcting for link loss in causal network inference caused by regulator interference. *Bioinformatics*, 30 (19): 2779-2786.

Wang, Y.Y. and Tsay, Y.F. (2011) *Arabidopsis* Nitrate Transporter NRT1.9 Is Important in Phloem Nitrate Transport. *The Plant Cell,* 23 (5): 1945-1957

Wehmeyer, N., & Vierling, E. (2000). The expression of small heat shock proteins in seeds responds to discrete developmental signals and suggests a general protective role in desiccation tolerance. *Plant Physiology*, 122(4): 1099-1108.

Williams, E.J. and Bowles, D.J. (2004). Coexpression of neighboring genes in the genome of *Arabidopsis thaliana*. *Genome Research,* 14 (6): 1060-1067.

Willmann, R., Lajunen, H.M., Erbs, G., Newman, M.A., Kolb, D., Tsuda, K., Katagiri, F., Fliegmann, J., Bono, J.J., Cullimore, J.V., Jehle, A.K. Gotz, F., Kulik, A., Molinaro, A., Lipka, V., Gust, A.A. and Nurnberger, T. (2011). *Arabidopsis* lysin-motif proteins LYM1 LYM3 CERK1 mediate bacterial peptidoglycan sensing and immunity to bacterial infection. *Proceedings of the National Academy of Sciences of the USA,* 108 (49): 19824-19829.

Windram, O., Madhou, P., McHattie, S., Hill, C., Hickman, R., Cooke, E., Jenkins, D.J. Penfold, C.A., Baxter, L., Breeze, E., Kiddle, S.J. Rhodes, J., Atwell, S., Kliebenstein, D.J. Kim, Y.S., Stegle, O., Borgwardt, K., Zhang, C., Tabrett, A., Legaie, R., Moore, J., Finkenstadt, B., Wild, D.L., Mead, A., Rand, D., Beynon, J., Ott, S., Buchanan-Wollaston, V. and Denby, K.J. (2012). *Arabidopsis* Defense against Botrytis cinerea: Chronology and Regulation Deciphered by High-Resolution Temporal Transcriptomic Analysis. *The Plant Cell*, 24 (9): 3530-3557.

Wirth, J., Chopin, F., Santoni, V., Viennois, G., Tillard, P., Krapp, A., Lejay, L., Daniel-Vedele, F. and Gojon, A. (2007). Regulation of root nitrate uptake at the NRT2.1 protein level in *Arabidopsis thaliana*. *Journal of Biological Chemistry,* 282 (32): 23541-23552.

Wolf, S., Hematy, K. and Hofte, H. (2012). Growth control and cell wall signaling in plants. *Annual Review of Plant Biology,* 63: 381-407.

Wu, C., Feng, J., Wang, R., Liu, H., Yang, H., Rodriguez, P.L., Qin, H., Liu, X. and Wang, D. (2011). HRS1 acts as a negative regulator of abscisic acid signaling to promote timely germination of *Arabidopsis* seeds. *PLoS One*, 7 (4): e35764-e35764.

Xu, G., Fan, X. and Miller, A.J. (2012) Plant nitrogen assimilation and use efficiency. *Annual Reviews of Plant Biology*, 63: 153-182.

Xu, M., Hu, T., McKim, S.M., Murmu, J., Haughn, G.W. and Hepworth, S.R. (2010). *Arabidopsis* BLADE ON PETIOLE1 and 2 promote floral meristem fate and determinacy in a previously undefined pathway targeting APETALA1 and AGAMOUS LIKE24. *The Plant Journal*, 63 (6): 974-989.

Xu, W., Campbell, P., Vargheese, A.K. and Braam, J. (1996). The *Arabidopsis* XET-related gene family: environmental and hormonal regulation of expression. *Plant Journal,* 9 (6): 879-889.

Yang, K. Z., Xia, C., Liu, X. L., Dou, X. Y., Wang, W., Chen, L. Q., ... & Ye, D. (2009). A mutation in Thermosensitive Male Sterile 1, encoding a heat shock protein with DnaJ and PDI domains, leads to thermosensitive gametophytic male sterility in *Arabidopsis*. *The Plant Journal*, 57 (5): 870-882.

Yanhui, C., Xiaoyuan, Y., Kun, H., Meihua, L., Jigang, L., Zhaofeng, G., Zhiqiang, L., Yunfei, Z., Xiaoxiao, W., Xiaoming, Q., Yunping, S., Li, Z., Xiaohui, D., Jingchu, L., Xing-Wang, D., Zhangliang, C., Hongya, G. and Li-Jia, Q. (2005). The MYB transcription factor superfamily of *Arabidopsis*: expression analysis and phylogenetic comparison with the rice MYB family. *Plant Molecular Biology,* 60 (1): 107-124.

Yoder, J. I. (1999). Parasitic plant responses to host plant signals: a model for subterranean plant-plant interactions. *Current Opinion in Plant Biology*, 2 (1): 65-70.

Yong, Z., Kotur, Z. and Glass, A.D.M. (2010) Characterization of an intact two-component high-affinity nitrate transporter from *Arabidopsis* roots. *The Plant Journal,* 63 (5): 739-748.

Zhang, H. and Forde, B.G. (1998) An *Arabidopsis* MADS box gene that controls nutrient-induced changes in root Architecture. *Science*, 279 (5349): 407-409.

Zhang, J. X., Wang, C., Yang, C. Y., Wang, J. Y., Chen, L., Bao, X. M. and Liu, J. (2010). The role of *Arabidopsis* AtFes1A in cytosolic Hsp70 stability and abiotic stress tolerance. *The Plant Journal*, 62 (4): 539-548.

Zhang, X.C., Wu, X., Findley, S., Wan, J., Libault, M., Nguyen, H.T., Cannon, S.B. and Stacey, G. (2007). Molecular evolution of lysin motif-type receptor-like kinases in plants. *Plant Physiology,* 144 (2): 623-636.

Zhu, Q., Zhang, J., Gao, X., Tong, J., Xiao, L., Li, W. and Zhang, H. (2010). The *Arabidopsis* AP2/ERF transcription factor RAP2.6 participates in ABA, salt and osmotic stress responses. *Gene,* 457 (1): 1-12.

Zhu, Y., Dong, A. and Shen, W.H. (2006). chromatin remodeling in *Arabidopsis* root growth. *The Plant Cell,* 18: 2879-92.

Zhuo, D., Okamoto, M., Vidmar, J.J. and Glass, D.M. (1999) Regulation of a putative high‐affinity nitrate transporter (Nrt2; 1At) in roots of *Arabidopsis thaliana*. *The Plant Journal*, 17 (5): 563-568.